THÈSE

En vue de l'obtention du

DOCTORAT DE L'UNIVERSITÉ DE TOULOUSE

Délivré par *l'Université Toulouse III - Paul Sabatier*
Discipline ou spécialité : *Anthropologie biologique*

Présentée et soutenue par *Adeline LE CABEC*
Le *18 Mars 2013*

Titre :

Anterior Dental Loading and Root Morphology in Neanderthals

JURY
Pr. Jean-Jacques HUBLIN (MPI-EVA, Leipzig, Allemagne)
Pr. José BRAGA (AMIS UMR 5288, Toulouse, France)
Pr. Olivier DUTOUR (EPHE, France)
Pr. Svante PÄÄBO (MPI-EVA, Leipzig, Allemagne)
Pr. Thomas MAGIN (TRM Leipzig, Leipzig, Allemagne)
Pr. Jean-Pierre JESSEL (IRIT, Toulouse, France)
Pr. Jean-Michel LOUBES (Institut de Mathématiques de Toulouse, Toulouse, France)
Dr. Paul TAFFOREAU (ESRF, Grenoble, France)

Ecole doctorale : *Biologie, Santé, Biotechnologies (BSB)*
Unité de recherche : *Dpt. Human Evolution (MPI-EVA) et Laboratoire AMIS UMR 5288*
Directeur(s) de Thèse : *Pr. Jean-Jacques HUBLIN, Pr. José BRAGA*
Rapporteurs : *Pr. Olivier DUTOUR, Pr. Richard KLEIN*

Anterior Dental Loading and Root Morphology in Neanderthals

Von der Fakultät für Biowissenschaften, Pharmazie und Psychologie

der Universität Leipzig

genehmigte

D I S S E R T A T I O N

zur Erlangung des akademischen Grades

Doctor rerum naturalium
Dr. rer. nat.

vorgelegt

von

M.Sc., B.Sc. Adeline Le Cabec

geboren am 11. Dezember 1984 in Saint-Brieuc (Côtes-d'Armor), Frankreich

Dekanin: Prof. Dr. Andrea Robitzki

Gutachter: Prof. Dr. Jean-Jacques Hublin

Prof. Dr. Richard Klein

Tag der Verteidigung: 18. März 2013

BIBLIOGRAPHICAL DESCRIPTION

Adeline Le Cabec, 2012

Anterior Dental Loading and Root Morphology in Neanderthals.

Faculty of Life Sciences, Pharmacy and Psychology, University of Leipzig
Prepared at the Dept. of Human Evolution, Max Planck Institute for Evolutionary Anthropology, Leipzig
In joint supervision with the University Paul Sabatier, Toulouse, France.

Cumulative Dissertation

246 pages, 266 bibliographical references, 18 Figures, 25 Tables.

Distinguishing Neanderthal and modern human incisors and canines can be challenging in the case of isolated teeth found in museum collections, or from unclear stratigraphic contexts. In addition, the crown morphology cannot be used in the case of heavily worn teeth. A preliminary study based on limited samples and linear measurements (Bailey, 2005) proposed that root length alone can taxonomically discriminate Neanderthals from Upper Paleolithic and extant modern humans.

This thesis investigates whether this remains true for a broader chronological and geographical sample of Neanderthals and modern humans, using micro-computed tomography. In addition to the taxonomic interest of investigating root size and shape, we discuss the functional implications of the anterior root morphology in the context of the 'teeth-as-tools' hypothesis and of para-masticatory activities.

The first part was published as: Le Cabec, A., Kupczik, K., Gunz, P., Braga, J., and Hublin, J.J. (2012). Long Anterior Mandibular Tooth Roots in Neanderthals Are Not the Result of their Large Jaws. ***Journal of Human Evolution***, 63, pp. 667-681. DOI: 10.1016/j.jhevol.2012.07.003. This part validates root length as a taxonomical tool to distinguish late Neanderthals from Upper Paleolithic and recent modern humans. Despite the absence of correlation between root size and symphyseal size, Neanderthals have large roots for the size of their jaws. It is hypothesized that the short roots of extant modern humans result from a negative allometry.

The second part was published as: Le Cabec, A., Gunz, P., Kupczik, K., Braga, J. and Hublin, J.J. (2013). Anterior Tooth Root Morphology and Size in Neanderthals: Taxonomic and Functional Implications. ***Journal of Human Evolution***, 64, pp. 169-193**.** DOI: 10.1016/j.jhevol.2012.08.011. Root morphology is explored across a chronologically and geographically large sample of fossil and extant hominids. Longer roots in Neanderthals may have resulted from the retention of an ancestral condition. The debated taxonomic attribution of some specimens is discussed in light of anterior tooth root morphology and shows that root length alone should not be sufficient for taxonomic diagnosis. The frequent presence of hypercementosis and its non-homogeneous distribution around the root apex in Neanderthal anterior teeth could reflect the loading regime exerted on the front teeth, likely used as a third hand.

Anterior Dental Loading and Root Morphology in Neanderthals

ACKNOWLEDGEMENTS

I express my sincere gratitude to Professor Jean-Jacques Hublin for accepting my application as a PhD student in the Department of Human Evolution at the Max Planck Institute for Evolutionary Anthropology, Leipzig, Germany. This provided me with a unique opportunity to learn to do research in an international context, to improve my English and my German, to get to know high level researchers from the many fields that represent the pluridisciplinary studies of Human Evolution. I have been lucky enough to take part in two scanning trips (in France and in Israel) with the two portable micro-CT scanners of the Max Planck. I had the opportunity to learn to operate one of them myself. The large collection of micro-CT data available at the MPI has enabled me to study large series of Neanderthal and early modern human fossils. Lastly, I sincerely enjoyed discussing my results with Professor Hublin, and sharing his enthusiasm and his knowledge. I also acknowledge the Max Planck Gesellschaft for funding this research.

I am grateful to Professor José Braga who encouraged me to apply for the PhD position at the Max Planck Institute. This has given me the opportunity to work in an international environment, with facilities which are unique and scarcely accessible for PhD work.

I thank Dr. Kornelius Kupczik for providing guidance and extensive comments and feedback for the two peer-reviewed manuscripts that form the core of this Ph.D. thesis. Moreover, he trained me to write my first abstracts and build my first posters and presentations.

I am sincerely thankful to Dr Philipp Gunz for the support and advice that he provided me during the last part of my thesis. I have enjoyed collaborating with him on the shape studies and following his advice and experience regarding scientific writing. He also made the scanning trip to Israel possible, which considerably enriched my thesis samples.

I want to thank Rico Tilgner for the many many times that he has helped me (always in a good mood and with patience!) with image processing issues, and especially for his code based on the Watershed. Thank you also to Andreas Winzer for the micro-CT scanning of many specimens of my thesis, and for his help with scanning

issues; and the trip to Les Eyzies will remain a good memory of a team work! My thanks go also to Patrick Schönfeld for his collaboration during the scanning trip in Israel. Thanks to Heiko Temming for training me to scan with the Skyscan micro-CT scanner of the Department of Human Evolution (MPI). I am far from forgetting the many long meetings about the P folders, the workflow for data processing and the database…! Thank you to Dennis Reinhardt for IT support.

I am thankful to Ms. Silke Streiber, Cornelia Schicke and Diana Carstens for their kind help with the diverse administrative issues during the whole time of my thesis at the Max Planck Institute. In particular, Silke and Conny have been of tremendous help for various aspects of the PhD and of life in Leipzig. Always available and ready to help, their good mood, their friendship and their efficiency have been really significant to me! Vielen Dank!

I am grateful to all the curators and people that granted or facilitated me (directly or indirectly) the access to fossil and modern specimens for this research.

Particular thanks go to Dr. Bence Viola for providing access to unpublished fossil dental material from Chagyrskaya and for allowing me to include these specimens in my thesis sample, as well as for helpful discussions in general.

Many thanks to Dr. Adam Sylvester for discussions about the PhD in general, and also for writing the R code for the computation of the surface area in the estimation of the missing root portion.

I also appreciate the significant help and support provided by Roger Mundry for getting me started with running statistical tests with R. Roger helped me patiently to improve some of my code. Many thanks for this!

Thank you to Alyson Reid for proofreading the English of my papers and of my thesis.

I am also obliged to the MPI library staff for providing me with bibliographical references with great efficiency, in particular to Ms. Lisa Kaufmann, who has been very helpful at the end of my thesis!

I would like to acknowledge Dr. David Begun, editor of the *Journal of Human Evolution*, and the five reviewers that have provided insightful comments and

suggestions on my two manuscripts. Their remarks have significantly improved the quality of the papers of my thesis.

I thank the Dental Group of the Max Planck Institute for diverse discussions and advice on my work, and also for some of the people concerned, for scanning teeth that have been included in my thesis sample: Dr. Robin Feeney, Dr. Tanya Smith, Dr. Matthew Skinner, Dr. Anthony Olejniczak, Dr. Kornelius Kupczik and Collin Moore.

I have appreciated working in the Department of Human Evolution, and first, I thank my office mates for a friendly working atmosphere: Nicolas Zwyns, Domingo Carlos Salazar García, Kate Britton, Fei Peng and Simon Neubauer. My best wishes to my MPI colleagues and friends: Christine Verna, Meir Barak, Bence Viola, Enza Spinapolice, Tracy Kivell, Marcello Mannino, Sireen El Zaatari, Collin Moore, Andre Strauss, Amanda Henry, Shannon McPherron, Fred Spoor, Philipp Nigst, Daniel Richter, Michael Richards, Benjamin Fuller, Tsenka Tsanova, Joseba Rios Garaizar, Claire Letourneux, Huynh Nhu Nguyen, Maura Pelligrini, Marie Soressi, Morgan Roussel, Caroline Souday, Nandini Singh, Heike Scherf, Olaf Nehlich, Sarah Freidline, Sahra Talamo, Anja Gumprich, Friederike Kachel, Melanie Bäuchle, Marjolein Bosch, Viktoria Oelze, Ying Ma, Yi Guo, Liu Huan, Tamara Dogandzic, Dawit Desta, Alexander Stößel and Uta Schwarz.

My thesis would not have been exactly the same without the eruption of the Eyjafjöll volcano, in southern Iceland in April 2010, while we were at the AAPA meeting in Albuquerque. I thank Ben Fuller and his family for their warm welcome during this amazing road trip to California with Ben, Marcello, Domingo and Heike! An unforgettable, incredible and relaxing time!

I would like to express my deepest appreciation to Dr. Paul Tafforeau and to Dr. Tanya Smith for giving me the great opportunity to join their project, between the ESRF (Beamline ID 19, European Synchrotron Radiation Facility, Grenoble, France) and Harvard University, on the dental enamel microstructure in hominids. I enjoy learning and benefitting from their expertise in dental studies and in X-Ray imaging. I am particularly grateful to Paul, for his understanding at the time when I was working both on the completion of my PhD and starting as a Junior Scientist. His kindness and his availability for discussions and advice have been crucial! In addition, I am very pleased that he accepted to take part in my thesis committee. I am also very grateful to Paul,

Claudia, Hélio and Sélène for their kindness and their warm welcome! I also thank my colleagues from ID 19 for their support: Anne Bonnin, Jean-David Moreau, Carmen Soriano, Bernhard Hesse, Martin Kundrat (for his encouragement!), Julio Cesar da Silva, Pierre Jean Gouttenoire, Pei Dong, Alexander Rack, Lukas Helfen, Elodie Boller, Cécile Olivier and Françoise Peyrin.

This thesis is for me the opportunity to thank Professor Yves Coppens, because he made me want to study human evolution. As early as my childhood, I enjoyed listening to his radio broadcasts, where he brought his knowledge and experience within my reach. I recognize his work of scientific popularization (which is not always appreciated in the scientific community), but which raised the interest of the general public in the study of human evolution and research in general.

I express my gratitude to Dr. Jean-Laurent Monnier (University of Rennes 1, France), who has been advising, supporting and encouraging me, for over a decade, about the orientation of my studies. His enthusiasm for archeology and for research in general has encouraged me to follow my dream to dedicate my studies to human evolution. I thank him also for sharing his experience and for his friendship.

Maria, Volker and Christiane Braütigam have been my ‘German family’, here in Leipzig. I am eternally grateful to them for their kindness, their love and practice of baroque music (Leipzig, the city of Bach). Thank you also for integrating me into the ‘German life’ and sharing nice moments with me: Volker, I will always remember the orchid hunting in the Erzgebirge! I have made significant progress in German thanks to their patience when speaking with me and correcting me during our very stimulating discussions. My friendly gratitude goes to Maria for her precious help, and for her consistent support of my thesis as well! Herzlichen Dank!

Last but not least, I sincerely thank my parents, Marie-Lise and Christian, as well as my little sister Floriane. They have always been present for me to cheer me up when the task sounded impossible to achieve, and this happened quite a few times! They always succeeded in convincing me to keep on walking and I wish to dedicate this work to them! My Mother, in particular, deserves this thesis as much as I do, for her absolutely unfailing patience, understanding, and affection! In addition, I acknowledge my grandparents, who got me interested very early in learning and in what I would call the Natural Sciences.

TABLE OF CONTENTS

FIGURES

- Part 1 -

- Part 2 -

TABLES

- Part 1 -

- Part 2 -

GENERAL INTRODUCTION

Based on skeletal and dental remains, Neanderthals are known to have occupied the Eurasian continent until ca. 30 ky ago. Morphological evidence clearly distinguishes them from modern humans (e.g., Vandermeersch, 1991). However, both groups sometimes occupied the same areas relatively closely in time and it becomes challenging to ascertain the taxonomical status of some fragmentary human remains (e.g., Bailey and Hublin, 2006). Furthermore, gene flow between groups, i.e. hybridization, cannot be discounted by the structure and the history of the Neanderthal and modern human genomes (Green et al, 2010) and recent analyses of ancient DNA have revealed that the modern human genome may have received a contribution of approximately 2.5% of Neanderthal DNA (Reich et al., 2010). It has been argued that some specimens present an ambiguous morphology and cannot be clearly attributed to Neanderthals or to modern humans (e.g., Hershkovitz et al., 2011; Hublin, 1998; Krause et al., 2007; Quam and Smith, 1998; Schwartz and Tattersall, 2000).

Teeth are the most commonly found hominid remains in sites, since they are the best preserved parts of the skeleton during the fossilization process, due to their high degree of mineralization (96% of calcium hydroxyapatite). The anterior Neanderthal teeth are generally described as large and robust, showing a distinctive combination of features (shoveling, lingual tubercle) that are seen much more frequently than in modern humans (e.g., Smith and Paquette, 1989). Morphological studies have focused on the metric and non-metric features (such as shoveling, marginal ridges and lingual tubercle) of the dental crown (e.g.: Tillier et al, 1989). Nonetheless, these types of criteria are of limited interest when dealing with heavily worn or taphonomically damaged crowns. A lot of dental remains are not found with associated jaws or craniofacial skeletal elements that would provide further morphological arguments for taxonomical diagnosis. This is especially the case for the anterior teeth (incisors and canines), which easily fall from jaws since they are single-rooted. Isolated and damaged teeth can also be found out of any clear stratigraphic context (e.g., Chech et al., 2003). Attributing these dental remains confidently to one taxonomic group or another is therefore sometimes problematic. In this situation, tooth root morphology may represent a valuable source of information. Root morphology is also essential to analyze from a

functional point of view and considering the differences in masticatory apparatus morphology between Neanderthals and modern humans, anterior teeth root morphology is of obvious interest.

Some scholars have already observed that the Neanderthal anterior tooth roots are markedly longer and more robust than those of modern humans (e.g., Koby, 1956; Trinkaus et al., 2000a). However, most of the time, these observations remain qualitative. To date, this statement is supported by only one quantitative study that compared root lengths in Neanderthals and Upper Paleolithic humans (Bailey, 2005). In this study only one linear measurement made with a caliper was taken into consideration and the analysis involved limited samples of fossils.

In this thesis, we intend to test whether Bailey's conclusions about root length are confirmed with larger samples, and can be extended to other root dimensions (linear, surface and volumetric measurements, as well as root shape).

Documenting the variability in anterior tooth root morphology will assess to what extent Neanderthals, early and recent modern humans can be distinguished. This study will involve a larger sample of Neanderthals, early modern humans, and recent modern humans. Our fossil samples should cover a larger geographical area and a broader chronological period to address the question of the polarity of the anterior tooth root morphology. Do modern humans display derived conditions in having presumably short roots? Are the large roots of Neanderthals derived? Or alternatively, could these large roots be the retention of an ancestral morphology?

It has been hypothesized that the overall larger teeth in Neanderthals could be linked with their overall larger dimensions (Trinkaus, 1978; Bailey, 2005). However, studies on recent humans have yielded conflicting results (Anderson et al., 1977 *contra* e.g., Henderson and Corruccini, 1976; Perzigian, 1981). Therefore comes the question whether longer roots in Neanderthals could result from their overall larger facial size. Is the anterior root size correlated with symphyseal size? Or with the overall mandibular size? We need to test whether long roots in Neanderthals could be a by-product of their jaw size.

Crèvecoeur and Trinkaus (2004) already noticed that Neanderthal and modern humans do not differ significantly in terms of symphyseal height and width. Then

considering the dental development and the difference in size of the anterior tooth germs between Neanderthals and recent modern humans, raises the question of how to accommodate the larger Neanderthal anterior tooth germs in a symphysis of similar dimensions to modern humans? Are teeth governing the growth of the mandible? Do the mandible and the space available in the jaw influence the dental development? (e.g., Dean and Beynon, 1991).

Aside from the taxonomic and developmental aspects of anterior root morphology, the functional significance of this morphology in the anterior tooth root of Neanderthals is still poorly investigated. Several hypotheses have attempted to interpret these large teeth and the cranio-facial architecture in Neanderthals. For some scholars, the establishment of part of this cranio-facial morphology could result from genetic drift without having much adaptive significance (Hublin, 1998; Weaver et al., 2007; Rae et al., 2011). Others (Couture, 1993) invoke morphogenetic processes as main driving factors. Purely adaptive hypotheses propose the adaptations to dry and cold climate (e.g., Coon, 1962; Franciscus and Trinkaus, 1988; Churchill, 1998). Finally, a purely functional hypothesis – the 'anterior dental loading hypothesis' – provides an interpretation for both craniofacial and dental morphology. This hypothesis states that Neanderthals would have used their anterior dentition as a tool, or as a third hand (e.g., Demes, 1987; Trinkaus, 1987; Smith and Paquette, 1989). This would be to perform para-masticatory (e.g.: cutting a piece of meat held between one hand and the front teeth while the other hand manipulates a stone tool), or non-masticatory activities (e.g.: tanning a piece of animal skin held between one hand and the front teeth). Recent microwear studies (Krueger, 2011) confirm that those activities would have been performed by Neanderthals, and not by early modern humans. This thesis aims to investigate whether differences between Neanderthal and modern humans in root size and shape could bring support to this hypothesis. Can we identify features in root morphology that could directly result from this supposed use of the anterior dentition as a third hand?

In this work, we intend to test whether Bailey's conclusions about root length are confirmed with larger samples, and can be extended to other root dimensions (linear, surface and volumetric measurements, as well as root shape). We will assess the quality of the separation between Neanderthals, early and recent modern humans. Furthermore, we will address the questions of the polarity of the root characters in the human lineage,

of the relation between root size and jaw size, and of the functional significance of the root morphology observed in Neanderthals. The variability in anterior tooth root morphology will be documented using micro-computed tomography, linear, surface and volumetric measurements, as well as geometric morphometrics techniques. This will involve a larger sample of Neanderthals, early modern humans, and recent modern humans. Our fossil samples cover a large geographical area (from Spain to Siberia, and from Germany to Israel and Morocco), and the modern samples involve many ethnicities from Africa, Eurasia and North America. All the samples span over a broad chronological period (from MIS 15 to MIS 1), including a few specimens from the lower and middle Paleolithic. We will finally discuss the functional significance of the anterior tooth root morphology in Neanderthals in the context of the 'anterior dental loading hypothesis'.

PART 1

Long Anterior Mandibular Tooth Roots in Neanderthals Are Not the Result of their Large Jaws

This part was published as:

Le Cabec A., et al., 2012. Long anterior mandibular tooth roots in Neanderthals are not the result of their large jaws, *Journal of Human Evolution*, 63, pp. 667-681.

http://dx.doi.org/10.1016/j.jhevol.2012.07.003

Received 26 October 2011; Accepted 8 July 2012; Available online 21 September 2012.

AUTHORS

Adeline Le Cabec [a,b], Kornelius Kupczik [a,c], Philipp Gunz [a], José Braga [b], Jean-Jacques Hublin [a].

AUTHOR'S AFFILIATIONS

[a] Department of Human Evolution, Max Planck Institute for Evolutionary Anthropology, Deutscher Platz 6, 04103 Leipzig, Germany

[b] UMR 5288 CNRS, Anthropobiologie et Imagerie Anatomique, 37 Allées Jules Guesde, 31000 Toulouse, France

[c] Institut für Spezielle Zoologie und Evolutionsbiologie, Friedrich-Schiller-Universität Jena, Erbertstrasse 1, 07743 Jena, Germany

AUTHOR CONTRIBUTIONS

ALC, KK, PG, JB and JJH designed the research. ALC processed the micro-CT data, segmented and generated the 3D models of the teeth, generated the surface models of the mandibles, collected the landmarks and semi-landmarks data, took the linear, surface and volumetric measurements, performed statistical analyses and wrote the paper. PG performed the geometric morphometrics analyses for the shape study, and estimated missing data for the incomplete mandibles. JJH provided the micro-CT and image processing facilities and the possibility for data acquisition. PG, KK and JJH provided comments on the paper and helped to improve the writing.

ABSTRACT

Tooth root length has been shown to taxonomically distinguish Neanderthals from modern humans. However, this may result from differences in jaw size between both taxa, although most previous studies have revealed a very low or non-existent correlation between tooth size and jaw size in recent modern humans. We therefore investigated, within a broader taxonomical frame, to what extent measurements on the anterior tooth roots and the symphyseal region covary.

Our samples comprise permanent mandibular incisors and canines from Mauer, Neanderthals, and extant and fossil modern humans *sensu lato*. Using micro-computed tomography, we took linear and cross-sectional surface area measurements of the roots and the symphyseal region and calculated the root volume. We also measured 3D landmarks to quantify the overall size of the mandible using centroid size. Furthermore, we analyzed the relationship between root size and symphyseal shape, based on Procrustes shape variables of semi-landmarks along the symphyseal outline.

Our results show that Neanderthals have significantly larger anterior tooth roots than recent modern humans in terms of root length, mid-sagittal surface area and volume, even after correction for mandibular size. In contrast, symphyseal height and width do not differ significantly between both taxa, whereas, without scaling, the mid-sagittal symphyseal surface area and the centroid size of the mandible do differ. Importantly, no significant correlation was found between any of the root and symphyseal measurements after correction for overall mandibular size. The shape analyses revealed that Neanderthals have a vertical symphyseal profile with an evenly-thick symphysis, whereas recent modern humans display an unevenly-thick symphysis, comprising a pronounced *incurvatio mandibularis* and a bony chin. These results suggest a negative evolutionary allometry for the recent modern human anterior root size. Therefore, root length and other root dimensions can be considered taxonomically relevant for distinguishing Neanderthals from modern humans.

KEYWORDS

Incisor, Canine, Mandibular symphysis, Micro-CT, Allometry, Pleistocene *Homo*.

INTRODUCTION

Neanderthal tooth roots are often described as strikingly longer than those of recent modern humans, especially in the anterior dentition (e.g., Patte, 1962; Smith, 1976a; Wolpoff, 1979; Paquette, 1985; Trinkaus, 2004). Anterior tooth root lengths of Upper Paleolithic humans fall within the range of the geographically diverse recent modern human samples mentioned in Bailey (2005). Therefore, root length has been proposed to taxonomically distinguish Neanderthals from modern humans (Paquette, 1985; Smith and Paquette, 1989; Bailey, 2005). It has been suggested that longer tooth roots in Neanderthals might be a by-product of their larger jaws or of their larger overall body mass, in comparison with modern humans (Trinkaus, 1978). Furthermore, Bailey (2005) hypothesized that root length and alveolar height might be strongly correlated. However, the hypothesis of a correlation between tooth size and jaw size in Neanderthals has been based on recent modern human studies (e.g., Smith et al., 1986, 1989). In the present study, we investigated whether longer anterior tooth roots in Neanderthals are a by-product of their mandibular size.

Empirical studies report surprisingly low correlations between measurements of the tooth crown (bucco-lingual and mesio-distal crown diameters, as well as height of the tooth crown) and the mandibular corpus in primates (Plavcan and Daegling, 2006). More specifically, focusing on modern humans, Anderson et al. (1977) have found correlations between body weight and the size of the anterior mandibular dentition (mesio-distal crown diameter). Other modern human studies have looked for correlations between tooth size (crown diameters) and diverse proxies for body size, such as stature (Garn and Lewis, 1958; Filipsson and Goldson, 1963; Wolpoff, 1971; Henderson and Corruccini, 1976), cranial measurements (Filipsson and Goldson, 1963; Kieser and Groeneveld, 1988; Plavcan and Daegling, 2006), femur length (Perzigian, 1981), and jaw size (Smith et al., 1986, 1989, one of the rare studies involving root length). Ozaki et al. (1987, 1988) have predicted that total tooth length and root length would be a reflection of stature. These studies reveal consistently a low correlation or an absence of correlation between ‘tooth size’ and estimates for body size. In most of these cases, tooth size is restricted to the size of the crown (diameter). However, there is little evidence for a strong correlation between crown size and root size in postcanine teeth (Smith et al., 1986, 1989), and there has been even less research done on the anterior dentition. Therefore, in the context of testing how useful root length is as a taxonomic

character to distinguish Neanderthals from modern humans, it appears that the most relevant approach is to investigate whether anterior tooth root size and symphyseal and mandibular sizes are significantly correlated in modern humans and in Neanderthals. We expand the study of root size to include cross-sectional surface and volume measurements.

Considering that Neanderthals are described as having large mandibles and anterior teeth, one might expect to observe a positive correlation between tooth root size and symphyseal/mandibular size in this taxon. In the case where no correlation could be found, we expect to find that root length could still be validated to distinguish Neanderthals from modern humans if the two distributions in root length are separated enough. The questions remain of how to accommodate large tooth roots in jaws that tend to be smaller than expected. Only a change in shape would enable the distribution of bone differentially within the same dimensions. It has been shown that Neanderthals and modern humans differ in symphyseal shape. Neanderthals tend to have a receding symphysis, whereas modern humans typically have a fully developed chin (e.g., Nicholson and Harvati, 2006; Mounier et al., 2009). We investigate whether the noticed differences in symphyseal shape are related to the observed differences in root length in Neanderthals and recent modern humans.

To test whether longer anterior roots in Neanderthals are a by-product of jaw size, we used high-resolution micro-computed tomography (micro-CT) to investigate the correlation between root size of the mandibular permanent incisors and canines and overall mandibular and symphyseal size in Neanderthals and modern humans. In addition, we analyzed the relationship between symphyseal shape and anterior tooth root size.

MATERIALS AND METHODS

SAMPLE

The fossil sample includes 13 Neanderthal mandibles, including eight adults and five subadults (see Tables 1 and 2). The Middle Pleistocene Mauer mandible (Schoetensack, 1908; Wagner et al., 2010) is included in this study as an attempt

Table 1. Samples of permanent teeth.

Taxon	Specimen	Chronological attribution
Homo heidelbergensis	Mauer	MIS 15 (609 ± 40 ka, Wagner et al., 2010).
Neanderthals	Ehringsdorf F 09	MIS 7 (~230 ka, Blackwell and Schwarcz, 1986)
	Ehringsdorf G1 10	
	Krp 55 (Mandible E)	MIS 5 (130 ± 10 ka, Rink et al., 1995)
	Krp 58 (Mandible H)	
	Krp 59 (Mandible J)	
	Krp 53 (Mandible C; I_2)	
	Krp 54 (Mandible D; I_2 and C,)	
	Regourdou 1	MIS 5 (Maureille and Tillier, 2008; Turq et al., 2008)
	Kebara 2	MIS 4 (60 ka, Valladas et al., 1987)
	Spy 1	MIS 4-3 (~60ka, cited in Mounier et al., 2009)
	Amud 1	MIS 3 (41,5 ka BP, Delson et al., 2000)
	Le Moustier 1	MIS 3 (40 ka, Valladas et al., 1986)
	Saint-Césaire	MIS 3 (36.3 ± 2.7 ka, Mercier et al., 1991)
Early modern humans	Qafzeh 9	MIS 5 (Grün and Stringer, 1991) (90-130ka, Mounier et al., 2009)
	Temara (Grotte des Contrebandiers, Aterian)	MIS 5 (between 107 ± 4 and 96 ± 4 ka, Jacobs et al., 2011)
Upper Paleolithic/Mesolithic modern humans	Oberkassel D999	MIS 2 (12 ka cal. BC, Street et al., 2006)
	Combe-Capelle	MIS 1 (7,596–7,577 ka cal. BC, Hoffmann et al., 2011)
Recent modern humans (ULAC)	1 (M, Germany); 13 (F, Germany), 58 (M, Norway); 66 (F, Norway/Sweden); 74, 151, 171 and 179 (M, Italy/Etruscan); 119 (F, Italy/Etruscan); 259 (M, Algeria); 522, 536, 566 and 607 (M, Egypt) ; 659 (F, Egypt) ; 752 (M, Sudan) ; 799-27 (U, Black American) ; 799-28 (U,U) ; 790, 797 and 806 (M, Afro-Americans/New Orleans) ; 801 (F, Afro-American/New Orleans).	MIS 1

MIS = Marine Isotopic Stage. For the recent modern humans (ULAC = University Leipzig Anatomical Collection), the catalog specimen number is followed in parentheses by sex estimation based on anthropological criteria (M = male, F = female, U = unknown) and geographical origin (U = unknown).
ka = thousands of years ago; BP = before present; cal. BP = calibrated years before present.

Table 2. Dental developmental stage of the Neanderthal juveniles using recent modern human standards.

Specimen	Dental stage	Dental age at death derived from modern human standards	Reference
Krapina 53 (Krp 53)	Right first and second permanent molars in functional occlusion (wear facets). Third permanent molar still in its crypt with a fully formed crown and no root formed yet. Right deciduous second molar is still present in the jaw.	11 years old	Wolpoff, 1979
Krapina 54 (Krp 54)	Third molars not erupted	15 years old	Wolpoff, 1979
Krapina 55 (Krp 55)	Third molars not erupted, but their roots estimated to be "partially complete" according to the size of its crypt	15 years old	Wolpoff, 1979
Ehringsdorf G1	The left M_3 has pierced the bony crypt.	-	Vleck, 1993
Le Moustier 1	Both M_3 erupting but not fully occluded yet (no wear facets).	15.5 ± 1.25 years (real age at 11.6–12.1 years, Smith et al, 2010)	Bilsborough and Thompson, 2005

to understand the ancestral condition in terms of the tooth size-jaw size relationship. In our study, early modern humans contemporaneous with some of our Neanderthals are represented by Qafzeh 9 (Vandermeersch, 1981) and Temara (Grotte des Contrebandiers; Vallois and Roche, 1958). The Magdalenian individual Oberkassel D999 (Henke, 1986) and the Mesolithic Combe-Capelle (Hoffmann et al., 2011) are also included for comparative purposes. Our modern comparative sample includes 22 recent modern human mandibles from the anatomical collection housed at the University of Leipzig, Germany. Information about sex, ethnicity and age estimated from dental and skeletal maturation is based on the records of the collection. For some specimens, calendar age was provided. Sex attribution of most crania was based on anthropological criteria, and may therefore not be fully reliable. While we labeled all specimens for which sex information was available as males and females in our figures, all statistical analyses were conducted on pooled-sex samples to avoid biasing our results. Although sex attribution is not reliable in fossils, we wish to report this information to assess if sexual dimorphism can contribute to the observed variability in root and jaw size within the recent modern humans. The individuals selected also represent various ethnicities (see Table 1). Only one extant individual (Hs 659) is a subadult with erupting M3s (bony crypt pierced by the tooth crown). Specimens were selected based on the state of preservation of the symphyseal region and on the formation of the roots of the incisors and canines (fully closed root apices). We also

avoided studying specimens showing any pathological conditions (e.g., visible osteological deformation of the mandibular symphysis or root resorption). Only adults (third molars in functional occlusion) and subadults (third molars not fully erupted, but second molar in functional occlusion) were selected to minimize the impact of major size and shape changes occurring earlier in jaw ontogeny.

MICRO-CT IMAGE ACQUISITION AND 3D MODEL GENERATION

The mandibles were scanned at the Max Planck Institute for Evolutionary Anthropology (Leipzig, Germany) on a BIR ARCTIS 225/300 industrial micro-CT scanner. Two types of acquisition were performed for most specimens (isotropic voxel-size ranging from 25.5 to 148.1 µm). An overview scan at a relatively low resolution allowed imaging of the complete mandible, while a high resolution scan focusing on the dentition was done for a more accurate quantification of dental tissue surface areas and volumes. Data for Spy 1 were produced on a Siemens Somatom 64 CT-scanner with an isometric pixel size of 0.299 mm and a slice thickness of 0.1 mm (NESPOS). The dental tissues (enamel, dentine, pulp) were segmented on the micro-CT data to obtain 3D models of the teeth. Each model was virtually cut at the cervical plane to isolate the crown and the root. Segmentation and 3D model processing protocols are provided in SOM 1. Fig. 1 illustrates the root and mandibular measurements taken.

ANTERIOR TOOTH ROOT SIZE

Root size was quantified by measuring the root length (RL) on the 3D models of the individual roots as the linear distance between the root apex and the center of the cervical plane of the tooth (using the ‘3D measurement’ tool in Avizo 6.2, Fig. 1B). Furthermore, the cross-sectional surface area of the root (CSRA) was computed from a mid-sagittal labio-lingually oriented section of the root through a plane defined by the root apex, and the labial and the lingual points of greatest curvature of the cemento-enamel junction (SurfaceCut module in Avizo; Fig. 1C). Root volume (RV) was obtained by adding up the root pulp volume and the volume of radicular dentine (Fig. 1D).

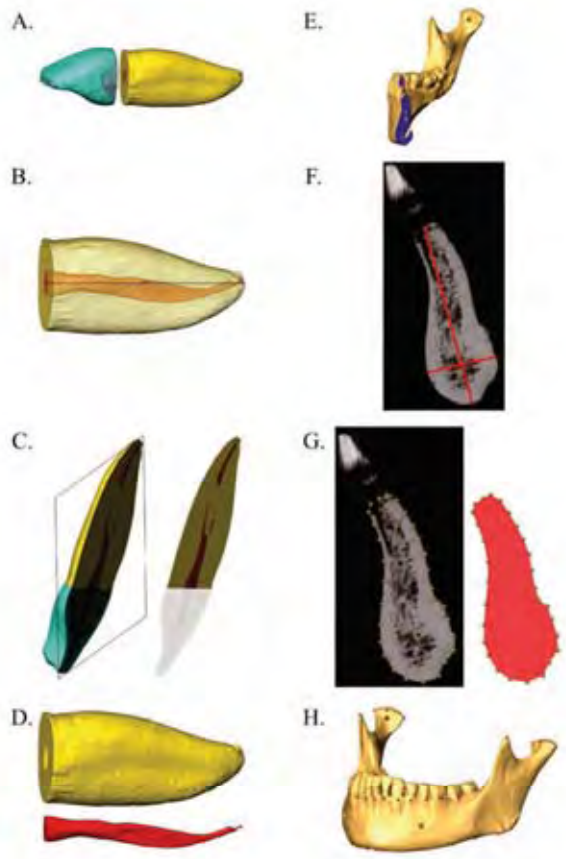

Figure 1. Measurements taken on the 3D models of the anterior tooth roots (A): root length (B), mid-sagittal surface area (C) and volume (D); and on the surface models of the mandibles (E): symphyseal height and width (F), mid-sagittal surface area (G) and estimation of the overall size by computing the centroid size from 3D landmarks (H).

SYMPHYSEAL AND OVERALL MANDIBULAR SIZE

Symphyseal size was estimated on a cross-section of the symphysis using a plane defined by infradentale, gnathion and genion (see Figs. 1E and 2). On this section, we measured the symphyseal height (SH) from infradentale to the lowest point of the symphyseal contour, and the symphyseal width (SW) as the largest dimension perpendicular to SH (Fig. 1F).

Three-dimensional curve semi-landmarks were collected along the outline of this mid-sagittal cross-section of the symphysis. The cross-sectional surface area of the symphysis (CSASy) was computed from the 2D surface enclosed by the semi-landmarks and generated by a Delaunay triangulation (De Berg et al., 2008; Delaunay 2D module in Avizo 6.2, see Fig. 1G and SOM 2 for details). In the event of damage to

the specimen, the missing parts of the symphyseal outline were visually estimated on the mid-sagittal cross-section by checking the portions of the symphysis through the micro-CT slices of the anterior portion of the mandibular corpus.

For each specimen, we computed its centroid size (CS) as an overall and absolute size measures, based on three-dimensional landmark coordinates (Table 3, Figs. 1H and 2, and see SOM 3 for details).

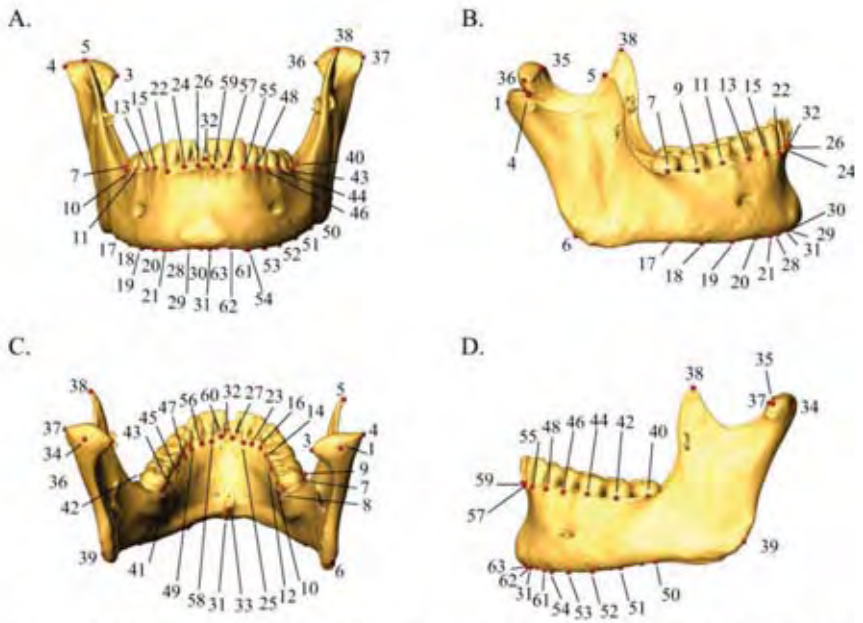

Figure 2. Labial (A), lateral right (B), lingual (C) and lateral left (D) views of the ULAC 58 modern human mandible showing the landmarks used for the computation of the centroid size. The landmarks are numbered and described in Table 3.

CORRELATION BETWEEN ROOT SIZE AND MANDIBULAR SIZE

The possible correlation between root size and symphysis/mandible size was tested by comparing the linear, surface and three-dimensional measurements of both anatomical entities, that is, root length with symphyseal height, cross-sectional area of the root with the cross-sectional area of the symphysis, root volume with the centroid size of the mandible (which gives an estimate for the overall size of the mandible) and, finally, root length with the mandibular centroid size. Correlations were computed separately within Neanderthals and recent modern humans to test for an intraspecific pattern, and with both samples pooled to look for an interspecific correlation. In addition, we computed these correlations after correction for centroid size. In the case of the interspecific correlation, the recent modern humans were scaled to the Neanderthal

size (using the ratio of the means of the centroid sizes of the late juveniles and adults of each taxon, see formula in Tables 5a and 5b), whereas each individual was scaled by its own centroid size when looking for an intraspecific correlation between root size and jaw size (each investigated variable was divided by the individual's centroid size).

SHAPE ANALYSIS OF THE CONTOUR OF THE SYMPHYSEAL CROSS-SECTION

Another set of 3D curve semi-landmarks was measured along the outline of the mid-sagittal section of the symphysis to quantify the shape variation using geometric morphometrics (Bookstein, 1991; Mitteroecker and Gunz, 2009). To provide the same number of homologous points for each specimen, these data points were resampled (to get 100 semi-landmarks per cross-section) and allowed to slide along the curve to minimize the bending energy between each specimen and the Procrustes average shape (Bookstein, 1997; Gunz et al., 2005). Datasets were then superimposed during a Generalized Procrustes Analysis, which means that all of the sets were translated, rotated and rescaled (Rohlf and Slice, 1990). A principal component analysis was then performed on the Procrustes coordinates of the specimens (i.e., in shape space). To illustrate the shape and size differences, we multiplied the Procrustes shape coordinates by the respective centroid size.

We used a permutation test (Good, 2000) based on Procrustes distance between the group means (Mitteroecker and Gunz, 2009) to test for significant shape differences between recent modern humans and Neanderthals.

STATISTICAL ANALYSES

Descriptive statistics are provided for all investigated taxa and variables. Since Neanderthals and recent modern humans are the largest samples, they were subjected to three kinds of statistical analyses. We emphasize that since we expected to find bigger roots for Neanderthals following the observations of Bailey (2005) on root length, we will use the term 'root size' generally to refer to root length, surface cross-sectional surface area, and volume. In other words, 'larger root' is used when all three dimensions

Table 3. Landmarks for overall size estimation of the mandible (centroid size).

	Bilateral landmarks		
	Right side	Left side	
Posterior condylion	1	34	Most posterior point of the condylion.
Anterior condylion	2	35	Most anterior point of the condylion.
Medial condylion	3	36	Most medial point of the condylion.
Lateral condylion	4	37	Most lateral point of the condylion.
Coronion	5	38	Tip of the coronoid process.
Gonion	6	39	Point on the mandibular angle which is directed most inferiorly, posteriorly, and laterally. Gonion is positioned at the highest point of the curvature.
LM3 lab.	7	40	Most superior point at the middle point of the labial side of the LM3 alveolar border.
LM3 ling.	8	41	Most superior point at the middle point of the lingual side of the LM3 alveolar border.
LM2 ling.	9	42	Most superior point at the middle point of the lingual side of the LM2 alveolar border.
LM2 lab.	10	43	Most superior point at the middle point of the labial side of the LM2 alveolar border.
LM1 lab.	11	44	Most superior point at the middle point of the labial side of the LM1 alveolar border.
LM1 ling.	12	45	Most superior point at the middle point of the lingual side of the LM1 alveolar border.
LP4 lab.	13	46	Most superior point at the middle point of the labial side of the LP4 alveolar border.
LP4 ling.	14	47	Most superior point at the middle point of the lingual side of the LP4 alveolar border.
LP3 lab.	15	48	Most superior point at the middle point of the labial side of the LP3 alveolar border.
LP3 ling.	16	49	Most superior point at the middle point of the lingual side of the LP3 alveolar border.
Bottom corpus LM3	17	50	Most inferior point of the inferior border of the mandibular body below LM3.
Bottom corpus LM2	18	51	Most inferior point of the inferior border of the mandibular body below LM2.
Bottom corpus LM1	19	52	Most inferior point of the inferior border of the mandibular body below LM1.
Bottom corpus LP4	20	53	Most inferior point of the inferior border of the mandibular body below LP4.

Table 3. *Continued.*

Bottom corpus LP3	21	54	Most inferior point of the inferior border of the mandibular body below LP3.
LC lab.	22	55	Most superior point at the middle point of the labial side of the LC alveolar border.
LC ling.	23	56	Most superior point at the middle point of the lingual side of the LC alveolar border.
LI2 lab.	24	57	Most superior point at the middle point of the labial side of the LI2 alveolar border.
LI2 ling.	25	58	Most superior point at the middle point of the lingual side of the LI2 alveolar border.
LI1 lab.	26	59	Most superior point at the middle point of the labial side of the LI1 alveolar border.
LI1 ling.	27	60	Most superior point at the middle point of the lingual side of the LI1 alveolar border.
Bottom corpus LC	28	61	Most inferior point of the inferior border of the mandibular body below LC.
Bottom corpus LI2	29	62	Most inferior point of the inferior border of the mandibular body below LI2.
Bottom corpus LI1	30	63	Most inferior point of the inferior border of the mandibular body below LI1.
			Mid-sagittal landmarks
Gnathion		31	Most anteroinferior point of mental symphysis (i.e. the lowest point on the inferior margin of the mandibular body in the mid-sagittal plane).
Infradentale		32	Highest point of the alveolar border between the lower central incisors.
Genion		33	Tip of the *spina mentalis*.

The landmark numbers are indicated on Fig. 2.

are considered, if not stated otherwise. As for the mandible and the symphysis, 'overall larger' will imply that the mandible/symphysis is larger for all three kinds of measurements (height and width of the symphysis, cross-sectional surface area of the symphysis, and centroid size of the mandible), and any other pattern will be specified. First, mandibular and root variables were compared between samples using the non-parametric Mann-Whitney U test (exact, two-tailed, $\alpha = 0.05$, U_{Min} reported) to test whether Neanderthals have significantly larger anterior tooth roots and/or a larger symphysis than modern humans. This was first performed with unscaled data, and then using the recent modern humans scaled to the Neanderthal size using the ratio of the means of the centroid sizes for each taxon (see above). Then, for each tooth type, we tested whether anterior tooth root size was correlated with jaw size, within recent modern humans and within Neanderthals, for the linear (RL versus SH), surface (CSRA versus CSASy) and 3D (RV versus CS) measurements using the Spearman rank order correlation test (exact, two-tailed, $\alpha = 0.05$, r_S reported, p values Bonferroni corrected). As explained above, we scaled the data to look for intra- and interspecific correlations.

Finally, and as described above, shape analyses were carried out on the semi-landmarks and landmarks datasets of the symphysis cross-sections, and of the overall mandible, respectively.

Statistical analyses and graphics were generated in R 2.12.1 (Calenge, 2006; Dray and Dufour, 2007; Peng et al., 2010; R Development Core Team, 2010; Hothorn and Hornik, 2011). Shape and form analyses, as well as the permutation tests, were performed in Mathematica (Wolfram, Inc.).

RESULTS

ANTERIOR TOOTH ROOT SIZE

Recent modern human males and females have anterior tooth roots of similar sizes (Figs. 3-5). Neanderthals have significantly absolutely larger mandibular incisor and canine roots than recent modern humans in terms of root length, surface area and volume ($p < 0.001$, Tables 4 and 5a). The separation is even much higher for the surface areas and volumes than for the root lengths (Figs. 3-5). This remains true even after correcting for mandible size (see Table 5a, results for scaled data). Figs. 3a-c highlights

the overlapping distribution of the two taxa in terms of root length. This is mainly due to the relatively shorter roots of Le Moustier 1 (Fig. 3) compared with most of the other Neanderthals. The separation between taxa is more clear-cut regarding the root volumes (Fig. 5) and even more so for the mid-sagittal cross-sectional surface area of the roots (Fig. 4), where little overlap is observed for the lateral incisor and the canine ($p \leq 0.01$; Tables 4 and 5a; Figs. 4a-c). For all root measurements, Mauer plots close to the Neanderthal mean (Figs. 3-5). Regarding the early modern humans, the root lengths of Qafzeh 9 fall in the upper range of the recent modern human variation (Fig. 3), while root volumes and cross-sectional surface areas overlap with those of Neanderthals and recent modern humans (for the canine), or fall within the lower range of the Neanderthal variation (for the incisors). The Aterian specimen, Temara, shows anterior tooth roots with cross-sectional surface areas and volumes falling in the upper end of the recent modern human range of variation. Temara's canine root length falls within the lower half of the modern human variation. Oberkassel D999's root lengths, cross-sectional surface areas, and volumes fall overall in the lower half the modern human range. The Mesolithic Combe-Capelle plots in the middle of the modern human variation for the root volumes and in its upper end for the root length and cross-sectional root surface areas.

SIZE OF THE SYMPHYSIS AND OVERALL SIZE OF THE MANDIBLE

Overall, Neanderthals do not differ from recent modern humans regarding symphyseal height and width, even after correction for overall mandibular size ($p > 0.05$; Tables 5b and 6; Figs. 3a-c). Recent modern human males have overall larger mandibles and a larger and more variable symphyseal height than females, while both sexes have a comparable range of root length (Fig. 3). Although the cross-sectional surface area of the symphysis is significantly larger in Neanderthals than in recent modern humans, both taxa do not differ after correction for overall mandibular size (Tables 5b and 6, Fig. 4). Male and female recent modern humans display no differences in the cross-sectional symphyseal area. The Neanderthal subadults cluster next to each other, in the lower end of the Neanderthal distribution. Mauer falls right in the middle of the Neanderthal distribution. Temara and Oberkassel fall within the recent modern human distribution. Combe-Capelle falls outside of the recent modern human distribution, having both larger symphyseal height and surface area for the size of its

Table 4. Descriptive statistics of the root variables.

			RL [mm]	CSRA [mm²]	RV [mm³]
H. heidelbergensis	Mauer (N=1)	I_1	16.5	102.6	292.7
		I_2	16.7	109.0	370.3
		C_1	20.8	141.0	565.9
Neanderthals	N=11	I_1	17.2 ± 2.5 [13.2-20.9]	107.9 ± 17.6 [81.7-132.9]	325.4 ± 59.2 [244.5-400.9]
	N=13	I_2	18.5 ± 2.0 [14.8-21.6]	121.5 ± 16.3 [86.2 -146.8]	402.0 ± 71.4 [281.2-507.6]
	N=12	C_1	21.1 ± 2.8 [17.2-25.6]	155.3 ± 28.5 [105.4-211.2]	630.2 ± 156.7 [339.5-902.3]
Fossil modern humans	Qafzeh 9 (N=1)	I_1	14.3	83.0	230.4
		I_2	16.2	97.1	296.0
		C_1	18.1	126.9	525.9
	Temara (N=1)	I_1	13.7	67.5	160.3
		I_2	14.0	79.3	211.2
		C_1	17.4	116.3	465.3
	Oberkassel D999 (N=1)	I_1	14.2	59.4	121.2
		I_2	16.2	67.4	149.2
		C_1	13.4	75.1	208.7
	Combe Capelle (N=1)	I_1	13.0	62.0	147.9
		I_2	15.5	80.2	194.2
		C_1	14.6	89.5	292.3
Recent modern humans	N=22	I_1	13.0 ± 1.6 [10.6-16.7]	60.4 ± 8.5 [45.3-77.3]	132.2 ± 23.1 [88.4-193.3]
		I_2	14.2 ± 1.7 [10.7-18.4]	71.0 ± 10.6 [49.4-92.2]	168.1 ± 34.4 [104.3-260.6]
		C_1	16.6 ± 1.8 [13.2-19.2]	98.6 ± 20.0 [67.7-139.0]	328.2 ± 95.5 [181.6-572.5]

N stands for sample size; mean ± standard deviation [minimum-maximum].

Table 5. Mann-Whitney U test results for comparison between recent modern humans and Neanderthals for the root variables (a) and for the mandibular variables (b).

(a)

Unscaled data		I_1 N_{Hn}=11 N_{Hs}=22	I_2 N_{Hn}=13 N_{Hs}=22	C, N_{Hn}=12 N_{Hs}=22
RL [mm]	U_{Min}	19	17	21
	p	***2.03e-05***	***1.54e-06***	***1.21e-05***
CSRA [mm²]	U_{Min}	0	2	11
	p	***1.03e-08***	***5.42e-09***	***7.11e-07***
RV [mm³]	U_{Min}	0	0	12
	p	***1.03e-08***	***1.35e-09***	***9.92e-07***

Scaled data		I_1 N_{Hn}=11 N_{Hs}=21	I_2 N_{Hn}=13 N_{Hs}=21	C, N_{Hn}=12 N_{Hs}=21
RL [mm]	U_{Min}	39	34	47
	p	***0.0017***	***1.07e-04***	***2.37e-03***
CSRA [mm²]	U_{Min}	6	10	39
	p	***4.65e-07***	***2.54e-07***	***6.88e-04***
RV [mm³]	U_{Min}	2	3	37
	p	***6.20e-08***	***1.19e-08***	***4.90e-04***

Table 5. *Continued.*

(b)

			Unscaled data	Scaled data
SH [mm]	N_{Hn}=13	U_{Min}	102	132
	N_{Hs}=22	*p*	*ns*	*ns*
SW [mm]	N_{Hn}=13	U_{Min}	142	80
	N_{Hs}=22	*p*	*ns*	*ns*
CSASy [mm²]	N_{Hn}=13	U_{Min}	68	127
	N_{Hs}=22	*p*	***0.01***	*ns*
CS	N_{Hn}=10	U_{Min}	99	102
	N_{Hs}=21	*p*	***0.00022***	*ns*

Minimal U values and p values (bolded when statistically significant) are reported. In the 'Scaled data' set, recent modern humans are scaled to the Neanderthals' size using the ratio of the means of the centroid sizes of each taxon, as follows:
mean(CS[modern humans])/mean(CS[Neanderthals]).
ns = for nonsignificant.

Table 6. Descriptive statistics of the mandibular variables.

		SH [mm]	SW [mm]	CSASy [mm²]	CS
H. heidelbergensis	Mauer (N=1)	31.5	15.6	451.0	408.5
Neanderthals	(N=13)	35.3 ± 5.6 [27.1-43.3]	15.2 ± 2.4 [12.7-22.1]	391.5 ± 106.4 [276.3-688.9]	393.8 ± 22.2 [360.7-420.2] (N=10)
Fossil modern humans	Qafzeh 9 (N=1)	38.6	13.8	417.4	380.2
	Temara (N=1)	31.8	12.1	285.2	396.3
	Oberkassel D999 (N=1)	31.1	14.3	269.5	350.2
	Combe Capelle (N=1)	37.2	20.3	420.2	355.9
Recent modern humans	N=22	32.7 ± 4.1 [26.9-42.4]	14.9 ± 1.9 [10.9-19.8]	315.5 ± 51.0 [205.8-419.3]	360.3 ± 17.9 [314.4-388.6] (N=21)

N = sample size; mean ± standard deviation [minimum-maximum].

(3a)

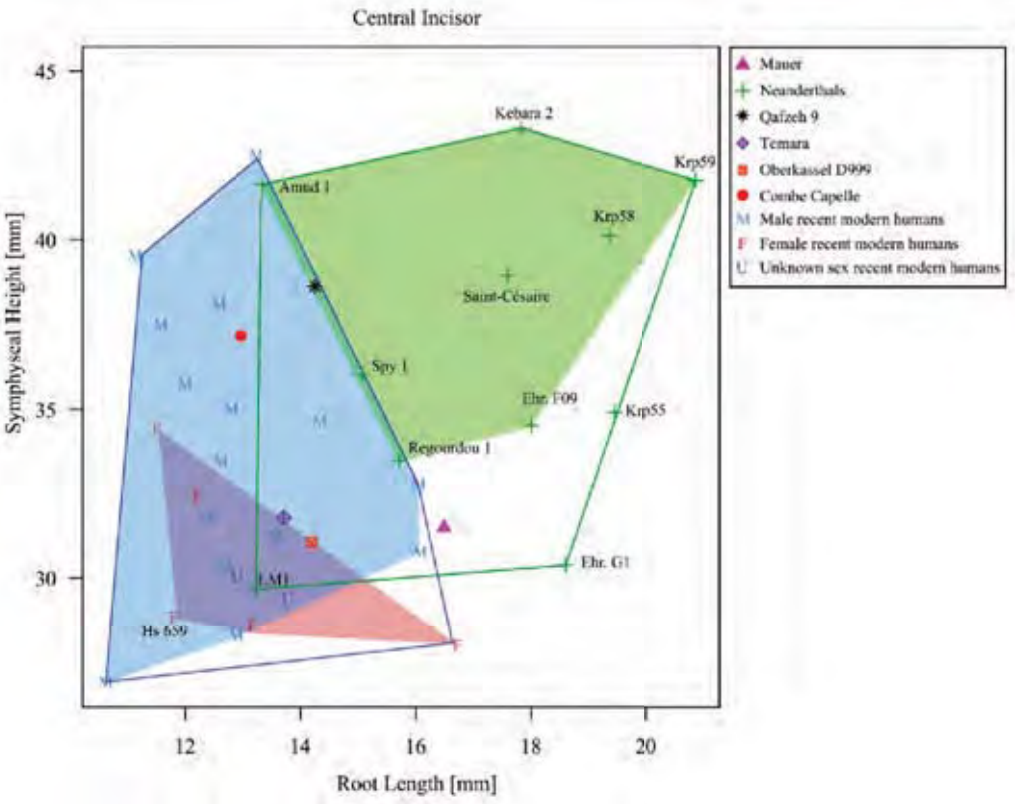
Central Incisor
Symphyseal Height [mm]
Root Length [mm]
Mauer
Neanderthals
Qafzeh 9
Temara
Oberkassel D999
Combe Capelle
Male recent modern humans
Female recent modern humans
Unknown sex recent modern humans
Kebara 2
Krp59
Amud 1
Krp58
Saint-Césaire
Spy 1
Ehr. F09
Krp55
Regourdou 1
Ehr. G1
LM1
Hs 659

(3b)

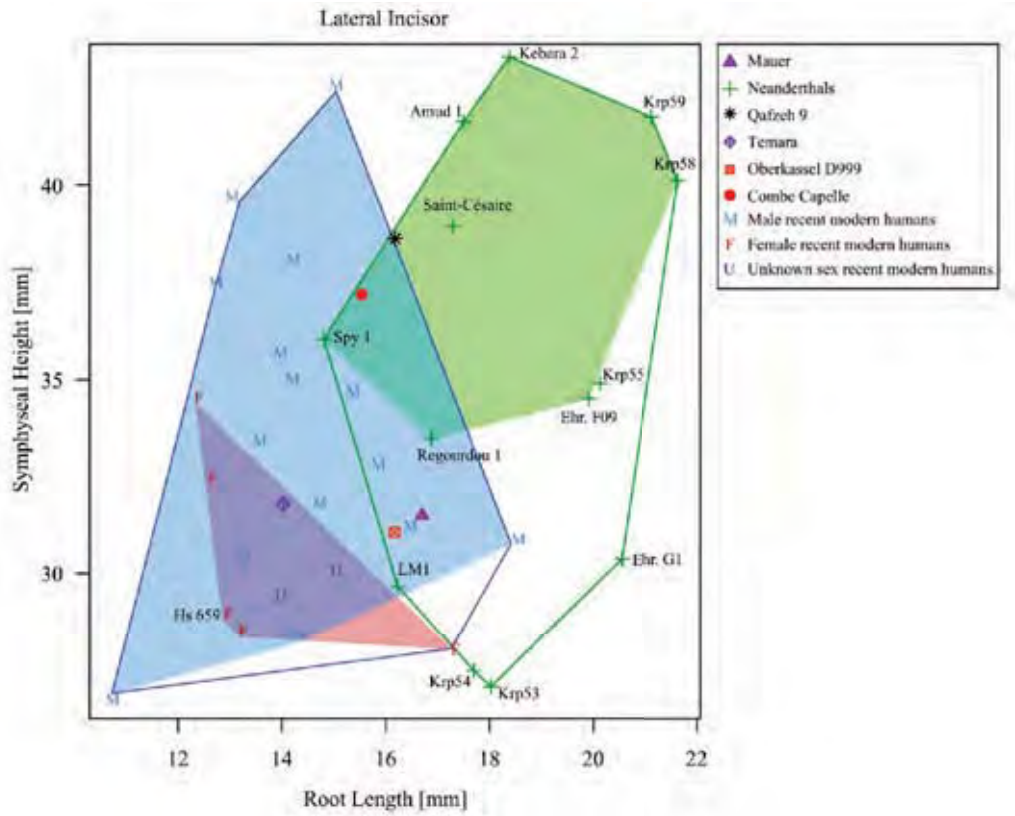
Lateral Incisor
Symphyseal Height [mm]
Root Length [mm]
Mauer
Neanderthals
Qafzeh 9
Temara
Oberkassel D999
Combe Capelle
Male recent modern humans
Female recent modern humans
Unknown sex recent modern humans
Kebara 2
Krp59
Amud 1
Krp58
Saint-Césaire
Spy 1
Krp55
Ehr. F09
Regourdou 1
Ehr. G1
LM1
Hs 659
Krp54
Krp53

(3c)

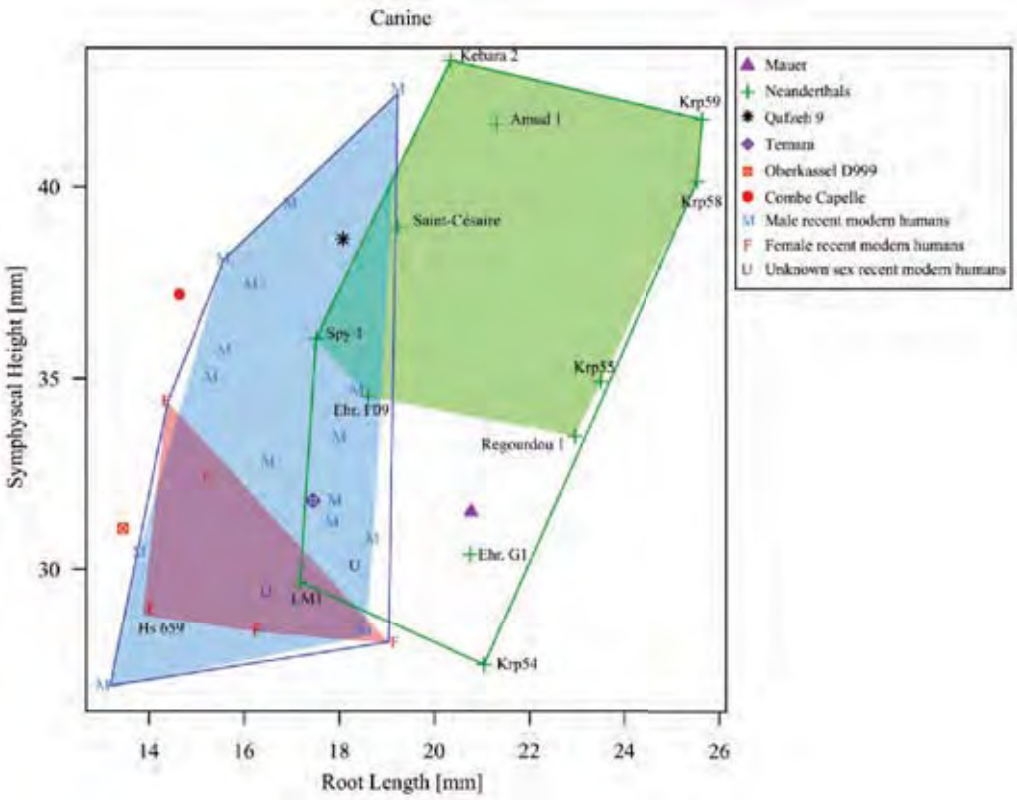

Figure 3. Scatterplot of the symphyseal height and the root length for the central incisor (a), lateral incisor (b) and canine (c). Convex hulls delineate the total Neanderthal (darker green outline), the fully adult Neanderthal (filled convex hulls with dashed outline) and recent modern human (purple) ranges. Male and female recent modern human ranges are represented as solid lines (convex hull shaded in blue and red, respectively). Krp 53, 54 and 55 are the Krapina subadults, Ehr. G1 stands for the Ehringsdorf G1 individual, Ehr. F09 for Ehringsdorf F09, LM1 for Le Moustier 1 and Hs 659 for the recent modern human subadult. While having larger anterior tooth roots, Neanderthals have a symphyseal height of comparable size with recent modern humans. (For interpretation of the references to color in this figure legend, the reader is referred to the web version of this article.)

(4a)

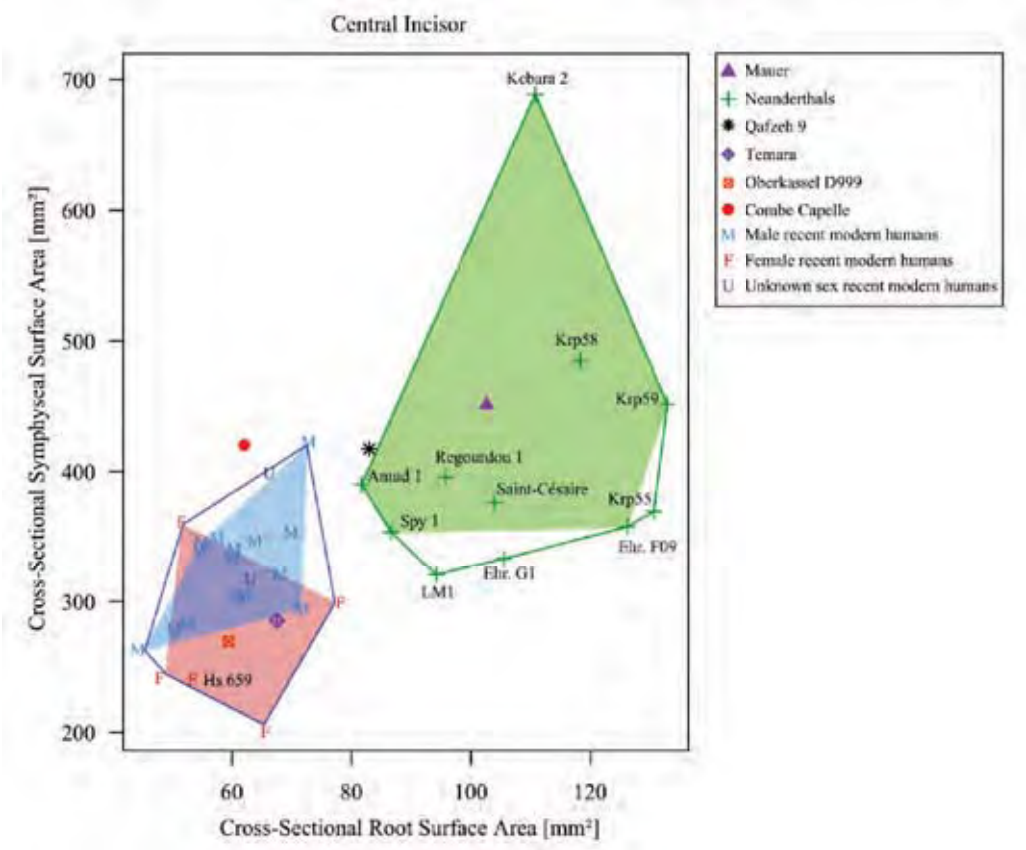
Central Incisor
Cross-Sectional Symphyseal Surface Area [mm²]
Cross-Sectional Root Surface Area [mm²]
Kebara 2
Krp58
Krp59
Regourdou 1
Amud 1
Saint-Césaire
Krp55
Spy 1
Ehr. F09
Ehr. G1
LM1
Hs 659
Mauer
Neanderthals
Qafzeh 9
Temara
Oberkassel D999
Combe Capelle
Male recent modern humans
Female recent modern humans
Unknown sex recent modern humans

(4b)

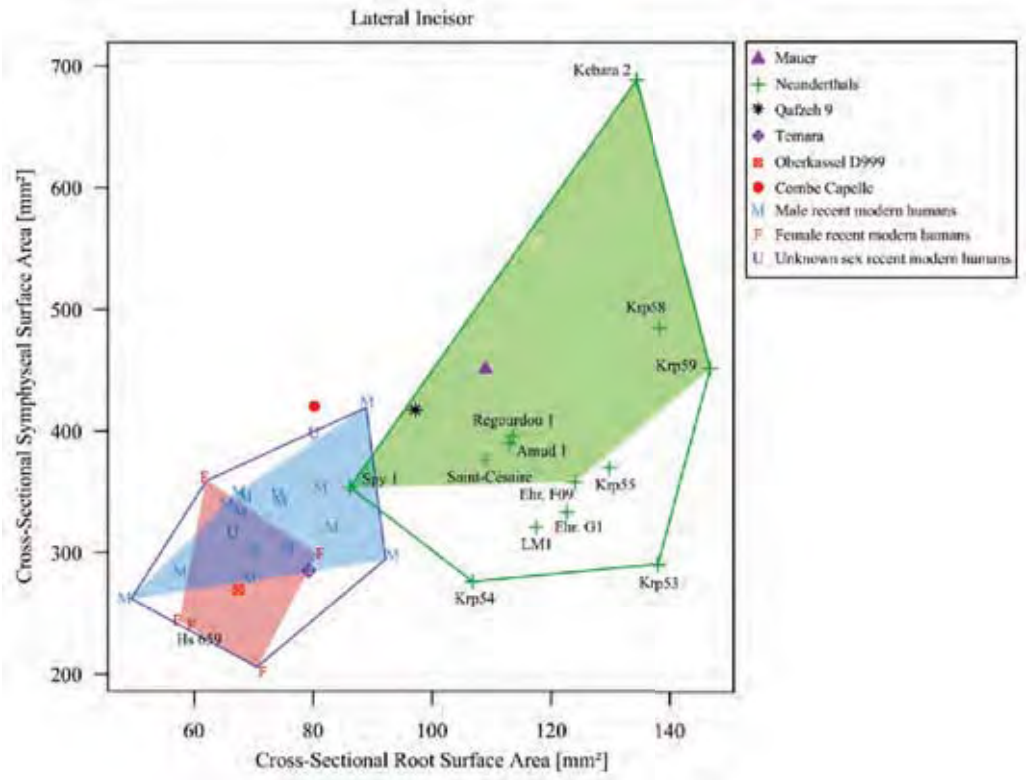
Lateral Incisor
Cross-Sectional Symphyseal Surface Area [mm²]
Cross-Sectional Root Surface Area [mm²]
Kebara 2
Krp58
Krp59
Regourdou 1
Amud 1
Spy 1
Saint-Césaire
Ehr. F09
Krp55
Ehr. G1
LM1
Krp54
Krp53
Hs 659
Mauer
Neanderthals
Qafzeh 9
Temara
Oberkassel D999
Combe Capelle
Male recent modern humans
Female recent modern humans
Unknown sex recent modern humans

(4c)

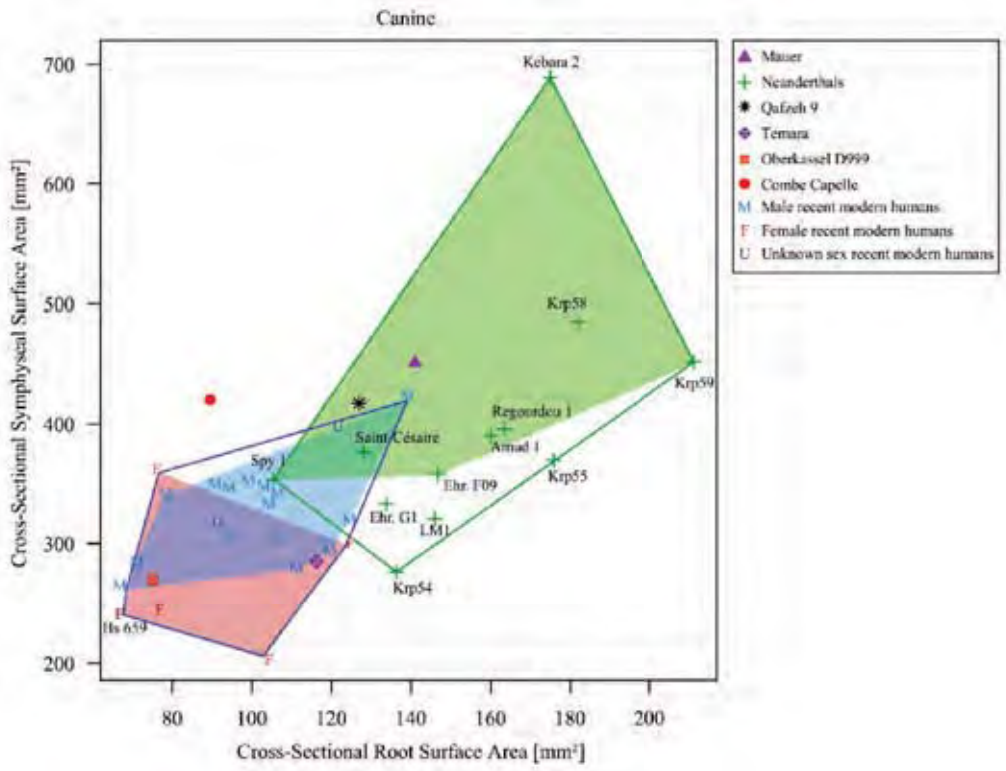

Figure 4. Scatterplot of the cross-sectional symphyseal surface area and the root surface area for the central incisor (a), lateral incisor (b) and canine (c). Convex hulls delineate the total Neanderthal (darker green outline), the fully adult Neanderthal (filled convex hulls with dashed outline) and recent modern human (purple) ranges. Male and female recent modern human ranges are represented as solid lines (convex hull shaded in blue and red, respectively). Neanderthals have significantly larger symphyseal and root surface areas than recent modern humans. (For interpretation of the references to color in this figure legend, the reader is referred to the web version of this article.)

(5a)

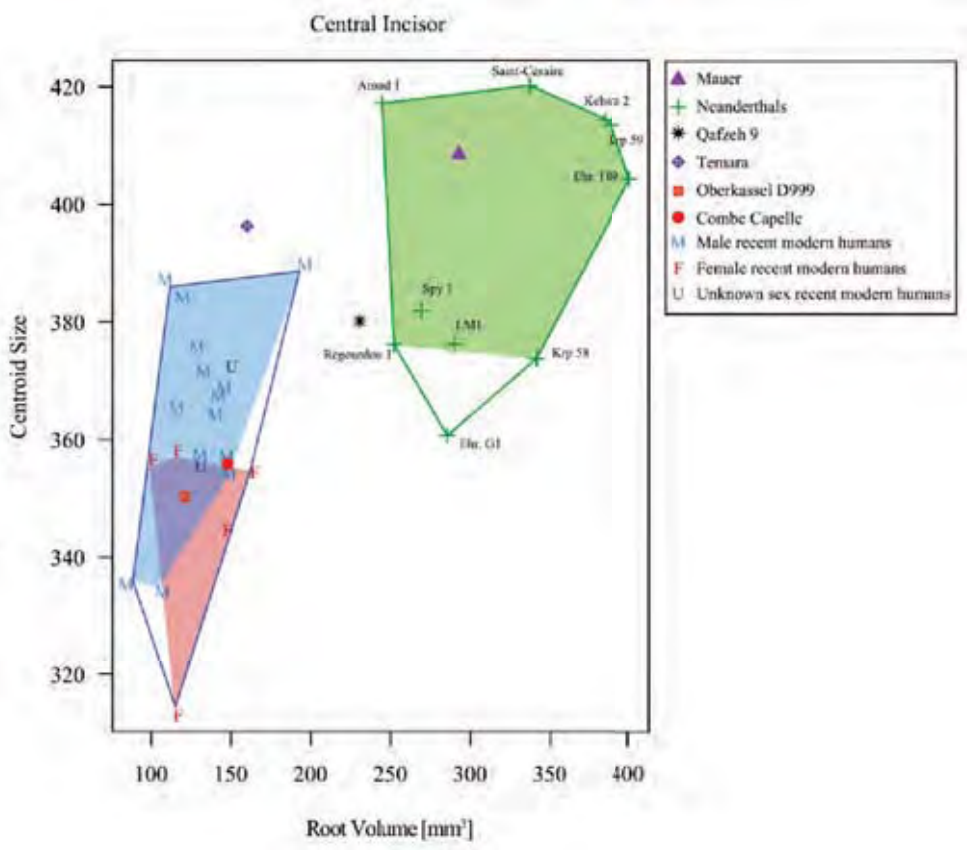
Central Incisor
Centroid Size
Root Volume [mm³]
Mauer
Neanderthals
Qafzeh 9
Tensura
Oberkassel D999
Combe Capelle
Male recent modern humans
Female recent modern humans
Unknown sex recent modern humans
Saint-Cesaire
Amud 1
Kebara 2
Krp 59
Ehr. F09
Spy 1
LM1
Regourdou 1
Krp 58
Ehr. G1

(5b)

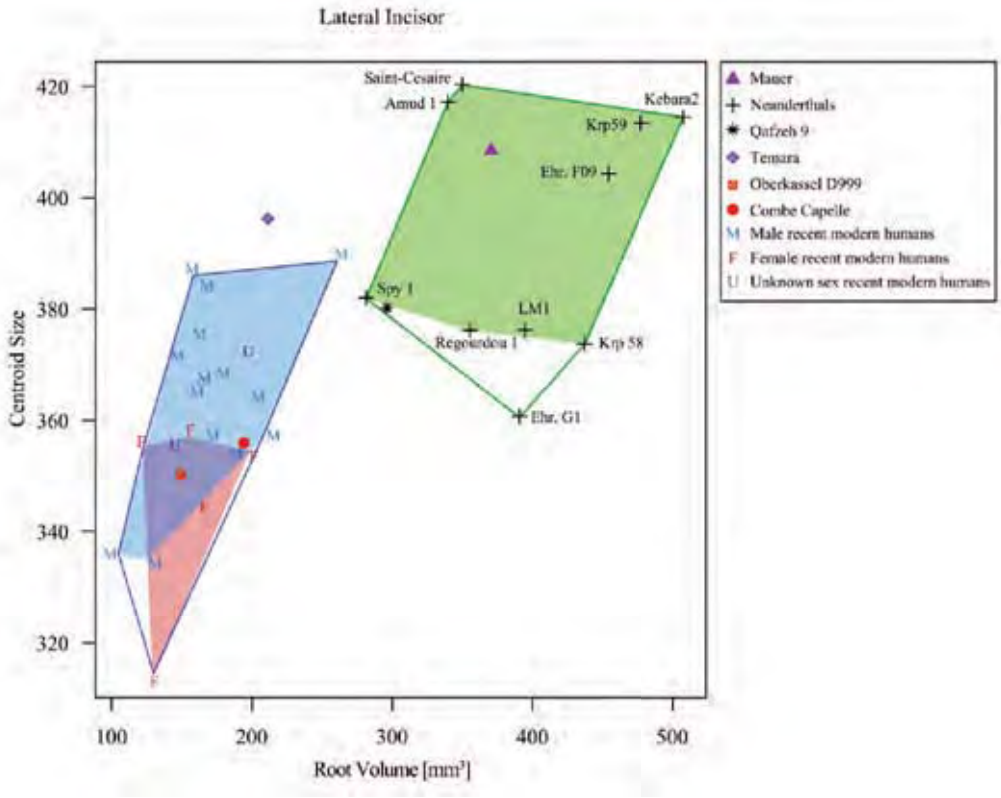
Lateral Incisor
Centroid Size
Root Volume [mm³]
Mauer
Neanderthals
Qafzeh 9
Tensura
Oberkassel D999
Combe Capelle
Male recent modern humans
Female recent modern humans
Unknown sex recent modern humans
Saint-Cesaire
Amud 1
Kebara2
Krp59
Ehr. F09
Spy 1
LM1
Regourdou 1
Krp 58
Ehr. G1

(5c)

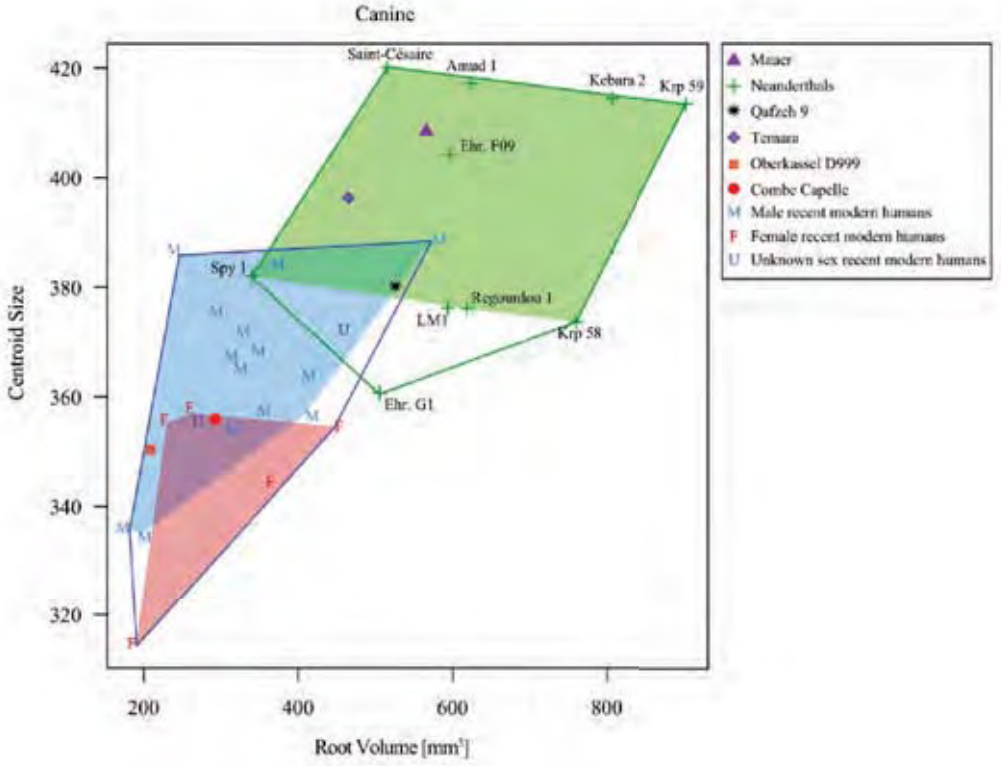

(5d)

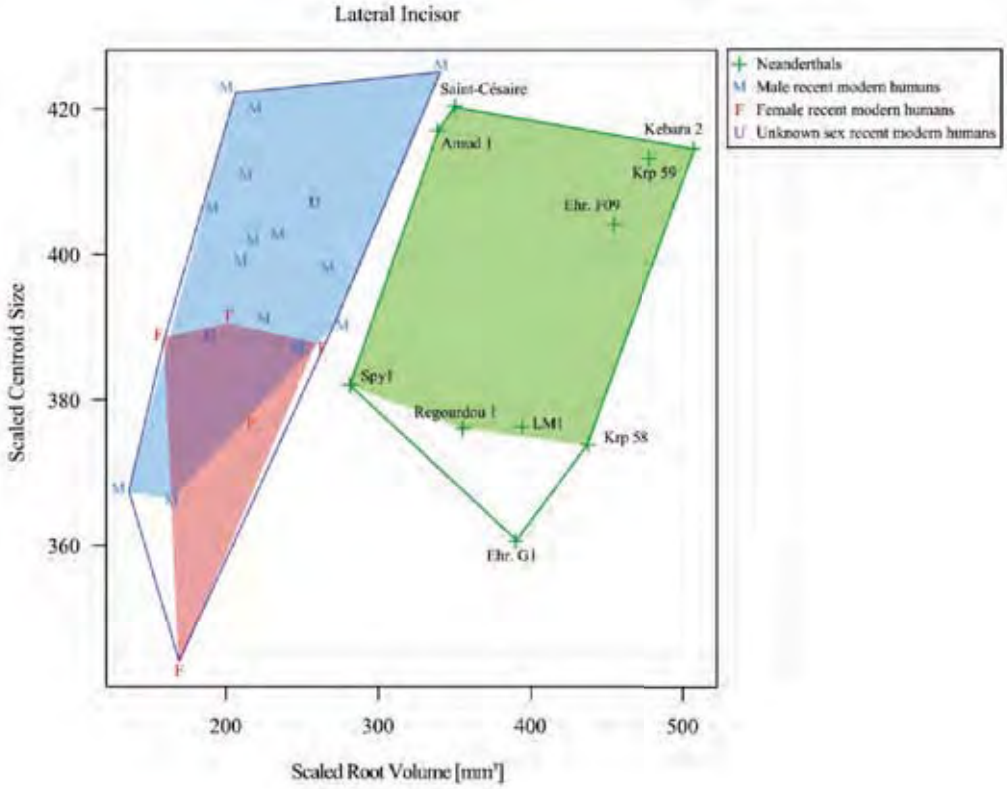

Figure 5. Scatterplot of the overall mandibular size (centroid size) and the root volume for the central incisor (a), lateral incisor (b) and canine (c). Convex hulls delineate the

total Neanderthal (darker green outline), the fully adult Neanderthal (filled convex hulls with dashed outline) and recent modern human (purple) ranges. Male and female recent modern human ranges are represented as solid lines (convex hull shaded in blue and red, respectively). Neanderthals have significantly larger overall mandibular centroid size and root volumes than recent modern humans. After correction for overall size (using the ratio described for Tables 5a and 5b), Neanderthals and recent modern humans still differ significantly in terms of root volume (d). (For interpretation of the references to color in this figure legend, the reader is referred to the web version of this article.)

anterior tooth roots. Regarding the overall and absolute size differences estimated from the centroid size of the mandibles, modern humans and Neanderthals differ significantly ($p = 0.00022$; Table 5b, Figs. 5a-c) with an overlap of one-third between the two distributions. This remains true after correction for size (Fig. 5d).

CORRELATION BETWEEN ROOT SIZE AND JAW SIZE

When Neanderthals and recent modern humans are pooled into one sample (Table 7a), root and symphyseal cross-sectional surface areas are significantly correlated. The same is true for the centroid size of the mandible, which correlates significantly with the root volume and the root length. However, when corrected for size, all correlations fail to reach statistical significance, meaning that there is no interspecific correlation between root size and jaw size.

In light of our results on root and jaw size, we computed ordinary least squares regressions of root dimensions on centroid size in this pooled sample of Neanderthals and recent modern humans. Although the results reach statistical significance, only 39-52% (the coefficient of determination) of the root size variance is explained by relationship to jaw size (Table 7a). Most of the Neanderthals have overall larger roots than expected (i.e., the Neanderthals plot above the regression line).

Intraspecifically, anterior tooth root size does not correlate significantly with symphyseal or overall mandibular size, neither within Neanderthals nor within recent modern humans (Table 7b). Although the cross-sectional surface areas of the Neanderthal mandibular canine root and of the symphysis correlate significantly ($p = 0.04$), the correction for individual size returns a non-significant correlation. Results remain unchanged whether we include or exclude the most juvenile specimens from our

analysis. To assess the effects of static allometry, we computed ordinary least squares regressions of log transformed root dimensions on log transformed mandibular/symphyseal dimensions in Neanderthals and in recent modern humans. For both taxa, our results show that measures of mandibular size explain only a small percent of the variation of root dimensions (Table 7b and SOM 4).

SHAPE ANALYSIS OF THE CONTOUR OF THE SYMPHYSEAL CROSS-SECTION AND OF THE MANDIBLE

Regarding the shape of the symphyseal cross-section, Neanderthals are much more variable than modern humans, and the ranges of both taxa overlap (Fig. 6). The subadult Neanderthals cluster close together, except for Krp 55. In terms of shape, Mauer falls within the cluster of subadult Neanderthals. Qafzeh 9 plots with the most robust recent modern humans and is close to Krp 58. Temara plots close to Qafzeh 9. The Oberkassel mandible falls in the middle of the recent modern human cloud as does the Hs 659 subadult, whereas Combe-Capelle is at the margin of this cloud, close to Kebara 2 and Regourdou 1.

In form space (i.e., combining both size and shape), the main trends are the same except that Krp 59 plots closer to Qafzeh 9, Krp 58, and the most robust recent modern humans. Temara falls right within the recent modern human range of variation. Mauer fits among the most robust Neanderthals, Kebara 2, and Krp 58 and 59.

Regarding the permutation tests for significance in symphyseal cross-sectional shape differences between recent modern humans and Neanderthals, we found only seven permutations (out of 10 001) that yielded Procrustes distances between the means that were equal to or greater than the actual distance ($p = 0.00069993$). The same statistic for the overall mandibular shape yielded 16 permutations out of 10,001 ($p = 0.00159984$). Both results confirm significant differences in shape for both symphyseal cross-section and overall mandibular shape between Neanderthals and recent modern humans (Figs. 6 and 7).

Table 7. Spearman rank order correlations to test whether root variables and mandibular variables correlate (a) interspecifically when recent modern humans and Neanderthals are pooled into one sample, and (b) intraspecifically in recent modern humans and in Neanderthals.

(a)

	SH vs RL [mm]			CSASy vs CSRA [mm²]			CS vs RV		
Tooth Type	I_1	I_2	C,	I_1	I_2	C,	I_1	I_2	C,
Unscaled data	r_s= 0.23	r_s= 0.32	r_s= 0.35	r_s= 0.62	r_s= 0.63	r_s= 0.59	r_s= 0.61	r_s= 0.67	r_s= 0.65
	ns	*ns*	*ns*	***7.94e-04***	***5.79 e-04***	***2.01 e-03***	***1.67e-04***	***1.67e-04***	***4.14e-04***
	r^2=0.09	r^2=0.13	r^2=0.19	**r^2=0.39**	**r^2=0.46**	**r^2=0.45**	**r^2=0.39**	**r^2=0.52**	**r^2=0.50**
Scaled data (only adults and older juveniles)	r_s= 0.02	r_s= 0.13	r_s= 0.24	r_s= 0.29	r_s= 0.33	r_s= 0.42	r_s= 0.15	r_s= 0.20	r_s= 0.34
	ns	*ns*	*ns*	*ns*	*ns*	*ns*	*ns*	*ns*	*ns*

	CS vs RL		
Tooth Type	I_1	I_2	C,
Unscaled data	r_s= 0.37	r_s= 0.53	r_s= 0.56
	ns	***6.57e-03***	***4.63e-03***
	r^2=0.39	**r^2=0.33**	**r^2=0.37**
Scaled data (only adults and older juveniles)	r_s= -2.42e-03	r_s= 0.16	r_s= 0.26
	ns	*ns*	*ns*

Table 7. *Continued.*

(b)

Tooth Type		SH vs RL [mm]			CSASy vs CSRA [mm²]			CS vs RV		
		I_1	I_2	C,	I_1	I_2	C,	I_1	I_2	C,
Neanderthals	Unscaled	r_s= 0.27 *ns* r^2=0.10	r_s= 0.26 *ns* r^2=0.05	r_s= 0.34 *ns* r^2=0.22	r_s= 0.33 *ns* r^2=0.13	r_s= 0.42 *ns* r^2=0.28	r_s= 0.71 ***0.04*** r^2=0.36	r_s= 0.15 *ns* r^2=0.18	r_s=-0.04 *ns* r^2=0.048	r_s=0.24 *ns* r^2=0.11
	Scaled	r_s= 0.27 *ns*	r_s= 0.13 *ns*	r_s= 0.53 *ns*	r_s= 0.32 *ns*	r_s= 0.42 *ns*	r_s= 0.65 *ns*	-	-	-
Recent modern humans	Unscaled	r_s= -0.23 *ns* r^2=0.03	r_s= -0.03 *ns* r^2=0.002	r_s= 0.04 *ns* r^2=0.03	r_s= 0.33 *ns* r^2=0.12	r_s= 0.36 *ns* r^2=0.22	r_s= 0.31 *ns* r^2=0.17	r_s= 0.25 *ns* r^2=0.16	r_s= 0.42 *ns* r^2=0.33	r_s= 0.46 *ns* r^2=0.38
	Scaled	r_s=-0.42 *ns*	r_s= -0.36 *ns*	r_s= -0.25 *ns*	r_s= 0.19 *ns*	r_s= 0.30 *ns*	r_s= 0.13 *ns*	-	-	-

Table 7. *Continued.*

Tooth Type		CS vs RL		
		I_1	I_2	C,
Neanderthals	Unscaled	r_s= -0.21 *ns* r^2=0.006	r_s= -0.18 *ns* r^2=4.46e10-6	r_s= -0.12 *ns* r^2=0.0003
	Scaled	-	-	-
Recent modern humans	Unscaled	r_s= -0.21 *ns* r^2=0.001	r_s= -0.18 *ns* r^2=0.10	r_s= -0.12 *ns* r^2=0.31
	Scaled	-	-	-

Note for (a) and (b): the coefficients of determination (r^2) computed for ordinary least squares regressions are reported for unscaled data (all variables log-transformed). r_S is the Spearman's rank order correlation coefficient. Bonferroni adjusted p values are bolded when significant. ns = nonsignificant.
Note for (a): In the 'scaled data', modern humans are scaled as explained in Tables 5a and 5b. Sample sizes for Neanderthals: I_1 N = 11, I_2 N = 13, C, N = 12; for recent modern humans N = 22 for all tooth types
Note for (b): Results are presented with both scaled and unscaled data so that each specimen is scaled by its own centroid size. The sample sizes for Neanderthals N = 10 and for recent modern humans N = 21 for all tooth types.

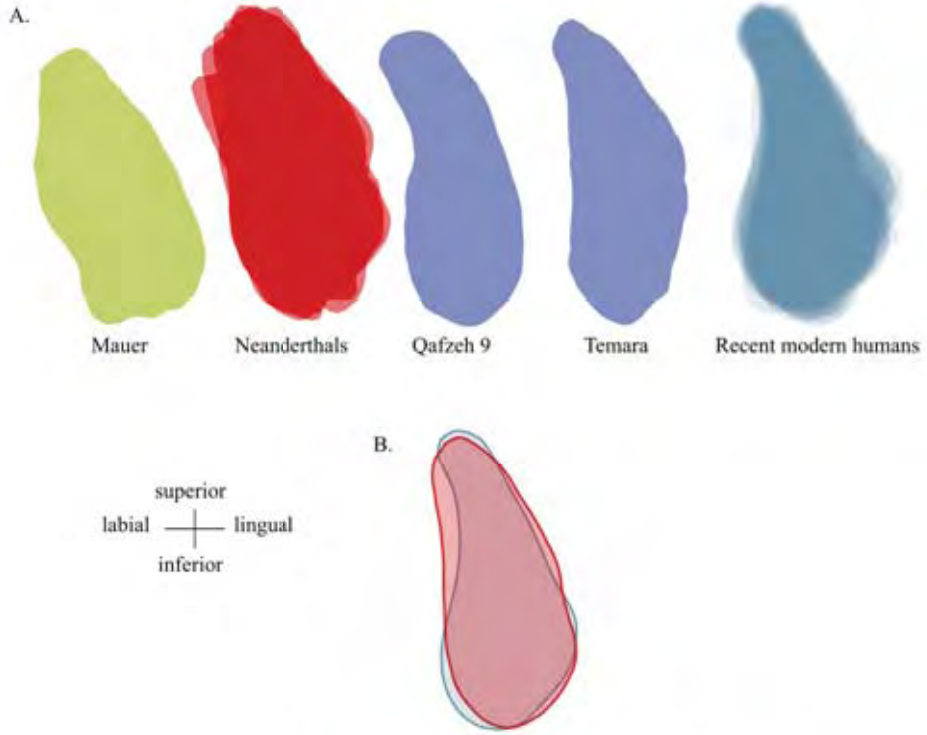

Figure 6. Shape outlines of the symphyseal cross-section for (A) Mauer (green), Neanderthals (red, all superimposed specimens), Qafzeh 9 and Temara (lavender), and recent modern humans (gray, all superimposed specimens), showing the evenly thick symphysis of Mauer, Neanderthals, Qafzeh 9, and Temara in a lesser extent, and the local variation in symphyseal thickness in recent modern humans. (B) Superimposed mean shapes of Neanderthals (red) and recent modern humans (gray). (For interpretation of the references to color in this figure legend, the reader is referred to the web version of this article.)

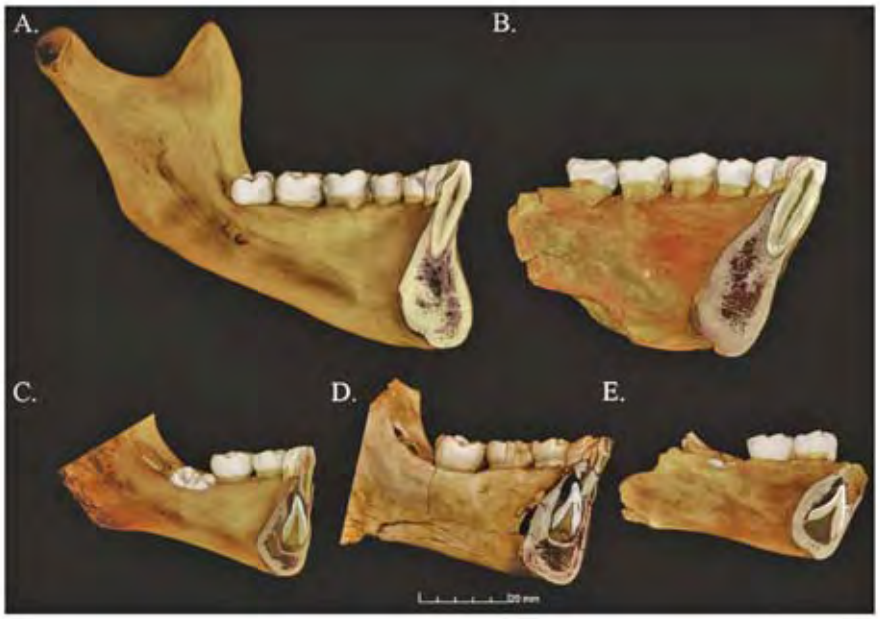

Figure 7. Labio-lingual sections of the symphyseal region through the alveolus of the central mandibular incisor in adult (A and B) and juvenile (C, D and E) Neanderthal and

modern human mandibles. Note the tear-drop outline of the symphyseal section in recent modern humans (adult ULAC 58: A; juvenile ULAC 81: C) and in the early modern human juvenile Qafzeh 10 (D), in contrast to the pillar shaped symphysis of the Neanderthals (adult Krapina 58: B; juvenile Gibraltar 2: E). This wider symphysis in Neanderthals may accommodate the eruption of a large tooth germ (see the difference in bicervical width between the modern human and Neanderthal). Gibraltar 2 and Qafzeh 10 (data publically available on the ESRF Paleontological Microtomographic Database after Smith et al., 2010) have been flipped for this figure.

DISCUSSION

Our research explores the validity of using anterior tooth root length as a taxonomic tool to distinguish Neanderthals from modern humans (proposed by Bailey, 2005). Whereas previous studies, which have investigated the correlation between tooth size and jaw size, have used only crown size as a proxy for tooth size and have been restricted to recent modern humans (e.g., Garn and Lewis, 1958; Filipsson and Goldson, 1963; Henderson and Corruccini, 1976), our micro-CT data allows us to study the relationship between root size and symphyseal size directly, and to extend this issue to fossil specimens, especially Neanderthals.

Our results regarding root length (Tables 4 and 5a) are in agreement with Bailey's (2005) findings. In terms of overall mandibular size (as measured by centroid size), our findings show that Neanderthals are significantly larger than recent modern humans (Tables 5b and 6), which confirm Nicholson and Harvati's (2006) results. This difference in mandibular size is accompanied by a significant difference in overall mandibular shape between Neanderthals and recent modern humans (see the results of our permutation tests and Bastir et al., 2007; Mounier et al., 2009). Neanderthals have large anterior tooth roots for the size of their mandibles, and, based on the observation of Mauer, one can speculate that this would be the primitive condition of the root-jaw size relationship. On the other hand and until the primitive condition has been ascertained by the study of more early *Homo* specimens, the most parsimonious statement we can make regarding the polarity of characters is that recent modern humans may be derived in having significantly smaller tooth roots for the size of their mandible.

Although Neanderthals and recent modern humans do not differ significantly in symphyseal height or width (see Tables 5b and 6; for the symphyseal height, results

confirmed by Crèvecoeur and Trinkaus, 2004: Table 3), the results of our permutation tests confirm a significant difference in symphyseal cross-sectional shape. Indeed, the mid-sagittal symphyseal surface area distinguishes both groups. In addition, Neanderthals have an overall evenly thick symphysis with a rather vertical profile (Mounier et al., 2009), while in modern humans, the symphysis thickness is subject to a localized variation (tear-drop shape of the section), with a relatively thin alveolar bone (pronounced *incurvatio mandibularis*), and a basal bone thickened by the presence of a chin (developed *tuber symphyseos* and central keel). Neanderthals show a greater variability due to the presence of morphological traits that participate in defining the modern human chin, such as in Amud 1, Krp 58, and Spy 1 as pointed out by Mounier et al. (2009). Our results show that this is also true in Saint-Césaire and Krp 55, which have a slightly developed chin yet different from the inverted 'T' shaped relief classically observed in recent modern humans (Schwartz and Tattersall, 2000). In addition, the MIS 7 Ehringsdorf F mandible, which shows a weak development of the *incurvatio mandibularis* and of the *tuber symphyseos* as also observed by Mounier et al. (2009), clusters close to those specimens. In a study including extant and extinct hominoids, Guy et al. (2008) concluded that symphyseal shape is not affected by size differences between males and females (except for *Gorilla* in their sample). It is therefore unlikely that the difference in mid-sagittal symphyseal shape that we document is related to sexually dimorphic differences within recent modern humans and Neanderthals. Moreover, we speculate that the distribution of the subadult Neanderthal specimens apart from the fully adult specimens might reveal an ontogenetic trajectory. Bastir et al.'s (2007) study on the facial ontogeny in Neanderthals and modern humans supports this hypothesis since it has shown that 'the differences in spatio-temporal aspects of postnatal ontogeny contribute to the establishment of differences in adult form' (Bastir et al., 2007: 1130).

After correction for overall mandibular size, we found no intraspecific or interspecific correlation between anterior tooth root size and symphyseal size for Neanderthals and recent modern humans. The results of our intraspecific regressions suggest that there is no or a negligible effect of static allometry on root size in both Neanderthals and recent modern humans. At the interspecific level, only the lower canine cross-sectional root surface area correlates with the symphyseal cross-sectional surface area in Neanderthals, with unscaled data. This may be due to sexual

dimorphism, although this cannot be tested on our Neanderthal sample since sex attribution is often debatable in fossils.

Whereas the symphyseal size becomes similar between both taxa after correcting for overall mandibular size (Table 5b), the anterior tooth roots remain significantly larger in Neanderthals than in modern humans (Table 5a). If Mauer is considered as a representative of the common ancestor between Neanderthals and recent modern humans (Mounier et al., 2009; Mounier, 2011; however see; Rosas and Bermúdez De Castro, 1998), and given the position of early modern human specimen Qafzeh 9 in the area of overlap of both taxa for all measured variables, long anterior tooth roots are probably the ancestral condition. This would suggest a negative allometry in root size in recent modern humans. Alternatively or in addition, it is possible that within the Neanderthal lineage there is a positive allometry for anterior root size, if the pre-Neanderthals and early *Homo* show the same type of root size/jaw size than Neanderthals. This question could be resolved in future studies by incorporating Middle Pleistocene specimens, such as from Sima de los Huesos, testing whether there is a significant increase of anterior root size independently from changes in jaw size within the Neanderthal lineage. Overall, our results are in favor of using root length as a taxonomic measurement to distinguish modern humans from Neanderthals.

While it is widely recognized that teeth and jawbones form a functional unit and influence each other during development (Boughner and Hallgrímsson, 2008), there is a long-standing debate about the relationship between size and morphology (i.e., overall shape) of tooth and mandibular bone.

Some researchers have posited that the shape of the bone is not determined by the shape and size of the dental crowns and roots alone (Lundström, 1951 for incisor crowding; Richardson, 1970 for third molar impaction). In great apes, it has been shown that early in ontogeny when dental development has not yet been completed, differences in mandibular shape are already established at the genus level (see Daegling, 1996 for comparison of *Gorilla* and *Pan*), as well as at the species level (see Boughner and Dean, 2008 for comparison of *Pan paniscus* and *Pan troglodytes*). In recent modern humans, mandibular molar teeth often start to mineralize in the mandibular ramus (Boughner and Hallgrímsson, 2008) and wisdom teeth sometimes emerge in the ramus due to lack of space in the tooth row (Richardson, 1970). Similarly, incisor crowding is a common

result of insufficient space in the jaw (Lundström, 1951; Howe et al., 1983). In addition, debates are still ongoing regarding whether the modern human chin is a functional adaptation to resist loads (Nicholson and Harvati, 2006; Gröning et al., 2011; contra; Dobson and Trinkaus, 2002). Whereas tooth development is complete once the root apex is closed, the jaw bone is still subject to growth processes involving both bone resorption and deposition, and later to remodeling due to aging (Coquerelle et al., 2010a).

However, other researchers support the theory that the bone merely accommodates the position, the size, and the shape of the developing tooth germs rather than adapting to biomechanical constraints during the mastication process (Sofaer, 1973; Frayer, 1978; Fukase, 2011, 2012).

Interestingly, Shea and Gomez (1988) found no strong association between postcanine tooth size (crown diameters) and body size (craniofacial measurements, body height and weight) in groups of human pygmies compared with non-pygmy groups, despite the fact that the mandibular first molar is often used as an estimate for body weight. They propose that skeletal growth and dental development are under the control of different growth factors, which would explain their relative independence. In light of our results, showing that Neanderthals have larger anterior roots for the size of their jaw in comparison with recent modern humans, the mandible would not be an ‘entity’ as such. Rather, it would be a group of modules that can independently develop and evolve, such as the anterior and posterior portions of the dental arch (Moskowitsch and Smith, 1993). This decoupling between the anterior and posterior part of the jaw can be seen in Temara, which has a relatively small symphysis for such a large mandible, and in Combe-Capelle, which shows the opposite pattern by having a large symphysis in an overall small mandible. Indeed, the symphyseal region seems to be stable in our study for the symphyseal height and width (see Table 5b) as opposed to the postcanine portion of the mandible. Although this was not specifically tested in the present study, Kupczik and Hublin (2010) noted that in general *Homo sapiens* has relatively shallow corpora compared with the height of the anterior portion of the mandible, which could be associated with the reduction of the postcanine dentition. In contrast, in fossil *Homo* other than *H. sapiens* the anterior and posterior corpus are roughly of equal height (Kupczik and Hublin, 2010). This previously discussed mandibular modularity would result from different selective pressures (Wolpoff, 1979;

Moskowitsch and Smith, 1993). On the one hand, interactions with the environment and manipulation of food would exert selective constraints acting on the anterior part of the mandible. On the other hand, comminution of the food particles would represent the major selective factor on the posterior part of the lower jaw. Following the theory by Moss and Rankow (1968), the teeth represent the functional matrix, which the growth of the alveolar process depends on. This is in agreement with Daegling's (1996) findings on mandibular growth in gorillas and chimpanzees. In other words, and as stated by Dean and Beynon (1991), the space available in the jaws for the developing teeth is determined by the jaw growth pattern. Emphasizing how narrow the anterior portion of the U-shaped mandible in great apes is, these authors explain how an increased antero-posterior cross-sectional area of the symphysis allows for the accommodation of the tooth germs in the alveolar bone. This has been investigated using Finite Element Analysis on *Macaca fascicularis* by Cobb and Panagiotopoulou (2011), who demonstrated that the spatial requirement for the developing incisors can constrain the future adult morphology and the functional adaptation of the symphysis. In light of our results in root size and cross-sectional symphyseal size, one could speculate that the evenly thick symphysis of the Neanderthals is adapted to accommodate the development and the migration of the anterior tooth germs that will eventually give rise to permanent large-rooted teeth. This hypothesis is in agreement with Tillier (1996), suggesting that the morphological variability observed in the posterior surface of the symphysis in the Roc de Marsal and Pech de l'Azé Neanderthal children may be related to the position of the developing permanent incisors in the bone. Bastir et al. (2007) also propose that the observed differences in shape trajectories of the alveolar region of the Neanderthal mandible could be related to ontogenetic differences in the maturation of the teeth. Fig. 7 illustrates this hypothesis, showing juvenile and adult modern humans with a tear-drop shaped symphyseal section, while the juvenile and adult Neanderthals show a pillar shaped symphysis. Note the wider permanent tooth germ in the Neanderthal child compared with the modern human, where the slender germ is located in a well defined crypt, and underneath a noticeable amount of cancelous bone.

Coquerelle et al. (2010b) have described in detail the growth pattern of the human mental symphysis. Prenatally, the symphysis is vertically oriented with a V-shaped basilar bone and a U-shaped alveolar bone. Postnatally, the alveolar bone is displaced backward while the mental region projects forward to give rise to the typical

modern human chin. This differs from Neanderthals, who do not display a chin as it is defined in modern humans: a central keel with bilateral mental *fossae*, lateral tubercles and a protruding *tuber symphyseos* (Schwartz and Tattersall, 2000; Mounier et al., 2009). In addition, Coquerelle et al. (2010a) observed that after two years of age, dental mineralization and mandibular form evolve more independently. Although this documented independence in growth could seem contradictory with the function that jaw and teeth obviously perform together, Boughner and Hallgrímsson (2008) regard the dentition and mandible as two functionally integrated modules, and argue that there has been a strong selection to coordinate the developmental pathways of both bony structure and teeth. These authors hypothesize that the timing of mandibular and dental development would be an indirect consequence of the need for coordination of growth trajectories.

In light of our results, Mauer essentially shows a Neanderthal-like morphology for its anterior tooth roots and its symphysis. These results could be interpreted in two ways. As suggested by some (e.g., Rosas and Bermúdez De Castro, 1998), Mauer could be simply seen as one of the oldest representatives of the Neanderthal clade. Alternatively, if Mauer represents a common ancestor to modern humans and Neanderthals (Rightmire, 1998), this implies that Neanderthals primarily retained the primitive conditions observed in Mauer. We are aware that due to the composition of our fossil samples and despite the inclusion of the Mauer specimen, the question of the polarity of the studied characters remains difficult to answer. Including older representatives of the genus *Homo* in this study could help to resolve the issue. The literature provides some insight into symphyseal height and width of some early *Homo* specimens (Guy et al., 2008). Unfortunately, to our knowledge, no micro-CT data of lower jaw with a preserved symphysis and *in situ* permanent lower incisors and canines are currently available for any adult or subadult early *Homo*. One noticeable exception is KNM-WT 15000, whose symphysis and anterior teeth are preserved. However, the specimen is a juvenile and its root apices are not fully closed. Despite the fact that the early modern human from Temara shows a complex pattern, combining small anterior tooth roots for a small symphysis and an overall large mandible, Qafzeh 9 is overall more similar to Neanderthals than to recent modern humans regarding the size of the anterior roots. This provides further support to the notion that Neanderthals essentially retained ancestral conditions. Although both Neanderthals and modern humans likely

display some proper derived conditions, this will need to be further investigated. The results obtained on early modern humans suggest that there is a negative evolutionary allometry in anterior root size developing within the modern human lineage. The oldest modern humans may therefore display a 'Neanderthal-like' pattern, that is, in fact, ancestral. This similarity may well be illustrated by the debate regarding the taxonomical status of the Tabun C2 mandible (Schwartz and Tattersall, 2000).

CONCLUSION

This study aimed to test whether anterior tooth root length, which has been shown to discriminate Neanderthals from modern humans, is a by-product of jaw size. We have investigated the correlation in size between the incisor and the canine roots and the symphyseal region in Neanderthals and modern humans, using micro-computed tomography. Our results show that Neanderthals have larger roots than expected for the size of their jaw compared with recent modern humans. Our results suggest that the effect of static allometry on root size in Neanderthals and in recent modern humans is negligible. Moreover, we have shown evidence for a negative evolutionary allometry in root size of recent modern humans, compared with the presumed ancestral condition. Therefore, root length and other root dimensions can be considered as taxonomically relevant to distinguish Neanderthals from modern humans, at least for the terminal forms of the clades. We have suggested that the significant difference in symphyseal shape between Neanderthals and recent modern humans may be an adaptation for the eruption and later accommodation of large permanent anterior teeth in Neanderthals. A larger sample including Neanderthals from more diverse time periods and geographical areas should help better understand the variability in root dimensions, in comparison with modern humans.

ACKNOWLEDGMENTS

We would like to thank the curators in charge of the material: Jean-François Tournepiche (Musée d'Angoulême, France), Jakov Radovčić (Croatian Natural History Museum, Croatia), Patrick Semal (Laboratory of Anthropology and Prehistory, Royal Belgian Institute of Natural Sciences) and NESPOS, Yoel Rak (Sackler School of

Medicine, Tel-Aviv University), Véronique Merlin-Langlade (Musée d'Art et d'Archéologie du Périgord), Patrick Périn (Musée d'archéologie nationale et Domaine national de Saint-Germain-en-Laye Château, France), Abdelwahed Ben-n'cer (Institut National des Sciences de l'Archéologie et du Patrimoine, Rabat, Morroco), Israel Hershkovitz (Sackler School of Medicine, Tel-Aviv University), Almut Hoffmann (Museum für Vor- und Frühgeschichte, Berlin), Ralf Schmitz (Rheinisches Landesmuseum für Archäologie, Kunst-und Kulturgeschichte, Bonn), Ullrich A. Glasmacher (Institut für Geowissenschaften, Heidelberg), Flora Groening and the Senckenberg (Forschungsstation für Quartärpaläontologie, Weimar), Bernard Vandermeersch, Christine Feja (Lehrsammlung Anatomie, Institut für Anatomie, Leipzig), the Rockefeller Museum (Jerusalem, Israel) and the Natural History Museum of London. We are grateful to Andreas Winzer and Heiko Temming for their micro-CT scanning expertise, to Rico Tilgner for his advice and expertise in image processing and software expertise, especially for writing and optimizing the Watershed segmentation algorithm, to Roger Mundry for his very helpful advice and support in using R statistical software and to Alyson Reid for English proof-reading. We acknowledge Paul Tafforeau for constructive comments and suggestions, as well as for collaboration on the preparation of Fig. 7. Scan data for Qafzeh 10 and Gibraltar 2 were provided by the ESRF Paleontological Microtomographic Database (http://paleo.esrf.eu/webgallery/index.php?/category/388). This research was funded by the Max Planck Society. We are very grateful to the editor, associate editor and two anonymous reviewers (especially Reviewer 2), whose insightful and constructive comments considerably improved the quality of this manuscript.

APPENDIX A. SUPPLEMENTARY DATA

Supplementary data related to this article can be found at http://dx.doi.org/10.1016/j.jhevol.2012.07.003 .

SUPPLEMENTARY ONLINE MATERIALS

SOM 1. Segmentation and 3D model processing.

Segmentation is an image processing step that consists of attributing each voxel of a micro-CT dataset to a user-defined material (here: enamel, dentine, pulp, cracks in the enamel and in the dentine). This attribution is based on the gray values of the voxels. The user defines each material by a range of gray values (e.g. white for the enamel, black for the air) and by his/her knowledge of the biological structure investigated (e.g. bone and root can display the same gray values, but they remain distinguishable if the periodontal space is preserved).

In order to facilitate the dental tissue segmentation in Avizo 6.2 (Mercury Systems), the reconstructed high resolution micro-CT slices were filtered using a median filter, followed by a mean-of-least-variance filter (each with a kernel size of three) to reduce the background noise while preserving and enhancing the edges (Kuwahara et al., 1976; Schulze and Pearce, 1994). Dental tissues (enamel, dentine and pulp) were semi-automatically segmented by thresholding and manual editing. Cracks in the enamel and dentine have been processed as distinct materials when they were clearly detectable on the scans, so as to avoid an overestimation of root volume and surface area. All modern human teeth and some of the best preserved fossil teeth (with good contrast) were segmented using a customized automated segmentation algorithm based on the watershed principle (Beucher and Lantuejoul, 1979). Minor manual editing was performed after running the algorithm, especially regarding cracks, which were always detected. Following this segmentation process, 3D surface models of the teeth were generated using a constrained smoothing algorithm in Avizo. Each tooth was then virtually divided into crown and root(s), by cutting the 3D models at the cervical plane defined by a best–fit plane between landmarks set on the uppermost enamel margins on the labial and lingual sides of the cemento-enamel junction.

SOM 2. Principle of the Delaunay triangulation used to generate the cross-sectional surface area of the mandibular symphysis.

Three-dimensional curve semi-landmarks were set along the outline of the midsagittal cross-section of the symphysis (Fig. A, example on Krp55, labial at the left hand side, lingual at the right hand side). The semi-landmarks are internally projected onto the plane (here the symphyseal cross-section) to generate a triangulated surface (with a 2D topology since the projections occur on a plane, Fig. B). The cross-sectional surface area of the symphysis (CSASy) is computed from this surface (Fig. C). The Delaunay algorithm links the semi-landmarks by groups of three to form triangles in a way that none of these triangles are overlapping, that the maximal surface area is covered by each triangle and that the minimum angles are maximized. In the end, the expected result is to get a surface patch enclosed by all the semi-landmarks. In the case of a very concave shape of the contour (e.g. in the case of the alveolar region of the symphysis of Combe-Capelle, Figs C to G), two sets of curve semi-landmarks were taken to compensate for the overestimation stemming from the Delaunay triangulation of the first set of semi-landmarks.

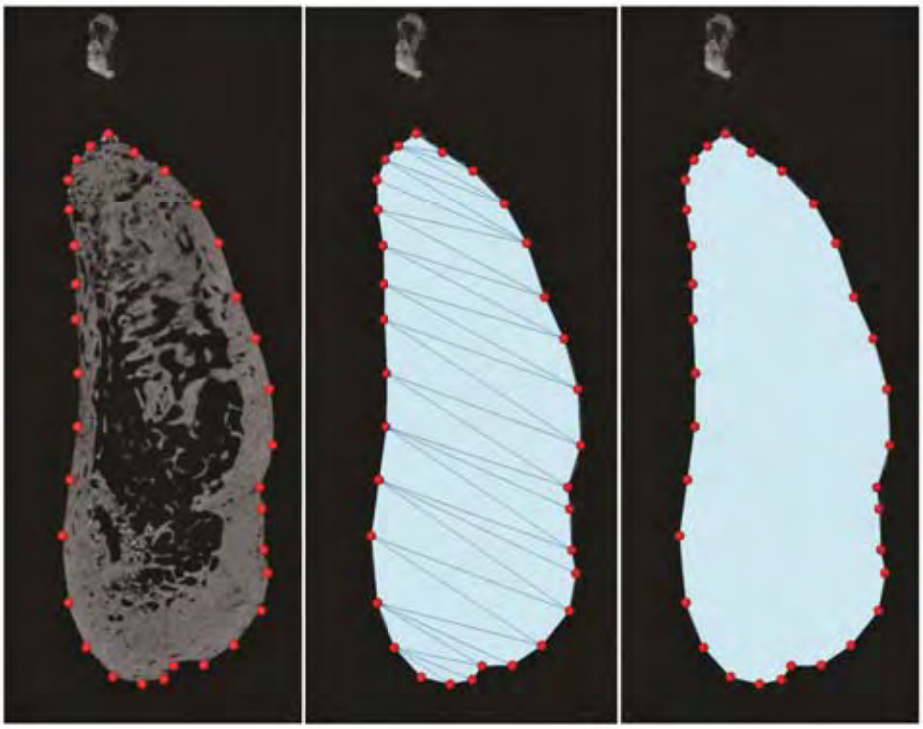

A. B. C.

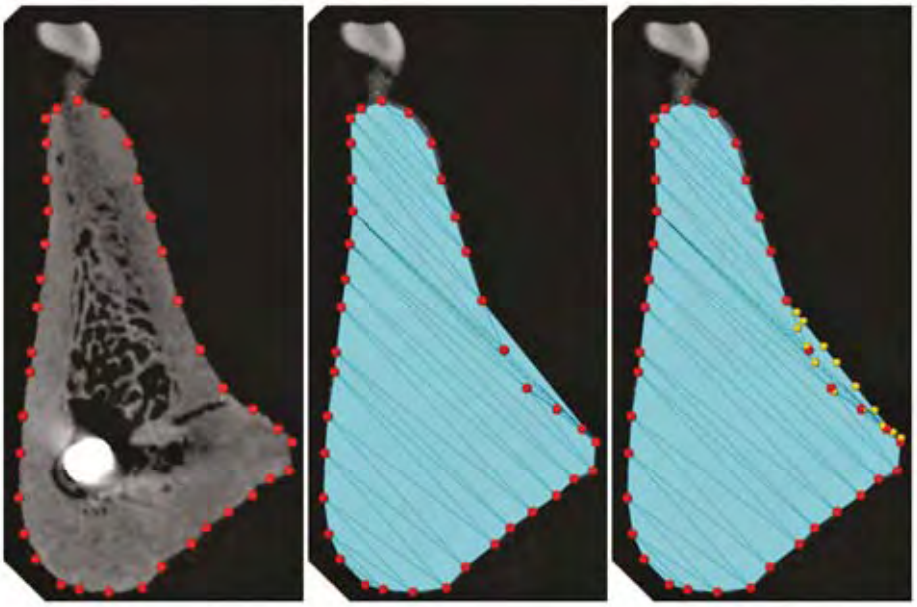

D. E. F.

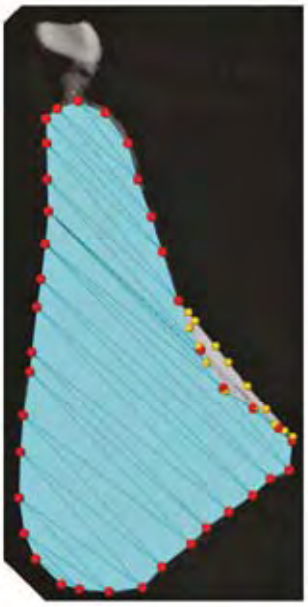

G.

In the case of the convex aspect of the lingual symphysis of Combe-Capelle, the pink surface area delimited by the yellow landmarks is subtracted from the blue surface area delimited by the red landmarks, to get the surface area of the section of the symphysis.

SOM.3. Centroid size computation.

Centroid size (CS) is defined as the square root of the summed squared distances between each landmark and the centroid (the average landmark) (Dryden and Mardia, 1998). Centroid size is a measure of scale used in geometric morphometrics, which has been shown to be uncorrelated with shape for small isotropic landmark variation (Bookstein, 1991; Mitteroecker and Gunz, 2009). When landmarks were missing, we estimated them following the protocol described in Gunz et al. (2009). Landmarks missing on one side were estimated using reflected relabeling. This requires the specification of paired (bilateral) and unpaired ("midsagittal") points (Mardia et al., 2000; Bookstein and Mardia, 2003; Bookstein, 2005). We reflected the landmarks along the medio-lateral axis (x-axis) while swapping the labels (labels of left and right side landmarks are interchanged); then these two configurations were superimposed with a Procrustes fit based on the available landmarks. Missing landmarks were then replaced by the mirrored landmarks. If missing data occurred on both sides of the specimen, or along the midline, landmarks were estimated using "geometric reconstruction" via a thin-plate spline (TPS) interpolation function (Gunz et al., 2009). A TPS interpolation was computed based on the subset of landmarks available in the incomplete specimen. This interpolation function was used to map the missing landmarks from the average reference shape onto the incomplete target, placing the landmark estimates so that the deformation between the reference and the incomplete specimen is as smooth as possible (for more details see: Gunz et al., 2009; Mitteroecker and Gunz, 2009).

SOM 4. Intraspecific ordinary least squares regressions of root size against mandibular/symphyseal size showing a quasi-absence of static allometry for both Neanderthals and recent modern humans. Data are not scaled and are log-log transformed. Graphs and computations have been performed in PAST (Hammer et al., 2001).

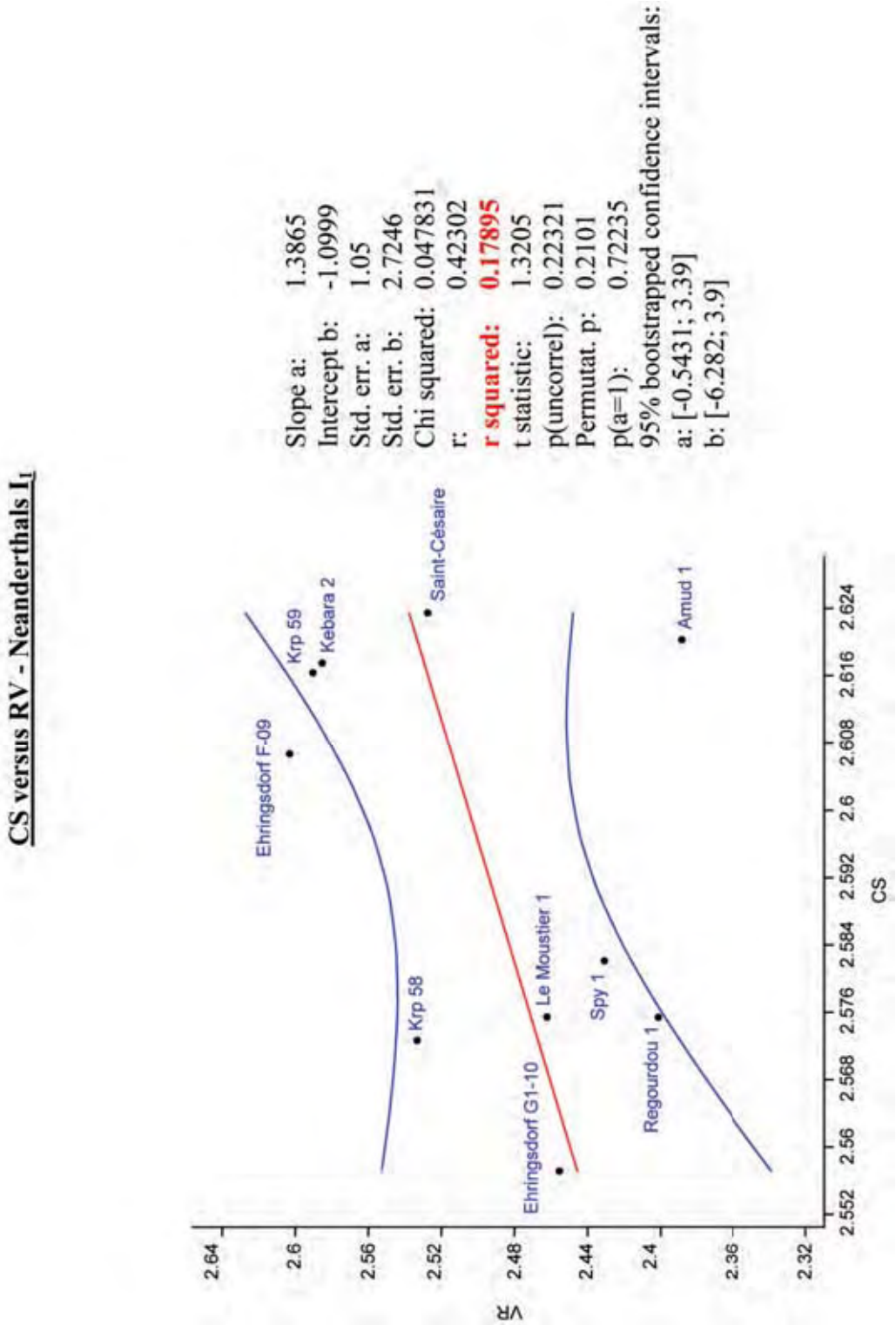

SOM 4. *Continued.*

CS versus RV - Neanderthals I_2

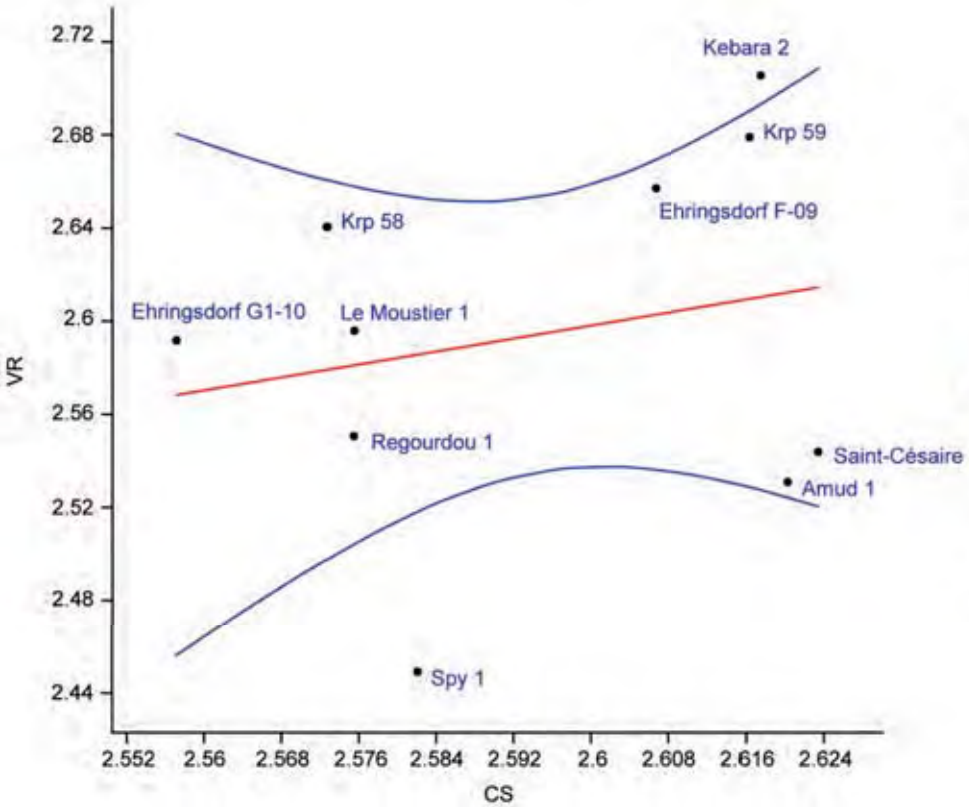

Slope a:	0.69594
Intercept b:	0.78865
Std. err. a:	1.1009
Std. err. b:	2.8567
Chi squared:	0.052582
r:	0.21811
r squared:	**0.047573**
t statistic:	0.63214
p(uncorrel):	0.54494
Permutat. p:	0.5442
p(a=1):	0.78941

95% bootstrapped confidence intervals:
a: [-1.564; 2.425]
b: [-3.698; 6.637]

SOM 4. *Continued.*

CS versus RV - Neanderthals C,

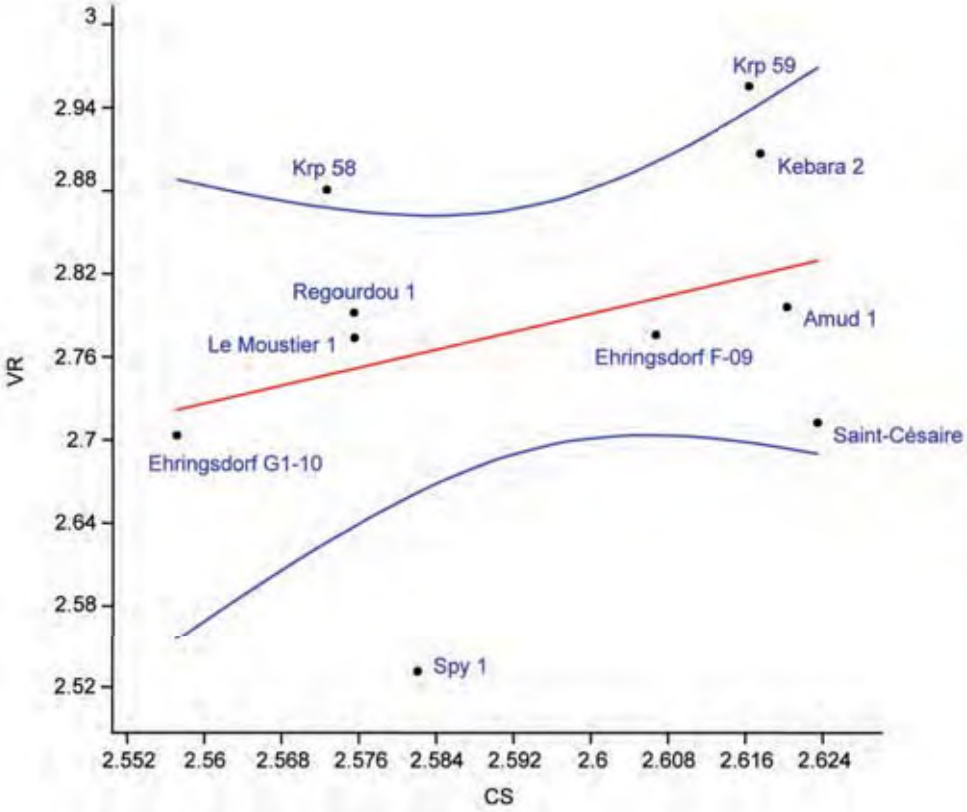

Slope a:	1,6225
Intercept b:	-1.4274
Std. err. a:	1.6326
Std. err. b:	4.2362
Chi squared:	0.11563
r:	0.33151
r squared:	**0.1099**
t statistic:	0.99386
p(uncorrel):	0.3494
Permutat. p:	0.3594
p(a=1):	0.71289

95% bootstrapped confidence intervals:
a: [-1.269; 4.264]
b: [-8.256; 6.126]

SOM 4. *Continued.*

CS versus RV - RMH I_1

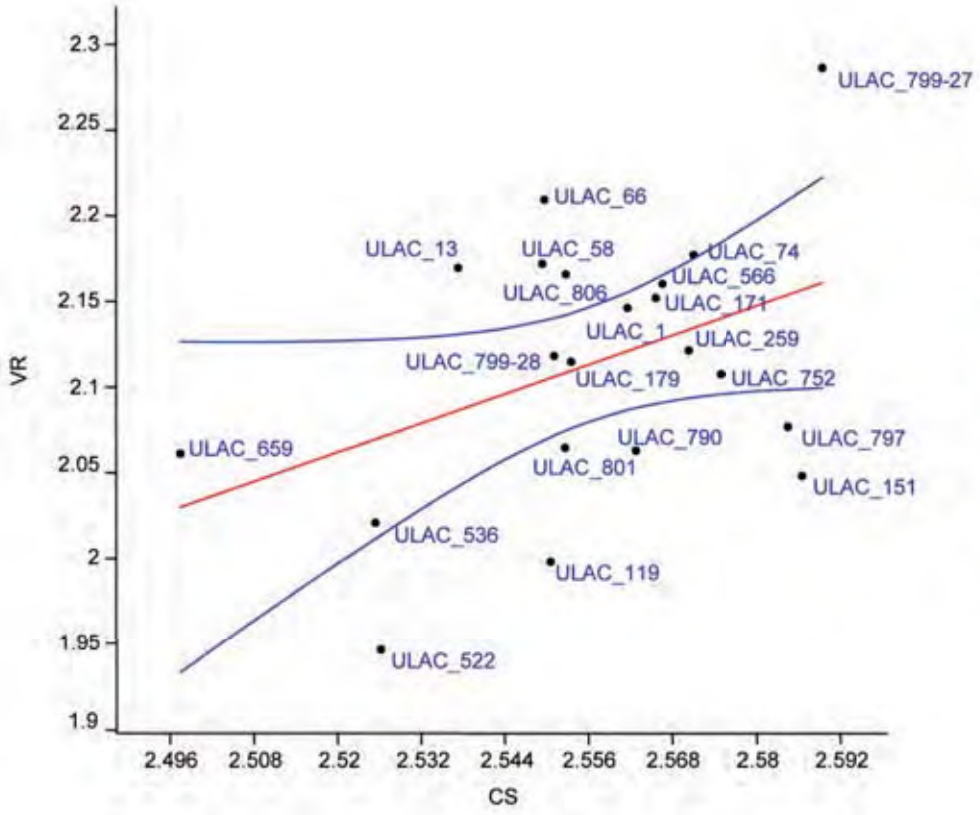

Slope a:	1.4222
Intercept b:	-1.5221
Std. err. a:	0.73887
Std. err. b:	1.8887
Chi squared:	0.1007
r:	0.40396
r squared:	**0.16319**
t statistic:	1.9249
p(uncorrel):	0.06935
Permutat. p:	0.0761
p(a=1):	0.57439

95% bootstrapped confidence intervals:
a: [-0.4544; 3.128]
b: [-5.884; 3.288]

SOM 4. *Continued.*

CS versus RV - RMH I_2

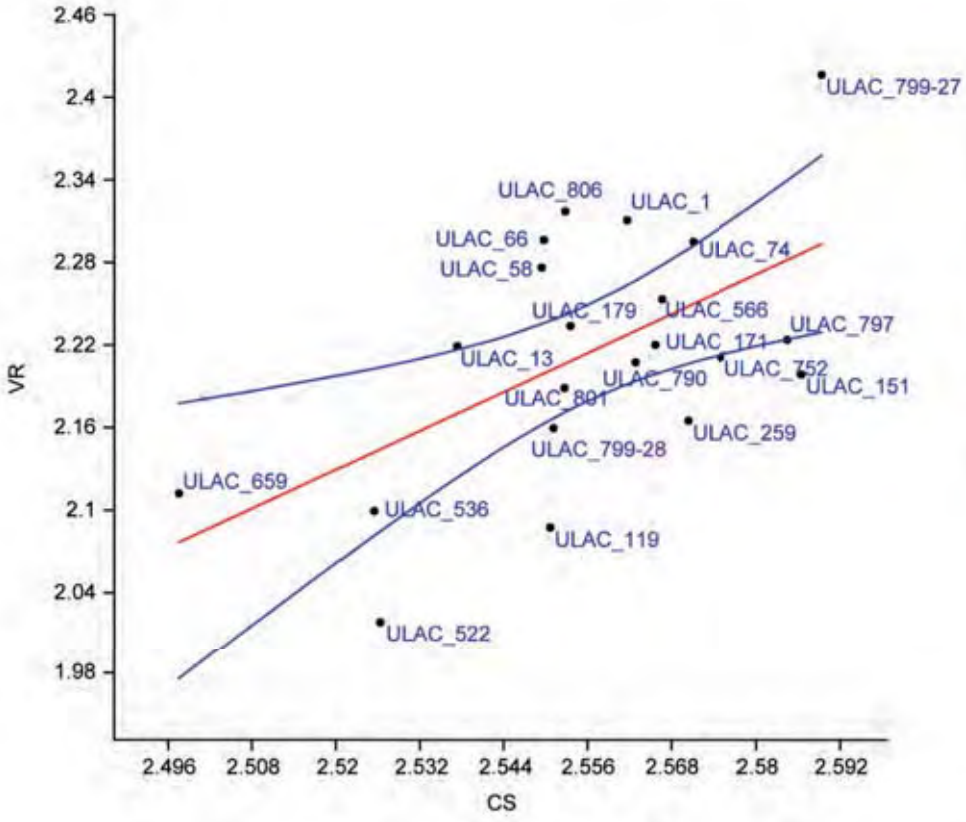

Slope a:	2.3563
Intercept b:	-3.8082
Std. err. a:	0.77261
Std. err. b:	1.9749
Chi squared:	0.11011
r:	0.57328
r squared:	**0.32865**
t statistic:	3.0498
p(uncorrel):	0.0065921
Permutat. p:	0.0064
p(a=1):	0.095288

95% bootstrapped confidence intervals:
a: [0.4633; 3.958]
b: [-7.914; 1.031]

SOM 4. *Continued.*

CS versus RV - RMH C.

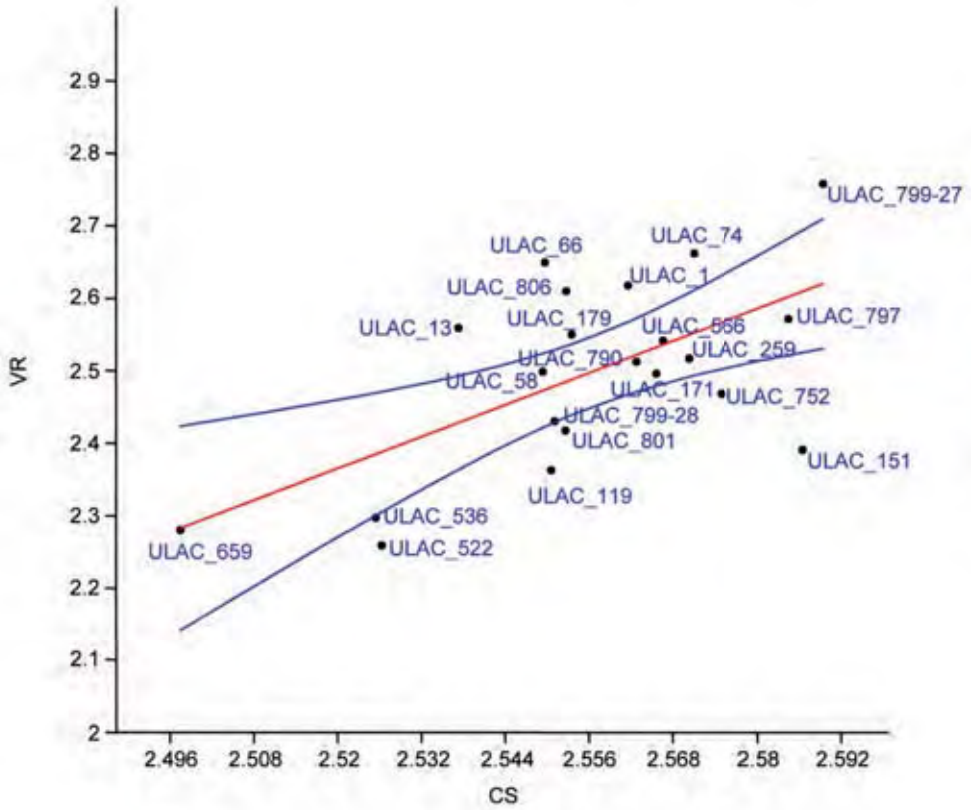

Slope a:	3.6678
Intercept b:	-6.8777
Std. err. a:	1.0777
Std. err. b:	2.7547
Chi squared:	0.21423
r:	0.61543
r squared:	**0.37876**
t statistic:	3.4035
p(uncorrel):	0.0029808
Permutat. p:	0.0028
p(a=1):	0.022888

95% bootstrapped confidence intervals:
a: [1.451; 6.465]
b: [-14.03; -1.214]

SOM 4. *Continued.*

CS versus RL - Neanderthals I_1

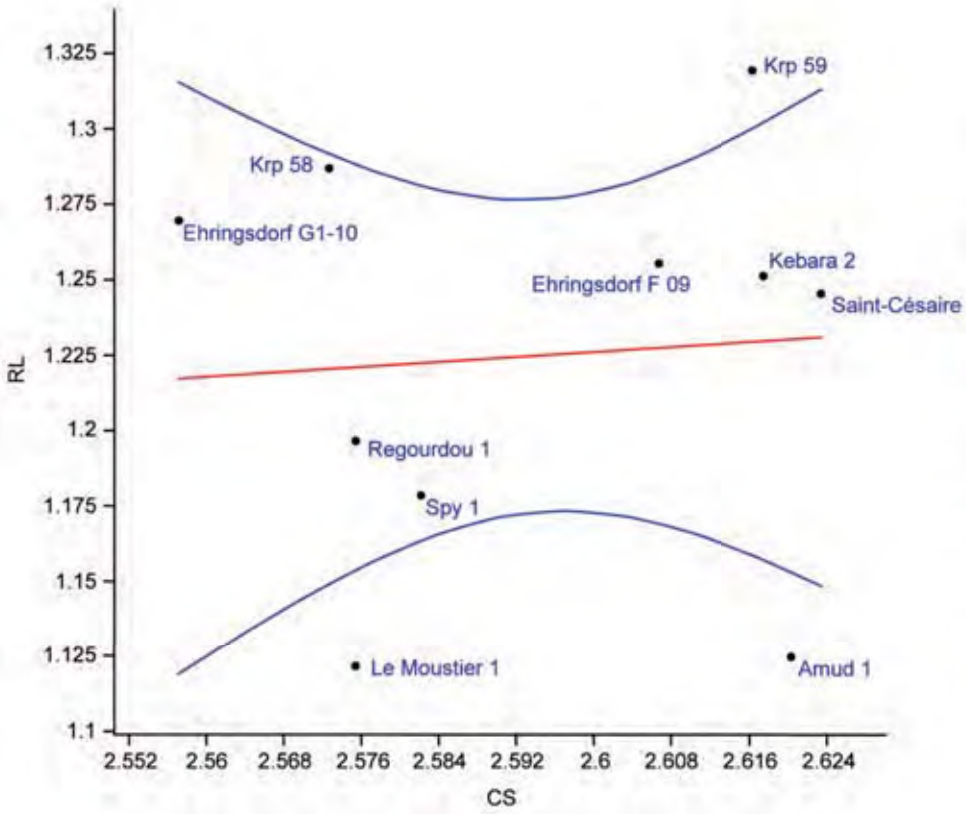

Slope a:	0.20434
Intercept b:	0.69463
Std. err. a:	0.96357
Std. err. b:	2.5003
Chi squared:	0.040279
r:	0.074766
r squared:	**0.00559**
t statistic:	0.21207
p(uncorrel):	0.83736
Permutat. p:	0.8291
p(a=1):	0.43288

95% bootstrapped confidence intervals:
a: [-1.977; 1.887]
b: [-3.664; 6.377]

SOM 4. *Continued.*

CS versus RL - Neanderthals I_2

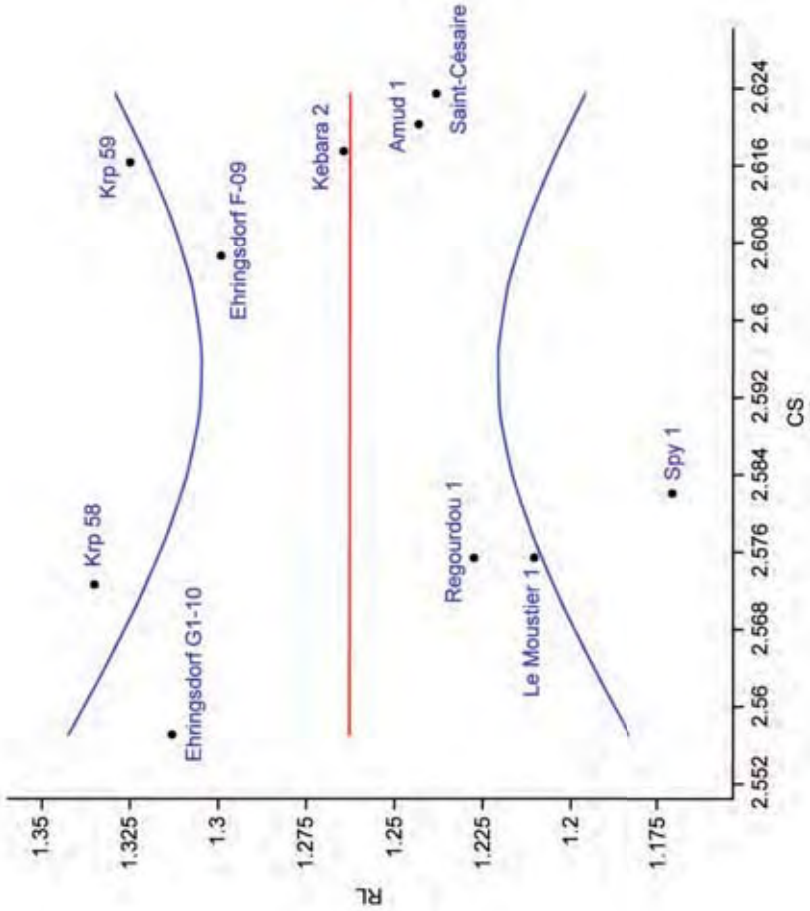

Slope a:	-0.0046774
Intercept b:	1.2747
Std. err. a:	0.78067
Std. err. b:	2.0257
Chi squared:	0.026439
r:	-0.0021183
r squared:	**4.4874e-06**
t statistic:	-0.0059916
p(uncorrel):	0.99537
Permutat. p:	0.9955
p(a=1):	0.2341

95% bootstrapped confidence intervals:
a: [-1.766; 1.081]
b: [-1.556; 5.868]

SOM 4. *Continued.*

CS versus RL - Neanderthals C,

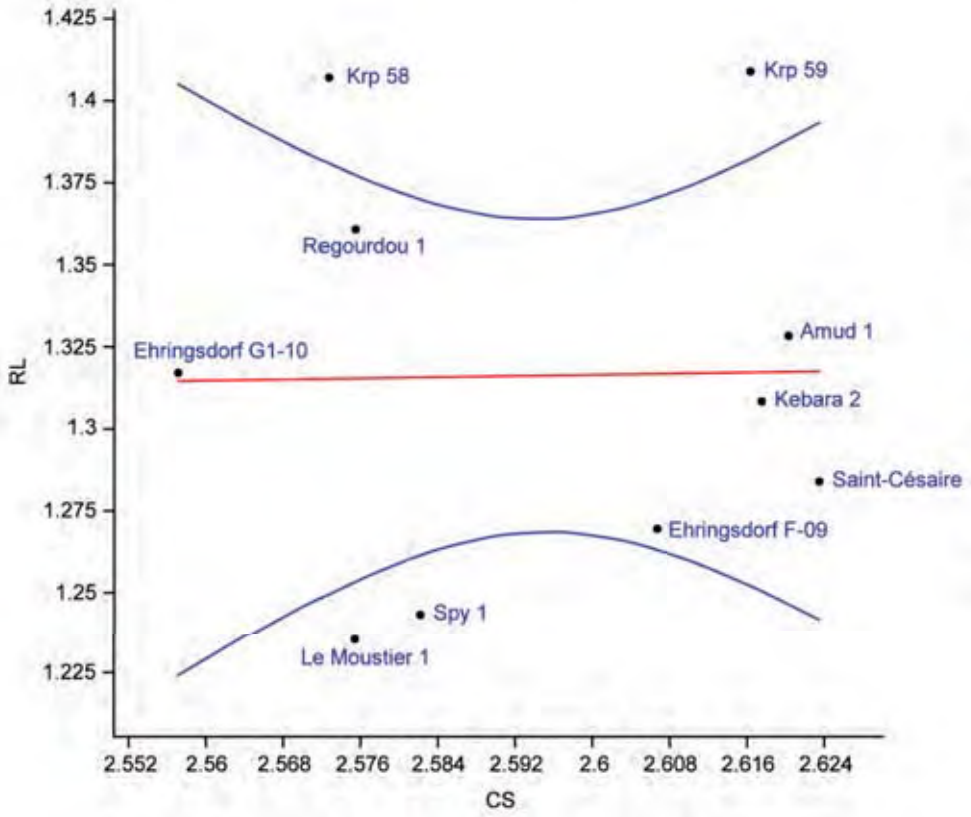

Slope a:	0.045302
Intercept b:	1.1987
Std. err. a:	0.88739
Std. err. b:	2.3026
Chi squared:	0.034162
r:	0.018046
r squared:	**0.00032567**
t statistic:	0.051051
p(uncorrel):	0.96054
Permutat. p:	0.9581
p(a=1):	0.31337

95% bootstrapped confidence intervals:
a: [-1.732; 1.643]
b: [-2.967; 5.858]

SOM 4. *Continued.*

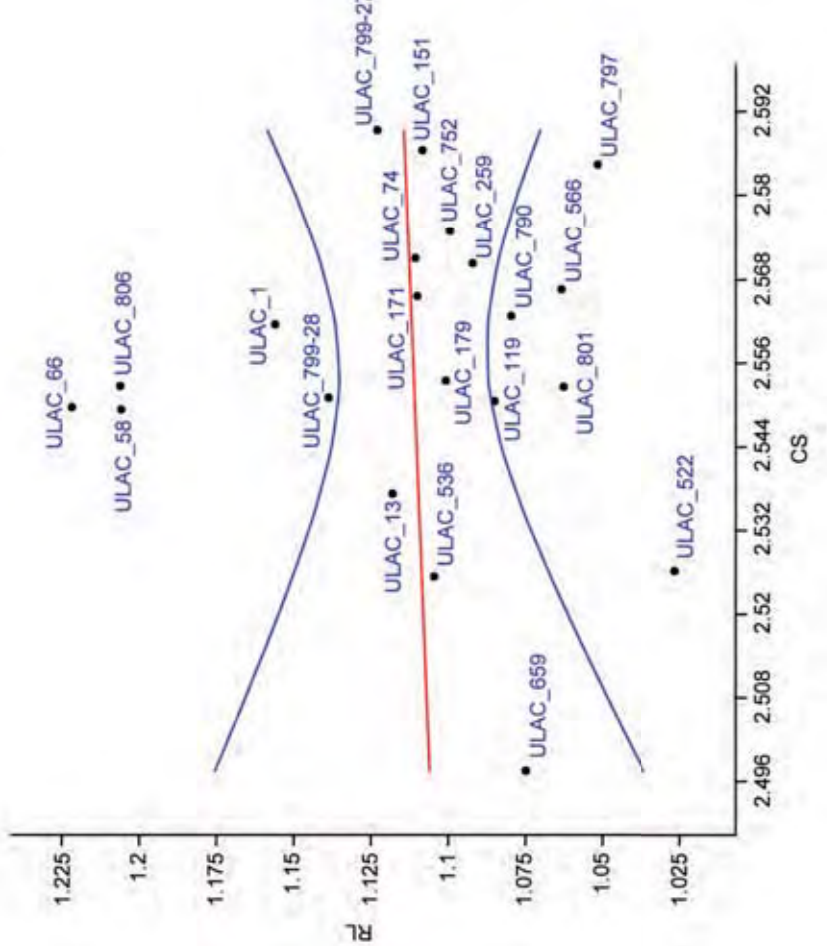

SOM 4. *Continued.*

CS versus RL - RMH I_2

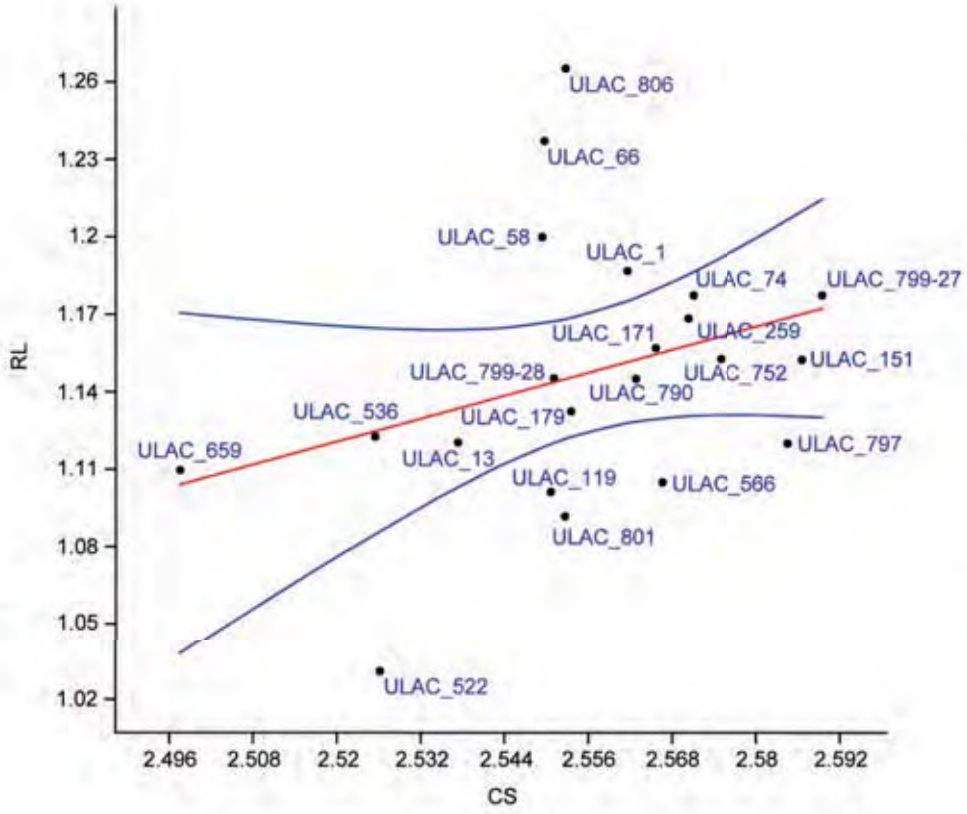

Slope a:	0.74038
Intercept b:	-0.74506
Std. err. a:	0.50843
Std. err. b:	1.2996
Chi squared:	0.047684
r:	0.31686
r squared:	**0.1004**
t statistic:	1.4562
p(uncorrel):	0.16166
Permutat. p:	0.1637
p(a=1):	0.61549

95% bootstrapped confidence intervals:
a: [-0.2143; 1.756]
b: [-3.365; 1.695]

SOM 4. *Continued.*

CS versus RL - RMH C.

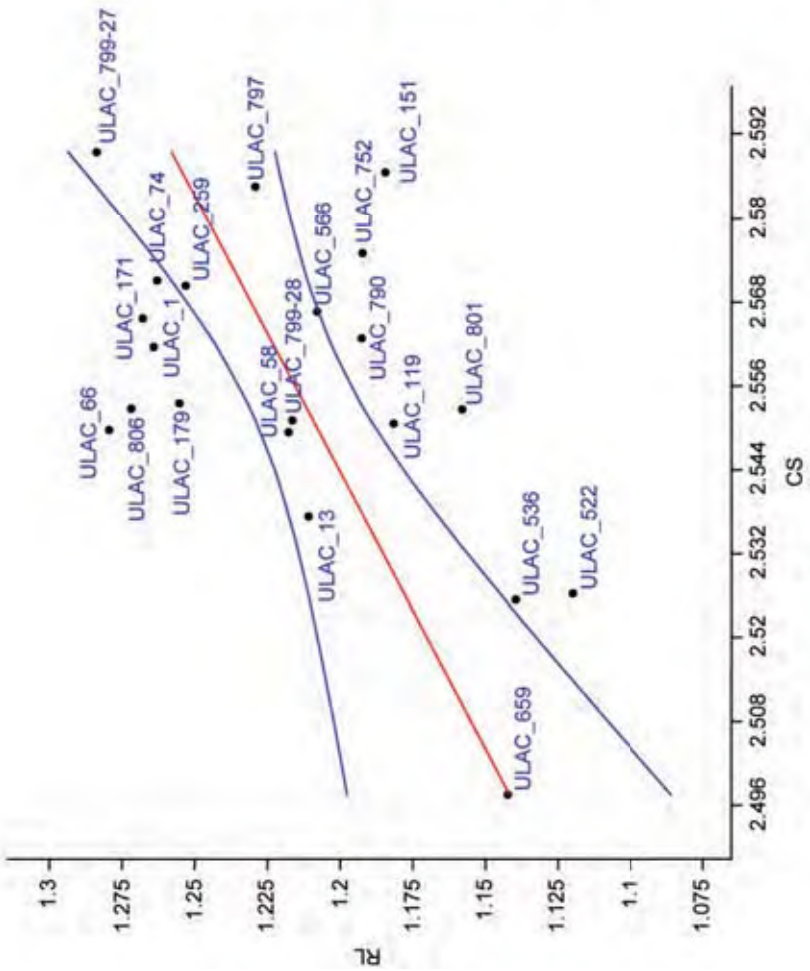

Slope a:	1.2635
Intercept b:	-2.0138
Std. err. a:	0.4279
Std. err. b:	1.0938
Chi squared:	0.033774
r:	0.56084
r squared:	**0.31454**
t statistic:	2.9527
p(uncorrel):	0.0081726
Permutat. p:	0.0081
p(a=1):	0.54539

95% bootstrapped confidence intervals:
a: [0.4358; 2.237]
b: [-4.514; 0.08875]

PART 2

Anterior Tooth Root Morphology and Size in Neanderthals: Taxonomic and Functional Implications

This part was published as:

Le Cabec A., et al. (2013). Anterior Tooth Root Morphology and Size in Neanderthals: Taxonomic and Functional Implications. *Journal of Human Evolution.* 64, pp. 169-193. http://dx.doi.org/10.1016/j.jhevol.2012.08.011

Received 19 December 2011; Accepted 8 August 2012; Available online 23 December 2012

AUTHORS

Adeline Le Cabec [a,b], Philipp Gunz [a], Kornelius Kupczik [a,c], José Braga [b], Jean-Jacques Hublin [a].

AUTHOR'S AFFILIATIONS

[a] Department of Human Evolution, Max Planck Institute for Evolutionary Anthropology, Deutscher Platz 6, 04103 Leipzig, Germany

[b] UMR 5288 CNRS, Anthropobiologie et Imagerie Anatomique, 37 Allées Jules Guesde, 31000 Toulouse, France

[c] Institut für Spezielle Zoologie und Evolutionsbiologie, Friedrich-Schiller-Universität Jena, Erbertstrasse 1, 07743 Jena, Germany

AUTHOR CONTRIBUTIONS

ALC, PG, KK, JB and JJH designed the study. ALC performed the scanning acquisition and micro-CT data reconstruction for some of the specimens studied, segmented the teeth, generated the 3D models and took the linear, surface and volumetric measurements. ALC designed and applied the method for the estimation of the missing portion of the developmentally or taphonomically incomplete roots. ALC collected the landmarks and curve and surface semi-landmarks. PG performed the geometric morphometric analysis for the root shape, and provided the R code for the PCA and CVA analyses.

PG, JJH and KK provided insightful comments on the text and contributed to improve the writing of the manuscript. JJH provided the facilities for micro-CT scanning, image processing, and for the scanning trips to Les Eyzies and Tel-Aviv. JB provided the micro-CT data for the 'Mandible 9726', scanned at the MEDES (Toulouse, France).

ABSTRACT

Comparing modern humans and Neanderthals, we have previously shown that recent modern humans (RMH) and Neanderthals differ in anterior root lengths, and that this difference cannot be explained by group differences in overall mandibular size. Here, we first document the evolutionary changes of root size and shape of the anterior upper and lower dentition in a broad chronological and geographical framework. We then use the size and shape differences between RMH and Neanderthals to classify several isolated teeth from Kebara cave and Steinheim, and to interpret the anterior tooth roots of the Tabun C2 mandible.

Our samples comprise permanent mandibular and maxillary incisors and canines from early *Homo*, Neanderthals, as well as extant and fossil modern humans (N=359). In addition to root length, we measured cervical root diameters and area, total root volume, root pulp volume and root surface area from µCT scans. We quantified root shape variation using geometric morphometrics.

Our results show that Neanderthals have not only significantly larger anterior roots than RMH overall, but also different root shapes for each tooth type. In the context of the 'teeth-as-tools' hypothesis, this could be an adaptation to better sustain high or frequent loads on the front teeth.

We demonstrate that the two isolated incisors stored with the Steinheim skull are very likely recent. Tabun C2 shows an anterior dentition similar in size and shape to Neanderthals while its molar roots are non-Neanderthal. Two of the five isolated teeth from Kebara are classified as Neanderthals.

Interestingly, early modern humans overlap with Neanderthals and RMH in root size and shape. Anterior roots of the Lower and Middle Pleistocene specimens are at least as large as Neanderthals, suggesting that Neanderthals retained a primitive pattern, which should prompt caution in the assessment of the earliest forms of modern humans.

KEYWORDS

Micro-CT; Incisors; Canines; Ancestral condition; Teeth-as-tools hypothesis

INTRODUCTION

Anterior tooth root length has been said to taxonomically distinguish Neanderthals from recent modern humans (Paquette, 1985; Smith and Paquette, 1989; Bailey, 2005). Descriptions of fossils have often remained qualitative, reporting 'long roots', and only the few studies mentioned above have attempted to quantify how long the Neanderthal anterior tooth roots actually are in comparison with modern humans. In the present study, we aim to document the variability of the anterior tooth root morphology in Neanderthals and modern humans in a broad geographical and chronological context. This knowledge could contribute not only to the taxonomical attribution of isolated teeth found during excavations or in museum collections, but also to the discussion of the uncertain taxonomy of some specimens. For example, debates are still going on regarding the taxonomic attribution of the Tabun C2 mandible (Hublin, 1998; Quam and Smith, 1998; Stefan and Trinkaus, 1998; Schwartz and Tattersall, 2000; Rak, 2002; Rak et al., 2002), five isolated teeth from the Kebara cave (Chech et al., 2003), and two isolated maxillary incisors supposedly from Steinheim. We will investigate how anterior tooth root morphology can contribute to this matter.

These large incisors have been related to the robusticity of the Neanderthal craniofacial skeleton, which is characterized by the combination of mid-facial prognathism and a large nasal aperture (Rak, 1986; Demes, 1987; Trinkaus, 1987; Smith and Paquette, 1989; Antón, 1990, 1994, 1996; Hublin, 1998; Rosas et al., 2006). However, we have recently shown that mandibular anterior tooth root size is not correlated with jaw size in either Neanderthals or recent modern humans. In addition, short roots in recent modern humans would result from a negative evolutionary allometry, while the longer roots in Neanderthals could result from the retention of an ancestral condition (Le Cabec et al., 2011, 2012). In comparison with earlier hominids, the early *Homo* incisors and canines have been described as increasing the size of their root and of their crown, which also display shoveling, labial convexity, marginal ridges and a lingual tubercle, although more weakly expressed than in Neanderthals (Patte, 1962; Wolpoff, 1999).

Whether the previously mentioned traits of the Neanderthal craniofacial skeleton have any adaptive significance remains debated. Although some authors have emphasized the role of drift in craniofacial Neanderthal evolution (Hublin, 1998;

Weaver et al., 2007; Rae et al., 2011), most explanations for the process of generating morphological variation in the Neanderthal face relate to developmental or adaptive issues. Churchill (1998) invokes mechanical and systemic effects on bone remodeling. In her study on the changes of orientation of the maxillary part of the face in Neanderthals, Couture (1993) argued that the Neanderthal face more likely results from morphogenetic processes rather than solely from the masticatory function, as proposed in many hypotheses discussed hereafter.

Purely adaptive hypotheses have been raised: adaptation to cold and dry climate (Coon, 1962; Franciscus and Trinkaus, 1988; Churchill, 1998; Franciscus, 1999, 2003; but see Rosas et al., 2006; Holton and Franciscus, 2008; Rae et al., 2011), or to an abrasive diet (Puech, 1981).

Finally, a purely biomechanical hypothesis, known as the 'anterior dental loading hypothesis', involves the dental and cranial morphology. The need for such a large anterior dentition would have been related to the whole evolution of the maxillofacial architecture of the Neanderthal face. This involves mid-facial prognathism and the steepness of the naso-alveolar *clivus*, which would better stand vertical forces exerted in a particular anterior dental loading regime (Smith, 1983; Rak, 1986; Demes, 1987; Spencer and Demes, 1993). Neanderthals would have used their anterior teeth for purposes other than incision of food, such as a tool or a third hand for para- and non-masticatory activities (Coon, 1962; Brace et al., 1964; Brace, 1975; Wallace et al., 1975; Smith, 1976a, b, 1983; Demes, 1987; Trinkaus, 1987; Smith and Paquette, 1989; Spencer and Demes, 1993; Fox and Frayer, 1997; Rosas et al., 2006; Rae et al., 2011). Here, we aim to discuss this hypothesis in light of the documented variability in anterior tooth root morphology. Regarding dental size, anterior tooth use and attrition, Neanderthals are often compared with the Inuit and Australian Aborigines (Molnar, 1971; Barrett, 1977; Hinton, 1981), who show relatively larger anterior teeth and a higher rate of attrition than other modern human populations. This pattern is thought to be an adaptive response to para-masticatory activities (Smith, 1976a) involving the processing of objects in contact with abrasive particles (sand), e.g., during skin preparation (Hylander, 1977). Wang et al. (2010) demonstrate that the Inuit and Neanderthals adopted two different morphological conformations of their mid-facial skeleton to adapt to high and frequent loads on their anterior dentition.

Since stable isotope studies portray Neanderthals as top-level carnivores (Richards et al., 2000, 2001, 2008), this would argue in favor of a highly demanding loading regime on the anterior dentition. As it has been documented in Arctic populations (Merbs, 1968), this may involve pre-ingestion processing steps, for instance slicing pieces of meat, following the 'stuff-and-cut' hypothesis (Koby, 1956; Brace, 1975), where Neanderthals would have clamped a piece of meat between their upper and lower incisors with one hand, while the other manipulates a stone tool to cut off the portion that sticks out from the lips (Patte, 1960; Ungar and Spencer, 1999).

The use of the anterior dentition as a tool has not only been suggested for Krapina (e.g., Lee, 2006), but also for earlier stages of evolution of the Neanderthal lineage, as well as for modern human hunter-gathers (e.g., the Natufians from Hayonim, in Eshed et al., 2006). The Middle Pleistocene European hominin dental remains from Boxgrove show considerable wear, secondary dentine and striations on the labial aspect of the crown and root (Hillson et al., 2010). The use of the teeth as a third hand has been suggested for Mauer and some teeth from Arago, based on complex microwear features and polished enamel surfaces (Puech, 1979; Lozano et al., 2008). Likewise, in the Sima de los Huesos dental remains, complex labial striations and microwear on the anterior teeth also attest that para-masticatory activities certainly have been performed by this population predating Neanderthals (Bermúdez de Castro et al., 1988, 2003; Bermúdez de Castro, 1993; Lozano-Ruiz et al., 2004; Lozano et al., 2008). It should however be emphasized that, despite marked entheses and powerful bony structures in the Neanderthal craniofacial skeleton (Rak, 1986; Demes, 1987), several studies suggest a poor efficiency in generating powerful anterior bite forces (Antón, 1990, 1994, 1996). Rather than being clearly more powerful in terms of muscular masticatory forces, Neanderthals could have exerted more frequent anterior dental loadings (O'Connor et al., 2005). Their anterior teeth are said to occlude in 'edge-to-edge' (Sakura, 1970; Puech, 1981; Ungar et al., 1997). The wear pattern observed in the Sima de los Huesos dental remains has led Bermúdez de Castro (1988) to suggest that the occlusion of these European Middle Pleistocene hominins was edge-to-edge. In this type of occlusion, incisal edges are in direct contact, whereas in modern humans the lingual face of the upper incisors covers the labial face of the lower incisors in an overbite. This mode and frequency of occlusion likely account for the higher rate of attrition in Neanderthals, without rejecting the possibility for para-masticatory activities. However, Kaifu and

colleagues (Kaifu, 2000; Kaifu et al., 2003) propose that edge-to-edge occlusion would have been the normal type of occlusion within the *Homo* lineage. They observe that in recent modern human populations with a heavily abrasive diet, the occlusion changes throughout life with a scissors occlusion in a mixed denture to an edge-to-edge occlusion when wear increases with ageing, i.e., involving a decrease in overjet (incisor lingual tipping) and overbite (occlusal wear). In this theory, occlusal wear would be the cause of the edge-to-edge bite (Ungar et al., 1997; Kaifu et al., 2003).

The present study aims to document the permanent maxillary and mandibular incisor and canine root size and shape in Neanderthals, in a broad chronological and geographical framework. Using a large set of linear, surface and volume measurements, as well as geometric morphometric techniques, we explore the taxonomic value of anterior tooth root size and shape to distinguish Neanderthals from early and recent modern humans. Finally, documenting anterior tooth root size and shape will contribute to the discussion on the anterior dental loading hypothesis in Neanderthals.

MATERIALS AND METHODS

SAMPLES

The samples under study comprise a total of 359 permanent mandibular and maxillary incisors (central and lateral) and canines from fossil and extant individuals from diverse chronological and geographical origins (Tables 1 and 2). We compare the anterior tooth root dimensions in a sample of 95 Neanderthal teeth, ranging from MIS 7 to MIS 3 and covering a large geographical area from Spain to Siberia and from Germany to Israel, with a sample of 26 teeth of penecontemporaneous (MIS 5) early modern humans (EMH) from Israel and Morocco, represented by specimens from Qafzeh and Skhul, and from Grotte des Contrebandiers (Temara) and Dar-es-Soltane II, respectively. Two isolated maxillary incisors are curated with the Steinheim skull (Gieseler, 1971; Adam, 2003; Street et al., 2006) despite the fact that, in the literature, there is no mention of their discovery at the Steinheim Quarry. However, their affiliation remains unknown since exploratory statistics have led us to question their taxonomic attribution, and even their provenience from the Steinheim site itself. In addition, we study how root dimensions position the Tabun C2 mandible, a specimen from the Levant, which is subject to intense debates regarding its taxonomic attribution (Quam and Smith, 1998;

Rak, 2002; Hublin, 2007) in our samples. Regarded as a Neanderthal by some researchers (e.g., Stefan and Trinkaus, 1998), Tabun C2 is contrastingly labeled as an early modern human by others (Rak et al., 2002). We also studied five isolated teeth without clear stratigraphic context from the Kebara Cave (Israel). For three of them, Chech and colleagues (2003) limit the chronological attribution to 'probably Mousterian'. The two other Kebara teeth are labeled in the collection of Tel-Aviv University as from 'unknown provenience', coming from the cleaning of the stratigraphic profile for one tooth and from the excavations by Turville-Petre for the other tooth. Taking advantage of our large comparative samples of Neanderthals and recent modern humans, we will test and discuss a possible taxonomic classification for these debated specimens, using a canonical variate analysis. A group of Upper Paleolithic and Epipaleolithic modern humans (UPEPIH) from MIS 2 and 1 brings together Ohalo II and Oberkassel (Upper Paleolithic) on the one hand, as well as Combe-Capelle and the Natufian Hayonim and Nahal-Oren (Epipaleolithic) specimens on the other hand (See Table 1). The KNM-WT 15000 *H. ergaster* specimen, Sangiran 4 and a few isolated teeth from Sangiran 7, as well as the Middle Pleistocene Mauer mandible (Schoetensack, 1908; Wagner et al., 2010), are included in our study to understand the ancestral condition in root dimensions. Our recent modern human comparative sample (RMH) comprises 167 teeth coming from clinical extractions and anatomical collections. Information on sex, ethnicity and age were either documented by the dental practitioners or are based on the records of the collections (estimations from dental and skeletal maturation). The individuals selected also represent various ethnicities (See Table 1). The comparative modern series were selected based on the state of preservation and on the stage of formation of the roots of the incisors and canines (fully closed root apices). However, we did include some specimens for which the root tip has been taphonomically broken or damaged, or that are developmentally incomplete. For these specimens, we computed an estimation of the root portion missing as explained later in this section. For specimens having both antimeres, we chose the best preserved side regarding the preservation of the root, of the cervical line and finally of the crown. It should be noted that due to preservation, the crown measurements for the Skhul IV mandibular canine were taken on the right tooth, while root measurements were performed on the left tooth. Specimens presenting pathological conditions were discarded.

Table 1. Fossil and extant specimens included in this study.

Chronological attribution	Taxon	Site	Specimen
Lower Pleistocene	*H. ergaster*	Nariokotome, Western Turkana, Kenya	KNM-WT 15000 A and B (1.53 ± 0.05 Ma, Delson et al., 2000).
	H. erectus	Sangiran, Indonesia Pucangan, Sangiran, Indonesia	Sangiran 4 (older than 1.5 Ma, Larick et al., 2001) S7-47, S7-48, S7-50 (older than 1.5 Ma, Larick et al., 2001)
MIS 15	*H. heidelbergensis*	Mauer, Heidelberg, Germany	Mauer (609 ± 40 ka, Wagner et al., 2010).
MIS 9 ?	*H. neanderthalensis ?*	Steinheim an der Murr, Ludwigsburg, Germany	Steinheim (250 or >300 ka, Street et al., 2006).
MIS 7	*H. neanderthalensis*	Weimar-Ehringsdorf, Germany	Ehringsdorf F 09, G1 10 and G3 12 (~230 ka, Blackwell and Schwarcz, 1986).
MIS 6	*H. neanderthalensis*	Abri Suard, La Chaise-de-Vouthon, France	S33 (Riss III, NESPOS).
	Early modern human or *H.neanderthalensis*	Tabun, Wadi el-Mughara, Mount Carmel, Israel	Tabun C2 (171 ± 17 ka, Mercier et al., 2000; 100-130 ka, Grün et al., 2005).
MIS 5	*H. neanderthalensis*	Abri Bourgeois-Delaunay, La Chaise-de-Vouthon, France HuSnjakovo rock shelter, Krapina, Croatia	BD1, BD20, BD 21, BD13, BD12, BD10, BD11, BD15, BD16 (135 ka, Condemi, 2001). Krp49 (Maxilla E), Krp50 (Maxilla F), Krp 53 (Mandible C), Krp 54 (Mandible D), Krp 55 (Mandible E), Krp 58 (Mandible H), Krp 59 (Mandible J), Krp D36, Krp D37, Krp D56, Krp D76, Krp D122, Krp D123, Krp D125, Krp D126, Krp D127, Krp D156, Krp D157, Krp D 158, Krp D159 and Krp D160 (130 ± 10 ka, Rink et al., 1995).
	Early modern humans	Qafzeh, Wadi el-Hadj, Israel Skhul, Wadi el-Mughara, Mount Carmel, Israel Grotte des Contrebandiers, Temara, Morocco	Qafzeh 8, 9, 11 and 15 (100-135 ka, Grün et al., 2005) Skhul IV (100-130 ka, Grün et al., 2005) Temara mandible (107 ± 4 - 96 ± 4 ka, Jacobs et al., 2011)
	H. neanderthalensis	Regourdou, Montignac, France Sclayn, Andenne, Belgium	Regourdou 1 (Maureille and Tillier, 2008; Turq et al., 2008) Scladina 1 (layer 4A, Pirson et al., 2008)

Table 1. *Continued.*

Chronological attribution	Taxon	Site	Specimen
MIS 5-4	*H. neanderthalensis*	Combe-Grenal, Domme, France	Combe-Grenal V, X, XI, 27 (75-65 ka, "relative chronology" by Guadelli & Laville, 1990, cited in Garralda and Vandermeersch, 2000)
	Early modern humans	Dar-es-Soltane II, Rabat, Morocco	Dar-es-Soltane II H4 mandible (121 ka, Schwenninger et al., 2010)
MIS 4	*H. neanderthalensis*	Kebara, Mount Carmel, Israel	Kebara 2 (60 ka, Valladas et al., 1987)
	H. neanderthalensis ?		KHM 27 and KMH 31 ("Probably Mousterian human remains", Chech et al., 2003)
	H. sapiens?		KMH 28 ("Probably Mousterian human remains", Chech et al., 2003 and records from Tel-Aviv University)
	H. sp?		Keb90-E19R2 (Turville- Petre's excavations) and KebA5N13-463 (unknown proveniance "Kebara dumps").
	H. neanderthalensis	Chagyrskaya Cave, Altai Mountains	Chagyrskaya 6 (end of MIS 4, Viola et al, 2012)
MIS 3	*H. neanderthalensis*	La Roche-à-Pierrot rock shelter, Saint-Césaire, France	Saint-Césaire 1 (36.3 ± 2.7 ka, Mercier et al., 1991)
		El Sidrón, Asturias, Spain	SD_331_ab, SD_703 and SD_599 (43 ka, Rosas et al., 2006)
		Le Moustier, France	Le Moustier 1 (40 ka, Valladas et al., 1986)
		Amud Cave, Israel	Amud 1 (41.5 ka, Delson et al., 2000)
		Spy Cave, Jemeppe-sur-Sambre, Belgium	Spy I (36 ka, Semal et al., 2009)
		Les Pradelles, Marillac-le-Franc, France	M71-C10 F12-93 (40-45 ka, Pérez-Pérez et al., 2003)
MIS 2	*H. sapiens*	Ohalo II, Sea of Galilee, Israel	Ohalo II H1 and H2 (19 ka, Nadel and Hershkovitz, 1991; Hershkovitz et al., 1995)
		Hayonim Cave, Ma'arat Hayonim, Mugharet el-Hamam, Galilee, Israel	Hayonim 8, 17, 19, 20, 25 (12.010 ± 180 ka, Belfer-Cohen, 1988; Bocquentin, 2003; Pinhasi et al., 2008)
		Bonn-Oberkassel, Germany	Oberkassel D999 (11.570 ± 100 ka, Street et al., 2006)
		Nahal-Oren, Mount Carmel, Israel	Nahal-Oren 8, 14, 16, 24 (11.300 - 10.500 BP, Belfer-Cohen, 1988; Bocquentin, 2003; Pinhasi et al., 2008)

Table 1. *Continued.*

Chronological attribution	Taxon	Site	Specimen
MIS 1	*H. sapiens*	Roc de Combe-Capelle, France	Combe-Capelle (7.596-7.577 ka cal. BC, Hoffmann et al., 2011)
		Jacobshaven, Disko Bay, Greenland	Mandible 9726 (mission of Ch. Rabot in 1895-17)
		Mandibles from the Anatomy collection, University of Leipzig, Germany from diverse geographical areas.	ULAC 1 (M, Germany); 13 (F, Germany), 58 (M, Norway); 66 (F, Norway/Sweden); 74, 151, 171 and 179 (M, Italy/Etruscan); 119 (F, Italy/Etruscan); 259 (M, Algeria); 522, 536, 566 and 607 (M, Egypt) ; 659 (F, Egypt) ; 752 (M, Sudan) ; 799-27 (U, Black American) ; 799-28 (U,U) ; 790, 797 and 806 (M, Afro-Americans/New Orleans) ; 801 (F, Afro-American/New Orleans).
		Marrakech, Morroco	M10, M15
		from diverse geographical areas, mostly Germany and Europe.	isolated permanent teeth from Max-Planck-Institute's collection of clinical extractions
		diverse ethnicities	isolated permanent teeth from Paul Brown's collection of clinical extractions.
		Romanian dental remains from the XX^{ieth} century	dental specimens from the Institutul de Antropologie "Francisc J. Rainer", Romania

MIS = Marine Isotopic Stage. For the recent modern humans from the ULAC collection, the catalog specimen number is followed in parentheses by sex estimation based on anthropological criteria (M = male, F = female, U = unknown) and geographical origin (U = unknown).
ka = thousands of years ago; BP = before present; cal. BP = calibrated years before present.

Table 2. Sample sizes by tooth type and taxonomical group.

	Maxillary dentition			Mandibular dentition			
	I^1	I^2	C'	I_1	I_2	C,	**Total**
H. erectus	1	-	2	-	1	-	**4**
H. ergaster	1	1	1	1	1	1	**6**
H. heidelbergensis	-	-	-	1	1	1	**3**
Steinheim	1	1	-	-	-	-	**2**
Neanderthals	17	18	12	17	15	16	**95**
Tabun C2	-	-	-	1	1	1	**3**
Early modern humans (EMH)	3	3	3	5	6	6	**26**
Upper Paleolithic and Epipaleolithic humans (UPEPIH)	6	6	8	9	10	10	**49**
Kebara isolated teeth	-	-	1	-	2	1	**4**
Recent modern humans (RMH)	24	22	12	39	47	23	**167**
Total	**53**	**51**	**39**	**73**	**84**	**59**	**359**

Abbreviations for the tooth types: I^1 = maxillary central incisor; I^2 = maxillary lateral incisor; C' = maxillary canine; I_1 = mandibular central incisor; I_2 = mandibular lateral incisor; C, = mandibular canine.

MICRO-CT IMAGE ACQUISITION AND 3D MODEL GENERATION

In situ and isolated teeth were scanned at the Max Planck Institute for Evolutionary Anthropology (Leipzig, Germany) on a BIR ARCTIS 225/300 industrial micro-CT scanner (most commonly used scan parameters: 130 kV, 100 µA, 0.25 to 0.5 mm brass filter, 0.144 degree of rotation step) or on a Skyscan 1172 micro-CT scanner (most commonly used scan parameters: 100 kV, 100 µA, 0.5 mm aluminum and 0.04 mm copper filters, 0.12 to 0.25 degree of rotation step, 360 degrees of rotation, 2 frames averaging). Acquisitions were performed to image the dentition at high resolution with an isotropic voxel-size ranging from 13.38 to 148.1 µm. This allows for a fine quantification of dental tissue surface areas and volumes. The specimens that were scanned at 13 µm were downsampled to 30 µm without compromising the quality of the image data (Skinner, 2008). Data for Spy 1 were produced on a Siemens Somatom 64 CT-scanner with an isometric pixel size of 0.299 mm and a slice thickness of 0.1 mm (NESPOS). The RMH 'Mandible 9726' was scanned at 41 µm on the XtremeCT micro-

scanner (Scanco) at the MEDES (Toulouse, France). To facilitate the dental tissue segmentation in Avizo 6.2 (Mercury Systems), the reconstructed high resolution micro-CT slices were filtered using a median filter followed by a mean-of-least-variance filter (each with a kernel size of three) to reduce the background noise while preserving and enhancing edges (Kuwahara et al., 1976; Schulze and Pearce, 1994). Dental tissues (enamel, dentine and pulp) were first semi-automatically segmented by thresholding and then the segmentation was manually edited. All modern human teeth and some of the best preserved fossil teeth (with good contrast) were segmented using a customized automated segmentation algorithm based on the watershed principle (Beucher and Lantuejoul, 1979). Minor manual editing was performed after running the algorithm, especially regarding cracks that may not have been well detected. Despite a very similar radiodensity to dentine (Pinheiro et al., 2008), in some cases hypertrophic cementum (conspicuous and irregularly thick accumulation of cementum on the surface of the apical root third) was detected on the micro-CT scans (Fig. 1). The hypertrophic cementum was thus segmented as a separate material following the segmentation protocol described above. For most of the Abri Bourgeois-Delaunay teeth under study, we identified demineralization on an even thickness of the root involving both dentine and hypertrophic cementum, when present. This may be the result of taphonomic processes. These demineralized tissues were segmented and attributed to dentine and cementum, respectively. Cracks in the enamel and dentine were segmented, as well as separate materials, when they were clearly detectable on the scans so as to avoid an overestimation of root volume and surface area, and of root length in case of a large transverse crack. Following this segmentation process, 3D surface models of the teeth were generated using a constrained smoothing algorithm in Avizo. We define the cervical plane by setting landmarks at the points of greatest curvature on the labial and lingual sides of the cemento-enamel junction and computing the best-fit plane based on a least squares criterion. Each tooth was then virtually divided into crown and root by cutting the 3D models at the previously defined cervical plane (Fig. 2A and B).

MEASUREMENT METHODS

Estimation of the missing apical portion of the root in taphonomically broken or developmentally incomplete specimens Some specimens with incomplete roots were included in the sample if the missing apical portion of the root was small. The roots may

have been incomplete for developmental reasons, due to post-mortem damage (during fossilization, excavation or handling for fossils) or in the case of recent specimens, because of damage occurring during clinical extractions. To avoid introducing biases into our samples, we estimated the missing portion in terms of root length, surface area and total volume. This was done by modeling the missing part as an elliptic cone. We tested for the reliability of this method by artificially cutting intact roots of known dimensions, and then estimating the missing portion. Our results (see Results section) consistently show a small amount of underestimation of the root values. For detailed explanations, see SOM Table 1.

Anterior tooth crown size (Table 3) Because occlusal and interproximal wear affect the mesio-distal diameter of the crown, as well as its volume, we limited the estimation of crown size to the maximum labio-lingual crown diameter (CrLL). This was measured following Martin's definition (M81(1) in Bräuer, 1988) as the maximal distance between the lingual and labial sides of crown, perpendicular to the mesio-distal diameter of the tooth (Fig. 2B). The volume of the pulp cavity in the crown is reported as well.

Anterior tooth root size (Table 3) Root size was quantified by measuring the root length (RL) on the 3D models of the individualized roots as the linear distance between the root apex and the center of the cervical plane of the tooth using the 3D tool measurement in Avizo 6.2 (Fig. 2C). The total root volume (RV) was calculated as the sum of the pulp cavity and dentine volumes (as well as the volume of hypertrophic cementum when this dental tissue has been segmented, Fig. 2D). The volume of the radicular pulp (RPV) was reported as well (Fig. 2D). On the cervical plane, we measured the cervical area (CA), as well as the labio-lingual and mesio-distal root diameters (Fig. 2E). The root surface area (RSA) was measured as the surface area of the radicular dentine (Fig. 2F). In addition, we measured the labial and lingual root surface areas (RSA Lab and RSA Ling) by cutting the 3D models of the root using a plane defined by three landmarks set at the root apex and at the point of greatest curvature of the cervical line on the mesial and on the distal aspects of the tooth (Figs. 2F and G). When we want to refer to all of the root variables at the same time, we use the term 'root size'.

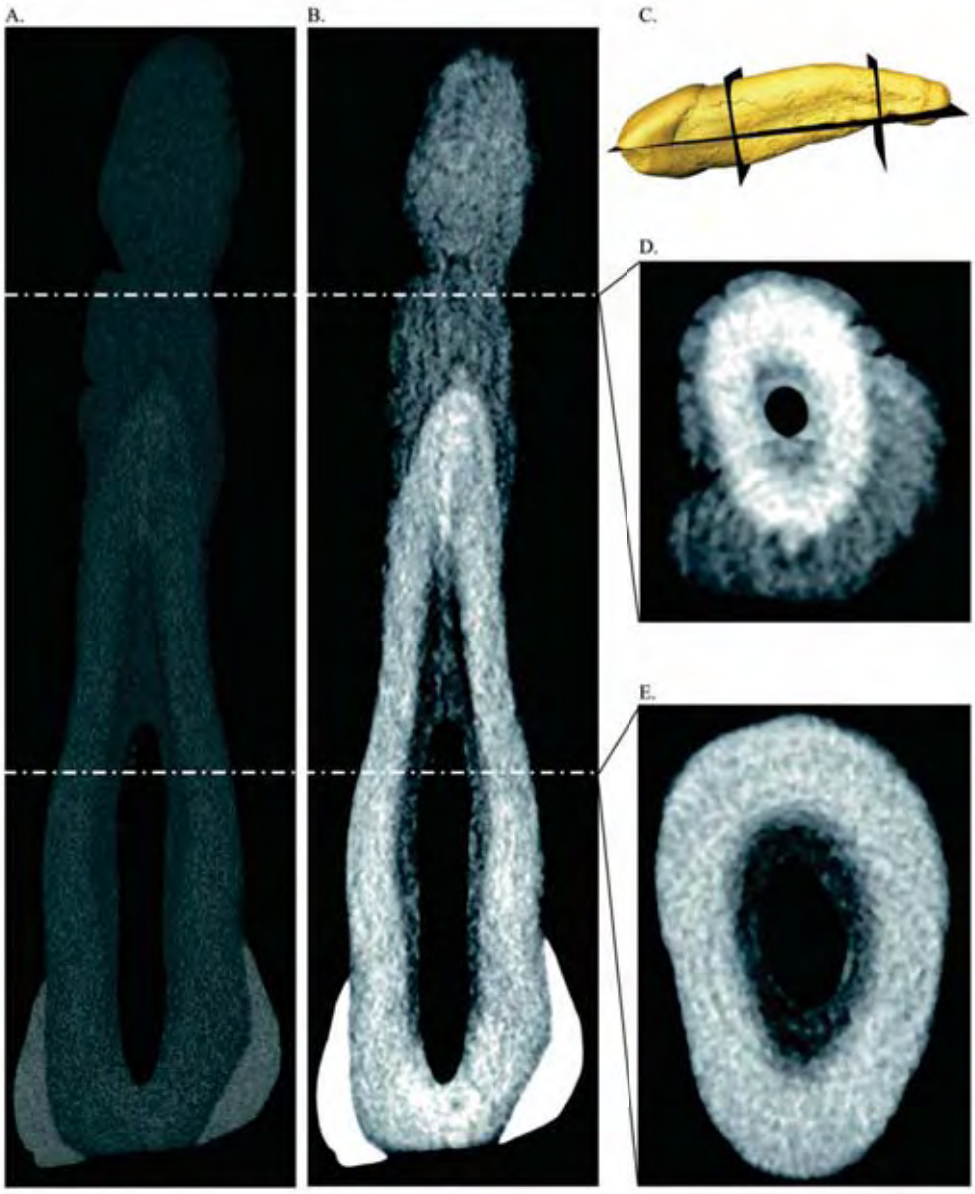

Figure 1. Visualization of hypercementosis and secondary dentine on the root of the Neanderthal maxillary canine BD15 (Abri Bourgeois-Delaunay, France). An iterative median filter (kernel size of seven, three iterations) was applied to the original micro-CT data (1A) to decrease the amount of noise in the pictures. Width and center of the window of gray values of the filtered stack were then modified to better identify the borders between materials, as shown on the mesio-distal slice (1B). Figure 1C gives the location of the filtered slice on the tooth. This image processing allows for clear distinction between the primary dentine and the overgrowth of cementum on the one hand (1D), and between primary and secondary dentine on the other hand (1E).

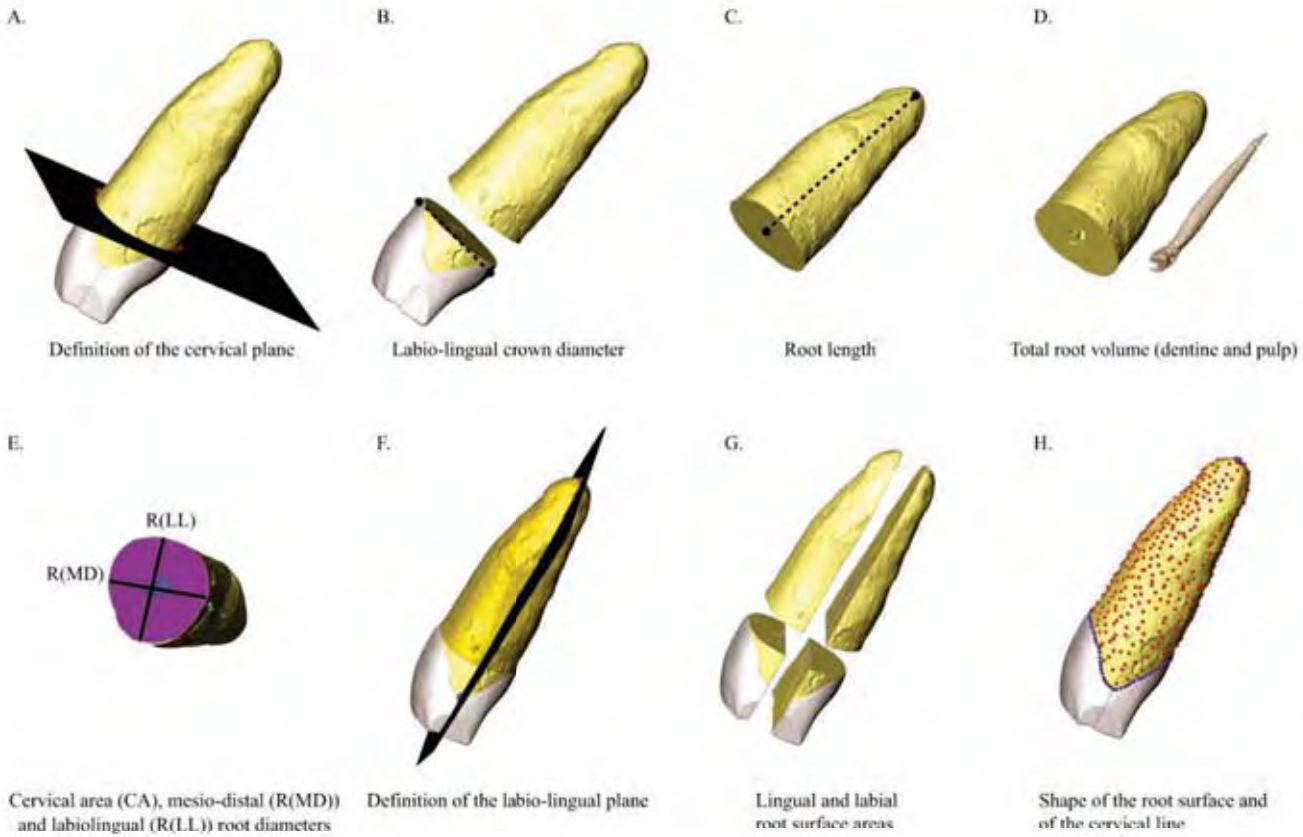

Figure 2. Techniques for crown and root measurements on the 3D models of the Saint-Césaire maxillary central incisor. After defining the cervical plane based on a best fit plane (2A), the tooth is virtually cut into a root and a crown (2B), which allows us to measure the maximum labio-lingual crown diameter (2B) and the root length (2C) from the center of the cervical plane to the root apex. The total root volume includes dentine and pulp (2D). Cervical diameters and surface area are measured on Fig. 2E. The root surface area [in dark yellow (web version)] is measured on the root (2F), and a labio-lingual cutting plane is defined to get the surface areas of the labial and of the lingual sides of the root (2G). Finally, Fig. 2 H shows that the shape analysis involves the cervical line and the root apex (blue semilandmarks) as well as the surface semilandmarks spread on the root surface (red).

Table 3. Definition of the metrics used in this study.

Metrics	Abbreviation	Complete definition	Dimension	Descriptive statistics
Maximum labio-lingual crown diameter	**CrLL**	Maximal distance between the lingual and labial sides of crown, perpendicular to the mesio-distal diameter of the tooth, following Martin's definition (M81(1) in Bräuer, 1988).	mm	Tables 4a and 4b
Root length	**RL**	Linear distance between the root apex and the center of the cervical plane of the tooth using the 3D tool measurement in Avizo 6.2.	mm	Tables 4a and 4b
Mesio-distal root diameter	**R(MD)**	In the mesio-distal direction, largest dimension of the root passing by the center of the cervical plane and parallel to this plane.	mm	SOM Tables 4a and 4b
Labio-lingual root diameter	**R(LL)**	In the labio-lingual direction, largest dimension of the root passing by the center of the cervical plane and parallel to this plane.	mm	SOM Tables 4a and 4b
Root surface area	**RSA**	Outer surface area of the radicular dentine.	mm^2	Tables 4a and 4b
Labial root surface area	**RSA Lab**	Surface area of the labial aspect of the root measured by cutting the 3D models of the root using a plane defined by three landmarks set at the root apex and at the greatest point of curvature of the cervical line on the mesial and on the distal aspects of the tooth.	mm^2	SOM Tables 4a and 4b
Lingual root surface area	**RSA Ling**	Surface area of the lingual aspect of the root measured by cutting the 3D models of the root using a plane defined by three landmarks set at the root apex and at the greatest point of curvature of the cervical line on the mesial and on the distal aspects of the tooth.	mm^2	SOM Tables 4a and 4b
Cervical area	**CA**	Surface area of the previously defined cutting plane between the crown and the root.	mm^2	SOM Tables 4a and 4b
Root volume	**RV**	Sum of the dentine and pulp volumes in the root.	mm^3	Tables 4a and 4b
Root pulp volume	**RPV**	Volume of the pulp cavity in the root.	mm^3	Tables 4a and 4b
Crown pulp volume	**CrPV**	Volume of the pulp cavity in the crown.	mm^3	SOM Tables 4a and 4b
	CrLL/RL	Ratio between the labio-lingual crown diameter and the root length.	dimensionless	SOM Tables 4a and 4b
	R(LL)/R(MD)	Ratio between the labio-lingual and the mesio-distal root diameters at the cervix.	dimensionless	SOM Tables 4a and 4b
	RSA lab/ling	Ratio between the labial and the lingual root surface areas.	dimensionless	SOM Tables 4a and 4b
	RSA/CA	Ratio between the root surface area and the cervical area.	dimensionless	SOM Tables 4a and 4b
	CrPV/RPV	Ratio between the volumes of the pulp in the crown and of the pulp in the root.	dimensionless	SOM Tables 4a and 4b
	RPV/RV	Ratio between the root pulp volume and the total root volume.	dimensionless	SOM Tables 4a and 4b

Although a detailed study about hypercementosis is beyond the scope of this paper, when hypertrophic cementum was identified on the µCT images and when a manual segmentation could be performed, we reported the volume of hypertrophic cementum for each specimen, and expressed its contribution to the total volume of the root as a percentage.

Root surface and cervical line shape analyses We selected a subset of teeth with complete roots, intact root surfaces and well preserved cervical lines (we work on the 3D models of the complete teeth). Small cracks were merged to the dentine as long as they did not disturb the overall morphology of the tooth. Specimens that are taphonomically distorted were otherwise discarded for this analysis. To investigate whether Neanderthals and recent modern humans differ in root shape, we used

geometric morphometric techniques, assessing shape differences using semilandmarks (Bookstein, 1997; Gunz et al., 2005, 2009). Geometric morphometric analyses require the analyzed points to be homologous (Bookstein, 1991; Mitteroecker and Gunz, 2009). To distribute the same number of points in homologous locations on every specimen we used the following protocol. For each tooth of interest, we first placed a landmark at the root apex (enlarged blue point on Fig. 2H), then a sequence of point coordinates was recorded along the cemento-enamel junction. Those semilandmarks were then resampled to 50 initially equidistant curve semilandmarks. We then placed 499 surface semilandmarks on the root surface of a reference specimen. This surface was delimited by the cervical landmarks and by the apical landmark. Those 499 points were then projected on the root surface of each tooth (following the protocol described in Gunz et al., 2005). By resampling the complex root surface to 500 surface semilandmarks, we are effectively smoothing the surface and thereby removing the confounding effect of surface irregularities. However, as equidistance is an intuitive, yet arbitrary way of distributing semilandmarks, this does not necessarily lead to geometric or biological correspondence of the points across specimens (Bookstein, 1997; Gunz et al., 2005). Likewise, the spacing of surface semi-landmarks is also arbitrary. Gunz et al. (2005) have shown that equidistance can lead to serious statistical and visualization artifacts. The semilandmarks were thus allowed to slide along their curve or surface to remove the effects of the arbitrary spacing by optimizing the position of the semilandmarks with respect to the average shape of the entire sample (average of the Procrustes shape coordinates). Allowing the points to slide along the cervical outline and the root surface then establishes geometric homology among the semilandmarks. For a technical description of the semilandmark algorithm, see Gunz et al. (2005).

STATISTICAL ANALYSES

Descriptive statistics are provided for all investigated groups and dental variables. Unless stated otherwise, we pooled the sexes for the RMH, since no reliable information is available for our fossil samples. Despite the fact that parametric tests are more powerful, non-parametric tests were preferred due to our relatively small sample sizes. First, crown and root variables were compared using the non-parametric Mann-Whitney U test (exact, two-tailed, α=0.05, U_{Min} reported) to determine whether Neanderthals have larger anterior tooth roots and/or larger crowns than RMH (our

largest samples). Then, we tested whether root size is correlated with crown size, within RMH and within Neanderthals, using the Spearman rank order correlation test (method: approximate, two-tailed, 1000 permutations, α=0.05, r_S reported; p values Bonferroni corrected). To assess multivariate trends in the data, we performed a principal component analysis (PCA) using the correlation matrix and a canonical variate analysis (CVA, see Mitteroecker and Bookstein, 2011 for discussion about these methods). For these multivariate analyses, we used all variables, except for crown pulp volume (since apposition of tertiary dentine at the roof of the pulp cavity can affect the results in Neanderthals).

TAXONOMIC AFFINITIES OF DEBATED SPECIMENS FROM ROOT DIMENSIONS

We used CVA to compute the likelihood of the anterior teeth of Steinheim, Tabun C2 and the Kebara Cave of belonging to one of the three reference groups that are Neanderthals, early and recent modern humans, using posterior probabilities. These three reference groups are made up of taxonomically conclusive dental remains. We used equal prior probabilities for all groups (p=1/3 to belong to each of the three groups). Posterior probabilities were computed using the 'leave-one-out' cross-validation technique.

All statistical analyses and graphics were generated in R 2.12.1 (Becker et al., 1988; Ligges and Maechler, 2003; Murrell, 2005; Weihs et al., 2005; Calenge, 2006; Dray and Dufour, 2007; Sarkar, 2008; Peng et al., 2010; R Development Core Team, 2010; Hothorn and Hornik, 2011). The cervical line and root surface shape analyses and the associated PCA were performed in Mathematica (Wolfram, Inc.).

RESULTS

ESTIMATION OF INCOMPLETE ROOTS

Virtually breaking off various amounts of the root tip on complete teeth show that overall all root variables remain underestimated in comparison with the actual values (see negative percentages in SOM Table 1). Differences between the intact teeth and the artificially cut teeth reveals a mean of -3.87% for the root length estimation, -3.86% for the root surface area, and finally -1.97% for the root volume estimation. We decided to include our total estimated values in the statistical analyses (only for root

length, surface area and total volume), since this may be more informative than reporting the actual measurements without reconstruction. Both corrected and non-corrected values are nonetheless reported in SOM Tables 2a and 2b, with the proportion of what is missing to the total corrected value. For some of the EMH (bolded and underlined in SOM Tables 2a and 2b), the estimation reveals a non-negligible portion of the root is missing (>15% for the root length and > 5% for the root surface area and volume), we have nonetheless reported these corrected values to document these scarce specimens.

ANTERIOR TOOTH CROWN SIZE

RMH males and females do not show significant differences in crown size (maximum labio-lingual crown diameter) in our sample. Although this has been tested, we remind that our samples are small and that various ethnicities have been sampled and pooled together here (see results of Mann-Whitney U tests in SOM Tables 3a and 3b). Neanderthals have significantly larger anterior tooth crowns and crown pulp volumes than RMH (Tables 4a, 4b, 5a and 5b, SOM Tables 4a and 4b). The range of EMH in crown size overlaps with both Neanderthals and RMH (Tables 4a and 4b).

ANTERIOR TOOTH ROOT SIZE

As for the crown, male and female RMH do not show a consistent pattern of sexual dimorphism in root dimensions (see results of Mann-Whitney U tests in SOM Tables 3a and 3b). However, for the mandibular lateral incisors, males display significantly larger root length, volume and surface area than females. For all root variables, Neanderthals have absolutely and significantly larger roots than RMH (Tables 4a, 4b, 5a and 5b, SOM Tables 4a and 4b). Neanderthals have significantly larger cervical root diameters than RMH. Consistently, in Neanderthals, the root surface area is greater on the labial side than on the lingual side, for both maxillary and mandibular teeth.

In recent modern humans, the canines and the mandibular lower incisors show a similar proportion of root surface area on the lingual and labial sides, the lingual surface being greater in central incisors, while the labial surface is larger in maxillary lateral incisors.

Table 4a. Descriptive statistics for the upper anterior dentition.

			CrLL [mm]	RL [mm]	RSA [mm²]	RV [mm³]	RPV [mm³]
H. erectus	S7_48	I^1	7.42	15.40	269.06	364.75	18.70
	S7_47	C'	10.93	21.52	458.72	755.07	43.42
	Sangiran 4	C'	11.82	21.68	543.59	868.67	90.62
H. ergaster	N=1	I^1	9.11	20.35	407.49	664.1	49.62
	N=1	I^2	7.9	18.84	425.32	464.92	27.32
Steinheim?	N=1	I^1	8.15	12.68	185.86	202.33	9.93
	N=1	I^2	6.08	13.95	191.90	200.82	9.52
Neanderthals	N=17	I^1	8.41 ± 0.58 [7.83-9.58] (6.88)	17.23 ± 2.40 [10.54-19.79] (13.95) *{15.7–19.7}*	315.31 ± 60.66 [162.90-409.32] (19.24)	452.00 ± 123.52 [195.84-693.61] (27.33)	37.25 ± 20.74 [2.00-85.97] (55.68)
	N=18	I^2	8.74 ± 0.60 [7.97-9.77] (6.83)	17.62 ± 1.85 [14.69-19.97] (10.48) *{15.0–19.2}*	343.08 ± 42.87 [252.79-409.22] (12.50)	487.24 ± 90.99 [310.68-633.22] (18.68)	31.36 ± 18.10 [9.25-81.67] (57.73)
	N=12	C'	9.69 ± 0.67 [8.76-11.01] (6.89)	22.51 ± 2.48 [17.69-25.16] (11.02) *{18.1–26.2}*	454.30 ± 60.28 [311.23-539.41] (13.27)	650.57 ± 98.94 [406.87-817.26] (15.21)	36.65 ± 14.84 [16.44-66.34] (40.50)
Isolated teeth from Kebara	KMH 27	I^2	8.22	15.41	305.82	450.19	21.05
	Keb90-E19R2	C'	8.00	14.73	238.83	280.58	13.78
EMH		I^1	N=3; 7.84 ± 0.66 [7.08-8.22] (8.36)	N=2; 16.61 ± 3.55 [14.10-19.12]	N=2; 265.76 ± 88.35 [203.29-328.23]	N=2; 346.74 ± 180.86 [218.85-474.63]	N=2; 18.21 ± 17.18 [6.06-30.36]
	N=3	I^2	7.39 ± 0.56 [6.80-7.91] (7.56)	15.08 ± 2.92 [11.71-16.79] (19.34)	230.04 ± 69.04 [150.49-274.29] (30.01)	266.53 ± 115.46 [137.44-359.94] (43.32)	21.66 ± 10.85 [11.67-33.20] (50.08)
	N=3	C'	9.03 ± 0.94 [8.25-10.07] (10.38)	18.19 ± 2.26 [15.65-19.96] (12.41)	315.30 ± 33.85 [295.05-354.38] (10.74)	426.43 ± 68.70 [384.88-505.73] (16.11)	28.79 ± 24.90 [10.09-57.06] (86.50)

Table 4a. *Continued.*

UPEPIH	N=6	I^1	7.52 ± 0.24 [7.23-7.86] (3.21)	13.50 ± 2.09 [10.61-15.80] (15.48)	220.25 ± 38.50 [166.18-276.11] (17.48)	274.95 ± 65.65 [197.44-388.04] (23.88)	10.87 ± 3.34 [5.71-16.22] (30.74)
	N=6	I^2	6.54 ± 0.51 [5.76-7.02] (7.75)	13.70 ± 1.82 [10.78-15.81] (13.26)	188.35 ± 33.39 [155.52-241.54] (17.73)	193.01 ± 47.14 [193.01-137.87] (24.43)	7.74 ± 3.21 [3.36-11.45] (41.45)
	N= 8	C'	8.98 ± 0.59 [7.79-9.74] (6.56)	16.90 ± 2.09 [12.55-19.57] (12.37)	278.24 ± 43.89 [216.30-342.31] (15.77)	343.56 ± 73.63 [229.55-459.33] (21.43)	16.36 ± 5.89 [7.13-25.08] (36.00)
RMH	N=24	I^1	7.12 ± 0.48 [6.28-8.45] (6.79)	12.94 ± 1.39 [11.08-16.32] (10.73)	192.33 ± 30.43 [142.58-262.53] (15.82)	225.60 ± 46.60 [147.75-333.03] (20.66)	8.74 ± 5.18 [1.61-24.05] (59.26)
	N=22	I^2	6.43 ± 0.46 [5.70-7.51] (7.11)	12.98 ± 1.41 [10.06-16.27] (10.84)	172.11 ± 28.01 [109.00-224.88] (16.27)	172.22 ± 39.65 [94.10-256.16] (23.02)	6.90 ± 4.99 [0.86-19.98] (72.33)
	N=12	C'	7.85 ± 0.63 [6.75-8.54] (8.05)	16.07 ± 1.43 [13.53-18.71] (8.89)	254.20 ± 37.79 [200.85-318.76] (14.87)	308.10 ± 71.25 [213.56-423.88] (23.13)	9.54 ± 4.05 [2.92-15.17] (42.42)

N = sample size. We report Mean ± standard deviation [minimum-maximum] (coefficient of variation). Ranges reported by Bailey (2005) are recalled in italics, in curly brackets. We describe the maximum labio-lingual crown diameter (CrLL), the root length (RL), the root surface area (RSA), the total root volume (RV) and the root pulp volume (RPV).

Table 4b. Descriptive statistics for the lower anterior dentition.

			CrLL [mm]	RL [mm]	RSA [mm²]	RV [mm³]	RPV [mm³]
H. erectus	S7_50	I_2	7.81	17.11	290.62	317.12	22.55
H. ergaster	N=1	I_1	6.66	19.39	280.28	289.62	6.26
	N=1	I_2	7.38	20.15	386.65	466.9	20.93
H. heidelbergensis	N=1	I_1	7.43	16.5	277.01	292.7	16.21
	N=1	I_2	7.91	16.7	313.7	370.3	21.78
	N=1	C,	8.71	20.8	410.58	565.9	44.7
Neanderthals	N=17	I_1	7.37 ± 0.31 [6.93-8.02] (4.17)	17.19 ± 1.93 [13.80-20.86] (11.25) *{15.7–16.6}*	300.66 ± 43.48 [195.57-358.86] (14.46)	330.34 ± 62.15 [200.08-421.73] (18.81)	12.76 ± 6.74 [5.16-24.89] (52.81)
	N=15	I_2	7.74 ± 0.67 [6.71-9.45] (8.60)	18.42 ± 2.03 [14.81-21.63] (11.02) *{15.3–17.9}*	335.93 ± 50.58 [240.21-403.59] (15.06)	396.22 ± 77.40 [258.89-507.60] (19.53)	21.01 ± 15.05 [6.63-63.03] (71.64)
	N=16	C,	8.83 ± 0.63 [7.97-10.61] (7.13)	20.71 ± 2.95 [16.05-25.64] (14.24) *{16.3–23.2}*	412.37 ± 97.14 [221.79-619.68] (23.56)	602.33 ± 152.63 [339.49-902.34] (25.34)	32.70 ± 19.12 [11.57-70.75] (58.48)
Kebara isolated teeth	KMH 28	I_2	7.10	15.67	282.49	331.41	25.10
	KebA5N13 -463	I_2	7.23	13.40	193.35	208.92	12.03
	KMH 31	C,	8.54	21.02	376.07	485.14	18.33
Tabun C2	N=1	I_1	6.97	18.29	294.98	330.08	11.45
	N=1	I_2	7.25	19.95	351.13	436.68	14.23
	N=1	C,	8.53	22.46	427.09	593.27	21.85

Table 4b. *Continued*

			CrLL [mm]	RL [mm]	RSA [mm²]	RV [mm³]	RPV [mm³]
EMH	N=5	I_1	6.42 ± 0.64 [5.69-7.14] (10.03)	14.43 ± 1.21 [13.71-16.56] (8.41)	194.72 ± 44.02 [122.46-229.11] (22.61)	183.89 ± 54.47 [98.89-230.43] (29.62)	11.11 ± 7.63 [4.39-22.66] (68.70)
	N=6	I_2	6.95 ± 0.53 [6.28-7.78] (7.58)	15.41 ± 1.58 [13.71-17.34] (10.23)	234 ± 47.76 [144.60-269.15] (20.33)	251.24 ± 70.02 [130.26-323.81] (27.87)	12.96 ± 6.17 [3.92-20.63] (47.63)
	N=6	C,	8.58 ± 0.65 [7.72-9.50] (7.63)	17.78 ± 1.31 [16.09-19.81] (7.37)	325.36 ± 49.56 [255.50-395.87] (15.23)	443.98 ± 101.06 [315.03-586.75] (22.76)	N=5; 41.15 ± 20.52 [15.66-62.45] (49.86)
UPEPIH	N=9	I_1	6.15 ± 0.37 [5.59-6.74] (6.09)	12.74 ± 0.84 [11.84-14.20] (6.61)	168.19 ± 17.40 [152.13-203.05] (10.34)	145.42 ± 21.53 [121.21-182.69] (14.81)	3.88 ± 1.60 [0.92-5.61] (41.20)
	N=10	I_2	6.49 ± 0.33 [5.98-6.90] (5.04)	14.73 ± 1.03 [13.31-16.17] (6.96)	199.10 ± 20.82 [180.57-236.90] (10.46)	180.07 ± 25.66 [149.23-232.89] (14.25)	5.09 ± 1.72 [1.77-6.71] (33.73)
	N=10	C,	7.87 ± 0.51 [7.15-8.82] (6.50)	15.92 ± 1.74 [13.45-18.88] (10.95)	258.27 ± 25.76 [215.69-307.67] (9.98)	295.50 ± 41.94 [208.71-373.61] (14.19)	13.17 ± 3.91 [5.78-19.98] (29.71)
RMH	N=39	I_1	5.92 ± 0.39 [5.14-6.71] (6.58)	12.67 ± 1.45 [10.12-16.66] (11.43)	154.29 ± 23.61 [115.34-200.65] (15.30)	127.49 ± 26.18 [75.48-193.28] (20.53)	4.04 ± 2.13 [1.17-11.21] (52.67)
	N=47	I_2	6.29 ± 0.42 [5.23-7.26] (6.61)	14.09 ± 1.42 [10.73-18.41] (10.11)	185.83 ± 26.15 [129.79-241.58] (14.07)	165.99 ± 32.34 [101.63-260.60] (19.48)	5.47 ± 2.88 [0.77-15.15] (54.67)
	N=23	C,	7.70 ± 0.72 [6.27-9.05] (9.41)	16.55 ± 1.80 [13.18-19.22] (10.88)	271.32 ± 53.55 [185.08-387.71] (19.74)	327.07 ± 93.48 [181.58-572.45] (28.58)	16.73 ± 9.36 [7.17-48.13] (55.98)

N = sample size. We report Mean ± standard deviation [minimum-maximum] (coefficient of variation). Ranges reported by Bailey (2005) are recalled in italics, in curly brackets. We describe the maximum labio-lingual crown diameter (CrLL), the root length (RL), the root surface area (RSA), the total root volume (RV) and the root pulp volume (RPV).

Table 5a. Mann-Whitney *U* test results for the comparison of the crown and root dimensions in the upper dentition between recent modern humans and Neanderthals.

		I^1 N_{Hn}=17 N_{Hs}=24	I^2 N_{Hn}=18 N_{Hs}=22	C^1 N_{Hn}=12 N_{Hs}=12
CrLL [mm]	U_{Min}	13	0	0
	p	***4.92e-09***	***1.76e-11***	***7.40e-07***
CrPV [mm³]	U_{Min}	63	30	8
	p	***9.03e-05***	***4.92e-07***	***4.96e-05***
R(MD) [mm]	U_{Min}	57	8	5.5
	p	***3.80e-05***	***1.16e-09***	***1.48e-05***
R(LL) [mm]	U_{Min}	2	0	0
	p	***5.28e-11***	***1.76e-11***	***7.40e-07***
RL [mm]	U_{Min}	29	5	2
	p	***2.95e-07***	***3.26e-10***	***2.96e-06***
RSA [mm²]	U_{Min}	24	0	1
	p	***9.58e-08***	***1.76e-11***	***1.48e-06***
RSA lab [mm²]	U_{Min}	7	0	1
	p	***5.94e-10***	***1.76e-11***	***1.48e-06***
RSA ling [mm²]	U_{Min}	61	2	9
	p	***6.89e-05***	***7.06e-11***	***7.17e-05***
CA [mm²]	U_{Min}	12	0	0
	p	***3.56e-09***	***1.76e-11***	***7.40e-07***
RV [mm³]	U_{Min}	19	0	1
	p	***2.75e-08***	***1.76e-11***	***1.48e-06***
RPV [mm³]	U_{Min}	29	16	0
	p	***2.88e-07***	***1.61e-08***	***7.40e-07***
CrLL/RL	U_{Min}	81	189	38.5
	p	***7.60e-4***	*ns*	*ns*
R(LL)/R(MD)	U_{Min}	201	192.5	46
	p	*ns*	*ns*	*ns*
RSA lab/ling	U_{Min}	4	59.5	30.5
	p	***1.39e-10***	***7.28e-05***	***0.015***
RSA/CA	U_{Min}	82	95	39
	p	***7.55e-04***	***0.0034***	*ns*
CrPV/RPV	U_{Min}	125.5	133	51
	p	***0.037***	*ns*	*ns*
RPV/RV	U_{Min}	74.5	113.5	18
	p	***3.69e-04***	***0.021***	***1.02e-03***

Minimal U values and p values [bold when statistically significant] are reported. Variables investigated are the maximum crown labio-lingual diameter (CrLL), the crown pulp volume (CrPV), the mesio-distal root diameter (R(MD)), the labio-lingual root diameter (R(LL)), the root length (RL), the root surface area (RSA), the surface areas of the labial and of the lingual aspects of the root (RSA lab and RSA ling respectively), the cervical area (CA), the total root volume (RV), the root pulp volume (RPV) and their ratios.

Table 5b. Mann-Whitney *U* test results for the comparison of the crown and root dimensions in the lower dentition between recent modern humans and Neanderthals.

		I_1	I_2	C_1
		N_{Hs}=17 N_{Hn}=39	N_{Hs}=15 N_{Hn}=47	N_{Hs}=16 N_{Hn}=23
CrLL [mm]	U_{Min}	0	9	36
	p	***1.02e-14***	***1.89e-12***	***4.77e-06***
CrPV [mm^3]	U_{Min}	194	199.5	121
	p	***0.013***	***0.002***	*ns*
R(MD) [mm]	U_{Min}	4.5	53	56.5
	p	***2.76 e-13***	***3.15e-08***	***0.00013***
R(LL) [mm]	U_{Min}	4	30	49
	p	***1.84e-13***	***5.41e-10***	***4.28e-05***
RL [mm]	U_{Min}	19	29.5	45.5
	p	***3.76e-11***	***4.91e-10***	***2.42e-05***
RSA [mm^2]	U_{Min}	1	1	35
	p	***3.06e-14***	***4.30e-14***	***3.94e-06***
RSA lab [mm^2]	U_{Min}	2	2	15
	p	***6.12e-14***	***8.60e-14***	***3.63e-08***
RSA ling [mm^2]	U_{Min}	36	5e56	48
	p	***1.73e-09***	***4.37e-08***	***3.65e-05***
CA [mm^2]	U_{Min}	2	34	55
	p	***6.12e-14***	***1.29e-09***	***0.0001***
RV [mm^3]	U_{Min}	0	1	19
	p	***1.02e-14***	***4.30e-14***	***1.10e-7***
RPV [mm^3]	U_{Min}	34	42.5	76
	p	***1.19e-09***	***5.83e-09***	***1.19e-07***
CrLL/RL	U_{Min}	210	248.5	113
	p	***0.029***	*ns*	***0.042***
R(LL)/R(MD)	U_{Min}	253.5	299	180
	p	*ns*	*ns*	*ns*
RSA lab/ling	U_{Min}	172	75	109.5
	p	***0.004***	***5.99e-07***	***0.033***
RSA/CA	U_{Min}	88.5	86.5	66
	p	***1.98e-06***	***1.06e-06***	***3.77e-04***
CrPV/RV	U_{Min}	145	145.5	114.5
	p	***6.16e-04***	***1.19e-03***	***0.047***
RPV/RPV	U_{Min}	282.5	233.5	184
	p	*ns*	*ns*	*ns*

Minimal U values and p values [bold when statistically significant] are reported. Variables investigated are the maximum crown labio-lingual diameter (CrLL), the crown pulp volume (CrPV), the mesio-distal root diameter (R(MD)), the labio-lingual root diameter (R(LL)), the root length (RL), the root surface area (RSA), the surface areas of the labial and of the lingual aspects of the root (RSA lab and RSA ling respectively), the cervical area (CA), the total root volume (RV), the root pulp volume (RPV) and their ratios.

Root pulp volume is the most variable parameter measured (highest coefficient of variations in Tables 4a and 4b). In the maxillary anterior teeth, the proportion of pulp to the total root volume is significantly greater in Neanderthals than in RMH. Neanderthals have proportionally a larger pulp cavity (SOM Table 5a). The ratio CrLL/RL and the proportion of pulp in the crown and in the root only differ for the I^1, i.e., compared with RMH, Neanderthals have a proportionally longer root for the size of their crown and they have relatively more pulp in the root than in the crown. In the mandibular dentition, the proportion of radicular pulp to the total root volume is overall similar in both taxa (SOM Table 5b). In contrast, Neanderthals have a relative larger radicular pulp for their coronal pulp volume, a relatively larger root for their crown size, and finally a labio-lingually broader cervix (CA, SOM Tables 5a and 5b) for the surface area of their root, compared with RMH.

The EMH from the Near East and Morocco are intermediate in root size between Neanderthals and RMH. Since our sample sizes of EMH are small, we also ran the Mann-Whitney U tests to compare EMH both with Neanderthals (SOM Tables 6a and 6b), and with RMH (SOM Tables 7a and 7b). The differences seem to be stronger between the Neanderthals and EMH, and more visible for the root surface area and volume in the lower dentition than for other measurements. Overall, the proportion of CrLL/RL, CrPV/RPV and RPV/RV do not differ significantly between EMH and the two comparative groups (RMH and Neanderthals, see Tables 4a, 4b, SOM Tables 5a3, 5a4, 5b3, 5b4, 6a and 6b). The UPEPIH always plot in the upper portion of the RMH variation.

Figure 3 gives an overview of the variability in root length and root pulp volume in our samples. Specimens represented are close to the mean of their taxonomic group. A chronological trend can be identified in Figure 4 when the root length is plotted against the maximum crown labio-lingual diameter. Neanderthals prior to MIS 4 are more robust in size than the rest of the Neanderthal sample, with greater variability. However, the fact that MIS 3 Neanderthals seem to have less variability in root and crown dimensions could be due to small sample size.

CROWN SIZE-ROOT SIZE CORRELATIONS

Overall, root size (root length) does not correlate with crown size (labio-lingual

diameter) in either Neanderthals or RMH (Table 6, $p>0.05$), except for the recent modern human mandibular canine. Similarly, root length is not correlated with any of the root diameters overall, except in the recent modern humans for the mesio-distal root diameter in the upper and lower canines, and for the labio-lingual root diameter in the central incisors and the lower canines. On the contrary, root length and root surface area are highly correlated for each tooth type in both taxa. The signal is weaker for the correlation between cervical and root surface areas (Table 6). In Neanderthals, only the correlations for maxillary and mandibular lateral incisors reach significance, whereas only the upper canines do not show significant correlations in RMH. Root pulp volume and total volume are not correlated (except for the lower canines in RMH) in either of the taxa tested. Neanderthals, having overall more voluminous anterior roots, show a much larger variability in their root pulp volumes than RMH. The volume of the pulp in the crown is correlated with the pulp volume in the root, except for the lower canines in both taxa, and for the lower lateral incisors in Neanderthals.

TOOTH WEAR AND ROOT PULP VOLUME

As explained in the Method section, Figure 1 highlights the deposition of an evenly thick layer of secondary dentine on the walls of the pulp chamber in some of the Bourgeois-Delaunay teeth. This phenomenon could possibly account for the large variability in pulp volume, observed in our samples. This could be related to the amount of wear found in our Neanderthals. To test this hypothesis, we scored the wear in our total sample following Smith (1984), and computed again the descriptive statistics for RPV, excluding from the samples the teeth with a considerable amount of wear (only stages 1 to 4 were kept, SOM Tables 8a and 8b). We are aware that the Neanderthal teeth are worn faster (in the frame of the teeth-as-tools hypothesis) over a shorter lifespan than in recent modern humans. Moreover, whereas the daily secretion rate of dentine is approximately the same between both taxa, the formation of the dentine in Neanderthals is faster (i.e., the root grows faster, Smith et al., 2010). This means that for a given stage of wear, a Neanderthal would have less secondary dentine deposited than an extant human. Our results show that Neanderthals still have significantly larger pulp volumes than RMH, for all tooth types, while only their lateral incisors are significantly more worn ($p<1.0e-3$ and $p<0.05$, respectively, SOM Table 8c).

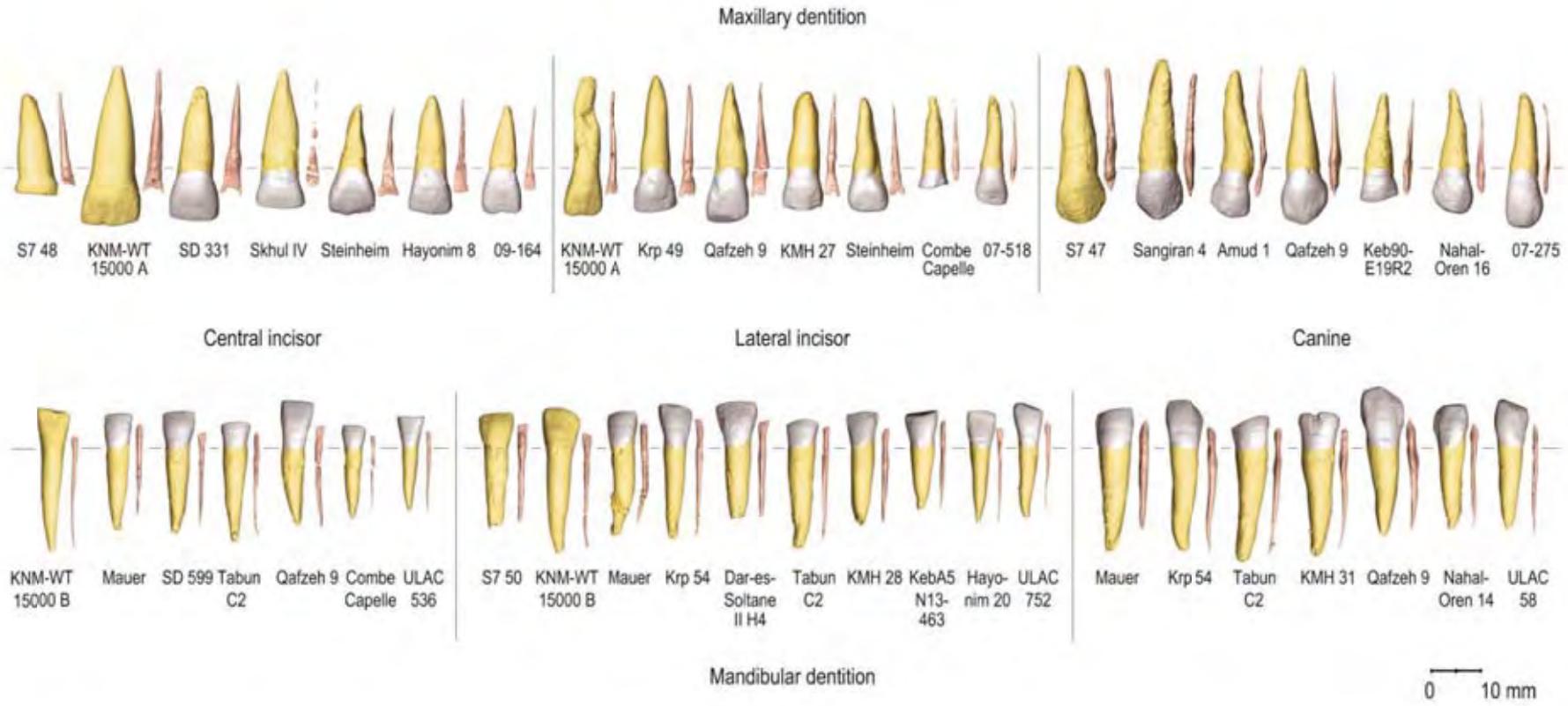

Figure 3. Anterior root morphology: overview of our total sample. Specimens (natural siding preserved) are displayed in anatomical position, in the labial view, with their extracted pulp at their right hand-side. We have chosen specimens close to the mean of their group in terms of size. Specimens for which taxonomical status is debated are also represented. This attempts to illustrate the variability in root length, root volume and root pulp volume. Because of the poor contrast between enamel and dentine, in the KNM-WT 15000 and Sangiran 7 teeth, a reliable distinction between both dental materials was not possible.

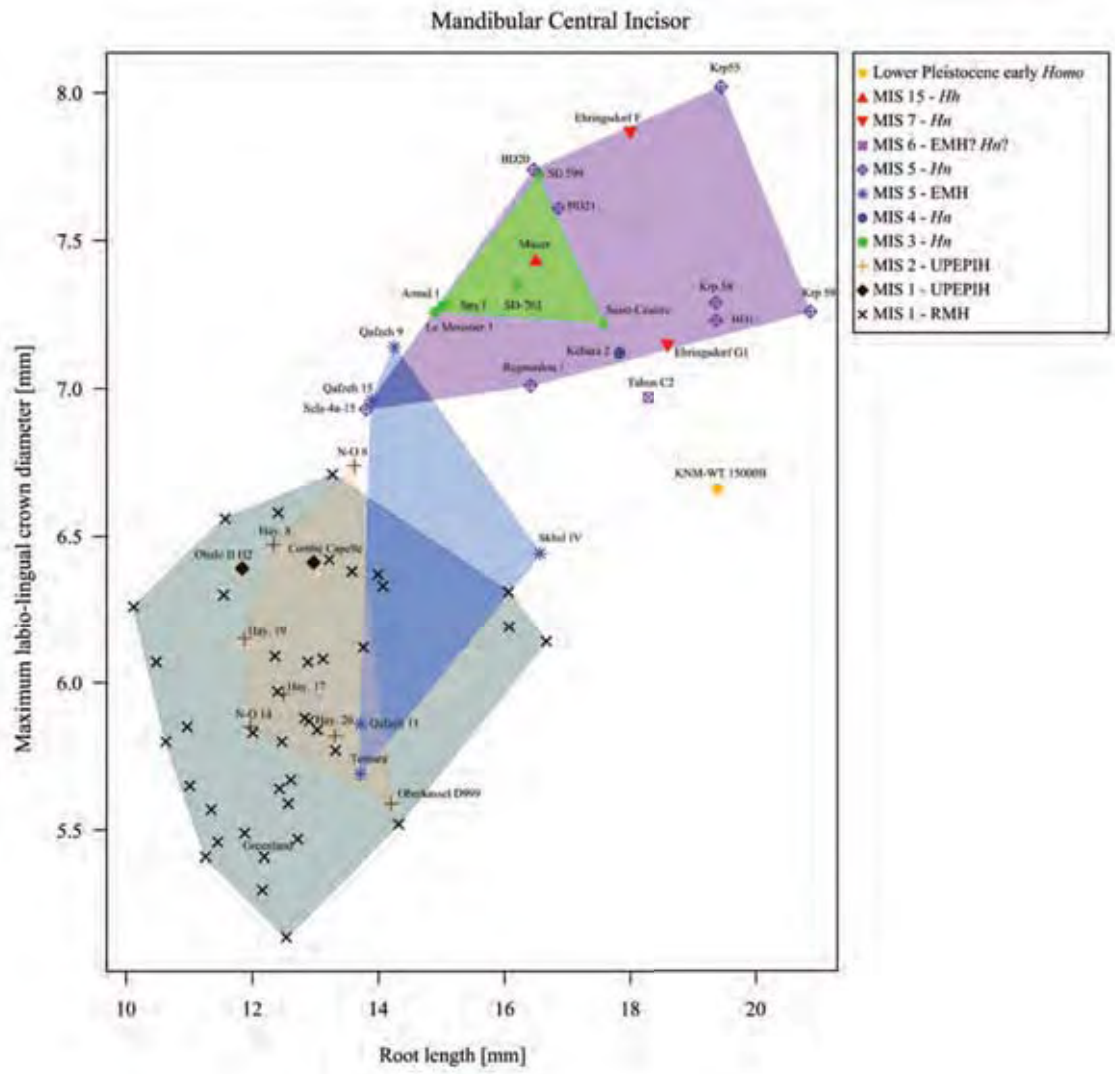

Figure 4. Pattern suggesting a chronological trend in our crown and root size data. A gradient is clearly visible, from the older specimens (at the right) toward the more gracile recent modern humans (at the very left). Note the smaller variability of MIS3 Neanderthals (this is possibly due to small sample size).

HYPERCEMENTOSIS

Hypercementosis was identified only (and in almost all specimens) in Neanderthals, in both upper and lower teeth. However, we were able to segment the cementum in eight maxillary teeth (six canines and two incisors) from Krapina, La Chaise-Abri-Bourgeois-Delaunay and Combe Grenal. We have however observed that the layer of cementum has often certainly been taphonomically broken, for instance in the Krapina specimens (Fig. 5), which implies that our preliminary quantifications underestimate the real amount of hypertrophic cementum developed on these teeth. These findings have been confirmed by direct observations on the original specimens

Table 6. Spearman Rank Order Correlations testing for statistical dependence among root and crown variables in recent modern humans and Neanderthals.

		CrLL vs. RL						CrLL vs. CA					
Tooth Type		I^1	I^2	C'	I_1	I_2	C,	I^1	I^2	C'	I_1	I_2	C,
Neanderthals	rho	0.60	0.47	-0.45	0.20	0.49	0.21	0.35	0.72	0.80	0.58	0.92	0.71
	p	*ns*	*ns*	*ns*	*ns*	*ns*	*ns*	*ns*	***0.009***	***0.001***	*ns*	***0.001***	***0.02***
Recent modern humans	rho	0.34	0.33	0.52	0.36	0.28	0.66	0.93	0.59	0.22	0.84	0.74	0.89
	p	*ns*	*ns*	*ns*	*ns*	*ns*	***0.008***	***0.0006***	***0.02***	*ns*	***0.0006***	***0.0006***	***0.0006***

		RL vs. CA						RSA vs. CA					
Tooth Type		I^1	I^2	C'	I_1	I_2	C,	I^1	I^2	C'	I_1	I_2	C,
Neanderthals	rho	0.29	0.23	-0.34	0.25	0.49	0.37	0.59	0.61	-0.02	0.58	0.69	0.42
	p	*ns*	*ns*	*ns*	*ns*	*ns*	*ns*	*ns*	*ns*	*ns*	*ns*	***0.04***	*ns*
Recent modern humans	rho	0.51	0.57	0.67	0.34	0.33	0.72	0.72	0.70	0.53	0.63	0.61	0.80
	p	*ns*	***0.04***	*ns*	*ns*	*ns*	***0.002***	***5.0e-4***	***9.0e-4***	*ns*	***1.0e-4***	***1.0e-4***	***1.0e-4***

		RL vs. RSA						RL vs. R(MD)					
Tooth Type		I^1	I^2	C'	I_1	I_2	C,	I^1	I^2	C'	I_1	I_2	C,
Neanderthals	rho	0.88	0.79	0.88	0.67	0.77	0.85	0.23	0.16	-0.31	0.19	0.61	0.62
	p	***0.0006***	***0.001***	***0.003***	***0.03***	***0.01***	***0.001***	*ns*	*ns*	*ns*	*ns*	*ns*	*ns*
Recent modern humans	rho	0.90	0.85	0.85	0.85	0.83	0.92	0.44	0.56	0.77	0.05	0.19	0.59
	p	***0.0006***	***0.0006***	***0.001***	***0.0006***	***0.0006***	***0.0006***	*ns*	*ns*	***0.03***	*ns*	*ns*	***0.02***

		RL vs. R(LL)						RSA Lab vs. RSA Ling					
Tooth Type		I^1	I^2	C'	I_1	I_2	C,	I^1	I^2	C'	I_1	I_2	C,
Neanderthals	rho	0.59	0.41	-0.36	0.42	0.34	0.32	0.62	0.32	0.27	0.28	0.61	0.57
	p	*ns*	*ns*	*ns*	*ns*	*ns*	*ns*	*ns*	*ns*	*ns*	*ns*	*ns*	*ns*
Recent modern humans	rho	0.55	0.28	0.62	0.47	0.26	0.72	0.52	0.36	0.12	0.49	0.65	0.77
	p	***0.04***	*ns*	*ns*	***0.02***	*ns*	***0.002***	***0.009***	*ns*	*ns*	***0.002***	***0.0001***	***0.0001***

Tabel 6. *Continued.*

Tooth Type	RPV vs. RV						RPV vs. CrPV					
	I^1	I^2	C'	I_1	I_2	C,	I^1	I^2	C'	I_1	I_2	C,
Neanderthals	0.19	0.03	0.01	-0.25	0.05	-0.02	0.75	0.74	0.81	0.70	0.54	0.44
	ns	*ns*	*ns*	*ns*	*ns*	*ns*	***0.01***	***0.01***	***0.02***	***0.01***	*ns*	*ns*
Recent modern humans	0.27	0.28	0.62	0.37	0.27	0.88	0.69	0.70	0.78	0.75	0.77	0.34
	ns	*ns*	*ns*	*ns*	*ns*	***0.001***	***0.002***	***0.004***	***0.03***	***0.0006***	***0.0006***	*ns*

Tooth Type	CrPV vs. CrLL					
	I^1	I^2	C'	I_1	I_2	C,
Neanderthals	0.30	0.25	0.05	-0.12	0.32	0.03
	ns	*ns*	*ns*	*ns*	*ns*	*ns*
Recent modern humans	0.22	0.34	0.54	0.10	0.10	0.52
	ns	*ns*	*ns*	*ns*	*ns*	*ns*

Samples sizes for Neanderthals: I^1 N=17, I^2 N=18, ' N=12, I_1 N=17, I_2 N=15 C, N=16. For recent modern humans: I^1 N=24, I^2 N=22, C' N=12, I_1 N=39, I_2 N=47, C, N=23. r_s = Spearman's rank order correlation coefficient. Bonferroni adjusted p values are italicized and bolded when significant. ns = nonsignificant.

from La Chaise and on pictures of the Krapina teeth. The proportion of hypertrophic cementum to the total volume of the root varies from 2% to 21% (Table 7). To better visualize the distribution of hypertrophic cementum, we computed the distance between the surfaces of underlying dentine and the layer of extra cementum. In Figure 5, the thickness of hypercementosis is expressed using a colormap. The scale is the same for all specimens to allow for an easier comparison. We observe a greater accumulation of hypertrophic cementum on the lingual and mesial aspects of the apical third of the root.

MULTIVARIATE STATISTICS

The results of the PCA and CVA analyses performed on our crown and root data (PC1 plotted against PC2 in Figs. 6a, 6b, 6c, SOM Fig. 1a, 1b and 1c) show a gradient from the robust early *Homo*, and progressing gradually towards the Neanderthals to the EMH, the UPEPIH and finally to the more gracile RMH group. For each tooth type, PC1 represents 'size' as the PC1 loadings are fairly similar for all of the variables considered in this analysis (Table 8). When PC2 is plotted against PC3, all groups overlap (Figs. 6 and SOM Figs. 1).

SHAPE OF THE CERVICAL LINE AND OF THE ROOT SURFACE

Since our data mainly reveal differences in overall size, the cervical shape analysis attempts to detect a morphological difference in shape at the cemento-enamel junction and on the root surface among our Neanderthal, EMH and RMH samples. Group mean differences in cervical shape and root shape reach statistical significance for all tooth types. The same pattern seems to emerge for all tooth types from the comparison of the Neanderthal and RMH mean root shape. For all tooth types, the mean shapes are different in shape space, but there is an overlap between groups even for tooth types for which separation is the best, such as the upper lateral incisor (Fig. 7). Therefore, we will limit the presentation of our results to this tooth type. Neanderthals have a more infero-superiorly convex root labially, with visibly more dentine spread on this surface, and a more infero-superiorly concave lingual root surface. We clearly noticed a greater curvature of the mesial and distal aspects of the RMH cervical line. This may be correlated with the fact that the cervical two thirds of the lingual aspect of the root are broader in RMH, more markedly than for the other tooth types. Despite the

Table 7. Proportion of hypertrophic cementum to the total root volume in cases where the hypertrophic cementum could be segmented.

Taxon	Specimen	Tooth type	Total Root volume [mm^3]	Volume of hypertrophic cementum [mm^3]	Percentage of hypercementosis
Neanderthals	Combe-Grenal 27	I^1	395.51	41.71	10.55
	Combe-Grenal X	I^2	352.35	24.59	6.98
	Krp D36	C'	817.26	15.59	1.91
	Krp D56	C'	731.3	24.65	3.37
	Krp D76	C'	678.01	20.81	3.07
	BD11	C'	656.55	126.08	19.2
	BD15	C'	650.64	136.81	21.03
	BD16	C'	734.51	122.05	16.62
			Mean ± SD	64.04 ± 53.89	10.34 ± 7.71
			[Min-Max]	[15.59-136.81]	[1.91-21.03]

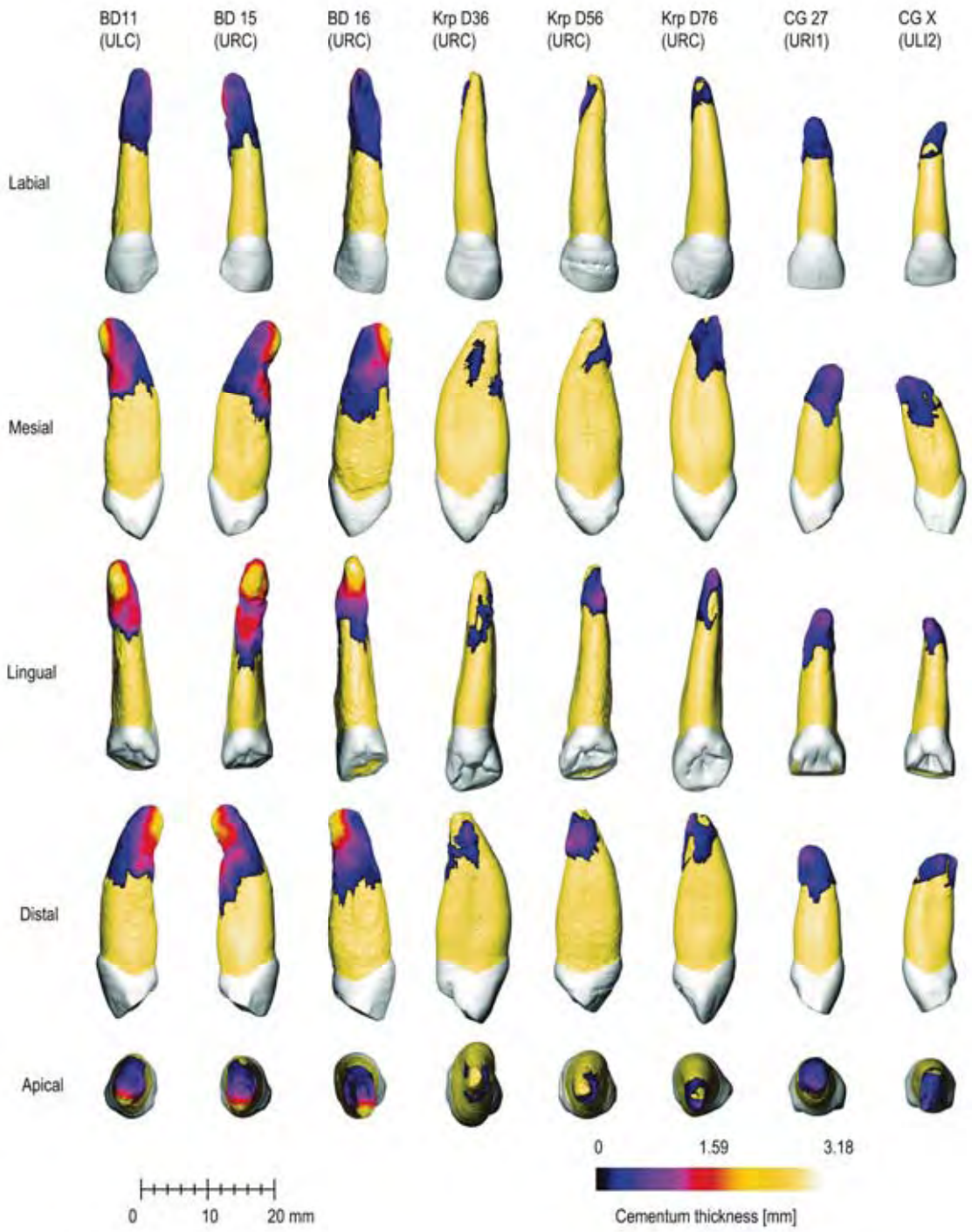

Figure 5. The pattern of distribution of the hypertrophic cementum is displayed using a colormap (which is proportional to thickness of cementum), on the 3D models of the maxillary incisors and canines for which segmentation of the extra cementum has been possible. 'ULC' stands for 'maxillary left canine', 'URC' for 'maxillary right canine', 'URI1' for 'maxillary right central incisor', 'ULI2' for 'maxillary left lateral incisor', and 'CG' for 'Combe-Grenal'. See Table 1 for specimen names.

Table 8. Loadings of the first principal component [PC1] revealing a size gradient from Neanderthals to recent modern humans.

	I^1	I^2	C'	I_1	I_2	C,
R(MD)	-0.28908	0.302567	-0.29914	-0.31113	-0.29104	-0.30773
R(LL)	-0.32824	0.326882	-0.31775	-0.33042	-0.32835	-0.32621
RL	-0.31737	0.305195	-0.30391	-0.29788	-0.30449	-0.31148
CrLL	-0.31305	0.320843	-0.31889	-0.32247	-0.31654	-0.31078
RPV^(1/3)	-0.26658	0.266626	-0.31116	-0.24614	-0.26416	-0.25226
RV^(1/3)	-0.34226	0.332664	-0.34524	-0.33994	-0.34254	-0.35221
RSA^(1/2)	-0.33876	0.332566	-0.33996	-0.33726	-0.34025	-0.31863
RSA lab^(1/2)	-0.32625	0.324471	-0.32464	-0.32307	-0.33051	-0.31878
RSA ling^(1/2)	-0.30986	0.313871	-0.30026	-0.31056	-0.30452	-0.32418
CA^(1/2)	-0.32334	0.330704	-0.29726	-0.33256	-0.33123	-0.33069

^(1/2) = the square root of a variable.^(1/3) = the cubic root of a variable.

fact that differences in root shape reach statistical significance and mean shapes do differ, the distinction among isolated teeth of Neanderthals, EMH and recent modern humans remains difficult, as distributions of the three groups in the PCA in shape space display a large amount of overlap for the other tooth types.

TAXONOMIC AFFINITIES FOR DEBATED SPECIMENS

Two isolated incisors labeled as 'Steinheim' at the Staatliches Museum für Naturkunde in Stuttgart, Germany, and stored in the same box as the Steinheim skull are in fact of uncertain origin. There is no mention in the literature of their discovery at the Steinheim quarry (Gieseler, 1971; Adam, 2003), and no manuscript record of their possible association with the Steinheim skull (personal communication from Reinhard Ziegler, curator at the Staatliches Museum für Naturkunde). Our results show that the two isolated incisors from Steinheim are clearly classified as recent modern humans (Fig. 6b and SOM Fig. 1a), questioning the suggestion that they belong to the Steinheim skull, and even to the Steinheim site. Even in the root shape analysis (Fig. 7), the upper lateral incisor from Steinheim plots in the middle of the RMH distribution.

Regarding the Tabun C2 mandible, all root and crown measurements show robust and large anterior teeth. Regarding the ratio CrLL/RL, Tabun C2 falls within

(6a)

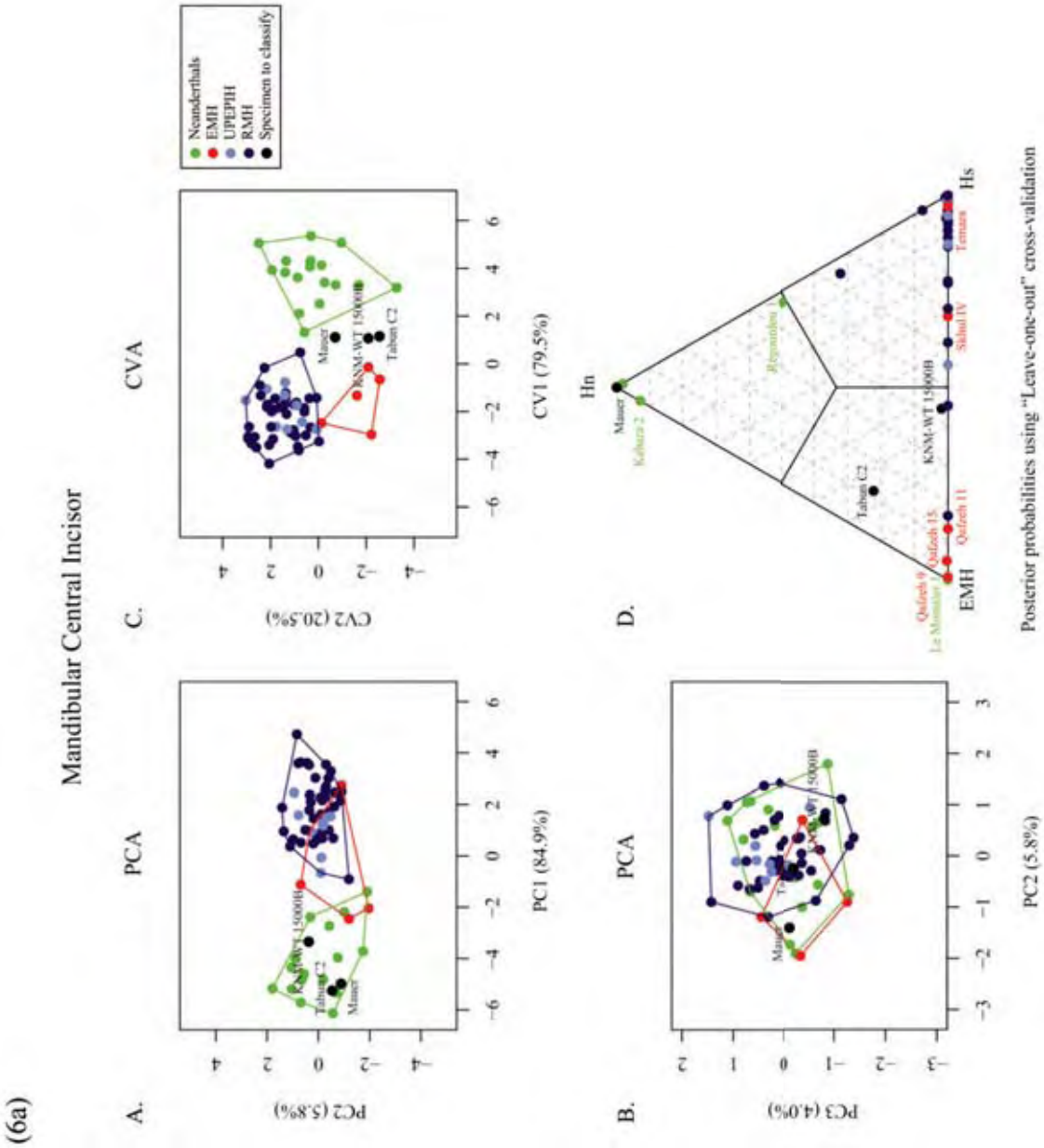
Mandibular Central Incisor
A.
PCA
PC2 (5.8%)
PC1 (84.9%)
KNM-WT 15000B
Taboun C2
Mauer
C.
CVA
CV2 (20.5%)
CV1 (79.5%)
Neanderthals
EMH
UPEPIH
RMH
Specimen to classify
B.
PCA
PC3 (4.0%)
PC2 (5.8%)
D.
Hn
Hs
EMH
Mauer
Kabwe 2
Taboun C2
KNM-WT 15000B
Qafzeh 11
Skhul IV
Tersan
Posterior probabilities using "Leave-one-out" cross-validation

(6b)

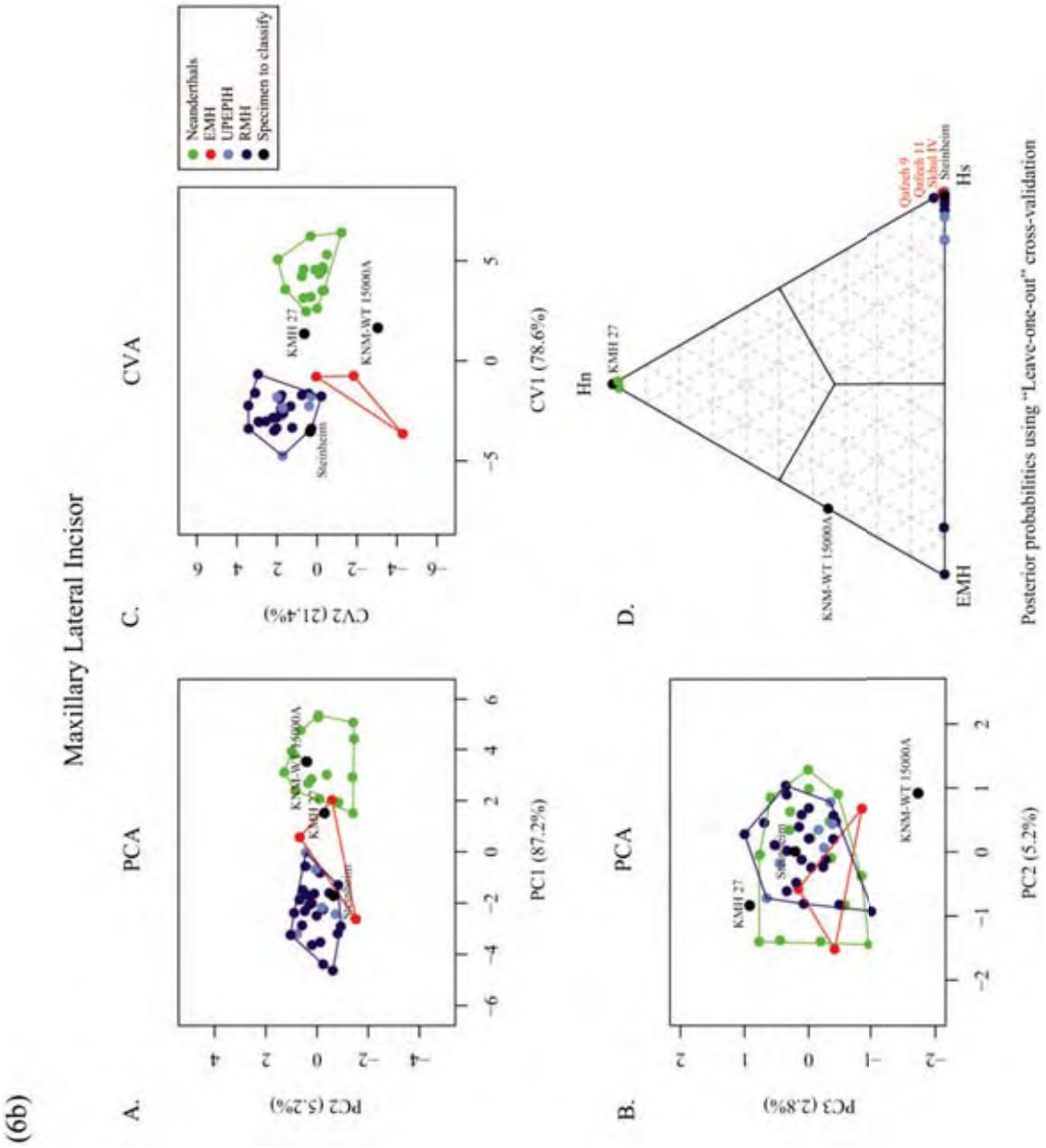
Maxillary Lateral Incisor
A.
PCA
PC2 (5.2%)
PC1 (87.2%)
KNM-WT 15000A
KMH 27
Specimen
C.
CVA
CV2 (21.4%)
CV1 (78.6%)
KMH 27
KNM-WT 15000A
Steinheim
Neanderthals
EMH
UPEPIH
RMH
Specimen to classify
B.
PCA
PC3 (2.8%)
PC2 (5.2%)
KMH 27
KNM-WT 15000A
D.
Hn
KMH 27
KNM-WT 15000A
Qafzeh 9
Qafzeh 11
Skhul IV
Steinheim
Hs
EMH
Posterior probabilities using "Leave-one-out" cross-validation

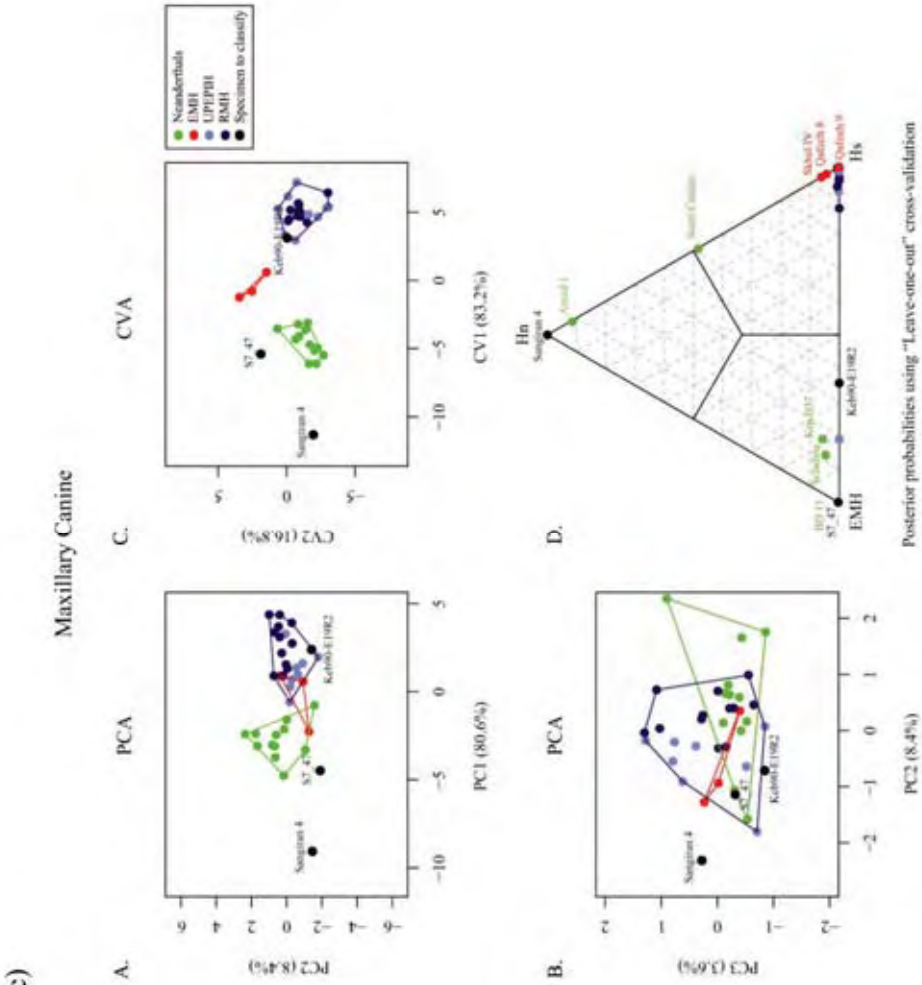

Figure 6. PCA, CVA and posterior probabilities for the I_1 (6a), I^2 (6b) and C' (6c) showing the size gradient (A. PC1 plotted against PC2), and the overwhelming signal of size in our data (B. PC2 plotted against PC3). The CVA attempts to best separate the group, while the posterior probability shows a classification of the debated specimens in our three main groups (the names of the outliers are reported to provide a more precise idea of the quality of the classification).

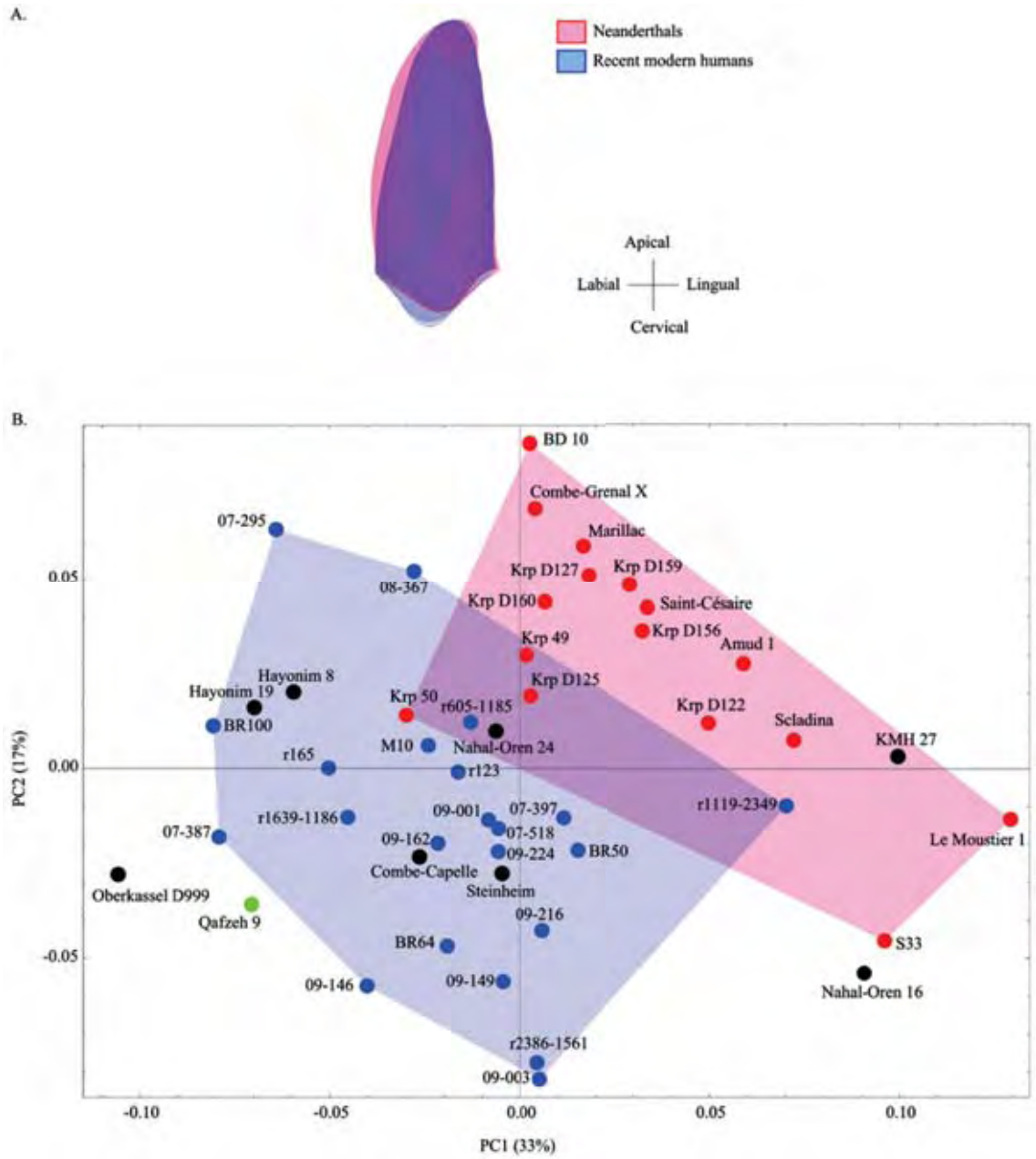

Figure 7. Root surface shape analysis in the maxillary lateral incisor. The superimposition of the Neanderthal (red) and of the recent modern human (blue) mean root shapes (A) allows us to see that the Neanderthal root is broader and more supero-inferiorly convex labially. This pattern is consistent for all tooth types. The PCA plot (B) shows separation between both groups despite a little overlap and that the Neanderthals and recent modern humans mean shapes are significantly different.

the lower end of the Neanderthal variation while it is excluded from the EMH variability (SOM Table 5b1). Compared with Neanderthals, Tabun C2 has a longer root and a smaller crown, for all anterior teeth (SOM Table 5b1, Table 4b). The Tabun C2 clearly plots with the Neanderthals in the PCA (Fig. 6a, SOM Fig. 1b and 1c), while it is more intermediate between Neanderthals and EMH in the CVA. Posterior probabilities attribute this specimen to EMH for the incisors, while the mandibular canine equiprobably attributes the Tabun C2 specimen to Neanderthals or recent modern humans. The anterior dentition of Tabun C2 displays closer affinities with Neanderthals in terms of size. Regarding root shape, the mandibular teeth do not allow for a good separation among groups in shape space, therefore Tabun C2 always falls in the overlapping area.

Finally, the taxonomic affinities of the five isolated teeth from the Kebara cave show that, for all of the analyses on the root and crown dimensions, KMH 27 (an I^2) and KMH 28 (an I_2) are likely to be attributed to Neanderthals (Fig. 6b and SOM Fig. 1b). In terms of root shape, KMH 27 still plots with the Neanderthals in shape space, whereas KMH 28 rather plots within the RMH distribution. The case of KMH 31 (a mandibular canine) is less clear-cut since the CVA classifies it as a modern human and the PCA places it in the Neanderthal cluster (SOM Fig. 1c). The root shape analysis instead places KMH 31 close to being within the Neanderthal cluster but also very close to the overlapping area with RMH. Keb90-E19R2 (a maxillary canine) falls within the recent modern human variation, posterior probabilities classify it as being closer to EMH than to RMH and its root shape is modern-human like. Lastly, KebA5N13-463 (an I_2) plots in the overlapping area between RMH and EMH, and is strongly attracted by the EMH pole in the posterior probabilities (SOM Fig. 1b). Its root shape is rather modern human like, but we must remain cautious since the distinction between groups is poor for the mandibular second incisor.

DISCUSSION

This study improves our knowledge of the variability in anterior tooth root size in Neanderthals, early modern humans and recent modern humans. This is of considerable interest for the taxonomic attribution of isolated teeth in the context of an unclear or disturbed stratigraphy, of remains that have been collected years ago during

old excavations (i.e., the isolated teeth from Kebara), and finally to contribute in discussing the status of debated specimens (such as Tabun C2). By using micro-computed tomography, yet undocumented aspects of the incisor and canine root morphology are reported, including root volume and surface area, root pulp volume, as well as the cemento-enamel junction and root shapes. In addition, this technique allows for the considerable broadening of the sample of *in situ* teeth for which the roots were previously inaccessible for study. Previous studies have stated that anterior tooth root length effectively distinguishes Neanderthals from RMH (Paquette, 1985; Smith and Paquette, 1989; Bailey, 2005). Our study confirms this finding with a geographically and chronologically larger sample, and draws attention to the overlapping distribution of these two taxa. In addition, we show the overlapping position of early modern humans, and document Upper Paleolithic and Epipaleolithic specimens.

TAXONOMIC IMPLICATIONS

Our data on root length enlarge the ranges provided by Bailey (2005) (See Tables 4a and 4b). Out of the four MIS 3 Sima de Las Palomas (SP) anterior teeth described by Walker et al. (2008), which had root length inferior to the ranges reported by Bailey (2005), only the SP26 mandibular canine remains out of our ranges with extremely short roots (14.5 mm whereas our minimum for the Neanderthal lower canines is at 16.05 mm, Table 4b). Neanderthals not only have overall longer anterior tooth roots than recent modern humans, but they also have significantly larger cervical root diameters, cervical area, root surface area, root volume, and root pulp volume, and as well as different cervical and root shapes. The larger root volumes in Neanderthals are expected since the root extension rate has been shown to be faster in Neanderthals than in modern humans (Smith et al., 2010). Regarding this difference in root shape, Koby (1956) and Trinkaus et al. (2000a) already qualitatively reported a labial convexity on the root of the Neanderthal permanent maxillary incisors of, respectively, Saint-Brais II (an I^1) and of Aubesier 4 and 9 (a left and a right I^2). Bermúdez de Castro (1988) also described this morphology in the maxillary lateral incisors of Sima de los Huesos.

One surprising finding in this study concerns the two Steinheim incisors. Both teeth, and in particular the maxillary lateral incisor, unexpectedly fall in our recent

modern human variability for all analyses performed. This questions the suggested Middle Pleistocene nature of these teeth. After careful observations of the skull, it appears very unlikely that they could refit on the Steinheim skull. After further investigation in the literature reporting the conditions of the discovery of the Steinheim remains and through communication with the curator in charge of the Steinheim skull, it appears that those dental remains have been stored by accident with the Steinheim skull, leading to this taxonomic confusion. Our analysis of root dimensions has allowed us to detect this and to safely rule out the option that those teeth could belong to the Steinheim cranium.

In addition, our data have yielded a comparative framework for studying five isolated teeth from the Kebara cave. Only two remains can be safely attributed to Neanderthals (KMH 27 and KMH 28). However, a large tooth could be erroneously classified as a Neanderthal.

The Tabun C2 mandible shows an anterior dentition fitting within the Neanderthal range of variation. In light of these results, we also examined its molar root morphology on the micro-CT scans. If Tabun C2 would actually have closer affinities to Neanderthals in root morphology, one would expect to see pyramidal or taurodontic roots (see Kupczik and Hublin, 2010). The crown body to root ratio defined in Wright (2007), here measured on the right molars of the specimen of interest, allows for a quick identification of taurodontism on 2D images. Actually, in contrast with the Neanderthal pattern, Tabun C2 has cynodont molar roots (all ratios being inferior to 1.10 with 0.65 for the first molar, 0.99 for the second, and 0.81 for the third molar). This means that the mesial and the distal roots diverge quite rapidly below the cervical plane and the pulp chamber clearly splits into two root canals over the three-quarters of the total root length (Fig. 8). Contrasting interpretations of the specimen have been proposed. On the one hand, Vandermeersch (1981) underlines the closer affinities of the Tabun C2 mandible with the Qafzeh-Skhul cluster rather than with Amud-Shanidar-Tabun C1. Rak et al. (2002) also show that the mandibular ramus morphology places Tabun C2 in the modern human cluster. On the other hand, Stefan and Trinkaus (1998) conclude to a stronger affinity with Neanderthals by studying the mandibular morphology and the size of the tooth crowns in the anterior dentition. Based on overall and symphyseal mandibular morphology, Schwartz and Tattersall (2000) also reject the idea that Tabun C2 is a modern human, and conclude that due to closer affinities with Neanderthals, it is

highly probable that Tabun C2 belongs to this taxon although it is not easily demonstrable. The attribution of Tabun C2 to the Neanderthals would be consistent with the occurrence at the top of the same stratigraphic level (Tabun C) of the Neanderthal skeleton of Tabun C1. However, to date, all of the EMH of the Levant have been in fact

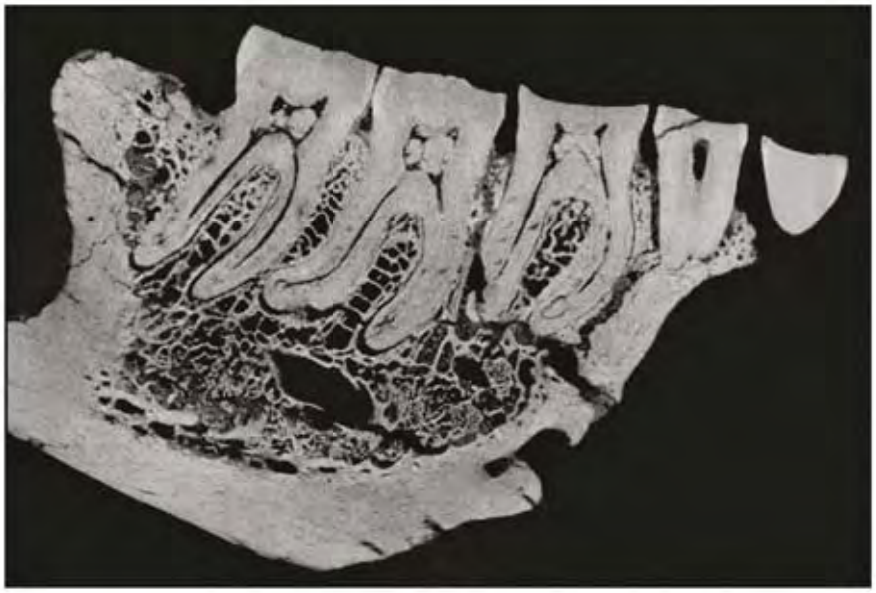

Figure 8. Mid-sagittal section through the high-resolution micro-CT scans of the Tabun C2 mandible showing for the right molars a modern-human like root (cynodont) and pulp canal morphology.

found in association with Tabun C Mousterian assemblages, while Neanderthal remains were yielded by Tabun B type Mousterian layers (Bar-Yosef, 1998; Quam and Smith, 1998; Bar-Yosef and Callander, 1999). It has therefore been suggested that the burial of the Tabun C1 skeleton could actually be intrusive from layer B into the top of layer C (Rak, 2002). Primarily, our results confirm the mosaic and ambiguous nature of the Tabun C2 specimen. However, one should emphasize that, as long as only the features entertained in this study are concerned, the most primitive representatives of the EMH group might be practically indistinguishable from Neanderthals. This might well be the case with Tabun C2 and anterior root length alone should not be considered as sufficient for taxonomic attribution in such cases.

POLARITY OF ANTERIOR TOOTH ROOT SIZE AND SHAPE

To assess the polarity of the root features that we have documented in this study, we need to discuss the different visions of the history of the Neanderthal lineage, and

the condition of specimens that are older than Neanderthals. It has been proposed, especially with the accretion model (Hublin, 1998, 2009), that along their evolution Neanderthals would have experienced a series of bottlenecks, periodically reducing their effective population size, resulting in genetic drift and possible decrease in morphological variability. Opponents (Hawks and Wolpoff, 2001) to this model advocate that a multiregional evolution model would better explain the Neanderthal morphology than a complete isolation of the Neanderthal populations. However, observations based on genetic (Serre et al., 2004; Green et al., 2008, 2010) and morphological studies (Trinkaus, 1993; Hublin, 1998; Maureille and Houët, 1998; Harvati et al., 2010) brought support to the accretion model. Martinón-Torres and colleagues (2012) refute the linearity of this model emphasizing that, based on discrete crown features, the Sima de Los Huesos individuals are more similar to Neanderthals than are Mauer, Arago and even some of the classic Neanderthals. Thus, these authors instead suggest the coexistence of several distinct human lineages in the European Middle Pleistocene (Martinón-Torres et al., 2012). This argumentation assumes that Mauer, Sima de Los Huesos and Arago are close in age, which is to date not generally accepted (Hublin, 2009; Endicott et al., 2010). Our data show that MIS 3 Neanderthals tend to have a lower variability in terms of crown and root size than pre-MIS 4 Neanderthals (Fig. 4), which would be consistent with the predictions of the accretion model. However, further investigations with larger sample sizes need to be conducted.

Our Lower and Middle Pleistocene specimens (Sangiran specimens, KNM-WT 15000 and Mauer) display an anterior tooth root size range that is equal to or greater than the Neanderthal condition. Since no further micro-CT data were accessible to study a large amount of Lower and Middle Pleistocene specimens, we relied on information collected from the literature to document crown size (labio-lingual diameter) and root length when available (See SOM 9 Tables 1 and 2). This limits the interpretation of the polarity in root character and a more detailed micro-CT study would improve the overview provided here. SOM Fig. 2a and b show how specimens from Dmanisi, Gran Dolina ATD6-H1, Sima de los Huesos, Arago, Lazaret and Pesada plot within the lower half of the Neanderthal variation, although the lower central incisor of Sima de los Huesos, two teeth from Dmanisi (D2677 and D2736) fall in the upper range of the Neanderthal distribution (see the results of our adjusted z-scores SOM 9 Table 3). We also collected root length data from a few more Neanderthals specimens (SOM 9 Table

3). They expectedly fall within the variation of our Neanderthal sample (SOM Fig. 2a and 2b).

This suggests that overall large anterior tooth roots are a retained ancestral condition, and not a Neanderthal characteristic. This has also been suggested by Martinón-Torres et al. (2012) who, based on discrete crown traits, proposed that Neanderthals would have retained ancestral characteristics present before the divergence of modern humans and Neanderthals, and later lost in recent modern humans. The Qafzeh and Skhul specimens overlap in distribution with Neanderthals and recent modern humans, perhaps simply because they date to a time closer to the event of divergence between modern humans and Neanderthals and are not yet derived for the concerned features. Interestingly, the much older Qesem mandibular canine (Hershkovitz et al., 2011), whose taxonomic status is uncertain, also falls in the area of overlap of our Neanderthals and early modern human distributions (SOM Fig.2a) in a similar way to Tabun C2. Alternatively, some have speculated that Qafzeh could be the result of the hybridization between Neanderthals and early modern humans in the Middle East (e.g., Martinón-Torres et al., 2012). Although it is impossible to test this hypothesis with our data, which is compatible with genetic data (Green et al., 2010), it cannot be excluded for Tabun C2.

In a previous study showing that root size is not correlated to mandible size (Le Cabec et al., 2012), we have highlighted that short roots in recent modern humans may result from a negative evolutionary allometry, whereas long anterior tooth roots in Neanderthals and early modern humans could be a retained ancestral condition. This is supported by the position of the European Middle Pleistocene specimens in comparison with our Neanderthals (SOM 9). The size gradient revealed by our data implies that a Neanderthal with relatively short roots (such as Scladina or Le Moustier 1) could be erroneously classified as a modern human, while a long-rooted early modern human (e.g., Dar-es-Soltane II H4) would be attributed to the Neanderthal group. However, the distinction between RMH and Neanderthals is clearer since the distributions overlap very little. Therefore, root dimensions do prove to be helpful in attempting to discuss taxonomic attributions for specimens that were found out of any clear and *in situ* stratigraphic context, or in defining taxonomic affinities for debated specimens. This has also been shown for molar tooth roots (Kupczik and Hublin, 2010). Our large

geographical and chronological samples provide us with a reasonable overview of the variability of anterior tooth root morphology along the Neanderthal lineage.

It is worth highlighting that these quantitative data and discussion focus on the permanent anterior dentition, but, to our knowledge, no quantitative studies are currently available yet for the root morphology of the deciduous dentition. However, qualitative description of Neanderthal deciduous teeth (incisors and canines) also underscores the fact that Neanderthal deciduous anterior teeth have labio-lingually larger crowns, more robust and longer roots, and larger pulp cavities than modern humans (Thoma, 1963; Ménard, 1984; Defleur et al., 1992; Vega-Toscano et al., 1994; Trinkaus et al., 2000b). Regarding root shape, Thoma (1963) observes a labial convexity similar to the permanent anterior teeth, whereas Ménard (1984) describes a lingual convexity, and others (Patte, 1962; Ménard, 1984; Defleur et al., 1992) a root labially straight or flat. Patte (1962) reports that in Krapina, while permanent incisors are found with a marked angle between the crown and the root (collum angle), deciduous incisors with a perfectly flat long axis have been found. In their study on the dental remains from La Grotte du Renne (Arcy-sur-Cure), Bailey and Hublin (2006) conclude that the maxillary deciduous incisor crowns of Neanderthals present discrete features (e.g., shoveling, labial convexity) that are present in the permanent teeth, although to a lesser frequency. This shows that for both dental generations, Neanderthals have overall larger teeth and also longer roots than recent modern humans. This would be in favor of a common ontogenetic signal in both dental generations, although the developmental pathways may differ. This latter hypothesis has been raised by Hughes et al. (2000) who stated that the deciduous crown size likely display a genetic underpinning as do the permanent teeth. Regarding deciduous molars metrics, Benazzi et al. (2011) also highlight the difference distinguishing Neanderthals from Upper Paleolithic humans. We have previously hypothesized that the pillar-shaped cross-sectional symphysis in Neanderthals could be an adaptation to allow large-rooted anterior teeth to erupt in a symphysis of similar size as in recent modern humans (Le Cabec et al., 2012).

In addition, recent studies have shown that both permanent and deciduous dentitions seem to share the same pattern of maturation within a taxon (Bayle et al., 2009a, b, 2010). However, it has been demonstrated in recent modern humans that both enamel and dentine rates of formation are faster in the deciduous dentition than in

permanent teeth (Liversidge and Molleson, 2004). Using Bayesian probabilities, Bayle and colleagues (2010) have shown that the sequences of maturation (for both permanent and temporary teeth) of the Roc-de-Marsal Neanderthal child and of the Gravettian Lagar Velho 1 child are not found in their large comparative sample of recent modern humans. Although different in sequences, both specimens share relatively delayed incisors and relatively advanced molar calcification for both dental generations. In contrast, the Upper Paleolithic La Madeleine 4 child absolute tooth size and relative dental tissue proportions fits within the range of recent modern humans (Bayle et al., 2009a).

Since we have highlighted a negative allometry in root size of the permanent anterior teeth in recent modern humans (Le Cabec et al., 2012), it would be worth investigating whether the difference in root size between both dental generations is the same for both taxa. If the deciduous anterior tooth roots were relatively larger than the permanent anterior roots in recent modern humans, this would mean that the deciduous dentition would have retained the ancestral condition in having long roots. We could then speculate that this would have been lost in the permanent dentition displaying shorter roots, to fit within a relatively smaller jaw in adult recent modern humans.

Overall, a better documentation of the early *Homo* anterior tooth root morphology would be required to assert this pattern of polarity.

FUNCTIONAL IMPLICATIONS REGARDING THE ANTERIOR DENTAL LOADING HYPOTHESIS

Despite the fact that we found no significant correlation between root size and crown size, and although this was not explicitly tested here, root size (and shape) may covary with crown shape. Indeed, Neanderthal maxillary incisor crowns have a pronounced labial convexity and a typical shovel-shaped lingual morphology (Tratman, 1950; Smith, 1976a; Mizoguchi, 1985; Smith and Paquette, 1989; Crummett, 1995) combining marginal ridges, a lingual fossa and a lingual tubercle. It has been proposed by Kirveskari and Alvesalo (1979) that shoveling (depth of the lingual fossa, in their study) varies with positive allometry with the mesio-distal diameter of the crown in maxillary incisors of modern humans. In comparison with hominids and modern populations, what characterizes Neanderthals for these non-metric traits is their degree

of expression as well as their frequency of occurrence (Bailey, 2006). Shoveling seems to be at least partly inherited genetically (Portin and Alvesalo, 1974; Blanco and Chakraborty, 1976), and it has been hypothesized that its strong prevalence in Neanderthals would be a retained ancestral characteristic (e.g., Bailey and Hublin, 2006).

Since the anterior teeth are often heavily worn and sometimes even show an irregular pattern of wear (Smith, 1976a, b; Wolpoff, 1979; Puech, 1981; Ungar et al., 1997), it has also been proposed that shoveling, involving both enamel and dentine (Tratman, 1950), would be a functional adaptation to optimize the incisal surface while wearing it down during incision, as well as during para- and non-masticatory processes (Trinkaus, 1986). This has been suggested as well by Bermúdez de Castro (1993) for the Sima de los Huesos hominids. Although he acknowledges the fact that Middle or early Late Pleistocene hominids have used their anterior dentition for non-masticatory purposes, he cannot confirm the hypothesis according to which their craniofacial morphology and their dental dimensions would be driven by an adaptation to high loads on the anterior dentition. Clement et al. (2012) reach the same conclusion for Neanderthals by examining tooth wear patterns. They further conclude that the amount of wear in the EMH is similar to that seen in Neanderthals, suggesting that EMH would have applied at least as high or as frequent loads on their anterior teeth, as Neanderthals. On the contrary, Krueger (2011) shows that the microwear pattern observed in EMH only testifies to a little amount of non-dietary anterior teeth use in these hominids. If the maxillary incisor crown is modeled as a wedge, an acute apex angle will remain sharp throughout the incision of tough and hard food, while a broader incisal edge would wear down blunt and lose efficiency in breaking hard food items (Ang et al., 2006). However, using FEA on the maxillary incisor crown, Magne and colleagues (1999) have shown that the lingual concavity of the modern human maxillary incisors represents an area of stress concentration, when the tooth is loaded on the incisal edge, perpendicular to the tooth axis. They state that the marginal ridges and the cingulum contribute to the decrease in the stress level on the lingual aspect of the crown. In this perspective, the pronounced lingual tubercle in Neanderthal incisors would represent an even more optimized adaptation to decrease the amount of stress generated from heavy or frequent loads on the labial portion of the anterior teeth.

Moreover, looking at fracture patterns by experimentally loading incisor and canine teeth, Schatz et al. (2001) find that upper canines display the best resistance to fracture. In contrast, maxillary and mandibular incisors have the smallest resistance to fracture, hence the advantage of having some kind of hyperstructures on the crowns that can already decrease the amount of stress to be transmitted to the root (Schatz et al., 2001). In this context, a larger root and a greater root surface area would further improve the sustainability of the tooth to high loads on the anterior dentition. In the present study, the maxillary incisors yield the strongest differences in root shape. Schatz et al. (2001) also conclude that root length is directly correlated with fracture energy, and a tooth with greater root length or surface area will better resist a force with a large magnitude than a short root with a small surface area. A greater root surface area would improve the attachment of the tooth in the jaw by increasing the surface of contact between the periodontal ligament and the supporting bony structures (e.g., Smith, 1983; Kupczik and Dean, 2008; Kupczik and Hublin, 2010). Kloehn (1938) pioneered the field of research on root surface area. He demonstrated that in any mammalian dentition, root surface area reflects the occlusal loads, which yields information on the dietary specializations and on the material properties of the processed items (food or others). This has been further investigated in primates (Spencer, 1998a, b, 2003; Kupczik and Dean, 2008). Kloehn (1938: 230) further claims that in the modern human dentition, “almost universally the greatest [root] surface is presented on the side where tension is known to occur.” Hylander (1977) reports a larger root surface area on the lingual side of Inuit vertically positioned maxillary incisors. He interprets this as an effective manner to concentrate a greater amount of periodontal fibers where compressive forces occur, which contradicts Kloehn (1938) who predicted a larger surface area on the labial side of the root. Our size and shape data reveal a greater root surface area on the labial side of the Neanderthal anterior teeth, which rather brings support to Kloehn’s (1938) views.

If Neanderthals were using their anterior teeth as a ‘third hand,’ the force applied on the maxillary front teeth would be linguo-labially oriented, and as predicted by Trinkaus (1978) an increase in labio-lingual diameter would be adaptatively advantageous. Such a force applied on the crown of a single-rooted tooth results in a slight rotation of the tooth around a fulcrum located between the half and the third of the apical part of the root (Smith and Burstone, 1984). This would produce compression

on the lingual apical half of the root and tension on the labial apical half. Such a loading regime is conceivable with clenching a piece of frozen meat (Barrett, 1977) or leather between the upper and lower front teeth. Our results are in agreement with Kloehn's (1938) prediction that the greater surface area occurs on the side of the root where tension occurs. Nonetheless, the combination of mid-facial prognathism, the large collum angle (crown-to-root angle) and labial convexity may change the pattern of distribution of stress. Harris and colleagues (1993) have proposed in a clinical study that class III malocclusion (mandibular protrusion, maxillary retrusion, both combined, and edge-to-edge bite as seen in Neanderthals) would developmentally induce a large collum angle, the crown being torqued lingually to the root axis. This strong angulation between the crown and the root in Neanderthals (Koby, 1956; Patte, 1960; Brabant and Sahly, 1964; Legoux, 1976) would be linked with the edge-to-edge occlusion. Therefore, a more convex labial root surface could be seen as an adaptation for a compromise between craniodental morphology and a highly demanding loading regime exerted on the anterior teeth.

Another adaptation lies in having an increased pulp chamber volume, which would improve the supply of nutrients for the tooth, but would also allow for deposition of tertiary dentine (as seen on the incisal surfaces of the Krapina 58 and 59 mandibles; also reported as 'secondary dentine' in some Neanderthal molars in Kupczik and Hublin, 2010) as compensation for high attrition rate, always keeping a minimum volume of pulp (Berry and Poole, 1976).

Another possible adaptation to sustain high or frequent occlusal loads on the anterior teeth has been observed in our samples in the form of hypercementosis. Hypertrophic cementum has been clearly identified and reconstructed in 3D for some of our Neanderthal maxillary canines and incisors (Fig. 5). The etiology of hypercementosis remains unclear although it is known to occur in normal vital teeth, with a possible correlation with age (e.g., Dastmalchi et al., 1990) and severe attrition (Gardner and Goldstein, 1931; Comuzzie and Steele, 1989; Gilbert, 1992; Trinkaus et al., 2008), and with stress due to traumatic occlusion (Guttman, 1912; Tratman, 1950; Weinberger, 1954; Spouge, 1973; Hylander, 1977; Garralda et al., 2004; Pinheiro et al., 2008; Waters-Rist et al., 2010). Several scholars have suggested that the appositional growth of cementum would preferentially occur under tensional forces, especially on the distal aspect of post-canine teeth during mesial drift (Dastmalchi et al., 1990;

Bosshardt and Selvig, 1997). In the frame of the teeth-as-tools hypothesis, and under the assumption that the tooth has a fulcrum between mid-root and the cervical root third, compressive forces would occur on the lingual aspect of the apical root third and on the labial aspect of the cervical root third. Tensional forces would occur on the labial aspect of the apical root third and the lingual aspect of the cervical third of the root. Our observations reveal that the repeated and frequent compression produced on the root may result in an excessive secretion of cementum on the lingual aspect of the apical root third. The surface of the hypertrophic cementum is markedly irregular since it is not part of the normal development of the tooth, but it can rather be seen as an active and constantly updated response to the biomechanical environment of the root, which is in agreement with what Kovacs (1967) called the 'eruptive phase'.

Cases of hypercementosis have already been reported for several Pleistocene hominin dental remains (Patte, 1960; Antunes and Cunha, 1992; Garralda and Vandermeersch, 2000; Henry-Gambier et al., 2004; Trinkaus et al., 2008; Martinón-Torres et al., 2011). Our results confirm Hartney's (1981) observations stating that hypercementosis seem to predominantly affect the maxillary dentition. Weinberger (1954), Bosshardt and Selvig (1997) and Martinón-Torres et al. (2011) noticed a larger amount of extra cementum on the mesial and distal aspects of the roots. On the contrary, and in agreement with what some authors have also observed (Philippas and Applebaum, 1967; Solheim, 1990), the hypertrophic cementum accumulates to a greater extent in our sample on the lingual and mesial aspects of the apical root third. Our observations of 'compensatory hypercementosis' (Pedersen, 1949) on the upper canines in Neanderthals are in agreement with Merbs' (1968) report on the use of the anterior dentition as a third hand in Inuit populations. Merbs (1968) states that forces applied to the lingual surface of the teeth will result in intense stresses in concentrated areas, and particularly at the root apex. Observation of our micro-CT data has shown a quasi omni-presence of hypercementosis on the apical portion of the incisor and canine roots in our Neanderthal sample. The amount and the spread of the hypercementosis over the root vary from one specimen to another (from traces to an amount comparable with the one seen in Combe-Grenal 27 on Fig.5). These results are preliminary and pending on an on-going study using new imaging techniques that will yield new insights into the quantitative documentation of hypercementosis.

In most modern clinical studies, hypercementosis is often seen as pathological (Spouge, 1973). It can be encountered, for instance, in patients affected by Paget's disease or by hyperpituitarism (i.e., acromegaly and gigantism, Pinheiro et al., 2008). Considering the intense and peculiar use of the anterior dentition in Inuit populations (Pedersen, 1949) and possibly in Neanderthals, we would argue that the frequent secondary changes undergone by the radicular tissues throughout adult life should be considered as common and non-pathological.

In conclusion, our observations on Neanderthals (larger anterior tooth roots, differences in maxillary incisor root shape and hypercementosis) bring some support to the ‘teeth-as-tools’ hypothesis (Brace et al., 1964; Smith and Paquette, 1989), or at least do not falsify it. This hypothesis states that Neanderthals used their front teeth as a third hand to perform para- and non-masticatory activities (e.g., 'stuff-and-cut' in Koby, 1956; Brace, 1962, 1975, 1979; Wallace et al., 1975). Although no evidence of ‘para-masticatory-related’ labial striations has been documented yet in early *Homo* (Lozano et al., 2008), we could speculate that the large anterior teeth that we have documented in this study could have been likely used in an opportunistic manner, as a third hand. Wolpoff (1999) argued that the increasing use of the large anterior dentition in early *Homo* would have to be related to the changes in technology involved in food preparation. Since the hyperstructures of the incisor crowns of Neanderthals are more strongly expressed than in early *Homo*, we can hypothesize that the Neanderthal anterior dentition was subject to a greater stress concentration, and that tooth use differed in intensity, frequency, and regarding the range of non-dietary activities performed.

CONCLUSION

This study has shown with geographically and chronologically broad samples that Neanderthals can be distinguished from modern humans using the size of their anterior tooth roots, at least when terminal forms of both lineages are considered. Their root shape is also significantly different, this difference being most evident in the maxillary incisors. Moreover, our results reveal that Neanderthals dated after MIS 4 tend to show a reduced variability compared with older Neanderthals, and this is

possibly related to genetic drift. We have further shown that the distribution of early modern human dental dimensions overlaps with both Neanderthals and recent modern humans. We identified a clear gradient in terms of tooth size, towards a gracilization of the roots in recent modern humans. We have shown, with the isolated teeth from Steinheim and Kebara Cave that anterior root dimensions can contribute to taxonomic attribution of fossil dental remains from uncertain stratigraphic provenience or subject to debate regarding their taxonomy. Since our early *Homo* specimens (Sangiran and KNM-WT 15000) and Tabun C2 have somewhat 'Neanderthal-like' anterior root dimensions, these large anterior tooth roots may not be a Neanderthal characteristic but rather a retained ancestral condition still present even in the earliest forms of modern humans. Nonetheless, the retention of longer roots and larger surface areas in Neanderthals can be seen as a functional adaptation to high or frequent loads exerted on the anterior dentition, as proposed by the 'teeth-as-tools' hypothesis. Preliminary results show that the presence of hypercementosis on a significant proportion of our Neanderthal teeth would lend some support to this, as a compensatory response to abnormally high loads.

ACKNOWLEDGEMENTS

We would like to thank the curators in charge of the material included in this study and the people who facilitated access to specimens: B. Arensburg, A. Barash, O. Bar-Yosef, E. Been, A. Ben-n'cer, D. Bonjean, P. Brown, J.-J. Cleyet-Merle, A.P. Derevianko, M.A. El Hajraoui, I. Fawzi, R. Feeney, C. Feja, U.A. Glasmacher, F. Gröning, M. Hänel, I. Hershkovitz, A. Hoffmann, O. Kullmer, S. Markin, E. Mbua, P. Mennecier, V. Merlin-Langlade, NESPOS, S. Pääbo, P. Périn, J. Radovčić, Y. Rak, S. Raoui, D. Reid, A. Rosas, A. Savariego, R. Schmitz, F. Schrenk, P. Semal, M.V. Shunkov, A. Soficaru, F. Spoor, J.-F. Tournepiche, M. Toussaint, B. Vandermeersch, C. Verna, B. Viola and R. Ziegler. We are grateful to A. Winzer, P. Schönfeld, H. Temming, T. Smith, M. Skinner and R. Feeney for their micro-CT scanning expertise. J. Abramov, A. Barash, E. Been, V. Eshed, S. Freidline, T. Kivell, T. Kuperman, S. Neubauer and V. Slon are acknowledged for their collaboration in the field. We are grateful to the following people for helpful discussions: B. Viola, C. Verna, S. Bortoluzzi, P. Tafforeau, B. Maureille, M. M. Barak, S. McPherron, D. Richter, J.-P.

Raynal and H. Dibble. We sincerely appreciate the contribution of A. Sylvester for writing the R code for the calculation of the cone surface area. We are indebted to R. Tilgner for his advice and expertise in image processing and software expertise, especially for writing and optimizing the Watershed segmentation algorithm, to R. Mundry for providing the R code for the Spearman correlation, for his very helpful advice and support in using R statistical software. We express our gratitude to the Max Planck Institute library staff and especially to L. Kaufmann, for their helpful support. We are very grateful to A. Reid for English proof-reading. We want to thank David Begun, as well as the associated editor and three anonymous reviewers for their comments and suggestions which greatly improved this manuscript. This research was funded by the Max Planck Society.

SOM Table 1. Reliability of the estimation of the incomplete apical root portion.

Tooth of interest	Percentage of the artificially cut total volume.	Difference in **root length** between the reconstruction and the actual value [in %].	Difference in **root surface area** between the reconstruction and the actual value [in %].	Difference in **root volume** between the reconstruction and the actual value [in %].
r123_LRI1	-1.17	-3.45	-1.81	-0.75
ULAC_74_LLI2	-2.71	-2.98	-3.39	-1.70
07_407_URC	-1.01	-4.78	-1.95	-1.95
ULAC_806_LRI1	-3.16	-8.41	-4.78	-4.78
r605_1185_URI2	-3.24	-4.12	-4.66	-4.66
KRP_D160_ULI2	-2.73	-1.43	-3.18	-3.18
Krp59_LRI2	-4.82	-8.12	-7.50	-7.50
BD20_LLI1	-5.76	-6.73	-6.65	-6.65
St_Cesaire_URC	-1.09	-0.26	-1.45	-1.45
Marillac_URI1	-3.90	+1.53	-3.19	-3.19
Average [Min; Max]	-2.96 [-5.76;-1.01]	**-3.87** [-8.41;+1.53]	**-3.86** [-7.50; -1.45]	**-1.97** [-4.21; -0.52]

The original micro-CT stack and the labels [of the model divided into crown and root] were reoriented and resampled in Avizo, using as reference an oblique slice oriented following the cervical plane previously defined to cut the tooth into individualized crown and root. In order to avoid biasing our result because of the resampling, we measured again on these new 3D models the root length, surface area and volume, as explained in the Materials and Methods section. We artificially cut the root tip in a plane parallel to the cervical plane using the crop editor in Avizo. The missing part was modeled as an elliptic cone. This does not mimic a natural cut, which would be irregular, but the goal of this experiment is to test the reliability of our estimation of the height of the elliptic cone, which we estimated before our very eyes, since the two radii are clearly identifiable on the scans at the break. After generating a 3D model from the artificially broken roots, we defined a labio-lingual plane by setting three landmarks on the 3D models of the incomplete teeth: one at the center of a plane parallel to the cervical plane at the broken apex and two landmarks at the greatest point of curvature of the cemento-enamel line on the labial and on lingual side of the tooth. A mesio-distal plane was similarly defined with the two last landmarks at the point of greatest curvature on the mesial and distal aspects of the cemento-enamel line. Using an oblique slice generated in Avizo 6.2, we resampled the micro-CT images according to these two planes, to get the midsagittal labio-lingual and mesio-distal slices through the broken root. Using a 3D linear measurement, we estimated the missing root length in both orientations, based on the long axis of the tooth and on the thickness of the dentine walls for the taphonomically broken teeth. These two measurements were then averaged to get the height of the elliptic cone representing the missing portion of the root. In the same way, we measured the radius at the break in the two planes, to get the major and minor radii of the elliptic cone, parallel to the long axis of the tooth and perpendicular to the height of the cone. The average height gives us the estimated missing root length, while the missing root surface area and root volume are computed from the average height and the two radii. Subsequently, we added these estimations to the actual measurements to get an estimation of the total root variables. Those estimations were then compared to the values measured on the intact specimens. The differences expressed in percentages are listed in the table above. Overall, our method tends to underestimate the actual values. Nonetheless, the descriptive statistics for each variable show that this is reliable enough, and would still be more accurate than including the incomplete value. In case of fossils, we consider that these approximations are

reasonable since the real root apex is not as slender and regular as the elliptic cone modeled and the fact that a root is never broken according to a plane exactly parallel to the cervical plane.

SOM Table 2a. Root length estimation for missing root apical portions in damaged or developmentally incomplete specimens.

Specimen	Tooth type	Side	Cause	rMD [mm]	rLL [mm]	rAv. [mm]	hMD [mm]	hLL [mm]	hAv. [mm]	RL meas. [mm]	Msg RL [mm]	%age Mis RL	Total estim. RL [mm]
S7_47	UC	L	t	*0.72*	*1.45*	1.09	0.58	1.20	*0.89*	20.63	0.89	**4.14**	21.52
S7_50	LI2	R	t	*1.16*	*2.1*	1.63	1.15	1.44	*1.30*	15.81	1.30	**7.57**	17.11
KNM-WT-15000A	UI2	L	d	*0.79*	*1.89*	1.3	0.82	0.99	*0.91*	17.93	0.91	**4.80**	18.84
KNM-WT-15000B	LI2	L	d	*0.62*	*0.98*	0.8	1.04	0.99	*1.02*	19.13	1.02	**5.04**	20.15
Le Moustier 1	LI1	L	t	*0.81*	*2.9*	1.9	1.17	2.16	*1.67*	13.23	1.67	**11.18**	14.90
Amud1	LI1	L	t	*1.23*	*2.27*	1.8	1.62	1.75	*1.69*	13.32	1.69	**11.23**	15.01
Regourdou 1	LI1	R	t	*0.43*	*1.18*	0.81	0.26	1.11	*0.69*	15.72	0.69	**4.18**	16.41
Le Moustier 1	LI2	R	t	*0.89*	*1.72*	1.3	0.47	0.53	*0.50*	16.23	0.50	**2.99**	16.73
Regourdou 1	LI2	R	t	*1.12*	*2.09*	1.6	0.78	1.05	*0.92*	16.88	0.92	**5.14**	17.80
Scla-4a-20	LI2	R	t	*1.13*	*2.05*	1.6	0.51	2.14	*1.33*	13.9	1.33	**8.70**	15.23
KMH 28	LI2	R	t?	*0.65*	*2.08*	1.4	0.87	0.93	*0.90*	14.77	0.90	**5.74**	15.67
KebA5N13-463	LI2	R	t	*0.68*	*1.11*	0.9	0.64	0.61	*0.63*	12.77	0.63	**4.67**	13.40
Ehringsdorf_G1_10	LC	R	d	*0.59*	*1.47*	1.0	0.88	0.72	*0.80*	20.75	0.80	**3.71**	21.55
Le Moustier 1	LC	R	t	*0.91*	*1.46*	1.2	0.5	0.48	*0.49*	17.18	0.49	**2.77**	17.67
Scla-4a-11	UI1	R	t/d	*1*	*1.07*	1.0	1.24	1.45	*1.35*	13.97	1.35	**8.78**	15.32
Krp D123	UI1	L	t	*1.32*	*1.69*	1.5	1.36	2.64	*2.00*	17.57	2.00	**10.22**	19.57
Krp D126	UI1	R	t/d	*1.03*	*1.43*	1.2	1.31	1.39	*1.35*	15.24	1.35	**8.14**	16.59
Krp D122	UI2	L	d	*0.72*	*1.8*	1.3	0.69	1.42	*1.06*	16.36	1.06	**6.06**	17.42

SOM Table 2a. *Continued.*

Specimen	Tooth type	Side	Cause	rMD [mm]	rLL [mm]	rAv. [mm]	hMD [mm]	hLL [mm]	hAv. [mm]	RL meas. [mm]	Msg RL [mm]	%age Mis RL	Total estim. RL [mm]
Krp 50 [Max. F]	UC	R	t	*1.68*	*1.79*	1.7	1.81	2.29	*2.05*	20.99	2.05	**8.90**	23.04
Scla-4a-16	UC	R	d	*0.5*	*0.83*	0.7	0.37	0.7	*0.54*	17.15	0.54	**3.03**	17.69
Qafzeh 8	UC	R	t	*1.78*	*2.3*	2.0	3.12	2.39	*2.76*	12.89	2.76	**17.61**	15.65
Qafzeh 11	LI1	R	t	*0.41*	*1.02*	0.7	0.48	0.81	*0.65*	13.07	0.65	**4.70**	13.72
Qafzeh 11	LC	R	t	*1.63*	*2.37*	2.0	2.68	2.25	*2.47*	13.62	2.47	**15.32**	16.09
Qafzeh 11	UI1	R	t	*1.4*	*1.6*	1.5	2.37	2.87	*2.62*	11.48	2.62	**18.58**	14.10
Qafzeh 11	UI2	R	t	*1.6*	*2.1*	1.9	4.05	4.04	*4.05*	7.66	4.05	**34.56**	11.71
Qafzeh 15	LI1	L	t/d?	*0.45*	*1.37*	0.9	0.26	0.49	*0.38*	13.51	0.38	**2.70**	13.89
Dar-Es-Sultane_II_H4	LI2	R	t	*1.14*	*2.32*	1.73	0.7	1.07	*0.89*	13.43	0.89	**6.18**	14.32
ULAC_179	LI2	L	d	*0.53*	*0.99*	0.8	0.32	0.93	*0.63*	13.56	0.63	**4.41**	14.19
09_222	UI1	R	t	*0.86*	*0.82*	0.8	0.96	0.97	*0.97*	13.87	0.97	**6.50**	14.84
07_155	UI1	R	t	*0.92*	*1.32*	1.1	1.12	0.97	*1.05*	11.35	1.05	**8.43**	12.40
r_123	UI2	L	t	*0.46*	*0.92*	0.7	0.45	1.22	*0.84*	11.18	0.84	**6.95**	12.02

We scored the reason why the root is incomplete as 't' for taphonomical break, 'd' for developmentally incomplete, 't/d' when the reason is uncertain between taphonomy and development. 'rMD' stands for the mesio-distal radius of the elliptic cone, 'rLL' for its labio-lingual radius, 'rAv.' for the average of both radii; 'hMD' and "hLL" for the height of the cone measured in the mesio-distal and in the labio-lingual plane respectively and 'hAv.' for the average of both heights. 'hMD', 'hLL' and 'hAv.' are italicized since they are used for further computations. 'RL meas.' stands for the measured root length [so incomplete], 'Total estim. RL' is the reconstructed root length summing the average height and the measured root length, and '%age Mis RL' is the percentage of the total root length represented by the portion of root that has been reconstructed [bold and underlined when superior to 15%].We notice that for Regourdou1 LI1, it is highly likely that the missing part of the root is actually some broken hypertrophic cementum.

SOM Table 2b. Root surface area and volume estimations for missing root apical portions in damaged or developmentally incomplete specimens.

Specimen	Tooth type	RSA meas. [mm²]	Misg RSA [mm²]	%age Misg RSA	Total estim RSA [mm²]	RV meas. [mm³]	Misg RV [mm³]	%age Misg RV	Total estim. RV [mm³]
S7_47	UC	454.16	4.56	**0.99**	458.72	754.09	0.97	**0.13**	755.07
S7_50	LI2	280.36	10.27	**3.53**	290.62	313.82	3.30	**1.04**	317.12
KNM-WT-15000A	UI2	419.12	6.20	**1.46**	425.32	463.50	1.42	**0.30**	464.92
KNM-WT-15000B	LI2	383.43	3.22	**0.83**	386.65	466.25	0.65	**0.14**	466.90
Le Moustier 1	LI1	256.77	13.04	**4.83**	269.80	289.87	4.10	**1.39**	293.97
Amud1	LI1	241.18	12.98	**5.11**	254.16	244.52	4.93	**1.98**	249.45
Regourdou 1	LI1	257.47	2.47	**0.95**	259.93	251.96	0.36	**0.14**	252.32
Le Moustier 1	LI2	325.29	5.27	**1.59**	330.56	394.30	0.80	**0.20**	395.10
Regourdou 1	LI2	319.84	8.78	**2.67**	328.62	355.33	2.24	**0.63**	357.57
Scla-4a-20	LI2	230.23	9.98	**4.16**	240.21	255.68	3.21	**1.24**	258.89
KMH 28	LI2	276.47	6.01	**2.13**	282.49	330.14	1.27	**0.38**	331.41
KebA5N13-463	LI2	190.37	2.98	**1.54**	193.35	208.42	0.49	**0.24**	208.92
Ehringsdorf_G1-10	LC	387.57	3.88	**0.99**	391.45	504.99	0.73	**0.14**	505.72
Le Moustier 1	LC	412.64	4.57	**1.10**	417.21	593.85	0.68	**0.11**	594.54
Scla-4a-11	UI1	239.46	5.52	**2.25**	244.98	327.83	1.51	**0.46**	329.34
Krp D123	UI1	357.72	11.81	**3.20**	369.53	576.45	4.67	**0.80**	581.12
Krp D126	UI1	281.84	7.01	**2.43**	288.85	387.65	2.08	**0.53**	389.74
Krp D122	UI2	360.61	6.04	**1.65**	366.65	510.62	1.43	**0.28**	512.06

SOM Table 2b. *Continued.*

Specimen	Tooth type	RSA meas. [mm²]	Misg RSA [mm²]	%age Misg RSA	Total estim RSA [mm²]	RV meas. [mm³]	Misg RV [mm³]	%age Misg RV	Total estim. RV [mm³]
Krp 50 [Max. F]	UC	430.75	14.64	**3.29**	445.39	617.58	6.46	**1.03**	624.03
Scla-4a-16	UC	309.50	1.73	**0.56**	311.23	406.63	0.23	**0.06**	406.87
Qafzeh 8	UC	274.54	21.92	**7.39**	296.46	376.86	11.81	**3.04**	388.67
Qafzeh 11	LI1	120.44	2.03	**1.66**	122.46	98.61	0.28	**0.29**	98.89
Qafzeh 11	LC	235.68	19.82	**7.76**	255.50	305.06	9.97	**3.17**	315.03
Qafzeh 11	UI1	189.07	14.23	**7.00**	203.29	212.71	6.15	**2.81**	218.85
Qafzeh 11	UI2	124.61	25.88	**17.20**	150.49	123.20	14.23	**10.36**	137.44
Qafzeh 15	LI1	216.32	2.27	**1.04**	218.59	214.76	0.24	**0.11**	215.00
Dar-Es-Sultane_II_H4	LI2	259.43	9.72	**3.61**	269.15	321.36	2.45	**0.76**	323.81
ULAC_179	LI2	197.91	2.26	**1.13**	200.17	171.28	0.34	**0.20**	171.63
09_222	UI1	207.87	3.38	**1.60**	211.25	235.64	0.71	**0.30**	236.36
07_155	UI1	162.77	5.33	**3.17**	168.10	181.08	1.33	**0.73**	182.41
r_123	UI2	153.21	2.30	**1.48**	155.51	140.44	0.37	**0.26**	140.81

'RSA meas.' stands for the measured root surface area [percentages bold and underlined when superior to 5%], and 'RV meas.' for the measured root volume [percentages bold and underlined when superior to 5%]. Further abbreviations follow the pattern used in the SOM Table 2a.

SOM Table 3a. Mann-Whitney U test results for the comparison between male and female RMH in the crown and root dimensions of the upper dentition.

		I^1	I^2	C'
		N_{HsF}=16 N_{HsM}=7	N_{HsF}=11 NHsM=10	N_{HsF}=2 N_{HsM}=10
CrLL [mm]	U_{Min}	47	30	2
	p	*ns*	*ns*	*ns*
R(MD) [mm]	U_{Min}	46	40.5	8
	p	*ns*	*ns*	*ns*
R(LL) [mm]	U_{Min}	45.5	31	1
	p	*ns*	*ns*	*ns*
RL [mm]	U_{Min}	43	49.5	8
	p	*ns*	*ns*	*ns*
RSA [mm²]	U_{Min}	41	42	3
	p	*ns*	*ns*	*ns*
RSA lab [mm^2]	U_{Min}	38	48	2
	p	*ns*	*ns*	*ns*
RSA ling [mm^2]	U_{Min}	46	39	8
	p	*ns*	*ns*	*ns*
RSA lab/ling [mm^2]	U_{Min}	46.5	48	7
	p	*ns*	*ns*	*ns*
CA [mm²]	U_{Min}	45.5	27	4
	p	*ns*	***0.049***	*ns*
RV [mm^3]	U_{Min}	47	35	3
	p	*ns*	*ns*	*ns*
RPV [mm^3]	U_{Min}	32	43	8
	p	*ns*	*ns*	*ns*

'N_{HsF}' and 'N_{HsM}' are the respective sample size for females and males in the recent modern human sample.
Since we sometimes have very small sample sizes, the following computation in R gives us the smallest p-value that we can accept for a result that is not a consequence of sample size: 2/[choose[N_1+N_2, N_1]], where N_1 and N_2 are the two sample sizes. All results reported here cannot be biased by the sample sizes according to this calculation.
For all root and crown variables investigated in this study, we detect no differences related to sexual dimorphism, except maybe in the cervical area of the maxillary lateral incisor

SOM Table 3b. Mann-Whitney U test results for the comparison between male and female RMH in the crown and root dimensions of the lower dentition.

		I_1 N_{HoF}=15 N_{HoM}=21	I_2 N_{HoF}=18 N_{HoM}=26	C_1 N_{HoF}=5 N_{HoM}=15
CrLL [mm]	U_{Min}	132	206.5	27
	p	*ns*	*ns*	*ns*
R(MD) [mm]	U_{Min}	113	194.5	35.5
	p	*ns*	*ns*	*ns*
R(LL) [mm]	U_{Min}	121	186.5	26.5
	p	*ns*	*ns*	*ns*
RL [mm]	U_{Min}	98	123	26
	p	*ns*	***0.01***	*ns*
RSA [mm²]	U_{Min}	93	124	29
	p	***0.04***	***0.01***	*ns*
RSA lab [mm²]	U_{Min}	97.5	136	25
	p	*ns*	***0.02***	*ns*
RSA ling [mm²]	U_{Min}	105	157	29
	p	*ns*	*ns*	*ns*
RSA lab/ling [mm²]	U_{Min}	121.5	230	34
	p	*ns*	*ns*	*ns*
CA [mm²]	U_{Min}	114	184	32
	p	*ns*	*ns*	*ns*
RV [mm³]	U_{Min}	98	129	31
	p	*ns*	***0.01***	*ns*
RPV [mm³]	U_{Min}	112	154	31
	p	*ns*	*ns*	*ns*

Abbreviations are as for SOM Table 4a. For all root and crown variables investigated in this study, we detect no differences related to sexual dimorphism, except for the root length, surface area and labial surface area in the incisors, the root volume and pulp volume in the lateral incisor. See SOM Table 3a for justification of the use of the test with small sample sizes.

SOM Table 4a. Complementary descriptive statistics for the upper anterior dentition. 'R(MD)' stands for mesio-distal root diameter, 'R(LL)' for labio-lingual root diameter, 'CA' for cervical area, 'CrPV' for crown pulp volume, 'RSA ling' and 'RSA lab' for surface area of the lingual and labial aspects of the root.

			R(MD) [mm]	R(LL) [mm]	CA [mm²]	CrPV [mm³]	RSA ling [mm²]	RSA lab [mm²]
H. erectus	S7_48	I^1	7.23	6.62	36.87	6.23	114.84	154.54
	S7_47	C'	7.29	10.57	61.08	19.01	183.08	272.05
	Sangiran 4	C'	7.1	11.61	66.01	17.37	244.03	300.84
H. ergaster	N=1	I^1	8.53	8.56	59.86	10.72	181.27	227.23
	N=1	I^2	5.01	8.33	36.61	7.79	199.88	220.98
Steinheim?	N=1	I^1	5.55	7.01	31.94	13.72	112.55	73.44
	N=1	I^2	5.34	6.04	26.16	8.43	94.95	97.13
Neanderthals	N=17	I^1	7.04 ± 1.08 [5.38-9.31] (15.29)	7.58 ± 0.49 [7.00-8.63] (6.46)	41.88 ± 8.00 [33.15-59.07] (19.10)	17.55 ± 8.23 [0.08-27.92] (46.88)	134.80 ± 26.61 [68.53-175.69] (19.74)	179.57 ± 39.54 [94.51-243.81] (22.02)
	N=18	I^2	6.11 ± 0.52 [5.40-7.22] (8.58)	7.96 ± 0.56 [7.28-9.30] (7.10)	39.59 ± 6.12 [31.22-53.29] (15.45)	11.44 ± 4.68 [2.84-22.96] (40.94)	138.43 ± 20.76 [97.84-182.97] (14.99)	204.81 ± 32.29 [155.26-269.03] (15.77)
	N=12	C'	6.18 ± 0.23 [5.84-6.51] (3.74)	9.35 ± 0.70 [8.66-10.98] (7.53)	46.18 ± 5.03 [40.00-55.84] (10.90)	11.78 ± 3.67 [6.70-18.93] (31.18)	198.33 ± 44.59 [122.17-311.58] (22.48)	255.37 ± 46.04 [170.41-314.42] (18.03)
Isolated teeth from Kebara	KMH 27	I^2	6.48	7.65	38.99	7.67	136.86	169.62
	Keb90-E19R2	C'	5.49	7.98	35.88	5.02	110.12	129.05

SOM Table 4a. *Continued.*

			R(MD) [mm]	R(LL) [mm]	CA [mm²]	CrPV [mm³]	RSA ling [mm²]	RSA lab [mm²]
EMH		I[1]	7.03 ± 1.19 [5.89-8.26] (16.88)	7.14 ± 0.80 [6.32-7.92] (11.22)	36.75 ± 9.30 [29.99-47.35] (25.30)	16.38 ± 13.15 [1.49-26.39] (80.27)	N=2; 121.21 ± 36.84 [94.22-181.18]	N=2; 137.70 ± 61.49 [94.22-181.18]
	N=3	I[2]	5.12 ± 1.06 [4.35-6.32] (20.62)	6.89 ± 0.44 [6.38-7.15] (6.45)	28.08 ± 5.23 [22.84-33.29] (18.61)	7.57 ± 6.48 [0.08-11.43] (85.70)	110.61 ± 43.45 [61.13-142.55] (39.28)	111.09 ± 41.14 [63.69-137.42] (37.03)
	N=3	C'	6.26 ± 0.22 [6.06-6.49] (3.47)	8.74 ± 1.16 [7.72-10.00] (13.24)	42.53 ± 4.69 [38.82-47.80] (11.02)	7.68 ± 6.65 [0.53-13.67] (86.51)	148.65 ± 20.70 [135.96-172.53] (13.92)	159.73 ± 21.91 [138.79-182.50] (13.72)
UPEPIH	N=6	I[1]	6.81 ± 0.42 [6.25-7.22] (6.19)	6.86 ± 0.36 [6.44-7.42] (5.26)	36.04 ± 3.85 [29.54-41.32] (10.68)	7.46 ± 3.80 [1.96-11.95] (50.91)	115.57 ± 20.07 [85.88-139.84] (17.36)	104.92 ± 19.18 [80.50-136.68] (18.28)
	N=6	I[2]	4.78 ± 0.35 [4.22-5.11] (7.32)	6.20 ± 0.52 [5.45-6.78] (8.46)	22.90 ± 3.26 [18.01-27.50] (14.24)	4.35 ± 1.67 [2.05-6.62] (38.32)	88.60 ± 18.55 [69.86-118.67] (20.93)	100.05 ± 15.08 [84.68-123.16] (15.07)
	N= 8	C'	5.71 ± 0.44 [5.10-6.32] (7.76)	8.68 ± 0.62 [7.31-9.26] (7.14)	27.11 ± 8.13 [21.58-41.05] (29.97)	6.86 ± 1.10 [5.56-8.74] (16.01)	127.16 ± 25.13 [95.80-171.55] (19.76)	151.48 ± 21.59 [120.93-180.15] (14.25)
RMH	N=24	I[1]	5.88 ± 0.49 [5.06-6.86] (8.33)	6.33 ± 0.36 [6.33-5.87] (5.74)	29.93 ± 3.48 [23.93-36.26] (11.62)	6.75 ± 5.26 [0.29-18.96] (77.88)	103.94 ± 18.07 [73.69-134.00] (17.39)	88.29 ± 16.66 [58.88-128.80] (18.87)
	N=22	I[2]	4.60 ± 0.47 [3.92-5.88] (10.22)	5.87 ± 0.43 [5.01-6.55] (7.40)	22.01 ± 3.12 [15.99-27.03] (14.17)	3.96 ± 2.25 [0.03-7.44] (56.72)	81.25 ± 14.70 [53.60-109.59] (18.09)	90.29 ± 18.29 [55.31-134.62] (20.26)
	N=12	C'	5.31 ± 0.51 [4.58-6.01] (9.66)	7.63 ± 0.65 [6.51-8.38] (8.47)	21.97 ± 0.13 [21.77-22.17] (0.60)	4.25 ± 3.06 [0-9.43] (71.97)	127.31 ± 28.02 [97.56-181.89] (22.01)	127.38 ± 25.01 [93.80-187.22] (19.64)

N stands for sample size; mean ± standard deviation [minimum-maximum].

SOM Table 4b. Complementary descriptive statistics for the lower anterior dentition.

			R(MD) [mm]	R(LL) [mm]	CrPV [mm^3]	CA [mm²]	RSA ling [mm^2]	RSA lab [mm^2]
H. erectus	S7_50	I_2	4.84	7.22	5.28	28.18	99.45	181.24
H. ergaster	N=1	I_1	4.4	6.66	2.7	24.02	119.67	160.98
	N=1	I_2	4.89	8.13	5.04	34.56	166.87	216.97
H. heidelbergensis	N=1	I_1	4.16	7.26	7.23	25.39	114.9	162.6
	N=1	I_2	4.44	7.72	8.18	30.24	119.04	195.08
	N=1	C,	6.28	8.92	12.39	45.09	152.1	259.25
Neanderthals	N=17	I_1	4.28 ± 0.26 [3.86-4.73] (6.00)	7.13 ± 0.39 [6.29-7.86] (5.40)	4.03 ± 2.82 [0-11.57] (70.08)	25.48 ± 2.86 [20.55-30.13] (11.21)	147.98 ± 31.95 [70.79-196.26] (21.59)	151.96 ± 27.38 [92.39-191.23] (18.02)
	N=15	I_2	4.57 ± 0.64 [3.29-6.42] (13.95)	7.55 ± 0.62 [6.14-8.71] (8.21)	5.44 ± 3.00 [1.59-12.11] (55.20)	28.51 ± 4.16 [18.03-35.72] (14.59)	147.26 ± 29.89 [70.31-192.64] (20.30)	187.96 ± 30.42 [124.32-228.22] (16.18)
	N=16	C,	5.80 ± 0.51 [4.30-6.44] (8.79)	8.88 ± 0.72 [7.52-10.52] (8.08)	7.16 ± 3.32 [2.14-13.47] (46.37)	42.24 ± 6.61 [25.61-54.46] (15.65)	192.48 ± 46.92 [78.24-280.29] (24.38)	237.98 ± 50.29 [150.11-340.78] (21.13)
Kebara isolated teeth	KMH 28	I_2	4.58	7.25	4.08	27.27	130.39	146.61
	KebA5N 13-463	I_2	4.56	7.16	4.65	27.97	92.27	98.47
	KMH 31	C,	6.43	8.47	7.36	43.89	165.08	212.02
Tabun C2	N=1	I_1	4.87	7.12	2.8	28.45	143.68	151.33
	N=1	I_2	5.25	7.42	3.12	31.71	149.92	201.59
	N=1	C,	6.37	8.66	6.49	45.14	201.31	226.62

SOM Table 4b. *Continued.*

			R(MD) [mm]	R(LL) [mm]	CrPV [mm^3]	CA [mm^2]	RSA ling [mm^2]	RSA lab [mm^2]
EMH	N=5	I_1	3.60 ± 0.40 [2.98-4.03] (11.03)	6.35 ± 0.73 [5.48-7.16] (11.43)	3.83 ± 2.52 [0.50-7.41] (65.75)	20.27 ± 4.55 [14.05-25.53] (22.42)	99.60 ± 18.91 [73.31-126.53] (18.98)	94.44 ± 32.20 [47.32-132.34] (34.10)
	N=6	I_2	4.60 ± 0.86 [3.88-6.08] (18.76)	6.37 ± 1.33 [3.68-7.11] (20.85)	6.12 ±2.91 [1.42-9.69] (47.56)	24.83 ± 4.31 [17.93-30.58] (17.37)	111.13 ± 20.89 [76.58-129.48] (18.80)	122.36 ± 30.47 [68.22-155.78] (24.90)
	N=6	C,	5.90 ± 0.50 [5.21-6.38] (8.49)	8.64 ± 0.50 [8.05-9.28] (5.78)	11.51 ± 4.54 [4.80-16.28] (39.45)	43.46 ± 6.17 [36.39-52.66] (14.19)	167.13 ± 28.26 [122.79-199.34] (16.91)	155.38 ± 32.85 [113.07-197.18] (21.14)
UPEPIH	N=9	I_1	3.60 ± 0.19 [3.19-3.82] (5.26)	5.98 ± 0.37 [5.41-6.62] (6.19)	2.40 ± 0.91 [0.96-3.53] (37.89)	17.94 ± 2.05 [14.01-21.04] (11.42)	92.48 ± 11 [75.38-113.19] (11.90)	75.92 ± 13.45 [54.82-99.41] (17.72)
	N=10	I_2	4.01 ± 0.25 [3.69-4.50] (6.34)	6.50 ± 0.35 [5.82-7.17] (5.32)	2.82 ± 0.60 [1.88-3.44] (21.22)	21.49 ± 2.12 [17.21-24.75] (9.85)	101.07 ± 11.96 [87.64-124.23] (11.83)	98.27 ± 11.58 [84.84-119.28] (11.79)
	N=10	C,	5.25 ± 0.45 [4.40-5.82] (8.58)	7.93 ± 0.47 [7.20-8.56] (5.87)	5.67 ± 1.64 [3.26-8.69] (28.86)	34.80 ± 4.41 [26.29-39.81] (12.66)	122.91 ± 16.03 [94.01-151.73] (13.04)	135.73 ± 18.46 [104.09-158.58] (13.60)
RMH	N=39	I_1	3.36 ± 0.27 [2.73-4.11] (8.07)	5.72 ± 0.36 [4.76-6.61] (6.27)	2.28 ± 1.46 [0.02-5.28] (63.99)	15.88 ± 2.09 [10.96-21.31] (13.13)	84.24 ± 14.40 [60.66-117.78] (17.09)	70.39 ± 13.77 [43.65-99.50] (19.57)
	N=47	I_2	3.65 ± 0.34 [3.01-4.47] (9.44)	6.20 ± 0.36 [5.49-6.99] (5.89)	2.70 ± 1.49 [0.02-6.21] (55.16)	19.00 ± 2.27 [15.22-26.04] (11.95)	92.27 ± 17.14 [28.03-123.13] (18.57)	92.32 ± 14.38 [62.82-128.01] (15.57)
	N=23	C,	5.18 ± 0.55 [4.01-6.41] (10.53)	7.85 ± 0.68 [6.77-9.21] (8.63)	5.28 ± 2.37 [2.33-13.87] (44.78)	33.62 ± 5.92 [24.49-47.81] (17.62)	132.35 ± 27.29 [83.62-183.70] (20.62)	139.57 ± 31.45 [98.64-234.10] (22.53)

N stands for sample size; mean ± standard deviation [minimum-maximum].

SOM Table 5a1. Descriptive statistics of the ratios for the upper anterior dentition.

			CrLL/RL	R(LL)/R(MD)	RSA/CA	CrPV/RPV	RPV/RV
H. erectus	S7_48	I^1	0.48	0.92	0.14	0.33	0.051
	S7_47	C'	0.51	1.45	0.13	0.44	0.058
	Sangiran 4	C'	0.55	1.64	0.12	0.19	0.104
H. ergaster	N=1	I^1	0.45	1.00	0.15	0.22	0.15
	N=1	I^2	0.42	1.66	0.09	0.29	0.09
Steinheim?	N=1	I^1	0.64	1.26	0.17	1.38	0.049
	N=1	I^2	0.44	1.13	0.14	0.89	0.047
Neanderthals	N=17	I^1	0.50 ± 0.079 [0.42-0.77] (15.80)	1.09 ± 0.13 [0.92-1.42] (12.15)	0.14 ± 0.028 [0.09-0.22] (20.76)	0.47 ± 0.19 [0.04-0.78] (40.23)	0.083 ± 0.047 [0.010-0.17] (56.58)
	N=18	I^2	0.50 ± 0.051 [0.43-0.63] (10.31)	1.31 ± 0.08 [1.17-1.46] (5.80)	0.12 ± 0.014 [0.10-0.15] (12.39)	0.42 ± 0.19 [0.19-1.00] (45.90)	0.067 ± 0.042 [0.022-0.16] (62.66)
	N=12	C'	0.44 ± 0.065 [0.35-0.55] (14.79)	1.51 ± 0.13 [1.38-1.85] (8.44)	0.10 ± 0.018 [0.08-0.14] (17.71)	0.34 ± 0.09 [0.23-0.56] (27.56)	0.060 ± 0.036 [0.025-0.16] (60.97)
Isolated teeth from Kebara	KMH 27	I^2	0.54	1.18	0.13	0.36	0.047
	Keb90-E19R2	C'	0.54	1.45	0.15	0.36	0.049

SOM Table 5a1. *Continued.*

			CrLL/RL	R(LL)/R(MD)	RSA/CA	CrPV/RPV	RPV/RV
EMH		I^1	N=2; 0.47 ± 0.049 [0.43-0.50]	N=3; 1.03 ± 0.14 [0.87-1.14] (13.65)	N=2; 0.13 ± 0.035 [0.10-0.15]	N=2; 0.48 ± 0.32 [0.25-0.70]	N=2; 0.076 ± 0.089 [0.013-0.14]
	N=3	I^2	0.50 ± 0.074 [0.44-0.58] (14.84)	1.38 ± 0.22 [1.13-1.53] (15.67)	0.13 ± 0.021 [0.11-0.15] (16.43)	0.31 ± 0.28 [0.01-0.57] (91.79)	0.092 ± 0.054 [0.039-0.15] (57.94)
	N=3	C'	0.50 ± 0.065 [0.43-0.56] (13.10)	1.39 ± 0.14 [1.27-1.54] (9.80)	0.13 ± 0.006 [0.13-0.14] (4.33)	0.25 ± 0.21 [0.05-0.46] (82.07)	0.063 ± 0.045 [0.026-0.11] (71.94)
UPEPIH	N=6	I^1	0.57 ± 0.075 [0.48-0.68] (13.33)	1.01 ± 0.07 [0.90-1.12] (7.38)	0.17 ± 0.019 [0.15-0.19] (11.17)	0.68 ± 0.34 [0.34-1.11] (49.21)	0.039 ± 0.0058 [0.029-0.05] (14.84)
	N=6	I^2	0.49 ± 0.082 [0.40-0.64] (16.94)	1.30 ± 0.10 [1.12-1.39] (7.75)	0.12 ± 0.011 [0.11-0.14] (9.13)	0.61 ± 0.24 [0.39-0.95] (39.10)	0.039 ± 0.0098 [0.024-0.05] (25.31)
	N= 8	C'	0.54 ± 0.086 [0.45-0.74] (16.01)	1.52 ± 0.12 [1.32-1.70] (7.94)	0.10 ± 0.044 [0.06-0.18] (43.24)	0.47 ± 0.18 [0.26-0.78] (37.58)	0.047 ± 0.010 [0.031-0.06] (22.38)
RMH	N=24	I^1	0.56 ± 0.059 [0.46-0.67] (10.56)	1.08 ± 0.08 [0.91-1.30] (7.66)	0.16 ± 0.019 [0.12-0.19] (11.85)	0.75 ± 0.46 [0.07-1.60] (61.44)	0.039 ± 0.023 [0.007-0.12] (59.35)
	N=22	I^2	0.50 ± 0.056 [0.36-0.62] (11.25)	1.28 ± 0.13 [0.98-1.50] (9.85)	0.13 ± 0.016 [0.11-0.17] (12.53)	0.61 ± 0.34 [0.03-1.14] (54.94)	0.041 ± 0.031 [0.005-0.14] (74.78)
	N=12	C'	0.49 ± 0.046 [0.44-0.60] (9.42)	1.44 ± 0.10 [1.32-1.68] (6.76)	0.09 ± 0.013 [0.07-0.11] (14.35)	0.40 ± 023 [0-0.67] (57.57)	0.031 ± 0.011 [0.012-0.05] (36.51)

N stands for sample size; mean ± standard deviation [minimum-maximum].

SOM Table 5a2. Mann-Whitney U test results for the comparison between Neanderthals and RMH in the ratios for the upper dentition.

		I^1 N_{Hn}=17 N_{RMH}=24	I^2 N_{Hn}=18 N_{RMH}=22	C' N_{Hn}=12 N_{RMH}=12
CrLL/RL	U_{Min}	81	189	38.5
	p	***7.60e-04***	*ns*	*ns*
R(LL)/R(MD)	U_{Min}	201	192.5	46
	p	*ns*	*ns*	*ns*
RSA/CA	U_{Min}	82	95	39
	p	***7.55e-04***	***3.42e-03***	*ns*
CrPV/RPV	U_{Min}	125.5	133	51
	p	***3.74e-02***	*ns*	*ns*
RPV/RV	U_{Min}	74.5	113.5	18
	p	***3.69e-04***	***2.07e-02***	***1.02e-03***

SOM Table 5a3. Mann-Whitney U test results for the comparison between Neanderthals and EMH in the ratios for the upper dentition.

		I^1	I^2	C'
		N_{Hn}=17 N_{EMH}=3	N_{Hn}=18 N_{EMH}=3	N_{Hn}=12 N_{EMH}=3
CrLL/RL	U_{Min}	13	23	8.5
	p	*ns*	*ns*	*ns*
R(LL)/R(MD)	U_{Min}	19.5	18	9
	p	*ns*	*ns*	*ns*
RSA/CA	U_{Min}	15	15.5	3.5
	p	*ns*	*ns*	***0.042***
CrPV/RPV	U_{Min}	17.5	23.5	13
	p	*ns*	*ns*	*ns*
RPV/RV	U_{Min}	16	18	18
	p	*ns*	*ns*	*ns*

We have checked that our small sample sizes have a negligible effect on our results, following the method described for SOM Tables 3a and 3b.

SOM Table 5a4. Mann-Whitney U test results for the comparison between EMH and RMH in the ratios for the upper dentition.

		I^1	I^2	C'
		N_{EMH}=3 N_{RMH}=24	N_{EMH}=3 N_{RMH}=22	N_{EMH}=3 N_{RMH}=12
CrLL/RL	U_{Min}	4.5	27	17.5
	p	*ns*	*ns*	*ns*
R(LL)/R(MD)	U_{Min}	30.5	22	12
	p	*ns*	*ns*	*ns*
RSA/CA	U_{Min}	8.5	30	0
	p	*ns*	*ns*	*2.20e-03* (1)
CrPV/RPV	U_{Min}	15	15.5	11.5
	p	*ns*	*ns*	*ns*
RPV/RV	U_{Min}	25	15.5	7.5
	p	*ns*	*ns*	*ns*

We have checked that our small sample sizes have a negligible effect on our results, following the method described for SOM Tables 3a and 3b.
It appears that the significance for the RSA/CA for the C' (1) could be biased by the sample size. This result is therefore not reliable.

SOM Table 5b1. Descriptive statistics of the ratios for the lower anterior dentition.

			CrLL/RL	R(LL)/R(MD)	RSA/CA	CrPV/RPV	RPV/RV
H. erectus	S7_50	I_2	0.46	1.49	0.10	0.23	0.071
H. ergaster	N=1	I_1	0.34	1.51	0.09	0.43	0.022
	N=1	I_2	0.37	1.66	0.09	0.24	0.045
H. heidelbergensis	N=1	I_1	0.45	1.75	0.09	0.45	0.55
	N=1	I_2	0.47	1.74	0.10	0.38	0.59
	N=1	C,	0.42	1.42	0.11	0.28	0.079
Neanderthals	N=17	I_1	0.43 ± 0.047 [0.35-0.50] (10.82)	1.67 ± 0.10 [1.51-1.89] (5.96)	0.09 ± 0.010 [0.07-0.11] (11.69)	0.29 ± 0.16 [0-0.68] (53.55)	0.041 ± 0.027 [0.013-0.10] (64.81)
	N=15	I_2	0.42 ± 0.044 [0.35-0.48] (10.27)	1.66 ± 0.12 [1.36-1.87] (7.04)	0.09 ± 0.010 [0.07-0.10] (11.61)	0.29 ± 0.14 [0.05-0.62] (49.05)	0.054 ± 0.036 [0.016-0.13] (66.00)
	N=16	C,	0.43 ± 0.065 [0.34-0.54] (15.09)	1.54 ± 0.13 [1.37-1.75] (8.18)	0.11 ± 0.041 [0.08-0.25] (37.37)	0.27 ± 0.15 [0.10-0.59] (58.16)	0.057 ± 0.037 [0.019-0.14] (63.72)
Kebara isolated teeth	KMH 28	I_2	0.45	1.58	0.10	0.16	0.076
	KebA5N1 3-463	I_2	0.54	1.57	0.14	0.39	0.058
	KMH 31	C,	0.41	1.32	0.12	0.40	0.038

SOM Table 5b1. *Continued.*

			CrLL/RL	R(LL)/R(MD)	RSA/CA	CrPV/RPV	RPV/RV
Tabun C2	N=1	I_1	0.38	1.46	0.10	0.24	0.035
	N=1	I_2	0.36	1.41	0.09	0.22	0.033
	N=1	C,	0.38	1.36	0.11	0.30	0.037
EMH	N=5	I_1	0.45 ± 0.05 [0.39-0.50] (11.09)	1.77 ± 0.08 [1.63-1.84] (4.58)	0.11 ± 0.011 [0.09-0.12] (10.76)	0.39 ± 0.24 [0.11-0.66] (61.03)	0.062 ± 0.038 [0.022-0.11] (61.02)
	N=6	I_2	0.46 ± 0.050 [0.38-0.50] (10.92)	1.45 ± 0.45 [0.61-1.83] (31.30)	0.11 ± 0.014 [0.09-0.12] (13.13)	0.46 ± 0.06 [0.36-0.53] (12.49)	0.056 ± 0.032 [0.015-0.11] (57.61)
	N=6	C,	0.48 ± 0.047 [0.40-0.53] (9.76)	1.47 ± 0.09 [1.34-1.60] (6.32)	0.13 ± 0.019 [0.11-0.16] (13.96)	0.37 ± 0.16 [0.24-0.64] (45.00)	0.095 ± 0.062 [0.041-0.20] (65.31)
UPEPIH	N=9	I_1	0.48 ± 0.046 [0.39-0.54] (9.41)	1.66 ± 0.09 [1.52-1.79] (5.35)	0.11 ± 0.009 [0.09-0.12] (8.36)	0.67 ± 0.20 [0.34-1.04] (29.63)	0.026 ± 0.011 [0.007-0.04] (40.73)
	N=10	I_2	0.44 ± 0.033 [0.37-0.49] (7.37)	1.63 ± 0.10 [1.40-1.75] (6.29)	0.11 ± 0.012 [0.09-0.13] (10.98)	0.61 ± 0.23 [0.36-1.14] (36.88)	0.028 ± 0.0085 [0.012-0.04] (30.40)
	N=10	C,	0.50 ± 0.061 [0.40-0.60] (12.15)	1.52 ± 0.10 [1.37-1.67] (6.89)	0.14 ± 0.015 [0.12-0.16] (11.18)	0.45 ± 0.14 [0.22-0.60] (30.45)	0.044 ± 0.0096 [0.028-0.06] (21.91)

SOM Table 5b1. *Continued.*

			CrLL/RL	R(LL)/R(MD)	RSA/CA	CrPV/RPV	RPV/RV
RMH	N=39	I_1	0.47 ± 0.054 [0.37-0.62] (11.44)	1.71 ± 0.12 [1.44-1.98] (7.03)	0.10 ± 0.013 [0.08-0.15] (12.80)	0.54 ± 0.29 [0.02-1.19] (53.00)	0.031 ± 0.014 [0.007-0.07] (44.75)
	N=47	I_2	0.45 ± 0.046 [0.36-0.58] (10.29)	1.71 ± 0.15 [1.30-2.10] (8.84)	0.10 ±0.012 [0.07-0.13] (11.98)	0.50 ± 0.23 [0.01-0.95] (47.36)	0.033 ± 0.017 [0.006-0.09] (50.76)
	N=23	C,	0.47 ± 0.040 [0.40-0.56] (8.54)	1.52 ± 0.13 [1.26-1.83] (8.32)	0.12 ± 0.014 [0.10-0.16] (11.56)	0.36 ± 0.14 [0.12-0.70] (39.74)	0.049 ± 0.014 [0.026-0.08] (28.26)

SOM Table 5b2. Mann-Whitney *U* test results for the comparison between Neanderthals and RMH in the ratios for the lower dentition.

		I_1	I_2	C_1
		N_{Hn}=17 N_{RMH}=39	N_{Hn}=15 N_{RMH}=47	N_{Hn}=16 N_{RMH}=23
CrLL/RL	U_{Min}	210	248.5	113
	p	***0.03***	*ns*	***0.042***
R(LL)/R(MD)	U_{Min}	253.5	299	180
	p	*ns*	*ns*	*ns*
RSA/CA	U_{Min}	88.5	86.5	66
	p	***1.98e-06***	***1.06e-06***	***3.77e-04***
CrPV/RPV	U_{Min}	145	145.5	114.5
	p	***6.16e-04***	***1.19e-03***	***0.047***
RPV/RV	U_{Min}	282.5	233.5	184
	p	*ns*	*ns*	*ns*

SOM Table 5b3. Mann-Whitney *U* test results for the comparison between Neanderthals and EMH in the ratios for the lower dentition.

		I_1	I_2	C,
		N_{Hn}=17 N_{EMH}=5	N_{Hn}=15 N_{EMH}=6	N_{Hn}=16 N_{EMH}=6
CrLL/RL	U_{Min}	33.5	26.5	26.5
	p	*ns*	*ns*	*ns*
R(LL)/R(MD)	U_{Min}	17	39	33.5
	p	*ns*	*ns*	*ns*
RSA/CA	U_{Min}	8	12	13
	p	*ns*	***6.34e-03***	***6.97e-03***
CrPV/RPV	U_{Min}	34.5	16	37.5
	p	*ns*	***5.75e-03***	*ns*
RPV/RV	U_{Min}	25	44	37
	p	*ns*	*ns*	*ns*

We have checked that our small sample sizes have a negligible effect on our results, following the method described for SOM Tables 3a and 3b.

SOM Table 5b4. Mann-Whitney *U* test results for the comparison between EMH and RMH in the ratios for the lower dentition.

		I_1	I_2	C_1
		N_{EMH}=5 N_{RMH}=39	N_{EMH}=6 N_{RMH}=47	N_{EMH}=6 N_{RMH}=23
CrLL/RL	U_{Min}	73.5	124.5	50
	p	*ns*	*ns*	*ns*
R(LL)/R(MD)	U_{Min}	59	100	47
	p	*ns*	*ns*	*ns*
RSA/CA	U_{Min}	84	134	50
	p	*ns*	*ns*	*ns*
CrPV/RPV	U_{Min}	71.5	118.5	55.5
	p	*ns*	*ns*	*ns*
RPV/RV	U_{Min}	55.5	68.5	50
	p	*ns*	***0.040***	*ns*

We have checked that our small sample sizes have a negligible effect on our results, following the method described for SOM Tables 3a and 3b.

SOM Table 6a. Mann-Whitney U test results for the comparison of the crown and root dimensions in the upper dentition between EMH and Neanderthals.

		I^1	I^2	C'
		N_{Hn}=17 N_{EMH}=3	N_{Hn}=18 N_{EMH}=3	N_{Hn}=12 N_{EMH}=3
CrLL [mm]	U_{Min}	18	0	11
	p	*ns*	***0.002***	*ns*
CrPV [mm^3]	U_{Min}	23	12.5	10
	p	*ns*	*ns*	*ns*
R(MD) [mm]	U_{Min}	24	13	14.5
	p	*ns*	*ns*	*ns*
R(LL) [mm]	U_{Min}	17	0	10
	p	*ns*	***0.002***	*ns*
RL [mm]	U_{Min}	12	15	4
	p	*ns*	*ns*	***0.048***
RSA [mm^2]	U_{Min}	10	2	1
	p	*ns*	***0.01***	***0.009***
RSA lab [mm^2]	U_{Min}	9	0	1
	p	*ns*	***0.002***	***0.009***
RSA ling [mm^2]	U_{Min}	11	17	4
	p	*ns*	*ns*	***0.048***
CA [mm^2]	U_{Min}	13	2	11
	p	*ns*	***0.006***	*ns*

SOM Table 6a. *Continued.*

		I^1 N_{Hn}=17 N_{EMH}=3	I^2 N_{Hn}=18 N_{EMH}=3	C' N_{Hn}=12 N_{EMH}=3
RV [mm^3]	U_{Min}	12	1	1
	p	*ns*	***0.003***	***0.009***
RPV [mm^3]	U_{Min}	8	18	13
	p	*ns*	*ns*	*ns*
CrLL/RL	U_{Min}	13	23	8.5
	p	*ns*	*ns*	*ns*
R(LL)/R(MD)	U_{Min}	19.5	18	9
	p	***0.56***	***0.40***	*ns*
RSA lab/ling	U_{Min}	23.5	2	3
	p	*ns*	***0.005***	***0.03***
RSA/CA	U_{Min}	15	15.5	3.5
	p	*ns*	*ns*	***0.042***
CrPV/RPV	U_{Min}	17.5	23.5	13
	p	*ns*	*ns*	*ns*
RPV/RV	U_{Min}	16	18	18
	p	*ns*	*ns*	*ns*

See SOM Table 3a for justification of the use of the test with small sample sizes.

SOM Table 6b. Mann-Whitney U test results for the comparison of the crown and root dimensions in the lower dentition between EMH and Neanderthals.

		I_1 N_{Hn}=17 N_{EMH}=5	I_2 N_{Hn}=15 N_{EMH}=6	C_1 N_{Hn}=16 N_{EMH}=6
CrLL [mm]	U_{Min}	4	12	42
	p	***0.0009***	***0.008***	*ns*
CrPV [mm^3]	U_{Min}	41	44	22
	p	*ns*	*ns*	*ns*
R(MD) [mm]	U_{Min}	4	42	43
	p	***0.0009***	*ns*	*ns*
R(LL) [mm]	U_{Min}	15	9	37.5
	p	***0.03***	***0.003***	*ns*
RL [mm]	U_{Min}	10	9	19
	p	***0.009***	***0.003***	***0.03***
RSA [mm^2]	U_{Min}	3	8	21
	p	***0.0005***	***0.002***	***0.049***
RSA lab [mm^2]	U_{Min}	7	4	6
	p	***0.003***	***0.0004***	***0.0008***
RSA ling [mm^2]	U_{Min}	7	13	31
	p	***0.003***	***0.01***	*ns*
CA [mm^2]	U_{Min}	14	20	45
	p	***0.02***	*ns*	*ns*

SOM Table 6b. *Continued.*

		I_1 N_{Hn}=17 N_{EMH}=5	I_2 N_{Hn}=15 N_{EMH}=6	C, N_{Hn}=16 N_{EMH}=6
RV [mm^3]	U_{Min}	3	7	19
	p	***0.0005***	***0.002***	***0.03***
RPV [mm^3]	U_{Min}	33	33	45
	p	*ns*	*ns*	*ns*
CrLL/RL	U_{Min}	33.5	26.5	26.5
	p	*ns*	*ns*	*ns*
R(LL)/R(MD)	U_{Min}	17	39	33.5
	p	***0.045***	*ns*	*ns*
RSA lab/ling	U_{Min}	33	18.5	11
	p	*ns*	***0.04***	***0.004***
RSA/CA	U_{Min}	8	12	13
	p	***2.58e-03***	***6.34e-03***	***6.97e-03***
CrPV/RPV	U_{Min}	34.5	16	37.5
	p	*ns*	***5.75e-03***	*ns*
RPV/RV	U_{Min}	25	44	37
	p	*ns*	*ns*	*ns*

See SOM Table 3a for justification of the use of the test with small sample sizes.

SOM Table 7a. Mann-Whitney U test results for the comparison of the crown and root dimensions in the upper dentition between EMH and RMH.

		I^1	I^2	C'
		$N_{EMH}=3$ $N_{Hs}=24$	$N_{EMH}=3$ $N_{Hs}=22$	$N_{EMH}=3$ $N_{Hs}=12$
CrLL [mm]	U_{Min}	12	5	4
	p	*ns*	***0.014***	***0.048***
CrPV [mm^3]	U_{Min}	19	21	11
	p	*ns*	*ns*	*ns*
R(MD) [mm]	U_{Min}	11	24.5	0
	p	*ns*	*ns*	***0.004***
R(LL) [mm]	U_{Min}	11.5	3	5
	p	*ns*	***0.006***	*ns*
RL [mm]	U_{Min}	28	19	8
	p	*ns*	*ns*	*ns*
RSA [mm^2]	U_{Min}	32	17	4
	p	*ns*	*ns*	***0.048***
RSA lab [mm^2]	U_{Min}	31	21	*4*
	p	*ns*	*ns*	***0.048***
RSA ling [mm^2]	U_{Min}	34	19	7
	p	*ns*	*ns*	*ns*
CA [mm^2]	U_{Min}	18	9	0
	p	*ns*	***0.045***	***0.004***

SOM Table 7a. *Continued.*

		I^1 N_{EMH}=3 N_{Hs}=24	I^2 N_{EMH}=3 N_{Hs}=22	C' N_{EMH}=3 N_{Hs}=12
RV [mm^3]	U_{Min}	35	18	6
	p	*ns*	*ns*	*ns*
RPV [mm^3]	U_{Min}	30	3	5
	p	*ns*	***0.0061***	*ns*
CrLL/RL	U_{Min}	4.5	27	17.5
	p	*ns*	*ns*	*ns*
R(LL)/R(MD)	U_{Min}	30.5	22	12
	p	*ns*	*ns*	*ns*
RSA lab/ling	U_{Min}	2	24	16.5
	p	***0.02***	*ns*	*ns*
RSA/CA	U_{Min}	8.5	30	0
	p	*ns*	*ns*	***2.20e-03***
CrPV/RPV	U_{Min}	15	15.5	11.5
	p	*ns*	*ns*	*ns*
RPV/RV	U_{Min}	25	11	7.5
	p	*ns*	*ns*	*ns*

See SOM Table 3a for justification of the use of the test with small sample sizes.

SOM Table 7b. Mann-Whitney U test results for the comparison of the crown and root dimensions in the lower dentition between EMH and RMH.

		I_1 N_{EMH}=5 N_{Hs}=39	I_2 N_{EMH}=6 N_{Hs}=47	C, N_{EMH}=6 N_{Hs}=23
CrLL [mm]	U_{Min}	49	45.5	25
	p	*ns*	***0.005***	***0.02***
CrPV [mm^3]	U_{Min}	55	45	14
	p	*ns*	***0.005***	***0.002***
R(MD) [mm]	U_{Min}	56	31	27
	p	*ns*	***0.001***	***0.02***
R(LL) [mm]	U_{Min}	48	55	24.5
	p	*ns*	***0.01***	***0.01***
RL [mm]	U_{Min}	25	76.5	43
	p	***0.005***	*ns*	*ns*
RSA [mm^2]	U_{Min}	39	50	32
	p	***0.03***	***0.008***	***0.047***
RSA lab [mm^2]	U_{Min}	46	53	48
	p	*ns*	***0.01***	*ns*
RSA ling [mm^2]	U_{Min}	50	66	26
	p	*ns*	***0.03***	***0.02***
CA [mm^2]	U_{Min}	38	35	13.5
	p	***0.03***	***0.002***	***0.001***

SOM Table 7b. *Continued.*

		I_1 N_{EMH}=5 N_{Hs}=39	I_2 N_{EMH}=6 N_{Hs}=47	C, N_{EMH}=6 N_{Hs}=23
RV [mm^3]	U_{Min}	39	41	25
	p	***0.03***	***0.003***	***0.02***
RPV [mm^3]	U_{Min}	29	37	37
	p	***0.008***	***0.002***	***0.007***
CrLL/RL	U_{Min}	73.5	124.5	50
	p	*ns*	*ns*	*ns*
R(LL)/R(MD)	U_{Min}	59	100	47
	p	*ns*	*ns*	*ns*
RSA lab/ling	U_{Min}	83	108.5	38
	p	*ns*	*ns*	*ns*
RSA/CA	U_{Min}	84	134	50
	p	*ns*	*ns*	*ns*
CrPV/RPV	U_{Min}	71.5	118.5	55.5
	p	*ns*	*ns*	*ns*
RPV/RV	U_{Min}	55.5	68.5	50
	p	*ns*	***0.040***	*ns*

See SOM Table 3a for justification of the use of the test with small sample sizes.

SOM Table 8a. Descriptive statistics for the upper anterior dentition, involving the teeth for which the wear stage is comprised between 1 and 4, following Smith (1984)'s scoring system. Neanderthals still have significantly larger RPV than RMH (see SOM. Table 8c).

			Wear stage	RPV [mm^3]
H. erectus	S7_47	C'	2	43.42
	Sangiran 4	C'	3	90.62
H. ergaster	N=1	I^1	2	49.62
	N=1	I^2	2	27.32
Steinheim?	N=1	I^1	3	9.93
	N=1	I^2	2	9.52
Neanderthals	N=7	I^1	3.0 ± 0.6 [2-4] (19.2)	54.96 ± 16.21 [42.42-85.97] (29.49)
	N=15	I^2	3.1 ± 1.0 [2-4] (33.7)	34.53 ± 18.14 [11.36-81.67] (52.55)
	N=12	C'	3.2 ± 1.0 [1-4] (32.5)	36.65 ± 14.84 [16.44-66.34] (40.50)
Isolated teeth from Kebara	Keb90-E19R2	C'	4	13.78
EMH	N=1	I^1	3	30.36
	N=2	I^2	2.0 ± 1.4 [1-3]	26.66 ± 9.26 [20.11-33.20]
	N=2	C'	3.0 ± 1.4 [2-4]	33.58 ± 33.21 [10.09-57.06] (98.92)
UPEPIH	N=3	I^1	3.3 ± 0.6 [3-4] (17.3)	10.96 ± 0.36 [10.71-11.37] (3.24)
	N=4	I^2	2.3 ± 0.5 [2-3] (22.2)	9.46 ± 2.17 [9.46-11.45] (22.96)
	N= 7	C'	3.0 ± 0.8 [2-4] (27.2)	16.40 ± 6.36 [7.13-25.08] (38.77)
RMH	N=24	I^1	2.9 ± 0.9 [1-4] (32.9)	8.74 ± 5.18 [1.61-24.05] (59.26)
	N=21	I^2	1.9 ± 1.1 [1-4] (59.7)	6.70 ± 5.03 [0.86-19.98] (74.98)
	N=12	C'	2.6 ± 1.2 [1-4] (45.1)	9.54 ± 4.05 [2.92-15.17] (42.42)

N stands for sample size; mean ± standard deviation [minimum-maximum].

SOM.Table 8b. Descriptive statistics for the lower anterior dentition, involving the teeth for which the wear stage is comprised between 1 and 4, following Smith (1984)'s scoring system. Neanderthals still have significantly larger RPV than RMH (see SOM Table 8c).

			Wear stage	RPV [mm^3]
H. ergaster	N=1	I_1	2	6.26
	N=1	I_2	2	20.93
Neanderthals	N=4	I_1	3.8 ± 0.5 [1-4] (13.3)	19.39 ± 4.16 [16.01-24.89] (21.44)
	N=7	I_2	3.6 ± 0.5 [3-4] (15.0)	29.18 ± 18.08 [7.28-63.03] (61.95)
	N=11	C,	2.6 ± 1.4 [1-4] (51.7)	36.49 ± 20.92 [13.77-70.75] (57.33)
Kebara isolated teeth	KMH 28	I_2	4	25.10
	KebA5N13-463	I_2	4	12.03
EMH	N=3	I_1	2.7 ± 1.5 [1-4] (57.3)	15.48 ± 6.70 [9.40-22.66] (43.27)
	N=5	I_2	3.4 ± 0.5 [3-4] (16.1)	14.77 ± 4.81 [9.40-20.63] (32.55)
	N=5	C,	2.4 ± 0.9 [2-4] (0.37)	41.15 ± 20.52 [15.66-62.45] (49.86)
UPEPIH	N=5	I_1	4.0 ± 0 [4-4] (0)	5.01 ± 0.41 [4.59-5.61] (8.28)
	N=10	I_2	3.4 ± 0.7 [2-4] (22.0)	5.49 ± 1.43 [2.93-6.71] (25.99)
	N=9	C,	3.0 ±0.7 [2-4] (23.6)	13.29 ± 4.13 [5.78-19.98] (31.09)
RMH	N=30	I_1	3.4 ± 0.8 [2-4] (24.0)	4.11 ± 2.31 [1.17-11.21] (56.22)
	N=40	I_2	2.7 ± 0.9 [1-4] (33.4)	5.57 ± 2.91 [0.77-15.15] (52.33)
	N=23	C,	2.8 ± 0.9 [1-4] (31.4]	16.73 ± 9.36 [7.17-48.13] (55.98)

SOM Table 8c. Mann-Whitney U test results for the comparison of the wear stage and root pulp volume (RPV), involving the teeth (upper and lower dentitions), for which the wear stage is comprised between 1 and 4, following Smith (1984)'s scoring system.

		I_1	I_2	C,	I^1	I^2	C'
		N_{Hn}=4 N_{RMH}=30	N_{Hn}=7 N_{RMH}=43	N_{Hn}=11 N_{RMH}=23	N_{Hn}=7 N_{RMH}=24	N_{Hn}=15 N_{RMH}=21	N_{Hn}=12 N_{RMH}=12
Wear	U_{Min}	46	71	116.5	80	64.5	50.5
	p	*ns*	***0.019***	*ns*	*ns*	***1. 39e-03***	*ns*
RPV [mm^3]	U_{Min}	0	9	44	0	8	0
	p	*4.31e-05*	***1.88e-06***	***1.69e-03***	*7.61e-07*	***2.41e-08***	*7.40e-07*

We checked for the effect of small sample sizes, as explained in SOM Table 3a, and the significant p-values that may be affected by the sample sizes is not bolded (these p-values are equal to the smallest p-values given by this verification).

SOM.9. Comparative data on root length from the literature.

Is the comparison of the measurements collected from the literature to the measurements taken in the present study reliable?

In the literature, root length is measured mostly from the labial side of the cervix of the tooth to the apex, and less frequently from the lingual aspect of the cervix. It is also often not mentioned which technique has been used to measure root length. Since we measured root length from the center of the cervical plane to the root tip on micro-CT data, it is worth evaluating whether this difference in measurement technique could potentially influence the comparison we aim to perform. In addition to the root length measurement we have described in the paper, we also measured the root length from the labial side and from the lingual aspect of the cervix (at the point of maximum curvature of the cervical line, approximately at the middle of the labial and lingual faces). For both supplementary root length measurement and for each tooth type and taxon, we computed the percentage of difference with the root length measured from the center of the cervical pulp. As we can see in the table below (SOM 9 - Table 1), overall and on average, the minimal errors are of -5.32% and -3.53% for the labial and for the lingual measurements, and the maximal errors are of -1.00% for the labial and of 0.02% for the lingual. We are aware of the fact that root shape can explain a portion of these differences between the three root length measurements, but also that our measurements are all taken on 3D models derived from micro-CT data while data from the literature are taken on real specimens using calipers, and finally that gathering data from different publications involves an inter-observer error. However, with these differences being inferior to 6% in absolute values, the comparison of the data collected from the literature with the micro-CT data presented in this study remains valid.

SOM 9.Table 1. Reliability of the comparison of root length data from this study and from the literature.

	UI1		UI2		UC		LI1		LI2		LC	
	%Lab.	%Ling.	%Lab.	%Ling.	%Lab.	%Ling.	%Lab.	%Ling.	%Lab.	%Ling.	%Lab.	%Ling.
H. er.	-3.87	-0.18	-3.82	-2.87	-4.05	-2.34	-2.84	0.41	-3.49	-0.77	-	-
Mauer	-	-	-	-	-	-	-3.58	-1.21	-4.85	0.54	-1.88	-2.12
Neand.	-3.51	-1.3	-4.63	-0.02	-1.69	-2.59	-4.63	0.92	-4.02	0.14	-0.95	-3.05
EMH	-4.04	-2.02	-4.79	-0.99	-1.94	-3.69	-2.07	-0.79	-2.94	-2.01	0.14	-5.11
RMH	-2.33	-3.76	-4.79	0.18	-2.54	-2.82	-2.79	-2.06	-3.21	-1.1	0.06	-5.04
UPEPIH	-2.67	-5.15	-5.02	0.14	-3.09	-3.41	-2.94	-3.08	-2.69	-1.57	-1.79	-4.47
Kebara	-	-	-6.89	0.6	-3.12	-4.34	-	-	-1.91	-2.54	-1.62	-2.14
Tabun C2	-	-	-	-	-	-	-2.19	-1.37	-4.26	0.9	-0.98	-2.76
Steinheim	-2.13	-5.21	-7.31	3.08	-	-	-	-	-	-	-	-
Average	-3.09	-2.94	-5.32	0.02	-2.74	-3.20	-3.01	-1.03	-3.42	-0.80	-1.00	-3.53

Root length comparative data for European Lower and Middle Pleistocene Humans and Neanderthals

A non-exhaustive compilation of root length data collected from the literature is presented in SOM 9 Table 2. It has to be noted that for the Dmanisi and the Sima de los Huesos (Atapuerca) specimens AT-5615 to AT-164, the buccal and lingual root lengths were measured by one of us (ALC) in Photoshop, by averaging two successive measurements taken respectively on Figures 3, 4, 18, 19 & 20 in Martinón-Torres et al. (2008) and Figures 1, 2, 3, 4, 5, 13, 14 & 15 in Martinón-Torres et al. (2012). For the I_1 (R) and I_1 (L) from Grotte du Portel, root length has been calculated by subtracting the crown height from the total tooth height (both provided in Brabant and Saly, 1964: 24.5-9.5 for the first tooth, 24.1-10 for the second tooth).

We computed adjusted z-scores (Maureille et al., 2001) on each specimen to test whether or not it is included in the 95% confidence interval of our samples of Neanderthals, EMH and RMH. To summarize the results, we used the following code in the SOM 9 Table 2:

In the three following graphs (SOM 9 – Fig. 1), we compare the AT-8 maxillary central incisor to the sample of Neanderthals, EMH and RMH.

- If AT-8 plots at 0, it means that its root length is similar to the mean of the comparative sample (Neanderthals, for example). We coded this situation as: Neand~0.

- If -1<AT-8<1, AT-8 plots in the 95% confidence interval of the Neanderthal sample; for -1<AT-8<0, we coded: Neand-; for 0<AT-8<1, Neand+.

- If AT-8<-1 and AT-8>1, AT-8 plots outside the 95% confidence interval of the Neanderthal sample; for AT-8<-1, we coded: <<Neand and for AT-8>1, >>Neand.

In the case where AT-8 plots at the limit of the 95% interval, we used the following codes: for AT-8~=-1, we coded: ≤Neand; and for AT-8~=1: ≥Neand.

Therefore, in the table (SOM 9 Table 2), we recorded for AT-8: Neand+; EMH~0; >>RMH.

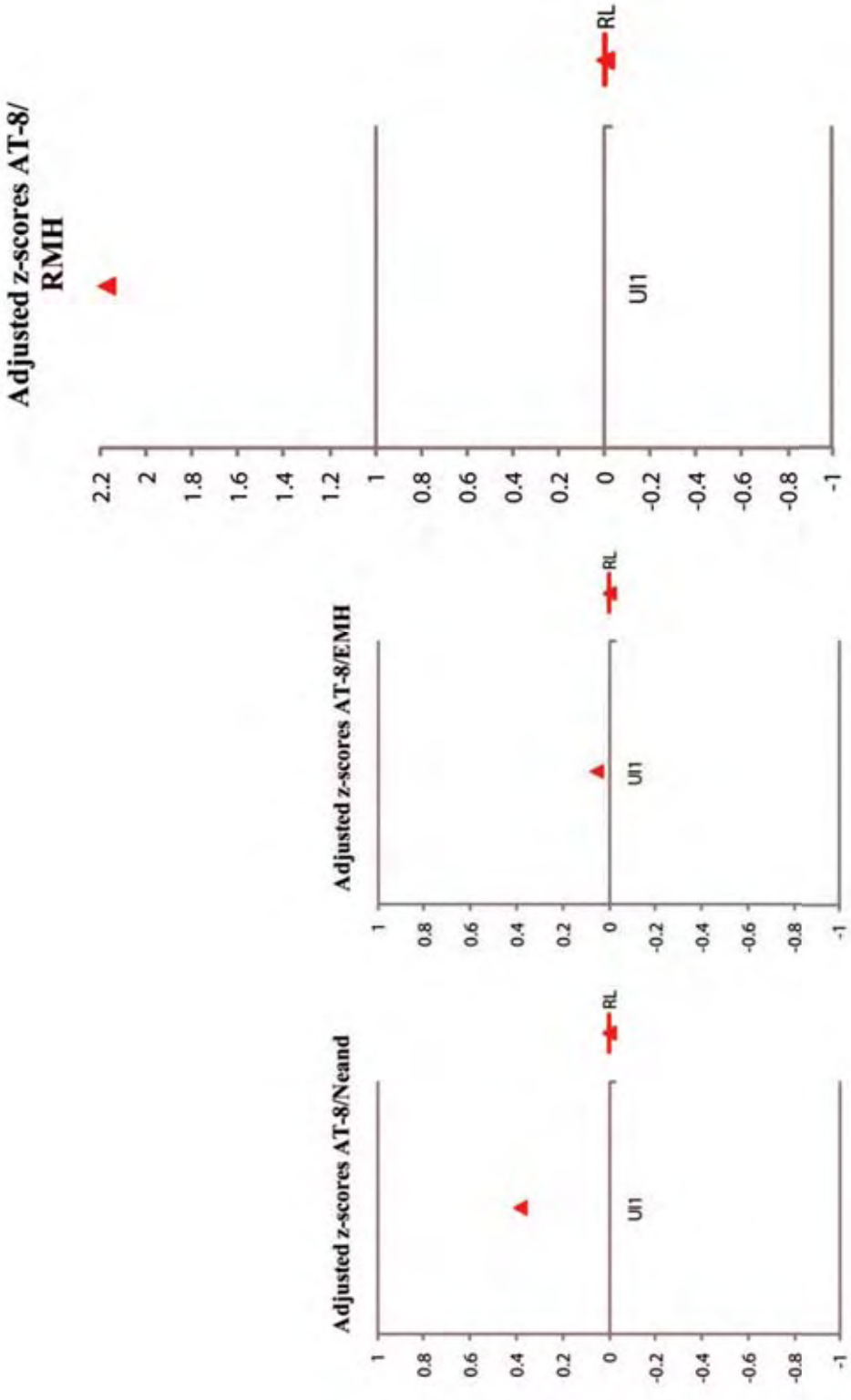

SOM 9. Figure 1. Adjusted z-scores for the comparison of root lengths collected in the literature to the samples used in this study.

SOM 9. Table 2. Root length comparative data for European Middle Pleistocene Humans and Neanderthals.

Site	Datation	Taxon	Specimen	Individual's age	Tooth type	Cr [mm]	Comparison with our samples	RL [mm]	Comparison with our samples	Side for RL	References
Damnisi, Republic of Georgia	1.8 Ma	*H. georgicus*	D3698	male subadult (D2700 /D2735, Rightmire et al., 2006)	I_2 (L)	7.6	Neand-EMH+ >RMH	16.87	Neand-EMH+ ≥RMH	Bucc.	Martinón-Torres et al. (2008)
								17.41	Neand-EMH+ >RMH	Ling.	
			D2678		C, (R)	9.2	Neand+ EMH+ ≥RMH	20.79	Neand~0 EMH+ >>RMH	Bucc.	
								21.69	Neand+ >EMH >>RMH	Ling.	
			D2736		I^1 (R)	7.8	Neand-EMH~0 RMH+	21.25	Neand+ EMH~0 >>RMH	Bucc.	
								19.73	Neand+ EMH~0 >>RMH	Ling.	
			D2677		I^2 (L)	6.9	<Neand EMH-RMH+	18.38	Neand+ EMH+ >>RMH	Bucc.	
								18.38	Neand+ EMH+ >>RMH	Ling.	
			D2732		C' (R)	9.9	Neand+ EMH+ >>RMH	17.38	≤Neand EMH~0 RMH+	Bucc.	
								18.65	Neand-EMH~0 RMH+	Ling.	

SOM 9. Table 2. *Continued.*

Site	Datation	Taxon	Specimen	Individual's age	Tooth type	Cr [mm]	Comparison with our samples	RL [mm]	Comparison with our samples	Side for RL	References
Gran Dolina, Sierra de Atapuerca, Ibeas de Juarros, Burgos, Spain	> 780 ka (>MIS 21)	EMPH (*Homo antecessor*)	ATD6-H1	<13 years (Bermúdez de Castro et al., 2006)	C, (L)	11.0	Neand+ EMH+ >>RMH	18.0	Neand- EMH~0≥RMH	Bucc.	Bermúdez de Castro et al. (1999)
Sima de los Huesos, Sierra de Atapuerca, Ibeas de Juarros, Burgos, Spain	400ka–500ka, (MIS 12–14) Bermùdez de Castro et al. (2003)	EMPH	AT-8	-	I^1 (L)	-	-	19.2	Neand+ EMH~0 >>RMH	Bucc.	Bermúdez de Castro (1988)
			AT-27	12.5-14.5 years (Lozano et al., 2008)	I^1 (L)	-	-	18.4	Neand+ EMH~0 >>RMH		
			AT-54	-	I^1 (R)	-	-	18.9	Neand+ EMH~0 >>RMH		
			AT-146	-	I^1 (R)	7.7	Neand- EMH~0 RMH+	19.0	Neand+ EMH~0 >>RMH		
			AT-7	-	I^2 (L)	-	-	19.0	Neand+ EMH+ >>RMH		
			AT-29	-	I^2 (R)	-	-	18.5	Neand+ EMH+ >>RMH		
			AT-53	-	I^2 (L)	-	-	16.0	Neand- EMH~0 ≥RMH		

SOM 9. Table 2. *Continued.*

Site	Datation	Taxon	Specimen	Individual's age	Tooth type	Cr [mm]	Comparison with our samples	RL [mm]	Comparison with our samples	Side for RL	References
Sima de los Huesos, Sierra de Atapuerca, Ibeas de Juarros, Burgos, Spain	400ka–500ka, (MIS 12–14) Bermùdez de Castro et al. (2003)	EMPH	AT-6	-	C'(L)	-	-	19.0	Neand- EMH+ RMH~0		
			AT-44	-	C'(L)	-	-	24.0	Neand+ EMH+ ≥RMH		
			AT-144	24-30 years (Lozano et al., 2008)	C'(R)	-	-	24.0	Neand+ EMH+ >RMH		
			AT-24	24-30 years (Lozano et al., 2008)	C, (R)	-	-	18.0	Neand- EMH~0 RMH+		
			AT-145	24-30 years (Lozano et al., 2008)	C, (L)	9.8	Neand+ EMH+ >RMH	20.9	Neand~0 EMH+ >>RMH		
			AT-5615	-	I^1 (R)	-	-	17.52	Neand~0 EMH~0 >RMH	Bucc.	Martinón-Torres et al. (2012)
								16.93	Neand- EMH~0 >RMH	Ling.	
			AT-197	-	I^1 (R)	-	-	16.01	Neand- EMH~0 >RMH	Bucc.	
								15.92	Neand- EMH~0 >RMH	Ling.	

SOM 9. Table 2. *Continued.*

Site	Datation	Taxon	Specimen	Individual's age	Tooth type	Cr [mm]	Comparison with our samples	RL [mm]	Comparison with our samples	Side for RL	References
Sima de los Huesos, Sierra de Atapuerca, Ibeas de Juarros, Burgos, Spain	400ka–500ka, (MIS 12–14) Bermùdez de Castro et al. (2003)	EMPH	AT-199	-	I^1 (L)	-	-	16.03	Neand-EMH~0 >RMH	Bucc.	Martinón-Torres et al. (2012)
								14.40	Neand-EMH~0 RMH+	Ling.	
			AT-280	-	I^1 (L)	-	-	16.18	Neand-EMH~0 >RMH	Bucc.	
								16.21	Neand-EMH~0 >RMH	Ling.	
			AT-954	-	I^1 (R)	-	-	15.60	Neand-EMH~0 RMH+	Bucc.	
								15.60	Neand-EMH~0 RMH+	Ling.	
			AT-165	-	I^1 (L)	-	-	20.36	Neand+ EMH+ >>RMH	Bucc.	
								20.20	Neand+ EMH+ >>RMH	Ling.	
			AT-1143	-	I^1 (L)	-	-	17.07	Neand-EMH~0 >RMH	Bucc.	
								16.76	Neand-EMH~0 >RMH	Ling.	

SOM 9. Table 2. *Continued.*

Site	Datation	Taxon	Specimen	Individual's age	Tooth type	Cr [mm]	Comparison with our samples	RL [mm]	Comparison with our samples	Side for RL	References
Sima de los Huesos, Sierra de Atapuerca, Ibeas de Juarros, Burgos, Spain	400ka–500ka, (MIS 12–14) Bermùdez de Castro et al. (2003)	EMPH	AT-2752	-	I^1 (L)	-	-	18.86	Neand+ EMH~0 >>RMH	Bucc.	Martinón-Torres et al. (2012)
								19.01	Neand+ EMH~0 >>RMH	Ling.	
			AT-3193	-	I^1 (R)	-	-	18.91	Neand+ EMH~0 >>RMH	Bucc.	
								17.75	Neand+ EMH~0 >>RMH	Ling.	
			AT-3194	-	I^1 (L)	-	-	18.60	Neand+ EMH~0 >>RMH	Bucc.	
								18.16	Neand+ EMH~0 >>RMH	Ling.	
			AT-4320	-	I^1 (L)	-	-	18.14	Neand+ EMH~0 >>RMH	Bucc.	
								18.42	Neand+ EMH~0 >>RMH	Ling.	
			AT-554	-	I^1 (L)	-	-	19.81	Neand+ EMH+ >>RMH	Bucc.	
								19.79	Neand+ EMH+ >>RMH	Ling.	

SOM 9. Table 2. *Continued.*

Site	Datation	Taxon	Specimen	Individual's age	Tooth type	Cr [mm]	Comparison with our samples	RL [mm]	Comparison with our samples	Side for RL	References
Sima de los Huesos, Sierra de Atapuerca, Ibeas de Juarros, Burgos, Spain	400ka–500ka, (MIS 12–14) Bermùdez de Castro et al. (2003)	EMPH	AT-961	-	I^2 (L)	-	-	16.32	Neand-EMH+ >RMH	Bucc.	Martinón-Torres et al. (2012)
								15.98	Neand-EMH+ >RMH	Ling.	
			AT-4321	-	I^2 (L)	-	-	16.75	Neand-EMH+ >RMH	Bucc.	
								16.47	Neand-EMH+ >RMH	Ling.	
			AT-4332	-	I^2 (R)	-	-	18.54	Neand+ EMH+ >>RMH	Bucc.	
								18.18	Neand+ EMH+ >>RMH	Ling.	
			AT-1444	-	I^2 (R)	-	-	16.39	Neand-EMH~0 >RMH	Bucc.	
								16.08	Neand-EMH~0 >RMH	Ling.	
			AT-1953	-	I^2 (L)	-	-	15.32	Neand-EMH~0 RMH+	Bucc.	
								15.25	Neand-EMH~0 RMH+	Ling.	

SOM 9. Table 2. *Continued.*

Site	Datation	Taxon	Specimen	Individual's age	Tooth type	Cr [mm]	Comparison with our samples	RL [mm]	Comparison with our samples	Side for RL	References
Sima de los Huesos, Sierra de Atapuerca, Ibeas de Juarros, Burgos, Spain	400ka–500ka, (MIS 12–14) Bermùdez de Castro et al. (2003)	EMPH	AT-4327	-	I^2 (R)	-	-	- 15.95	- Neand-EMH~0 ≥RMH	Bucc. Ling.	Martinón-Torres et al. (2012)
			AT-2769	-	I^2 (R)	-	-	- 17.19	- Neand-EMH+ >RMH	Bucc. Ling.	
			AT-2272	-	I^2 (L)	-	-	- 17.73	- Neand~0 EMH+ >RMH	Bucc. Ling.	
			AT-2280	-	I^2 (R)	-	-	- 17.16	- Neand-EMH+ >RMH	Bucc. Ling.	
			AT-820	-	I^2 (L)	-	-	- 18.53	- Neand+ EMH+ >RMH	Bucc. Ling.	
			AT-962	-	I^2 (R)	-	-	- 18.53	- Neand+ EMH+ >RMH	Bucc. Ling.	
			AT-3195	-	I^2 (R)	-	-	- 19.48	- Neand+ EMH+ >>RMH	Bucc. Ling.	

SOM 9. Table 2. *Continued.*

Site	Datation	Taxon	Specimen	Individual's age	Tooth type	Cr [mm]	Comparison with our samples	RL [mm]	Comparison with our samples	Side for RL	References
Sima de los Huesos, Sierra de Atapuerca, Ibeas de Juarros, Burgos, Spain	400ka–500ka, (MIS 12–14) Bermùdez de Castro et al. (2003)	EMPH	AT-3196	-	I^2 (L)	-	-	-	-	Bucc.	Martinón-Torres et al. (2012)
								17.49	Neand~0 EMH+ >RMH	Ling.	
			AT-5608	-	I^2 (R)	-	-	-	-	Bucc.	
								16.81	Neand- EMH+ >RMH	Ling.	
			AT-1754	-	I^2 (L)	-	-	-	-	Bucc.	
								16.45	Neand- EMH+ >RMH	Ling.	
			AT-958	-	C'(L)	-	-	21.32	Neand- EMH+ >RMH	Bucc.	
								20.82	Neand- EMH+ >RMH	Ling.	
			AT-1757	-	C'(L)	-	-	21.65	Neand- EMH+ >RMH	Bucc.	
								21.62	Neand- EMH+ >RMH	Ling.	
			AT-4333	-	C'(R)	-	-	20.69	Neand- EMH+ >RMH	Bucc.	
								20.82	Neand- EMH+ >RMH	Ling.	

SOM 9. Table 2. *Continued.*

Site	Datation	Taxon	Specimen	Individual's age	Tooth type	Cr [mm]	Comparison with our samples	RL [mm]	Comparison with our samples	Side for RL	References
Sima de los Huesos, Sierra de Atapuerca, Ibeas de Juarros, Burgos, Spain	400ka–500ka, (MIS 12–14) Bermúdez de Castro et al. (2003)	EMPH	AT-4335	-	C'(L)	-	-	18.92	Neand-EMH~0 RMH+	Bucc.	Martinón-Torres et al. (2012)
								20.30	Neand-EMH+ >RMH	Ling.	
			AT-3292	-	C'(L)	-	-	-	-	Bucc.	
								24.30	Neand+ EMH+ >>RMH	Ling.	
			AT-2392	-	C'(L)	-	-	-	-	Bucc.	
								24.13	Neand+ EMH+ >>RMH	Ling.	
			AT-558	-	C'(R)	-	-	-	-	Bucc.	
								22.23	Neand~0 EMH+ >>RMH	Ling.	
			AT-3255	-	C'(R)	-	-	-	-	Bucc.	
								24.38	Neand~0 EMH+ >>RMH	Ling.	
			AT-163	-	C'(L)	-	-	-	-	Bucc.	
								23.83	Neand+ EMH+ >>RMH	Ling.	
			AT-5616	-	C'(R)	-	-	-	-	Bucc.	
								23.77	Neand+ EMH+ >>RMH	Ling.	

SOM 9. Table 2. *Continued.*

Site	Datation	Taxon	Specimen	Individual's age	Tooth type	Cr [mm]	Comparison with our samples	RL [mm]	Comparison with our samples	Side for RL	References
Sima de los Huesos, Sierra de Atapuerca, Ibeas de Juarros, Burgos, Spain	400ka–500ka, (MIS 12–14) Bermùdez de Castro et al. (2003)	EMPH	AT-5622	-	C'(L)	-	-	-	-	Bucc.	Martinón-Torres et al. (2012)
								23.91	Neand+ EMH+ >>RMH	Ling.	
			AT-609	-	I_1 (R)	-	-	13.15	Neand- EMH- RMH+	Bucc.	
								13.37	Neand- EMH- RMH+	Ling.	
			AT-3252	-	I_1 (R)	-	-	16.42	Neand- EMH+ >RMH	Bucc.	
								-	-	Ling.	
			AT-2775	-	I_1 (L)	-	-	17.55	Neand+ EMH+ >RMH	Bucc.	
								16.51	Neand- EMH+ >RMH	Ling.	
			AT-2730	-	I_1 (L)	-	-	15.72	Neand- EMH+ ≥RMH	Bucc.	
								14.76	Neand- EMH+ RMH-	Ling.	
			AT-3250	-	I_1 (R)	-	-	19.27	Neand+ >EMH >>RMH	Bucc.	
								16.78	Neand- EMH+ >RMH	Ling.	

SOM 9. Table 2. *Continued.*

Site	Datation	Taxon	Specimen	Individual's age	Tooth type	Cr [mm]	Comparison with our samples	RL [mm]	Comparison with our samples	Side for RL	References
Sima de los Huesos, Sierra de Atapuerca, Ibeas de Juarros, Burgos, Spain	400ka–500ka, (MIS 12–14) Bermùdez de Castro et al. (2003)	EMPH	AT-3199	-	I_1 (L)	-	-	19.59	Neand+ >EMH >>RMH	Bucc.	Martinón-Torres et al. (2012)
								18.54	Neand+ >EMH >>RMH	Ling.	
			AT-166	-	I_1 (R)	-	-	13.57	Neand- EMH- RMH+	Bucc.	
								-	-	Ling.	
			AT-1474	-	I_1 (L)	-	-	-	-	Bucc.	
								13.59	Neand- EMH- RMH+	Ling.	
			AT-3241	-	I_1 (L)	-	-	13.61	Neand- EMH- RMH+	Bucc.	
								-	-	Ling.	
			AT-282	-	I_2 (R)	-	-	17.59	Neand- EMH+ >RMH	Bucc.	
								17.50	Neand- EMH+ >RMH	Ling.	
			AT-592	-	I_2 (R)	-	-	17.09	Neand- EMH+ >RMH	Bucc.	
								17.35	Neand- EMH+ >RMH	Ling.	

SOM 9. Table 2. *Continued.*

Site	Datation	Taxon	Specimen	Individual's age	Tooth type	Cr [mm]	Comparison with our samples	RL [mm]	Comparison with our samples	Side for RL	References
Sima de los Huesos, Sierra de Atapuerca, Ibeas de Juarros, Burgos, Spain	400ka–500ka, (MIS 12–14) Bermûdez de Castro et al. (2003)	EMPH	AT-2278	-	I_2(L)	-	-	15.05	Neand-EMH-RMH+	Bucc.	Martinón-Torres et al. (2012)
								15.03	Neand-EMH-RMH+	Ling.	
			AT-597	-	I_2(L)	-	-	15.02	Neand-EMH-RMH+	Bucc.	
								15.32	Neand-EMH~0 RMH+	Ling.	
			AT-55	-	I_2(R)	-	-	14.98	Neand-EMH-RMH+	Bucc.	
								14.51	Neand-EMH-RMH+	Ling.	
			AT-3937	-	I_2(L)	-	-	-	-	Bucc.	
								17.86	Neand-EMH+ >RMH	Ling.	
			AT-2776	-	I_2(L)	-	-	-	-	Bucc.	
								16.97	Neand-EMH+ ≥RMH	Ling.	
			AT-3256	-	I_2(R)	-	-	17.81	Neand-EMH+ >RMH	Bucc.	
								-	-	Ling.	

SOM 9. Table 2. *Continued.*

Site	Datation	Taxon	Specimen	Individual's age	Tooth type	Cr [mm]	Comparison with our samples	RL [mm]	Comparison with our samples	Side for RL	References
Sima de los Huesos, Sierra de Atapuerca, Ibeas de Juarros, Burgos, Spain	400ka–500ka, (MIS 12–14) Bermùdez de Castro et al. (2003)	EMPH	AT-1123	-	I_2 (R)	-	-	18.59	Neand~0 EMH+ >RMH	Bucc.	Martinón-Torres et al. (2012)
								-	-	Ling.	
			AT-276	-	C, (L)	-	-	19.42	Neand- EMH+ >RMH	Bucc.	
								20.31	Neand- EMH+ >RMH	Ling.	
			AT-578	-	C, (L)	-	-	19.61	Neand- EMH+ >>RMH	Bucc.	
								20.95	Neand~0 EMH+ >>RMH	Ling.	
			AT-1952	-	C, (R)	-	-	18.24	Neand- EMH+ >RMH	Bucc.	
								19.40	Neand- EMH+ >RMH	Ling.	
			AT-161	-	C, (L)	-	-	16.24	Neand- EMH- RMH-	Bucc.	
								16.59	Neand- EMH- RMH~0	Ling.	

SOM 9. Table 2. *Continued.*

Site	Datation	Taxon	Specimen	Individual's age	Tooth type	Cr [mm]	Comparison with our samples	RL [mm]	Comparison with our samples	Side for RL	References
Sima de los Huesos, Sierra de Atapuerca, Ibeas de Juarros, Burgos, Spain	400ka–500ka, (MIS 12–14) Bermùdez de Castro et al. (2003)	EMPH	AT-3886	-	C, (R)	-	-	19.31	Neand-EMH+ >>RMH	Bucc.	Martinón-Torres et al. (2012)
								20.21	Neand-EMH+ >>RMH	Ling.	
			AT-593	-	C, (R)	-	-	19.21	Neand-EMH+ >RMH	Bucc.	
								20.18	Neand-EMH+ >>RMH	Ling.	
			AT-164	-	C, (L)	-	-	-	-	Bucc.	
								18.66	Neand-EMH+ >RMH	Ling.	
			average ± standard deviation (sample size)	-	I^1	7.75±0.34 (24)	-	-	-	-	
				-	I^2	7.76±0.28 (24)	-	-	-	-	
				-	C'	9.88±0.52 (24)	-	-	-	-	
				-	I_1	6.56±0.31 (26)	-	-	-	-	
				-	I_2	7.3±0.34 (30)	-	-	-	-	
				-	C,	8.66±0.66 (29)	-	-	-	-	

SOM 9. Table 2. *Continued.*

Site	Datation	Taxon	Specimen	Individual's age	Tooth type	Cr [mm]	Comparison with our samples	RL [mm]	Comparison with our samples	Side for RL	References
Arago	(de Lumley et al., 1971)	EMPH	Arago LXI		I^1 (R)	-	-	17.4	Neand~0 EMH~0 >RMH	Bucc.	Bermúdez de Castro (1988)
			Arago LX		I^2 (R)	-	-	17.6	Neand~0 EMH+ >RMH		
			Arago LIX		C'(R)	-	-	19.0	Neand- EMH+ RMH+		
Qesem Cave, Israel	400-200ka	Neand.? EMH?			C, (L)	8.3	Neand- EMH- RMH+	18,6	Neand- EMH+ >RMH	?	Hershkovitz et al. (2011)
Galeria Pesada, Almonda Karstic system, Torres Novas, Portugal	MIS 7	EMPH	Pesada I	-	C, (L)	10.0	Neand+ EMH+ >RMH	18.8	Neand- EMH+ >RMH	?	Trinkaus et al. (2003)
Lazaret, near Nice, France	MIS 6 (Puech and Albertini, 1981)	EMPH	Lazaret I	16-20 years (Bermúdez de Castro et al., 2004)	C, (R)	-	-	19.8	Neand- EMH+ >RMH	Bucc.	Bermúdez de Castro (1988)
La Ferrassie, Dordogne, France	71 to 50-35 ka (Klein, 1999)	Neand.	La Ferrassie 2		I^1 (R)	-	-	16.8	Neand- EMH~0 >RMH	Bucc.	Bermúdez de Castro (1988)

SOM 9. Table 2. *Continued.*

Site	Datation	Taxon	Specimen	Individual's age	Tooth type	Cr [mm]	Comparison with our samples	RL [mm]	Comparison with our samples	Side for RL	References
Grotte du Portel, Ariège, France	MIS 3-4	Neand.		~11years	I_1 (R)	7.0	Neand-EMH+ >RMH	15	Neand-EMH+ RMH+	?	Brabant and Sahly (1964)
					I_1 (L)	7.0	Neand-EMH+ >RMH	14.1	Neand-EMH- RMH+	?	
					I_2 (R)	7.60	Neand-EMH+ >RMH	-	-	?	
					C, (R and L)	8.80	Neand~0 EMH+ RMH+	18	Neand-EMH~0 ≥RMH	?	
Abri-Rousseau, Angles-sur-l'Anglin, Vienne, France	Mousterian	Neand.	Abri-Rousseau		I^1 (L)	8.4	Neand0 EMH+ >RMH	17.6	Neand+ EMH0 >RMH	Ling.	Patte (1960)
Saint-Brais II, Switzerland	35-45ka	Neand.	Saint-Brais II	16-18 years ?	I^1 (L)	9.0	Neand+ EMH+ >RMH	19.4	Neand+ EMH~0 >RMH	?	Koby (1956)
Grotte du Renne, Arcy-sur-Cure, Yonne, France	Chatelperronian	Neand.	« Tooth N°7 »		C, (L)	9.8	Neand+ EMH+ >RMH	18	Neand-EMH~0 RMH+	Ling.?	Bailey and Hublin (2006)

SOM 9. Table 2. *Continued.*

Site	Datation	Taxon	Specimen	Individual's age	Tooth type	Cr [mm]	Comparison with our samples	RL [mm]	Comparison with our samples	Side for RL	References
Sima de las Palomas del Cabezo Gordo, Murcia, Spain	<43-40ka cal. BP	Neand.	SP24		I^1(L)	-	-	15.5	Neand- EMH~0 RMH+	?	Walker et al. (2008)
			SP79		I^1 (L)	-	-	16.0	Neand- EMH~0 >RMH		
			SP90		I^1 (L)	-	-	16.4	Neand- EMH~0 >RMH		
			SP43		I^2 (L)	-	-	20.4	Neand+ EMH+ >RMH		
			SP48		I^2 (R)	-	-	14.3	Neand- EMH- RMH+		
			SP35		C' (L)	-	-	21.1	Neand- EMH+ >RMH		
			SP74		C'(L)	-	-	18.1	Neand- EMH~0 RMH+		
			SP19		I_1 (L)	7.0	Neand- EMH+ >RMH	15.0	Neand- EMH+ RMH+		
			SP21		I_1 (R)	6.6	Neand- EMH+ RMH+	13.9	Neand- EMH- RMH+		

SOM 9. Table 2. *Continued.*

Site	Datation	Taxon	Specimen	Individual's age	Tooth type	Cr [mm]	Comparison with our samples	RL [mm]	Comparison with our samples	Side for RL	References
Sima de las Palomas del Cabezo Gordo, Murcia, Spain	<43-40ka cal. BP	Neand.	SP20		I_2 (L)	6.8	Neand- EMH- RMH+	16.8	Neand- EMH+ RMH+	?	Walker et al. (2008)
			SP18		C, (L)	8.6	Neand- EMH0 RMH+	18.2	Neand- EMH+ >RMH		
			SP26		C, (R)	7.6	Neand- EMH- RMH~0	14.5	≤Neand ≤EMH <RMH		
			SP44		C, (R)	-	-	21.9	Neand+ >EMH >>RMH		
			SP82		C, (L)	9.1	Neand+ EMH+ RMH+	16.6	Neand- EMH- RMH~0		
Hortus	MIS 3 (Szmidt et al., 2010)	Neand.	Hortus IV	-	C, (L)	-	-	18.6	Neand- EMH+ >RMH	Bucc.	Bermúdez de Castro (1988)
			Hortus VII	-	I^1 (R)	-	-	18.3	Neand+ EMH~0 >RMH		
				-	I^2 (R)	-	-	17.9	Neand+ EMH+ >RMH		
			Hortus VIII	-	I^1 (R)	-	-	15.9	Neand- EMH~0 >RMH		
					I^2 (R)	-	-	14.9	Neand- EMH~0 RMH+		

SOM 9. Table 2. *Continued.*

Site	Datation	Taxon	Specimen	Individual's age	Tooth type	Cr [mm]	Comparison with our samples	RL [mm]	Comparison with our samples	Side for RL	References
Hortus	MIS 3 (Szmidt et al., 2010)	Neand.	Hortus VIII		C'(R)	-	-	19.6	Neand- EMH+ >RMH		
			Hortus IX	-	I^1 (R)	-	-	16.0	Neand- EMH~0 ≥RMH		
					I^2 (L)	-	-	20.5	Neand+ EMH+ >>RMH		
			Hortus X	-	I^1 (R)	-	-	18.7	Neand+ EMH~0 >>RMH		
					I^2 (L)	-	-	17.3	Neand- EMH+ >RMH		
			Hortus XI	-	I^2 (R)	-	-	17.0	Neand- EMH+ >RMH		
			Hortus XII	-	I^1 (R)	-	-	17.6	Neand+ EMH~0 >RMH		
					I^2 (R)	-	-	18.0	Neand+ EMH+ >RMH		
			Hortus XIIbis	-	I^1 (R)	-	-	18.0	Neand+ EMH~0 >RMH		
					I^2 (R)	-	-	17.8	Neand~0 EMH+ >RMH		

SOM Figs. 2a and 2b show graphically how the data collected from the literature (buccal side was chosen for our measurements of root lengths on the pictures) plot with the micro-CT data of this study.

(1a)

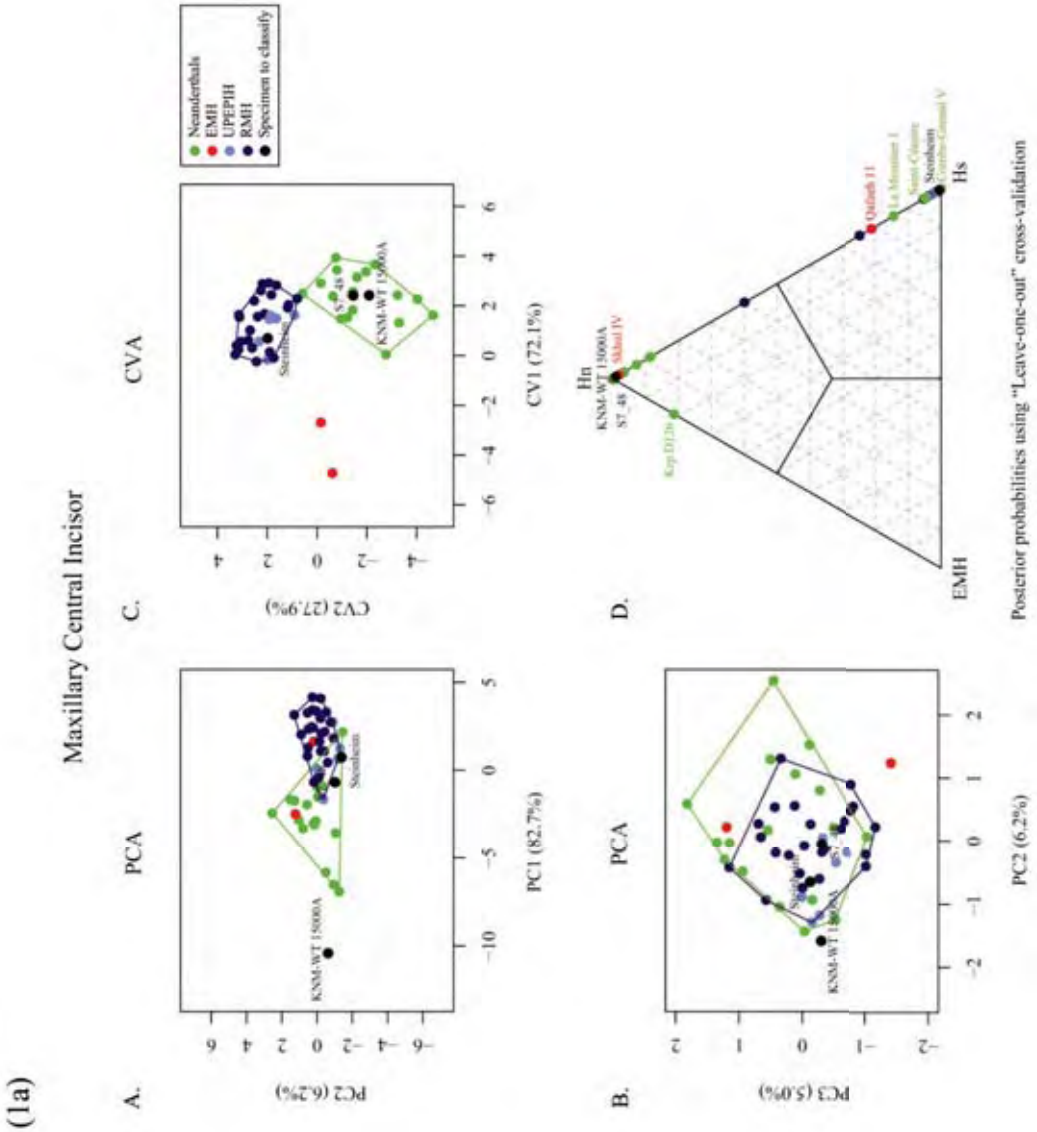
Maxillary Central Incisor
A.
PCA
PC2 (6.2%)
PC1 (82.7%)
KNM-WT 15000A
Steinheim
C.
CVA
CV2 (27.9%)
CV1 (72.1%)
Neanderthals
EMH
UPEPIH
RMH
Specimen to classify
B.
PCA
PC3 (5.0%)
PC2 (6.2%)
D.
Hn
Hs
EMH
Posterior probabilities using "Leave-one-out" cross-validation

(1b)

Mandibular Lateral Incisor

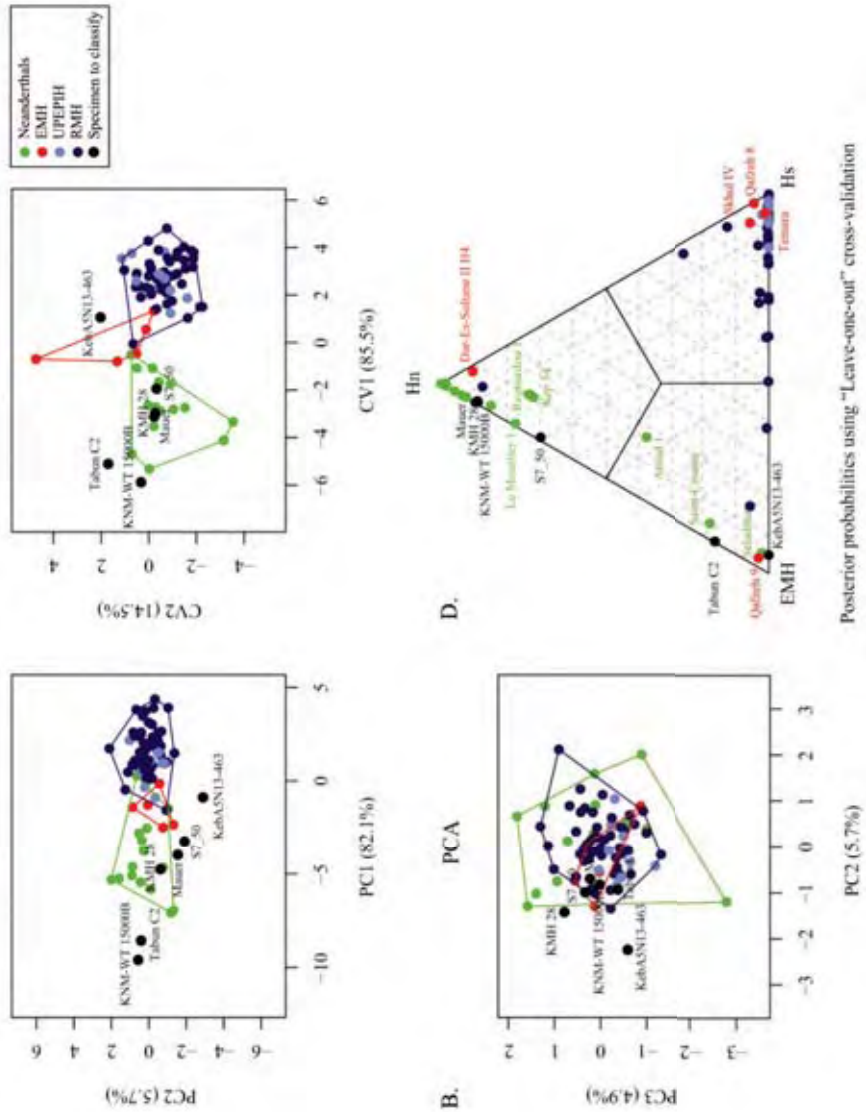

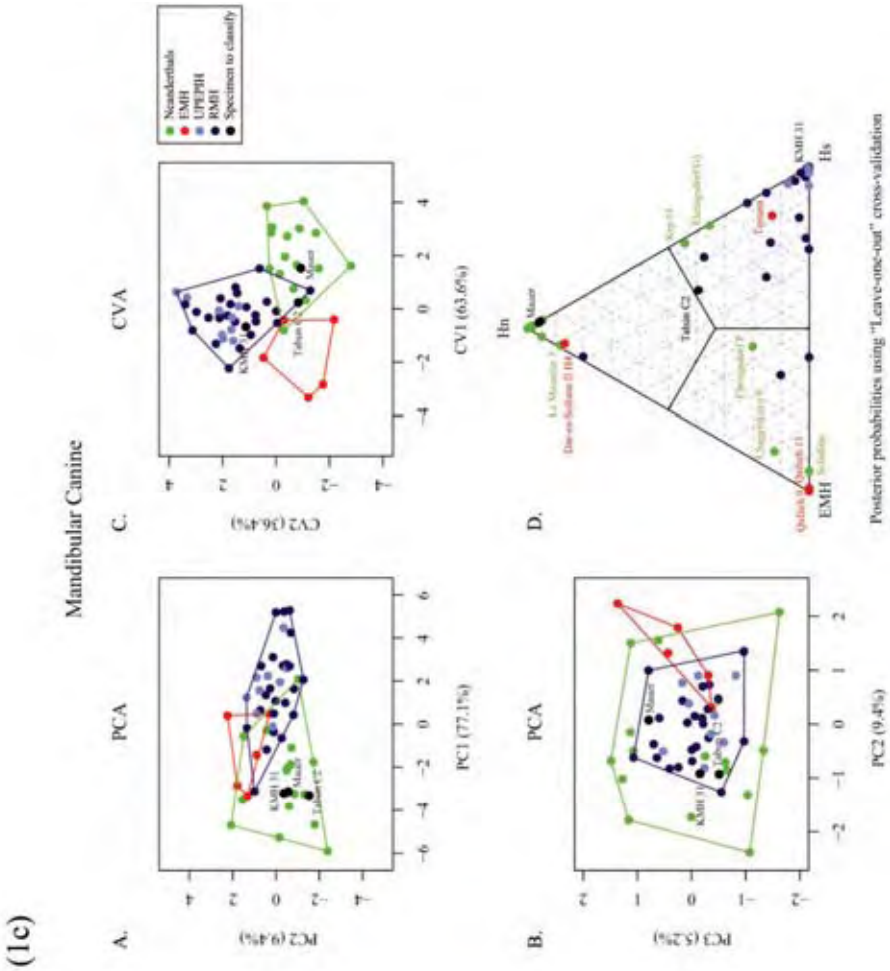

SOM Figure 1. PCA, CVA and posterior probabilities for the I^1 (1a), I_2 (1b) and C, (1c) showing the size gradient (A. PC1 plotted against PC2), and the overwhelming signal of size in our data (B. PC2 plotted against PC3). The CVA attempts to best separate the group, while the posterior probability shows a classification of the debated specimens in our three main groups (the names of the outliers are reported to provide a more precise idea of the quality of the classification).

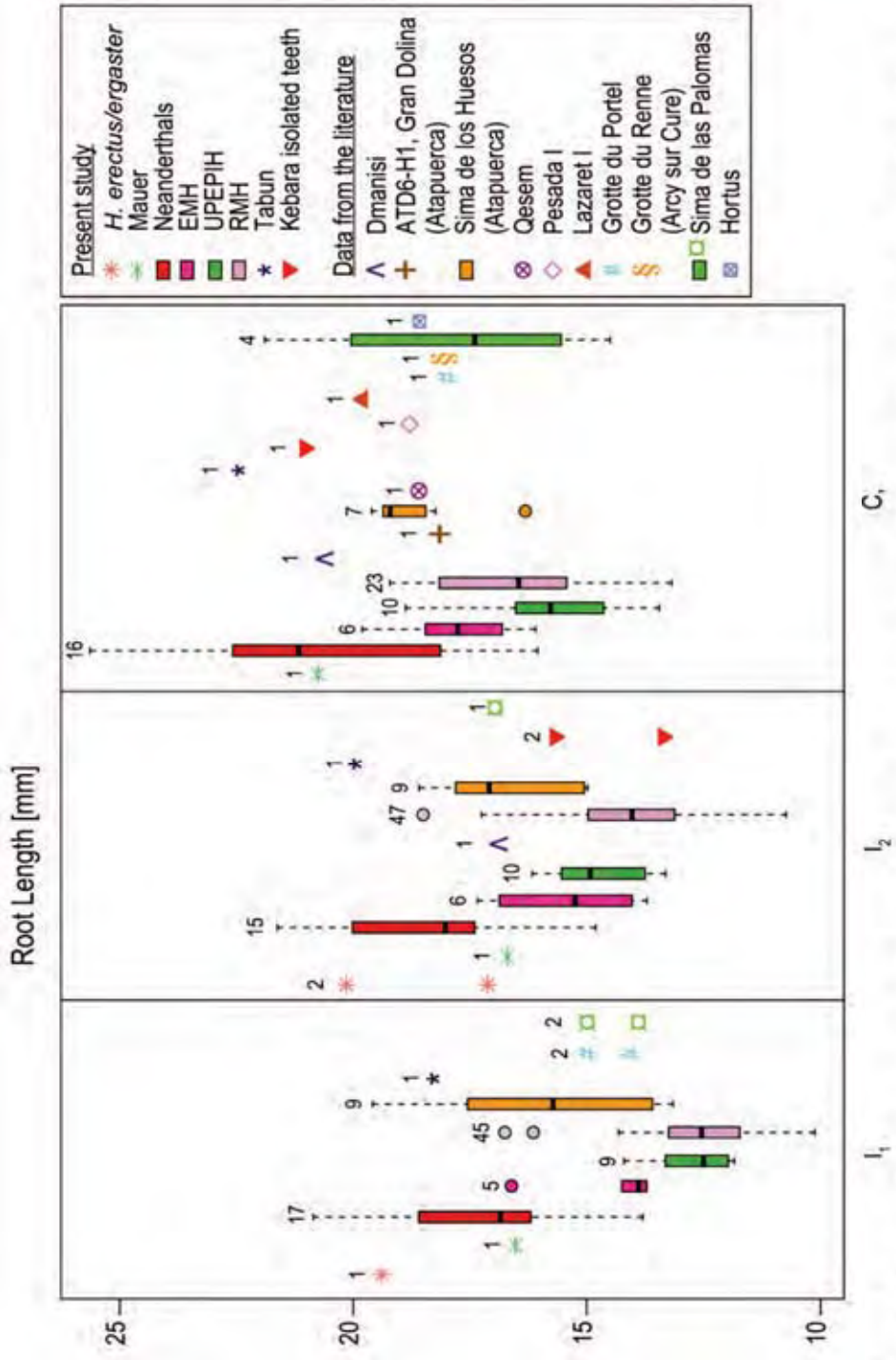

SOM Figure 2a. Comparison of our samples with supplementary root length (lower dentition) collected (or measured on pictures) from the literature, for Lower and Middle Pleistocene hominins. The figures above the boxplots are sample sizes. See SOM 9 for detailed references and statistics.

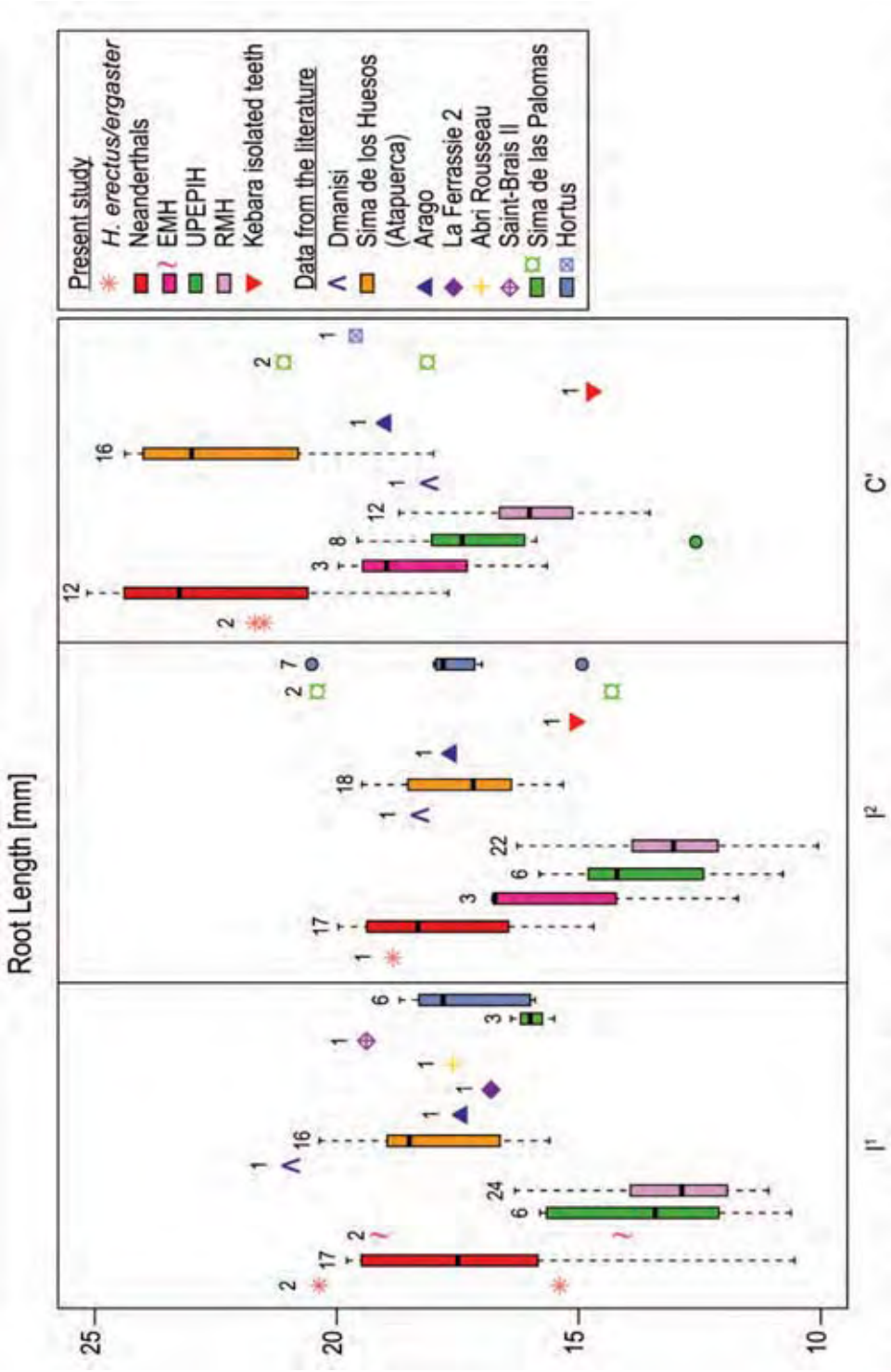

SOM Figure 2b. Comparison of our samples with supplementary root length (upper dentition) collected (or measured on pictures) from the literature, for Lower and Middle Pleistocene hominins. The figures above the boxplots are sample sizes. See SOM 9 for detailed references and statistics.

REFERENCES

Adam, K.D., 2003. Der *Homo steinheimensis* im Spannungsfeld von Alt- und Neumenschen. Veröffentlichungen des Landesamtes für Archäologie 57, 29–42.

Anderson, D.L., Thompson, G.W., Popovich, F., 1977. Tooth, chin, bone and body size correlations. Am. J. Phys. Anthropol. 46, 7–11.

Ang, K.Y., Lucas, P.W., Tan, H.T.W., 2006. Incisal orientation and biting efficiency. J. Hum. Evol. 50, 663–672.

Antón, S.C., 1990. Neandertals and the anterior dental loading hypothesis: a biomechanical evaluation of bite force production. Kroeber Anthropol. Soc. Pap. 71, 67–76.

Antón, S.C., 1994. Mechanical and other perspectives on Neandertal craniofacial morphology. In: Corruccini, R.S., Ciochon, R.L. (Eds.), Integrative Paths to the Past: Palaeoanthropological Advances in Honor of F. Clark Howell. Prentice Hall, Englewood Cliffs, pp. 677–695.

Antón, S.C., 1996. Tendon-associated bone features of the masticatory system in Neandertals. J. Hum. Evol. 31, 391–408.

Antunes, M.T., Cunha, A.S., 1992. Neanderthalian remains from Figueira Brava cave, Portugal. Geobios 25, 681–692.

Bailey, S.E., 2005. Diagnostic dental differences between Neandertals and Upper Paleolithic modern humans: getting to the root of the matter. In: Zadzinska, E. (Ed.), Curr. Trends Dent. Morphol. Res. Univeristy of Łódź Press, Łódź (Poland), pp. 201–210.

Bailey, S.E., 2006. Beyond shovel-shaped incisors: Neandertal dental morphology in a comparative context. Period. Biol. 108(3), 253–267.

Bailey, S.E., Hublin, J.-J., 2006. Dental remains from the Grotte du Renne at Arcy-sur-Cure (Yonne). J. Hum. Evol. 50, 485–508.

Bar-Yosef, O., 1998. The chronology of the Middle Paleolithic of the Levant. In: Akazawa, T., Aoki, K., Bar-Yosef, O. (Eds.), Neandertals and Modern Humans in Western Asia. Springer, New York, pp. 39–56.

Bar-Yosef, O., Callander, J., 1999. The woman from Tabun: Garrod's doubts in historical perspective. J. Hum. Evol. 37, 879–885.

Barrett, M.J., 1977. Masticatory and non-masticatory uses of teeth. In: Wright, R.V.S. (Ed.), Stone Tools as Cultural Markers: Change, Evolution and Complexity. Australian Institute of Aboriginal Studies, Canberra, pp. 18–23.

Bastir, M., O'Higgins, P., Rosas, A., 2007. Facial ontogeny in Neanderthals and modern humans. Proc. Roy. Soc. B 274, 1125–1132.

Bayle, P., Braga, J., Mazurier, A., Macchiarelli, R., 2009a. Brief communication: High-resolution assessment of the dental developmental pattern and characterization of tooth tissue proportions in the late upper Paleolithic child from La Madeleine, France. Am. J. Phys. Anthropol. 138, 493–498.

Bayle, P., Braga, J., Mazurier, A., Macchiarelli, R., 2009b. Dental developmental pattern of the Neanderthal child from Roc de Marsal: a high-resolution 3D analysis. J. Hum. Evol. 56, 66–75.

Bayle, P., Macchiarelli, R., Trinkaus, E., Duarte, C., Mazurier, A., Zilhão, J., 2010. Dental maturational sequence and dental tissue proportions in the early Upper Paleolithic child from Abrigo do Lagar Velho, Portugal. Proc. Natl. Acad. Sci. 107, 1338–1342.

Becker, R.A., Chambers, J.M., Wilks, A.R., 1988. The New S Language. Wadsworth & Brooks/Cole, Pacific Grove.

Belfer-Cohen, A., 1988. The Natufian settlement at Hayonim cave: a hunter-gatherer band, on the threshold of agriculture. Ph.D. Dissertation, Hebrew University, Jerusalem, Israel.

Benazzi, S., Douka, K., Fornai, C., Bauer, C.C., Kullmer, O., Svoboda, J., Pap, I., Mallegni, F., Bayle, P., Coquerelle, M., 2011. Early dispersal of modern humans in Europe and implications for Neanderthal behaviour. Nature 479, 525–528.

Bermúdez de Castro, J.M., 1988. Dental remains from Atapuerca/Ibeas (Spain) II. Morphology. J. Hum. Evol. 17, 279–304.

Bermúdez de Castro, J.M., 1993. The Atapuerca dental remains. New evidence (1987-1991 excavations) and interpretations. J. Hum. Evol. 24, 339–371.

Bermúdez de Castro, J.M., Bromage, T.G., Jalvo, Y.F., 1988. Buccal striations on fossil human anterior teeth: evidence of handedness in the middle and early Upper Pleistocene. J. Hum. Evol. 17, 403–412.

Bermúdez de Castro, J.M., Carbonell, E., Gómez, A., Mateos, A., Martinón-Torres, M., Muela, A., Rodríguez, J., Sarmiento, S., Varela, S., 2006. Paleodemografía del hipodigma de fósiles de homininos del nivel TD6 de Gran Dolina (Sierra de Atapuerca, Burgos): estudio preliminar. Estudios Geológicos 62, 145–154.

Bermúdez de Castro, J.M., Martinón-Torres, M., Lozano, M., Sarmiento, S., Muela, A., 2004. Paleodemography of the Atapuerca: Sima De Los Huesos Hominin

Sample: A Revision and New Approaches to the Paleodemography of the European Middle Pleistocene Population. J. Anthrop. Res. 60, 5–26.

Bermùdez de Castro, J.M., Martinon-Torres, M., Sarmiento, S., Lozano, M., Arsuaga, J.L., Carbonell, E., 2003. Rates of anterior tooth wear in Middle Pleistocene hominins from Sima de los Huesos (Sierra de Atapuerca, Spain). Proc. Natl. Acad. Sci. 100, 11992–11996.

Bermúdez de Castro, J.M., Rosas, A., Nicolás, M.E., 1999. Dental remains from Atapuerca-TD6 (Gran Dolina site, Burgos, Spain). J. Hum. Evol. 37, 523–566.

Berry, D.C., Poole, D.F., 1976. Attrition: possible mechanisms of compensation. J. Oral Rehabil. 3, 201–206.

Beucher, S., Lantuejoul, C., 1979. Use of watersheds in contour detection. In: International Workshop on Image Processing: Real-Time Edge and Motion Detection/Estimation, Rennes, France, September 17-21, 1979, pp. 1–12.

Bilsborough, A., Thompson, J.L., 2005. The dentition of the Le Moustier 1 Neandertal. In: Ullrich, H. (Ed.), The Neandertal Adolescent Le Moustier 1: New Aspects, New Results. Staatliche Museen Zu Berlin. Preussicher Kulturbesitz,Berlin, pp. 157–186.

Blackwell, B., Schwarcz, H.P., 1986. U-Series analyses of the lower travertine at Ehringsdorf, DDR. Quat. Res. 25, 215–222.

Blanco, R., Chakraborty, R., 1976. The genetics of shovel shape in maxillary central incisors in man. Am. J. Phys. Anthropol. 44, 233–236.

Bocquentin, F., 2003. Pratiques funéraires, paramètres biologiques et identités culturelles au Natoufien: une analyse archéo-anthropologique. Ph.D. Dissertation, University of Bordeaux I, Bordeaux, France.

Bookstein, F.L., 1991. Morphometric Tools for Landmark Data: Geometry and Biology. Cambridge University Press, Cambridge, 435 p.

Bookstein, F.L., 1997. Landmark methods for forms without landmarks: morphometrics of group differences in outline shape. Med. Image Anal. 1, 225–243.

Bookstein, F.L., 2005. After Landmarks. In: Slice, D.E. (Ed.), Modern Morphometrics in Physical Anthropology. Kluwer Academic/Plenum Publishers, Springer US, New York, pp. 49–71.

Bookstein, F.L., Mardia, K.V., 2003. The five components of directional asymmetry. In: Aykroyd, R.G., Mardia, K.V., Langdon, M.J. (Eds.), Stochastic Geometry, Biological Structure, and Images, pp. 35–40.

Bosshardt, D.D., Selvig, K.A., 1997. Dental cementum: the dynamic tissue covering of the root. Periodontol. 2000 13, 41–75.

Boughner, J., Dean, M., 2008. Mandibular Shape, Ontogeny and Dental Development in Bonobos (*Pan paniscus*) and Chimpanzees (*Pan troglodytes*). Evol. Biol. 35, 296–308.

Boughner, J.C., Hallgrímsson, B., 2008. Biological spacetime and the temporal integration of functional modules: A case study of dento-gnathic developmental timing. Dev. Dyn. 237, 1–17.

Brabant, H., Sahly, A., 1964. Étude des dents néandertaliennes découvertes dans la Grotte du Portel, en Ariège (France). Bull. Group. Int. Rech. Sci. Stomatol. 7, 237–254.

Brace, C.L., 1962. Cultural factors in the evolution of the human dentition. In: Montagu, M.F.A. (Ed.), Culture and the Evolution of Man. Oxford University Press, New York, pp. 343–354.

Brace, C.L., 1975. Comment on ‘Did La Ferrassie I use his teeth as tools?’ Curr. Anthropol. 16, 396–397.

Brace, C.L., 1979. Krapina, 'Classic' Neanderthals, and the evolution of the European face. J. Hum. Evol. 8, 527–550.

Brace, C.L., Agogino, G.A., Brothwell, D.R., Clark, W.E.L.G., Coon, C.S., Farmer, M.F., T, S.G., Givens, R.D., Howell, F.C., Howells, W.W., Koenigswald, G.H.R.V., Kurth, G., Montagu, A., Muller-Beck, H., Narr, K.J., Thoma, A., Tobias, P.V., Weckler, J.E., 1964. The fate of the 'Classic Neanderthals: A consideration of hominid catastrophism [and comments and reply]. Curr. Anthropol. 5, 3–43.

Bräuer, G.O., 1988. Osteometrie. In: Martin, R., Knussmann, R. (Eds.), Anthropologie: Handbuch der Vergleichenden Biologie Des Menschen. Band 1: Wesen un Methoden der Anthropologie. Teil 1: Wissenschaftstheorie, Geschichte, Morphologische Methoden. Gustav Fischer, Stuttgart, pp. 160–232.

Calenge, C., 2006. The package 'adehabitat' for the R software: A tool for the analysis of space and habitat use by animals. Ecol. Model. 197, 516–519.

Chech, M., Vandermeersch, B., Arensburg, B., Tillier, A.M., 2003. New human remains from Kebara Cave (Mount Carmel). The place of the Kebara hominids in the Levantine Mousterian fossil record. Paléorient 29, 35–62.

Churchill, S.E., 1998. Cold adaptation, heterochrony, and Neandertals. Evol. Anthropol. 7, 46–60.

Clement, A.F., Hillson, S.W., Aiello, L.C., 2012. Tooth wear, Neanderthal facial morphology and the anterior dental loading hypothesis. J. Hum. Evol. 62, 367–376.

Cobb, S.N., Panagiotopoulou, O., 2011. Balancing the spatial demands of the developing dentition with the mechanical demands of the catarrhine mandibular symphysis. J. Anat. 218, 96–111.

Comuzzie, A.G., Steele, D.G., 1989. Enlarged occlusal surfaces on first molars due to severe attrition and hypercementosis: Examples from prehistoric coastal populations of Texas. Am. J. Phys. Anthropol. 78, 9–15.

Condemi, S., 2001. 8 - Les Dents - Les Néandertaliens de La Chaise (Abri Bourgeois-Delaunay). Paris: Editions du CTHS.

Coon, C.S., 1962. The Origin of Races. Alfred A. Knopf, New York.

Coquerelle, M., Bayle, P., Bookstein, F., Braga, J., Halazonetis, D., Katina, S., Weber, G., 2010a. The association between dental mineralization and mandibular form: a study combining additive conjoint measurement and geometric morphometrics. J. Anthropol. Sci. 88, 129–150.

Coquerelle, M., Bookstein, F.L., Braga, J., Halazonetis, D.J., Weber, G.W., 2010b. Fetal and infant growth patterns of the mandibular symphysis in modern humans and chimpanzees (*Pan troglodytes*). J. Anat. 217, 507–520.

Couture, C., 1993. Changements de position du massif facial et de l'articulation temporo-mandibulaire dans la lignée néandertalienne. Organisation cranio-maxillo-faciale des Néandertaliens. C.R. Acad. Sci. 316, 1627–1633.

Crèvecoeur, I., Trinkaus, E., 2004. From the Nile to the Danube: a comparison of the Nazlet Khater 2 and Oase 1 early modern human mandibles. Anthropologie (Brno) 42, 229–239.

Crummett, T.L., 1995. The Three Dimensions of Shovel-Shaping. Aspects of Dental Biology: Palaeontology, Anthropology and Evolution. International Institute for the Study of Man, Florence, pp. 305–313.

Daegling, D.J., 1996. Growth in the mandibles of African apes. J. Hum. Evol. 30, 315–341.

Dastmalchi, R., Poison, A., Bouwsma, O., Proskin, H., 1990. Cementum thickness and mesial drift. J. Clin. Periodontol. 17, 709–713.

De Berg, M., Cheong, O., Van Kreveld, M., Overmars, M., 2008. Chap. 9 : Delaunay Triangulations - Height Interpolation. In: De Berg, M., Cheong, O., Van Kreveld, M., Overmars, M. (Eds.), Computational geometry: algorithms and applications. Third edition. Springer-Verlag New York, pp. 191–218.

De Lumley, H., de Lumley, M.A., Piveteau, J., 1971. Découverte de restes humains anténéandertaliens datés du début du Riss à la Caune de l'Arago (Tautavel, Pyrénées-Orientales). C R Acad Sci [II] 272, 1739–1742.

Dean, M.C., Beynon, A.D., 1991. Tooth crown heights, tooth wear, sexual dimorphism and jaw growth in hominoids. Z. Morph. Anthropol. 78, 425–440.

Defleur, A., Dutour, O., Vandermeersch, B., 1992. Étude de deux dents humaines provenant des niveaux moustériens de la Baume Néron (Soyons, Ardèche). Bull. Mém. Soc. Anthropol. Paris 4, 127–134.

Delson, E., Tattersall, I., Van Couvering, J.A., Brooks, A.S. (Eds.), 2000. Encyclopedia of Human Evolution and Prehistory. Garland Pub. Inc., New York.

Demes, B., 1987. Another look at an old face: biomechanics of the Neandertal facial skeleton reconsidered. J. Hum. Evol. 16, 297–303.

Dobson, S.D., Trinkaus, E., 2002. Cross-sectional geometry and morphology of the mandibular symphysis in Middle and Late Pleistocene *Homo*. J. Hum. Evol. 43, 67–87.

Dray, S., Dufour, A.B., 2007. The 'ade4' package: implementing the duality diagram for ecologists. J. Stat. Software 22, 1–20.

Dryden, I., Mardia, K., 1998. Statistical shape analysis. Wiley, Chichester, 346 p.

Endicott, P., Ho, S.Y.W., Stringer, C., 2010. Using genetic evidence to evaluate four palaeoanthropological hypotheses for the timing of Neanderthal and modern human origins. J. Hum. Evol. 59, 87–95.

Eshed, V., Gopher, A., Hershkovitz, I., 2006. Tooth wear and dental pathology at the advent of agriculture: New evidence from the Levant. Am. J. Phys. Anthropol. 130, 145–159.

Filipsson, R., Goldson, L., 1963. Correlation between tooth width, width of the head, length of the head, and stature. Acta Odontologica Scandinavica 21, 359–365.

Fox, C.L., Frayer, D.W., 1997. Non-dietary marks in the anterior dentition of the Krapina Neanderthals. Int. J. Osteoarchaeol. 7, 133–149.

Franciscus, R.G., 1999. Neandertal nasal structures and upper respiratory tract 'specialization'. Proc. Natl. Acad. Sci. 96, 1805–1809.

Franciscus, R.G., 2003. Internal nasal floor configuration in *Homo* with special reference to the evolution of Neandertal facial form. J. Hum. Evol. 44, 701–729.

Franciscus, R.G., Trinkaus, E., 1988. The Neandertal nose. Am. J. Phys. Anthropol. 75, 209–210.

Frayer, D.W., 1978. Evolution of the dentition in Upper Paleolithic and Mesolithic Europe. University Kansas Publications in Anthropology, Lawrence.

Fukase, H., 2011. Relationship between canine dimorphism and mandibular morphology in the hamadryas baboon and the Japanese monkey. Am. J. Phys. Anthropol. 144, 607–616.

Fukase, H., 2012. Interspecies difference in placement of developing teeth and its relationship with cross-sectional geometry of the mandibular symphysis in four primate species including modern humans. Am. J. Phys. Anthropol. 147, 217–226.

Gardner, B.S., Goldstein, H., 1931. The significance of hypercementosis. Dent. Cosmos 73, 1065–1069.

Garn, S.M., Lewis, A.B., 1958. Tooth-size, body-size and "giant" fossil man. Am. Anthropol. 60, 874–880.

Garralda, M.D., Maureille, B., Rigaud, J.P., Vandermeersch, B., 2004. La molaire néandertalienne de la grotte Vaufrey (Dordogne, France). Bull. Mém. Soc. Anthropol. Paris 16, 189–199.

Garralda, M.D., Vandermeersch, B., 2000. Les Néandertaliens de la grotte de Combe-Grenal (Domme, France). Paléo 12, 213–259.

Gieseler, W., 1971. Germany. Steinheim. In: Oakley, K.P., Campbell, B.G., Molleson, T.I. (Eds.), Catalogue of Fossil Hominids - Part II: Europe. The British Museum (Natural History), London, pp. 206–207.

Gilbert, J.-M., 1992. III. Etude odontologique. Gallia Préhist. 34, 282–284.

Good, P.I., 2000. Permutation Tests. Analyzing the Large Number of Variables in Biomedical and Satellite Imagery. John Wiley & Sons, Inc., Hoboken, pp. 5–21.

Green, R.E., Krause, J., Briggs, A.W., Maricic, T., Stenzel, U., Kircher, M., Patterson, N., Li, H., Zhai, W., Fritz, M.H.-Y., Hansen, N.F., Durand, E.Y., Malaspinas, A.-S., Jensen, J.D., Marques-Bonet, T., Alkan, C., Prüfer, K., Meyer, M., Burbano, H.A., Good, J.M., Schultz, R., Aximu-Petri, A., Butthof, A., Höber, B., Höffner, B., Siegemund, M., Weihmann, A., Nusbaum, C., Lander, E.S., Russ, C., Novod, N., Affourtit, J., Egholm, M., Verna, C., Rudan, P., Brajkovic, D.,

Kucan, Ž., Gušic, I., Doronichev, V.B., Golovanova, L.V., Lalueza-Fox, C., de la Rasilla, M., Fortea, J., Rosas, A., Schmitz, R.W., Johnson, P.L.F., Eichler, E.E., Falush, D., Birney, E., Mullikin, J.C., Slatkin, M., Nielsen, R., Kelso, J., Lachmann, M., Reich, D., Pääbo, S., 2010. A draft sequence of the Neandertal genome. Science 328, 710–722.

Green, R.E., Malaspinas, A.S., Krause, J., Briggs, A.W., Johnson, P.L.F., Uhler, C., Meyer, M., Good, J.M., Maricic, T., Stenzel, U., 2008. A complete Neandertal mitochondrial genome sequence determined by high-throughput sequencing. Cell 134, 416–426.

Gröning, F., Liu, J., Fagan, M.J., O'Higgins, P., 2011. Why do humans have chins? Testing the mechanical significance of modern human symphyseal morphology with finite element analysis. Am. J. Phys. Anthropol. 144, 593–606.

Grün, R., Stringer, C., 1991. Electron spin resonance dating and the evolution of modern humans. Archaeometry 33, 153–199.

Grün, R., Stringer, C., McDermott, F., Nathan, R., Porat, N., Robertson, S., Taylor, L., et al., 2005. U-series and ESR analyses of bones and teeth relating to the human burials from Skhul. J. Hum. Evol. 49, 316–334.

Guadelli, J.L., Laville, H., 1990. L'environnement climatique de la fin du Moustérien à Combe-Grenal et à Camiac. Confrontation des données naturalistes et implications. In : C. Farizy (Ed.), Paléolithique moyen récent et Paléolithique supérieur ancien en Europe. Mem. du Musée de Préhistoire d'Ile de France: 43–48.

Gunz, P., Mitteroecker, P., Bookstein, F., 2005. Semilandmarks in three dimensions. In: Slice, D.E. (Ed.), Modern Morphometrics in Physical Anthropology. Springer, New York, pp. 73–98.

Gunz, P., Mitteroecker, P., Neubauer, S., Weber, G.W., Bookstein, F.L., 2009. Principles for the virtual reconstruction of hominin crania. J. Hum. Evol. 57, 48–62.

Guttman, B., 1912. The etiology of hypercementosis. Dent. Cosmos 54, 244–245.

Guy, F., Mackaye, H.-T., Likius, A., Vignaud, P., Schmittbuhl, M., Brunet, M., 2008. Symphyseal shape variation in extant and fossil hominoids, and the symphysis of *Australopithecus bahrelghazali*. J. Hum. Evol. 55, 37–47.

Hammer Ø, Harper D.A.T, Ryan P.D, 2001. PAST: Paleontological Statistics Software Package for Education and Data Analysis. Palaeontologia Electronica 4 (1), 1–9. Version 2.15. Available online at http://folk.uio.no/ohammer/past/.

Harris, E.F., Hassankiadeh, S., Harris, J.T., 1993. Maxillary incisor crown-root relationships in different angle malocclusions. Am. J. Orthod. Dentofac. 103, 48–53.

Hartney, P.C., 1981. La recherche paléo-odontologique sur une population d'Iroquois de l'Ontario (Canada). Bull. Mém. Soc. Anthropol. Paris 8, 43–61.

Harvati, K., Hublin, J.-J., Gunz, P., 2010. Evolution of middle-late Pleistocene human cranio-facial form: a 3-D approach. J. Hum. Evol. 59, 445–464.

Hawks, J.D., Wolpoff, M.H., 2001. The accretion model of Neandertal evolution. Evolution 55, 1474–1485.

Henderson, A.M., Corruccini, R.S., 1976. Relationship Between Tooth Size and Body Size in American Blacks. J. Dent. Res. 55, 94–96.

Henke, W., 1986. Die magdalénienzeitlichen Menschenfunde von Oberkassel bei Bonn. Bonner Jahrbücher 186, 317–366.

Henry-Gambier, D., Maureille, B., White, W., 2004. Vestiges humains des niveaux de l'Aurignacien ancien du site de Brassempouy (Landes). Bull. Mém. Soc. Anthropol. Paris 16, 49–87.

Hershkovitz, I., Smith, P., Sarig, R., Quam, R., Rodríguez, L., García, R., Arsuaga, J.L., Barkai, R., Gopher, A., 2011. Middle Pleistocene dental remains from Qesem Cave (Israel). Am. J. Phys. Anthropol. 144, 575–592.

Hershkovitz, I., Speirs, M., Frayer, D., Nadel, D., Wish-Baratz, S., Arensburg, B., 1995. Ohalo II H2: A 19,000-year-old skeleton from a water-logged site at the Sea of Galilee, Israel. Am. J. Phys. Anthropol., 96, 215–234.

Hillson, S.W., Parfitt, S.A., Bello, S.M., Roberts, M.B., Stringer, C.B., 2010. Two hominin incisor teeth from the middle Pleistocene site of Boxgrove, Sussex, England. J. Hum. Evol. 59, 493–503.

Hinton, R.J., 1981. Form and patterning of anterior tooth wear among aboriginal human groups. Am. J. Phys. Anthropol. 54, 555–564.

Hoffmann, A., Hublin, J.-J., Hüls, M., Terberger, T., 2011. The *Homo aurignaciensis hauseri* from Combe-Capelle - A Mesolithic burial. J. Hum. Evol. 61, 211–214.

Holton, N.E., Franciscus, R.G., 2008. The paradox of a wide nasal aperture in cold-adapted Neandertals: a causal assessment. J. Hum. Evol. 55, 942–951.

Hothorn, T., Hornik, K., 2011. exactRankTests: Exact Distributions for Rank and Permutation Tests 0.8-20. http://cran.r-project.org/web/packages/exactRankTests/index.html.

Howe, R.P., McNamara Jr, J.A., O'Connor, K.A., 1983. An examination of dental crowding and its relationship to tooth size and arch dimension. Am. J. Orthod. 83, 363–373.

Hublin, J.-J., 1998. Climatic changes, paleogeography, and the evolution of the Neandertals. In: Akazawa, T., Aoki, K., Bar-Yosef, O. (Eds.), Neandertals and Modern Humans in Western Asia. Plenum Press, New York, pp. 295–310.

Hublin, J.-J., 2007. Origine et évolution des Néandertaliens. In: Vandermeersch, B., Maureille, B. (Eds.), Les Néandertaliens. Biologie et Cultures. Éditions du CTHS, Paris, pp. 95–107.

Hublin, J.J., 2009. The origin of Neandertals. Proc. Natl. Acad. Sci. 106, 16022–16027.

Hughes, T., Dempsey, P., Richards, L., Townsend, G., 2000. Genetic analysis of deciduous tooth size in Australian twins. Arch. Oral Biol. 45, 997–1004.

Hylander, H., 1977. The adaptive significance of Eskimo craniofacial morphology. In: Dahlberg, A.A., Graber, T.M. (Eds.), Orofacial Growth and Development. Mouton De Gruyter, The Hague, pp. 129–169.

Jacobs, Z., Meyer, M.C., Roberts, R.G., Aldeias, V., Dibble, H., El Hajraoui, M.A., 2011. Single-grain OSL dating at La Grotte des Contrebandiers (‘Smugglers’ Cave’), Morocco: improved age constraints for the Middle Paleolithic levels. J. Archaeol. Sci. 38, 3631–3643.

Kaifu, Y., 2000. Tooth wear and compensatory modification of the anterior dentoalveolar complex in humans. Am. J. Phys. Anthropol. 111, 369–392.

Kaifu, Y., Kasai, K., Townsend, G.C., Richards, L.C., 2003. Tooth wear and the 'design' of the human dentition: a perspective from evolutionary medicine. Am. J. Phys. Anthropol. 122, 47–61.

Kieser, J.A., Groeneveld, H.T., 1988. Allometric relations of teeth and jaws in man. Am. J. Phys. Anthropol. 77, 57–67.

Kirveskari, P., Alvesalo, L., 1979. Quantification of the shovel shape of incisor teeth. Ossa 6, 151–156.

Klein, R.G., 1999. The human career: Human biological and cultural origins. University of Chicago Press (Chicago) 1024 p.

Kloehn, S.J., 1938. The significance of root form as determined by occlusal stress. Angle Orthod. 8, 213–230.

Koby, F.E., 1956. Une incisive Néandertalienne trouvée en Suisse. Verhandenlungen der Nuturforschers Gesellschaft in Basel 67, 1–15.

Kovacs, I., 1967. Contribution to the ontogenetic morphology of roots of human teeth. J. Dent. Res. 46, 865–874.

Krause, J., Orlando, L., Serre, D., Viola, B., Prüfer, K., Richards, M.P., Hublin, J.-J., Hänni, C., Derevianko, A.P., Pääbo, S., 2007. Neanderthals in central Asia and Siberia. Nature 449, 902–904.

Krueger, K.L., 2011. Dietary and behavioral strategies of Neandertals and anatomically modern humans: Evidence from anterior dental microwear texture analysis. Ph.D. Dissertation, University of Arkansas.

Kupczik, K., Dean, M.C., 2008. Comparative observations on the tooth root morphology of *Gigantopithecus blacki*. J. Hum. Evol. 54, 196–204.

Kupczik, K., Hublin, J.-J., 2010. Mandibular molar root morphology in Neanderthals and Late Pleistocene and recent *Homo sapiens*. J. Hum. Evol. 59, 525–541.

Kuwahara, M., Hachimura, K., Eiho, S., Kinoshita, M., 1976. Processing of RI-angiocardiographic images. In: Preston, K., Onoe, M. (Eds.), Digital Processing of Biomedical Images. Plenum Press, New York, pp.187–202.

Larick, R., Ciochon, R. L., Zaim, Y., Sudijono, Suminto, Rizal, Y., Aziz, F., et al., 2001. Early Pleistocene $^{40}Ar/^{39}Ar$ ages for Bapang Formation hominins, Central Jawa, Indonesia. Proc. Natl. Acad. Sci., 98, 4866–4871.

Le Cabec, A., Kupczik, K., Gunz, P., Braga, J., Hublin, J.-J., 2011. Does anterior tooth root size correlate with symphyseal size in Neanderthals and modern humans? In: Abstracts of the Inaugural Meeting for the European Society for the Study of Human Evolution, Leipzig, Germany, September 2011, p. 18.

Le Cabec, A., Kupczik, K., Gunz, P., Braga, J., Hublin, J.J., 2012. Long anterior mandibular tooth roots in Neanderthals are not the result of their large jaws. J. Hum. Evol. 63, 667–681.

Lee, S., 2006. Patterns of dental sexual dimorphism in Krapina and Predmosti: A new approach. Period. Biol. 108, 417–424.

Legoux, P., 1976. Les dents de la Chaise de Vouthon. Etude pathologique et radiologique. Bull. Mém. Soc. Anthropol. Paris 3, 345–361.

Ligges, U., Maechler, M., 2003. scatterplot3d - An R package for visualizing multivariate data. J. Stat. Software 8, 1–20.

Liversidge, H.M., Molleson, T., 2004. Variation in crown and root formation and eruption of human deciduous teeth. Am. J. Phys. Anthropol. 123, 172–180.

Lozano, M., Bermúdez de Castro, J.M., Carbonell, E., Arsuaga, J.L., 2008. Non-masticatory uses of anterior teeth of Sima de los Huesos individuals (Sierra de Atapuerca, Spain). J. Hum. Evol. 55, 713–728.

Lozano-Ruiz, M., Bermúdez de Castro, J.M., Martinón-Torres, M., Sarmiento, S., 2004. Cutmarks on fossil human anterior teeth of the Sima de los Huesos Site (Atapuerca, Spain). J. Archaeol. Sci. 31, 1127–1135.

Lundström, A., 1951. The aetiology of crowding of the teeth (based on studies of twins and on morphological investigations) and its bearing on orthodontic treatment (expansion or extraction). Trans. Eur. Orthod. Soc., 176–191.

Magne, P., Versluis, A., Douglas, W.H., 1999. Rationalization of incisor shape: experimental-numerical analysis. J. Prosthet. Dent. 81, 345–355.

Mardia, K.V., Bookstein, F.L., Moreton, I.J., 2000. Statistical Assessment of Bilateral Symmetry of Shapes. Biometrika 87, 285–300.

Martinón-Torres, M., Bermúdez de Castro, J.M., Gómez-Robles, A., Margvelashvili, A., Prado, L., Lordkipanidze, D., Vekua, A., 2008. Dental remains from Dmanisi (Republic of Georgia): Morphological analysis and comparative study. J. Hum. Evol. 55, 249–273.

Martinón-Torres, M., Bermúdez de Castro, J.M., Gómez-Robles, A., Prado-Simón, L., Arsuaga, J.L., 2012. Morphological description and comparison of the dental remains from Atapuerca-Sima de los Huesos site (Spain). J. Hum. Evol. 62, 7–58.

Martinón-Torres, M., Martín-Francés, L., Gracia, A., Olejniczak, A., Prado-Simón, L., Gómez-Robles, A., Lapresa, M., Carbonell, E., Arsuaga, J.L., Bermúdez de Castro, J.M., 2011. Early Pleistocene human mandible from Sima del Elefante (TE) cave site in Sierra de Atapuerca (Spain): A palaeopathological study. J. Hum. Evol. 61, 1–11.

Maureille, B., Houët, F., 1998. La variabilité morpho-métrique du nez: Dérive génique dans la lignée néeandertalienne? Biométrie humaine et anthropologie 16, 27–33.

Maureille, B., Rougier, H., Houët, F., Vandermeersch, B., 2001. Les dents inférieures du Néandertalien Regourdou 1 (site de Regourdou, commune de Montignac,

Dordogne): Analyses métriques et comparatives. Paléo (Les Eyzies de Tayac-Sireuil), 183–200.

Maureille, B., Tillier, A.-M., 2008. Répartition géographique et chronologique des sépultures néandertaliennes. In: Vandermeersch, B., Cleyet-Merle, J.-J., Jaubert, J., Maureille, B., Turq, A. (Eds.), Première Humanité, Gestes Funéraires des Néandertaliens. Catalogue d'Exposition, Musée National de Préhistoire, Les Eyzies-de-Tayac. Réunion des Musées Nationaux, Paris, pp. 66–74.

Ménard, J., 1984. L'incisive temporaire supérieure centrale gauche moustérienne de tradition acheuléenne du Pech-de-l'Azé IV (Dordogne). Bull. Mém. Soc. Anthropol. Paris 1, 19–24.

Merbs, C.F., 1968. Anterior tooth loss in Arctic populations. S.J. Anthropol. 24, 20–32.

Mercier, N., Valladas, H., Joron, J.-L., Reyss, J.-L., Léveque, F., Vandermeersch, B., 1991. Thermoluminescence dating of the late Neanderthal remains from Saint-Césaire. Nature 351, 735–739.

Mercier, N., Valladas, H., Froget, L., Joron, J-L., Ronen, A., 2000. Datation par thermoluminescence de la base du gisement paléolithique de Tabun (Mont Carmel, Israël). C. R. Acad. Sci., Paris (Sciences de la Terre et des Planètes) 330, 731–738.

Mitteroecker, P., Bookstein, F., 2011. Linear discrimination, ordination, and the visualization of selection gradients in modern morphometrics. Evol. Biol. 38, 100–114.

Mitteroecker, P., Gunz, P., 2009. Advances in Geometric Morphometrics. Evol. Biol. 36, 235–247.

Mizoguchi, Y., 1985. Shoveling: A Statistical Analysis of its Morphology. University of Tokyo Press, Tokyo.

Molnar, S., 1971. Human tooth wear, tooth function and cultural variability. Am. J. Phys. Anthropol. 34, 175–189.

Moskowitsch, M., Smith, P., 1993. A note on functional implications of morphological variation in the human mandible. Int. J. Anthropol. 8, 53–60.

Moss, M.L., Rankow, R.M., 1968. The Role of the Functional Matrix in Mandibular Growth. Angle Orthod. 38, 95–103.

Mounier, A., 2011. Définition du taxon *Homo heidelbergensis* Schoetensack, 1908: analyse phénétique du massif facial supérieur des fossiles du genre *Homo* du Pléistocène moyen. Bull. Mem. Soc. Anthropol. Paris 23, 1–37.

Mounier, A., Marchal, F., Condemi, S., 2009. Is *Homo heidelbergensis* a distinct species? New insight on the Mauer mandible. J. Hum. Evol. 56, 219–246.

Murrell, P., 2005. R Graphics. Chapman & Hall/CRC Press, Boca Raton.

Nadel, D., Hershkovitz, I., 1991. New Subsistence Data and Human Remains from the Earliest Levantine Epipalaeolithic. Curr. Anthropol., 32, 631–635.

Nicholson, E., Harvati, K., 2006. Quantitative analysis of human mandibular shape using three-dimensional geometric morphometrics. Am. J. Phys. Anthropol. 131, 368–383.

O'Connor, C.F., Franciscus, R.G., Holton, N.E., 2005. Bite force production capability and efficiency in Neandertals and modern humans. Am. J. Phys. Anthropol. 127, 129–151.

Ozaki, T., Satake, T., Kanazawa, E., 1987. Morphological significance of root length variability in comparison with other crown dimensions. I - Basic statistics and sex difference. J. Nihon Univ. Sch. Dent. 29, 233–240.

Ozaki, T., Satake, T., Kanazawa, E., 1988. Morphological significance of root length variability in comparison with other crown dimensions. II - Correlation between crown and root measurements. J. Nihon Univ. Sch. Dent. 30, 11–21.

Paquette, S.P., 1985. Patterns of variation in the permanent maxillary anterior tooth roots: A different approach to the problem of anterior dental reduction during the transition from archaic to modern *Homo sapiens*. M.A. Thesis, University of Tennessee.

Patte, E., 1960. Découverte d'un Néandertalien dans la Vienne. L'Anthropologie 64, 512–517.

Patte, E., 1962. La Dentition des Neanderthaliens. Masson et Cie, Paris.

Pedersen, P.O., 1949. The East Greenland Eskimo Dentition. Numerical Variations and Anatomy. A Contribution to Comparative Ethnic Odontography. Meddelelser om Grønland 142. C.A. Reitzel, Copenhagen.

Peng, R.D., Murta, A., Murdoch, D., Rowlingson, B., 2010. gpclib: General Polygon Clipping Library for R. R package version 1.5-1. http://CRAN.R-project.org/package=gpclib.

Pérez-Pérez, A., Espurz, V., Bermúdez de Castro, J. M., de Lumley, M. A., Turbón, D., 2003. Non-occlusal dental microwear variability in a sample of Middle and Late Pleistocene human populations from Europe and the Near East. J. Hum. Evol., 44, 497–513.

Perzigian, A.J., 1981. Allometric analysis of dental variation in a human population. Am. J. Phys. Anthropol. 54, 341–345.

Philippas, G.G., Applebaum, E., 1967. Age changes in the permanent upper lateral incisor. J. Dent. Res. 46, 1002–1009.

Pinhasi, R., Eshed, V., Shaw, P., 2008. Evolutionary changes in the masticatory complex following the transition to farming in the southern Levant. Am. J. Phys. Anthropol., 135, 136–148.

Pinheiro, B.C., Pinheiro, T.N., Capelozza, A.L.A., Consolaro, A., 2008. A scanning electron microscopic study of hypercementosis J. Appl. Oral Sci. 16, 380–384.

Pirson, S., Court-Picon, M., Haesaerts, P., Bonjean, D., Damblon, F., 2008. New data on geology, anthracology and palynology from the Scladina Cave pleistocene sequence: preliminary results. Memoirs of the Geological Survey of Belgium, 55, 71–93.

Plavcan, J.M., Daegling, D.J., 2006. Interspecific and intraspecific relationships between tooth size and jaw size in primates. J. Hum. Evol. 51, 171–184.

Portin, P., Alvesalo, L., 1974. The inheritance of shovel shape in maxillary central incisors. Am. J. Phys. Anthropol. 41, 59–62.

Puech, P.-F., 1979. The diet of early man: evidence from abrasion of teeth and tools. Curr. Anthropol. 20, 590–592.

Puech, P.-F., 1981. Tooth wear in La Ferrassie Man. Curr. Anthropol. 22, 424–430.

Puech, P.-F., Albertini, H., 1981. Enamel pits of the Lazaret man. J. Hum. Evol. 10, 449–452.

Quam, R.M., Smith, F.H., 1998. A reassessment of the Tabun C2 mandible. In: Akazawa, T., Aoki, K., Bar-Yosef, O. (Eds.), Neandertals and Modern Humans in Western Asia. Springer, New York, pp. 405–421.

R Development Core Team, 2010. R: A Language and Environment for Statistical Computing. 2.12.1 Ed. R Foundation for Statistical Computing, Vienna, Austria. http://www.r-project.org/.

Rae, T.C., Koppe, T., Stringer, C.B., 2011. The Neanderthal face is not cold adapted. J. Hum. Evol. 60, 234–239.

Rak, Y., 1986. The Neanderthal: a new look at an old face. J. Hum. Evol. 15, 151–164.

Rak, Y., 2002. Does any Mousterian cave present evidence of two hominid species? In: Akazawa, T., Aoki, K., Bar-Yosef, O. (Eds.), Neandertals and Modern Humans in Western Asia. Springer, New York, pp. 353–366.

Rak, Y., Ginzburg, A., Geffen, E., 2002. Does *Homo neanderthalensis* play a role in modern human ancestry? The mandibular evidence. Am. J. Phys. Anthropol. 119, 199–204.

Reich, D., Green, R.E., Kircher, M., Krause, J., Patterson, N., Durand, E.Y., Viola, B., Briggs, A.W., Stenzel, U., Johnson, P.L.F., Maricic, T., Good, J.M., Marques-Bonet, T., Alkan, C., Fu, Q., Mallick, S., Li, H., Meyeer, M., Eichler, E.E., Stoneking, M., Richards, M., Talamo, S., Shunkov, M.V., Derevianko, A.P., Hublin, J.-J., Kelso, J., Slatkin, M., Pääbo, S., 2010. Genetic history of an archaic hominin group from Denisova Cave in Siberia. Nature 468,1053–1060.

Richards, M.P., Pettitt, P.B., Stiner, M.C., Trinkaus, E., 2001. Stable isotope evidence for increasing dietary breadth in the European mid-Upper Paleolithic. Proc. Natl. Acad. Sci. 98, 6528–6532.

Richards, M.P., Pettitt, P.B., Trinkaus, E., Smith, F.H., Paunović, M., Karavanić, I., 2000. Neanderthal diet at Vindija and Neanderthal predation: The evidence from stable isotopes. Proc. Natl. Acad. Sci. 97, 7663–7666.

Richards, M.P., Taylor, G., Steele, T., McPherron, S.P., Soressi, M., Jaubert, J., Orschiedt, J., Mallye, J.B., Rendu, W., Hublin, J.J., 2008. Isotopic dietary analysis of a Neanderthal and associated fauna from the site of Jonzac (Charente-Maritime), France. J. Hum. Evol. 55, 179–185.

Richardson, M.E., 1970. The Early Developmental Position of the Lower Third Molar Relative to Certain Jaw Dimensions. Angle Orthod. 40, 226–230.

Rightmire, G.P., 1998. Human evolution in the Middle Pleistocene: the role of *Homo heidelbergensis*. Evol. Anthropol. 6, 218–227.

Rightmire, G.P., Lordkipanidze, D., Vekua, A., 2006. Anatomical descriptions, comparative studies and evolutionary significance of the hominin skulls from Dmanisi, Republic of Georgia. J. Hum. Evol. 50, 115–141.

Rink, W.J., Schwarcz, H.P., Smith, F.H., Radovcic, J., 1995. ESR dating of Krapina hominids. Nature 378, 24.

Rohlf, F.J., Slice, D., 1990. Extensions of the Procrustes method for the optimal superimposition of landmarks. Syst. Biol. 39, 40–59.

Rosas, A., Bastir, M., Martínez-Maza, C., Garcia-Tabernero, A., Lalueza-Fox, C., 2006. Inquiries into Neanderthal cranio-facial development and evolution: ‘accretion’ vs ‘organismic’ models. In: Harvati, K., Harrison, T. (Eds.), Neanderthals Revisited: New Approaches and Perspectives. Springer, Dordrecht, pp. 37–70.

Rosas, A., Bermúdez De Castro, J.M., 1998. The Mauer mandible and the evolutionary significance of *Homo heidelbergensis*. Geobios 31, 687–697.

Sakura, H., 1970. Dentition of the Amud Man. In: Suzuki, H., Takai, F. (Eds.), The Amud Man and his Cave Site. Academic Press of Japan, Tokyo, pp. 207–218.

Sarkar, D., 2008. Lattice: Multivariate Data Visualization with R. Springer Verlag, New York.

Schatz, D., Alfter, G., Göz, G., 2001. Fracture resistance of human incisors and premolars: morphological and patho-anatomical factors. Dent. Traumatol. 17, 167–173.

Schoetensack, O., 1908. Der Unterkiefer des *Homo heidelbergensis* aus den Sanden von Mauer bei Heidelberg: Ein Beitrag zur Palaeontologie des Menschen. Verlag von Wilhelm Engelmann, Leipzig.

Schulze, M.A., Pearce, J.A., 1994. A morphology-based filter structure for edge-enhancing smoothing. Proceedings of the 1994 IEEE International Conference on Image Processing, Austin, TX, pp. 530–534.

Schwartz, J.H., Tattersall, I., 2000. The human chin revisited: what is it and who has it? J. Hum. Evol. 38, 367–409.

Schwenninger, J.-L., Collcutt, S.N., Barton, N., Bouzouggar, A., Clark Balzan, L., El Hajraoui, M.A., Nespoulet, R., Debénath, A., 2010. A new luminescence chronology for Aterian cave sites on the Atlantic coast of Morocco. In : Garcea, E.A. (Ed.), South-Eastern Mediterranean Peoples between 130,000 and 10,000 years ago. Oxbow Books, Oxford, pp.18–36.

Semal, P., Rougier, H., Crevecoeur, I., Jungels, C., Flas, D., Hauzeur, A., Maureille, B., et al., 2009. New data on the late Neandertals: Direct dating of the Belgian Spy fossils. Am. J. Phys. Anthropol., 138, 421–428.

Serre, D., Langaney, A., Chech, M., Teschler-Nicola, M., Paunovic, M., Mennecier, P., Hofreiter, M., Possnert, G., Pääbo, S., 2004. No evidence of Neandertal mtDNA contribution to early modern humans. Plos Biol. 2, 313–317.

Shea, B.T., Gomez, A.M., 1988. Tooth scaling and evolutionary dwarfism: An investigation of allometry in human pygmies. Am. J. Phys. Anthropol. 77, 117–132.

Skinner, M., 2008. Enamel-dentine junction morphology of extant hominoid and fossil hominin lower molars. Ph.D. Dissertation, The George Washington University.

Smith, B.H., 1984. Patterns of molar wear in hunter-gatherers and agriculturalists. Am. J. Phys. Anthropol. 63, 39–56.

Smith, F.H., 1976a. The Neandertal remains from Krapina: a descriptive and comparative study. University of Tennessee Department of Anthropology Reports of Investigations 15, 1–359.

Smith, F.H., 1976b. On anterior tooth wear at Krapina and Ochoz. Curr. Anthropol. 17, 167–168.

Smith, F.H., 1983. Behavioral interpretation of changes in craniofacial morphology across the archaic/modern *Homo sapiens* transition. In: Trinkaus, E. (Ed.), The Mousterian Legacy: Human Biocultural Change in the Upper Pleistocene. BAR Int. Ser. 164, Oxford, pp. 141–163.

Smith, F.H., Paquette, S.P., 1989. The adaptive basis of Neandertal facial form, with some thoughts on the nature of modern human origins. The emergence of modern humans. Cambridge University Press, Cambridge, pp. 181–210.

Smith, P., Wax, Y., Adler, F., 1989. Population variation in tooth, jaw, and root size: A radiographic study of two populations in a high-attrition environment. Am. J. Phys. Anthropol. 79, 197–206.

Smith, P., Wax, Y., Adler, F., Silberman, U., Heinic, G., 1986. Post-pleistocene changes in tooth root and jaw relationships. Am. J. Phys. Anthropol. 70, 339–348.

Smith, R.J., Burstone, C.J., 1984. Mechanics of tooth movement. Am. J. Orthod. 85, 294–307.

Smith, T.M., Tafforeau, P., Reid, D.J., Pouech, J., Lazzari, V., Zermeno, J.P., Guatelli-Steinberg, D., Olejniczak, A.J., Hoffman, A., Radovčić, J., Makaremi, M., Toussaint, M., Stringer, C., Hublin, J.-J., 2010. Dental evidence for ontogenetic differences between modern humans and Neanderthals. Proc. Natl. Acad. Sci. 107, 20923–20928.

Sofaer, J.A., 1973. A Model Relating Developmental Interaction and Differential Evolutionary Reduction of Tooth Size. Evolution 27, 427–434.

Solheim, T., 1990. Dental cementum apposition as an indicator of age. Scand. J. Dent. Res. 98, 510–519.

Spencer, M.A., 1998a. Force production in the primate masticatory system: electromyographic tests of biomechanical hypotheses. J. Hum. Evol. 34, 25–54.

Spencer, M.A., 1998b. Tooth root morphology and diet in primates. Am. J. Phys. Anthropol. 105, 206.

Spencer, M.A., 2003. Tooth-root form and function in platyrrhine seed-eaters. Am. J. Phys. Anthropol. 122, 325–335.

Spencer M.A., Demes, B., 1993. Biomechanical analysis of masticatory system configuration in Neandertals and Inuits. Am. J. Phys. Anthropol. 91, 1–20.

Spouge, J.D., 1973. Oral Pathology. CV Mosby, Saint Louis.

Stefan, V.H., Trinkaus, E., 1998. Discrete trait and dental morphometric affinities of the Tabun 2 mandible. J. Hum. Evol. 34, 443–468.

Street, M., Terberger, T., Orschiedt, J., 2006. A critical review of the German Paleolithic hominin record. J. Hum. Evol. 51, 551–579.

Szmidt, C.C., Moncel, M.-H., Daujeard, C., 2010. New data on the Late Mousterian in Mediterranean France: First radiocarbon (AMS) dates at Saint-Marcel Cave (Ardèche). Comptes Rendus Palevol 9, 185–199.

Thoma, A., 1963. The dentition of the Subalyuk Neandertal child. Z. Morph. Anthropol. 54, 127–150.

Tillier, A.-M., 1996. The Pech de l'Azé and Roc de Marsal children (middle paleolithic, France): Skeletal evidence for variation in Neanderthal ontogeny. Hum. Evol. 11, 113–119.

Tratman, E.K., 1950. A comparison of the teeth of people: Indo-European racial stock with mongoloid racial stock. Dent. Rec. 70, 63–88.

Trinkaus, E., 1978. Dental remains from the Shanidar adult Neanderthals. J. Hum. Evol. 7, 369–382.

Trinkaus, E., 1986. The Neandertals and modern human origins. A. Rev. Anthropol. 15, 193–218.

Trinkaus, E., 1987. The Neandertal face: evolutionary and functional perspectives on a recent hominid face. J. Hum. Evol. 16, 429–443.

Trinkaus, E., 1993. Variability in the position of the mandibular mental foramen and the identification of Neandertal apomorphies. Riv. Antropol. 71, 259–274.

Trinkaus, E., 2004. Dental crown dimensions of Middle and Late Pleistocene European humans. In: Rubio, S. (Ed.), Miscelánea en Homenaje a Emiliano Aguirre. Museo Arqueológico Reg., Alcalá de Henares, pp. 392–398.

Trinkaus, E., Lebel, S., Bailey, S.E., 2000a. Middle Paleolithic and recent human dental remains from the Bau de l'Aubesier, Monieux (Vaucluse). Bull. Mém. Soc. Anthropol. Paris 12, 207–226.

Trinkaus, E., Maley, B., Buzhilova, A.P., 2008. Brief communication: paleopathology of the Kiik-Koba 1 Neandertal. Am. J. Phys. Anthropol. 137, 106–112.

Trinkaus, E., Marks, A.E., Brugal, J.-P., Bailey, S.E., Rink, W.J., Richter, D., 2003. Later Middle Pleistocene human remains from the Almonda Karstic system, Torres Novas, Portugal. J. Hum. Evol. 45, 219–226.

Trinkaus, E., Ranov, V.A., Lauklin, S., 2000b. Middle Paleolithic human deciduous incisor from Khudji, Tajikistan. J. Hum. Evol. 38, 575–583.

Turq, A., Jaubert, J., Maureille, B., Laville, D., 2008. Le cas des sépultures Néandertaliennes du sud-ouest: et si on les vieillissait? In: Vandermeersch, B., Cleyet-Merle, J.-J., Jaubert, J., Maureille, B., Turq, A. (Eds.), Première Humanité, Gestes Funéraires des Néandertaliens. Réunion des Musées Nationaux, Paris, pp. 40–41.

Ungar, P.S., Fennel, K.J., Gordon, K., Trinkaus, E., 1997. Neandertal incisor beveling. J. Hum. Evol. 32, 407–421.

Ungar, P.S., Spencer, M.A., 1999. Incisor microwear, diet, and tooth use in three Amerindian populations. Am. J. Phys. Anthropol. 109, 387–396.

Valladas, H., Geneste, J.-M., Joron, J.-L., Chadelle, J.-P., 1986. Thermoluminescence dating of Le Moustier (Dordogne, France). Nature 322, 452–454.

Valladas, H., Joron, J.L., Valladas, G., Arensburg, B., Bar-Yosef, O., Belfer-Cohen, A., Goldberg, P., Laville, H., Meignen, L., Rak, Y., Tchernov, E., Tillier, A.M., Vandermeersch, B., 1987. Thermoluminescence dates for the Neanderthal burial site at Kebara in Israel. Nature 330, 159–160.

Vallois, H.V., Roche, J., 1958. La mandibule acheuléenne de Témara. C. R. Acad. Sci. [II] 246, 3113–3116.

Vandermeersch, B., 1981. Les Hommes Fossiles de Qafzeh (Israël). C.N.R.S., Cahiers de Paléontologie (Paléoanthropologie), Paris.

Vandermeersch, B., 1991. La ceinture scapulaire et les membres supérieurs. In: Bar-Yosef, O., Vandermeersch, B. (Eds.), Le squelette moustérien de Kebara 2. Éditions du CNRS, Paris, pp. 157–178.

Vega-Toscano, L.-G., Garralda, M.-D., Tillier, A.-M., Garcia-Sanchez, M., 1994. Les dents d'enfant des niveaux moustériens de la grotte de Carihuela (Grenade-Espagne). Paléo 6, 79–88.

Viola, B., Markin, S.V., Buzhilova, A.P., Mednikova, M.B., Dobrovolskaya, M.V., Le Cabec, A., Shunkov, M.V., Derevianko, A.P., Hublin, J.-J., 2012. A Neanderthal

mandible fragment from Chagyrskaya Cave (Altai Mountains, Russian Federation). In: Abstracts of the 2nd Annual Meeting of the European Society for the Study of Human Evolution, Bordeaux, France, September 2012, p. 189.

Vleck, E., 1993. Fossile Menschenfunde von Weimar-Ehringsdorf. Konrad Theiss Verlag, Stuttgart.

Wagner, G.A., Krbetschek, M., Degering, D., Bahain, J.-J., Shao, Q., Falguères, C., Voinchet, P., Dolo, J.-M., Garcia, T., Rightmire, G.P., 2010. Radiometric dating of the type-site for *Homo heidelbergensis* at Mauer, Germany. Proc. Natl. Acad. Sci. 107, 19726–19730.

Walker, M.J., Gibert, J., Lopez, M.V., Lombardi, A.V., Pérez-Pérez, A., Zapata, J., Ortega, J., Higham, T., Pike, A., Schwenninger, J.-L., Zilhão, J., Trinkaus, E., 2008. Late Neandertals in Southeastern Iberia: Sima de las Palomas del Cabezo Gordo, Murcia, Spain. Proc. Natl. Acad. Sci. 105, 20631–20636.

Wallace, J.A., Barrett, M.J., Brown, T., Brace, C.L., Howells, W.W., Koritzer, R.T., Sakura, H., Stloukal, M., Wolpoff, M.H., Žlábek, K., 1975. Did La Ferrassie I use his teeth as a tool? [and comments and reply]. Curr. Anthropol. 16, 393–401.

Wang, Q., Wright, B.W., Smith, A., Chalk, J., Byron, C.D., 2010. Mechanical impact of incisor loading on the primate midfacial skeleton and its relevance to human evolution. Anat. Rec. 293, 607–617.

Waters-Rist, A., Bazaliiskii, V.I., Weber, A., Goriunova, O.I., Katzenberg, M.A., 2010. Activity-induced dental modification in holocene siberian hunter-fisher-gatherers. Am. J. Phys. Anthropol. 143, 266–278.

Weaver, T.D., Roseman, C.C., Stringer, C.B., 2007. Were Neandertal and modern human cranial differences produced by natural selection or genetic drift? J. Hum. Evol. 53, 135–145.

Weihs, C., Ligges, U., Luebke, K.R., Raabe, N., 2005. klaR analyzing German business cycles. In: Baier, D., Decker, R., Schmidt-Thieme, L. (Eds.), Data Analysis and Decision Support. Springer-Verlag, Berlin, pp. 335–343.

Weinberger, A., 1954. The clinical significance of hypercementosis. Oral Surg. Oral Med. Oral Pathol. 7, 79–87.

Wolpoff, M.H., 1971. A Functional Measure of Tooth Size. Southwest. J. Anthropol. 27, 279–286.

Wolpoff, M.H., 1979. The Krapina dental remains. Am. J. Phys. Anthropol. 50, 67–113.

Wolpoff, M.H., 1999. Paleoanthropology. McGraw-Hill, New York.

Wright, T., 2007. The molecular control of and clinical variations in root formation. Cells Tissues Organs 186, 86–93.

SUMMARY

SUMMARY

Within karstic contexts, dental remains of Neanderthals and modern humans can both be found in similar stratigraphic conditions, whether because the occupation of the cave by the two taxa was close in time, or because stratigraphic layers were disturbed by taphonomic factors. Finding a discriminating feature that could distinguish both groups is crucial for the correct taxonomic designation and interpretation of the human remains. This holds true in the case where a Mousterian site can have been contaminated by modern remains (from the Upper Paleolithic or more recent times), or alternatively, in the context of pene-contemporaneous occupation of the place by both taxa, for the sites of the late Middle Paleolithic and of the early Upper Paleolithic.

In this context, tooth root length, especially for the permanent anterior teeth, has been proposed to reliably distinguish Neanderthals from extant modern humans. Anatomical descriptions of the Neanderthal anterior teeth have often underlined their long and robust roots. However, only one study has quantitatively investigated the value of root length to distinguish Neanderthals from Upper Paleolithic and extant modern humans (Bailey, 2005).

Several interpretations attempt to explain the long and robust roots of the Neanderthal dentition. For some authors, these long roots are the consequence of the cranio-facial architecture seen in Neanderthals, while for others, the maxillary region of the Neanderthal face has adapted to such long and robust teeth. Other scholars hypothesize that these long teeth result from genetic drift. Finally, several researchers see these large roots as a biomechanical adaptation to sustain high or frequent loads exerted on the anterior dentition of the Neanderthals, especially while performing para- and non-masticatory activities.

This thesis investigates the variability in root size and shape of the permanent maxillary and mandibular incisors and canines, in Neanderthals, early and recent modern humans. It analyses large samples of Neanderthals and early modern humans, covering a long chronological period and a broad geographical area. Using micro-computed tomography, this study aims to confirm and extend the results on root length

to other linear, surface and volumetric measurements taken on 3D models of the anterior tooth roots. In addition, root shape was investigated using geometric morphometric techniques, by collecting anatomical landmarks, as well as curve and surface semi-landmarks.

The first part of this work confirms that root length and volume distinguish Neanderthals from recent modern humans. Neanderthals have significantly larger root length, cross-sectional root surface area, root volume and overall mandibular size than recent modern humans. Both taxa have significantly different symphyseal cross-sectional shapes, while symphyseal height and width are similar in both groups. Although root size and mandible/symphyseal size are not correlated, Neanderthals have large roots for the size of their jaw. When modern humans are scaled to the size of the Neanderthals (using the centroid size of the mandible as an estimate of its overall size), their roots remains overall smaller than those of Neanderthals. The short roots observed in recent modern humans can be interpreted as the result of negative allometry in root size. The condition of the Mauer specimen, displaying long roots, suggests that Neanderthals would have retained an ancestral condition. In addition, Neanderthals could also display a positive allometry for root size, but confirming this hypothesis requires an increase in the early *Homo* samples. The difference in cross-sectional symphyseal shape in Neanderthals can be interpreted as a way of accommodating large permanent tooth roots in a symphysis of comparable size to modern humans.

This part of our study validates that root length and volume can be used to distinguish taxonomically late Neanderthals from recent and Upper Paleolithic modern humans.

The second part of this thesis strengthens the validity of root size (e.g. length, volume, surface area) as a proxy to distinguish the permanent anterior teeth of Neanderthals from those of modern humans. This analysis addresses a larger series of fossils dating from MIS 15 to MIS 2, in addition to a few specimens from the Lower Pleistocene; and ranging from Germany to Israel and from Siberia to Spain. X-ray micro-computed tomography gives access to yet unexplored specimens, regarding their

root morphology. This non-destructive technique allows for surface and volumetric quantifications, as well as for the analysis of the root surface shapes using geometric morphometric techniques.

Plotting root length against the labio-lingual crown diameter allowed us to identify a chronological trend towards a gracilization of the anterior tooth roots in recent modern humans. MIS 4 Neanderthals seem to have a lower variability than earlier Neanderthals. Importantly, early modern humans are found to overlap in several dimensions with both Neanderthals and recent modern humans. This observation, and the study of a limited number of early *Homo*, strengthens the conclusion reached in the first part of this thesis that overall longer and larger roots in Neanderthals would result from the retention of an ancestral condition. As a result, early modern humans might be difficult to distinguish from Neanderthals on the ground of the root dimensions of their anterior dentition. This could be the case for the Tabun C2 specimen (dated to circa 100-130 ka to 171 ka, Israel), where root morphology unfortunately does not allow any definitive conclusion, regarding its taxonomical status. Tabun C2 is shown to have anterior roots having a size and shape similar to Neanderthals. Since its molar roots do not display the characteristic taurodontic shape commonly observed in Neanderthals, Tabun C2 is better interpreted as being an early modern human, still retaining the robust ancestral root features.

Nonetheless, the taxonomical usefulness of root metrics and morphology is well illustrated by the cases of Steinheim (dated to 250 or >300 ka, Germany) and of five isolated teeth from the Kebara Cave (some of them are dated as ‘probably Mousterian’, Israel). Root size and shape eliminate the possibility that the incisors attributed to the Middle Pleistocene skull of Steinheim could belong to this specimen. They are more likely modern and recent, and were likely accidentally associated to the skull in storage. In Kebara, among five isolated teeth recovered in the Mousterian layers of the cave, two can safely be classified as Neanderthals while two others are more likely modern. The taxonomical status of the last tooth remains uncertain.

From a functional perspective, the size and shape of the Neanderthal anterior roots could be interpreted as a functional adaptation to sustain high or frequent loads exerted on the front teeth. This may lend support to the ‘Teeth-as-tools’ hypothesis, stating that Neanderthals were using their anterior dentition as a third hand, for non- and

para-masticatory activities. The use of the anterior teeth as a third hand has already been proposed, given the strong and irregular amount of wear in the anterior dentition in Neanderthals and other Middle Pleistocene hominids, and the results yielded by the microwear studies. We suggest that the labial convexity of the root would be in continuity with the one observed on the shovel-shaped crown. In combination with the lingual tubercle, this morphology would improve the distribution and the release of the stresses and avoid the fracture of the tooth under a demanding loading regime.

Although it has been observed throughout almost the entire Neanderthal sample, hypertrophic cementum could be successfully segmented only in eight teeth. The preferential distribution of the hypercementosis around the root apex could reflect the direction of the main forces exerted on the incisal surface, during the use of the anterior teeth as a third hand. The hypercementosis constitutes another argument supporting the 'teeth-as-tools' hypothesis.

This thesis considerably improves our knowledge of the anterior root size and shape in Neanderthals, fossil and extant humans, in a broad geographical and chronological context. Root morphology has proven its capacity to significantly contribute to the taxonomical attribution of isolated teeth from museum collections, old excavations or found in unclear stratigraphic contexts. We however stress that caution should be kept in mind, and that root length should not be taken as sufficient for a taxonomic determination, specifically when dealing with early forms of modern humans. The combination of metric and discrete features always strengthens a diagnosis.

Micro-CT scanning acquisitions of more numerous specimens of early *Homo* and of earlier hominids would yield a better understanding of the polarity of the anterior tooth root characters, and possibly about the functional significance of these morphological root features. Biomechanical modelling (e.g., using Finite Element Analysis) of the different loading regimes that Neanderthals could have been exerting on their anterior teeth, would yield a better understanding of the importance of the functional adaptation in the Neanderthal root and maxillo-facial morphology.

RESUME

En contexte karstique, les restes dentaires, à la fois de Néanderthaliens et d'Hommes modernes, peuvent être découverts dans des contextes archéologiques similaires, soit que l'occupation de la grotte par les deux taxons ait été proche dans le temps ou soit que les couches archéologiques aient été perturbées par des facteurs taphonomiques. Déterminer une caractéristique discriminante qui pourrait distinguer les deux taxons est crucial. Ceci est valable dans le cas où un site moustérien aurait pu être contaminé par des restes modernes (du Paléolithique Supérieur ou plus récents), mais aussi, dans le cas d'une occupation péné-contemporaine d'un site par les deux taxons, pour les sites du Paléolithique moyen tardif, et du Paléolithique supérieur ancien.

La longueur des racines dentaires, surtout celles des dents antérieures permanentes, a été proposée pour distinguer de façon fiable les dents isolées de Néanderthaliens et d'Hommes modernes récents. Les descriptions anatomiques des dents antérieures Néanderthaliennes ont en effet souvent souligné la robustesse et la longueur de leurs racines. Cependant, à ce jour, une seule étude quantitative a analysé l'intérêt taxonomique de la longueur des racines pour distinguer les Néanderthaliens des Hommes du Paléolithique Supérieur et des Hommes modernes récents et elle n'a porté que sur des échantillons limités (Bailey, 2005).

Plusieurs interprétations ont été proposées pour expliquer les racines longues et robustes de la denture néanderthalienne. Pour certains auteurs, ces longues racines sont la conséquence de l'architecture crânio-faciale observée chez les Néanderthaliens, alors que pour d'autres, ce serait plutôt la région maxillaire de la face néanderthalienne qui se serait adaptée à de telles dents, longues et robustes. D'autres scientifiques ont émis l'hypothèse qu'une partie de la morphologie faciale néanderthalienne pourrait résulter d'un phénomène de dérive génique. Enfin, plusieurs chercheurs voient ces grandes racines comme une adaptation biomécanique pour supporter des forces fréquentes ou de grande magnitude, exercées sur la dentition antérieure des Néanderthaliens, en particulier lors d'activités para- et non-masticatrices.

Cette thèse étudie la variabilité en taille et en conformation[1] des racines des incisives et canines permanentes, mandibulaires et maxillaires, chez les Néanderthaliens et les Hommes modernes anciens et récents. Cette recherche porte sur des échantillons conséquents de Néanderthaliens et d'Hommes modernes anciens, couvrant une large période chronologique et une vaste zone géographique. Au moyen de la micro-tomographie assistée par ordinateur, cette étude a pour objectif de valider les résultats sur la longueur des racines et d'analyser d'autres mesures linéaires, surfaciques et volumétriques, prises sur les modèles tridimensionnels des racines des dents antérieures. De plus, la conformation racinaire a été étudiée au moyen de techniques de géométrie morphométrique, en collectant les coordonnées de points anatomiques de référence ainsi que de points de référence répartis sur des courbes et des surfaces des racines.

La première partie de cette thèse confirme que la longueur et le volume des racines de la denture antérieure distingue les Néanderthaliens des Hommes modernes récents. Les Néanderthaliens se caractérisent par des longueurs racinaires, des surfaces de section longitudinale racinaire, des volumes racinaires et une taille générale de la mandibule significativement supérieurs à ceux des Hommes modernes récents. Les deux taxons ont une conformation en section de la symphyse mandibulaire significativement différente, alors que la hauteur et la largeur de la symphyse sont similaires dans les deux groupes. En dépit du fait que la taille des racines et la taille de la mandibule/symphyse ne soient pas corrélées, les Néanderthaliens ont de grandes racines par rapport à la taille de leurs mâchoires. Lorsque hommes modernes et Néanderthaliens sont ramenés à la même taille (en utilisant la taille centroïde de la mandibule comme approximation de sa taille globale), leurs racines restent en général plus petites que celles des Néanderthaliens. Les racines courtes observées chez les hommes modernes récents peuvent être interprétées comme résultant d'une allométrie négative de la taille des racines. L'analyse du spécimen de Mauer, qui possède de longues racines antérieures, suggère que les Néanderthaliens auraient retenu une condition ancestrale. Les Néanderthaliens pourraient aussi montrer une allométrie positive pour la taille de leurs racines, mais confirmer cette hypothèse requerrait d'augmenter la taille de l'échantillon des premiers représentants du genre *Homo*. La différence en conformation de la

[1] A noter qu'en Anglais, « form » inclut « size » et « shape ». Pour éviter toute confusion lors de la traduction, « shape » est traduit en Français par « conformation », et « form » par « forme ».

symphyse en section chez les Néanderthaliens peut être interprétée comme un moyen d'accommoder des germes de dents permanentes de grande taille dans une région symphysaire de taille comparable à celle des Hommes modernes. Cette partie de l'étude valide l'hypothèse que la longueur et le volume des racines des dents antérieures peuvent être utilisés pour distinguer les Néanderthaliens des Hommes modernes, sur un plan taxonomique.

La seconde partie de cette thèse renforce la validité de la taille des racines (par exemple, longueur, volume, surface) en tant que moyen de distinguer les dents antérieures permanentes des Néanderthaliens de celles des Hommes modernes. Ceci s'applique à un large échantillon de fossiles datant du stade isotopique 15 au stade isotopique 2, auxquels il faut ajouter quelques spécimens du Pléistocène Inférieur, et s'étendant de l'Allemagne à Israël, et de l'Espagne à la Sibérie. La micro-tomographie aux rayons X assistée par ordinateur permet d'accéder à des spécimens jusqu'alors inexplorés, quant à leur morphologie racinaire. De surcroît, cette technique non-destructive rend possible des quantifications surfaciques et volumétriques, ainsi que des analyses de la conformation des surfaces racinaires au moyen de techniques de la géométrie morphométrique.

Un graphique confrontant la longueur racinaire et le diamètre labio-lingual de la couronne permet d'identifier une tendance chronologique vers une gracilisation des racines des dents antérieures chez les Hommes modernes récents. Les Néanderthaliens du stade isotopique 4 semblent avoir une variabilité inférieure à celle des Néanderthaliens datant d'avant le stade 4. Enfin, la distribution des Hommes modernes anciens se superpose partiellement à celles des Néanderthaliens et des Hommes modernes récents. Cette observation, combinée à l'analyse de quelques représentants anciens du genre *Homo* inclus dans cette étude, renforce l'hypothèse émise dans le premier chapitre, suivant laquelle les racines globalement plus grandes et plus longues des Néanderthaliens résulteraient de la rétention d'une condition ancestrale. De ce fait, les hommes modernes anciens peuvent se révéler difficiles à distinguer des néanderthaliens pour ce qui est des dimensions des racines de la denture antérieure. Ce pourrait être le cas pour le spécimen de Tabun C2 (daté d'environ 100,000-130,000 ans à 171,000 ans, Israël), dont la morphologie racinaire ne permet malheureusement pas de

conclure de façon définitive quant au statut taxonomique de ce spécimen. Tabun C2 possède des racines antérieures de taille et de conformation similaires à celles des Néanderthaliens. Puisque ses molaires ne présentent pas la conformation taurodonte caractéristique, communément observée chez les Néanderthaliens, la meilleure interprétation est de considérer Tabun C2 comme un Homme moderne ancien, retenant encore les traits racinaires robustes ancestraux.

Néanmoins, l'utilité taxonomique de la morphologie et des mesures racinaires est très bien illustrée par les cas de Steinheim (daté à 250,000 ou >300,000 ans, Allemagne) et de cinq dents isolées provenant de la Grotte de Kébara (Israël), certaines d'entre elles sont désignées comme « probablement moustériennes ». La taille et la conformation racinaires permettent d'exclure que les incisives attribuées au crâne pléistocène moyen de Steinheim puissent appartenir à ce spécimen, et d'en déduire qu'elles sont plus vraisemblablement le résultat d'une intrusion accidentelle de dents modernes dans la boîte où est entreposé celui-ci. Parmi les cinq dents isolées des niveaux moustériens de la Grotte de Kébara, deux d'entre elles peuvent être classées avec confiance comme étant néanderthaliennes, alors que deux autres appartiennent plus probablement à des Hommes modernes. Le statut taxonomique de la dernière dent reste incertain.

D'un point de vue fonctionnel, la taille et la conformation des dents antérieures néanderthaliennes peuvent être interprétées comme une adaptation fonctionnelle répondant à des forces fréquentes ou de grande magnitude exercées sur les dents antérieures. Ceci soutiendrait l'hypothèse des « dents-utilisées-comme-des-outils », stipulant que les Néanderthaliens utilisaient leur dentition antérieure comme une troisième main, pour des activités non- ou para-masticatrices. L'utilisation des dents antérieures comme une troisième main a été proposée pour expliquer l'usure importante et irrégulière de la dentition antérieure chez les Néanderthaliens et d'autres hominidés du Pléistocène Moyen. Les résultats des études de micro-usure dentaire semblent confirmer cette interprétation. Nous suggérons que la convexité labiale des racines serait en continuité avec celle observée sur les couronnes à morphologie dite « en pelle ». En combinaison avec le tubercule lingual, cette morphologie améliorerait la distribution et le relâchement des contraintes et éviterait la fracture de la dent sous un régime de charges mécaniques trop contraignant.

Bien qu'il ait été observé dans la quasi-totalité de l'échantillon néanderthalien, le cément hypertrophique n'a pu être segmenté que dans huit dents. La distribution préférentielle de l'hypercémentose autour de l'apex racinaire pourrait refléter la direction des forces principales exercées sur la surface incisale, durant l'utilisation des dents antérieures comme une troisième main. L'hypercémentose constitue un autre argument pour soutenir l'hypothèse des « dents-utilisées-comme-des-outils ».

Cette thèse améliore considérablement notre connaissance de la taille et de la conformation des racines des dents antérieures chez les Néanderthaliens, les Hommes fossiles et actuels, dans un large contexte géographique et chronologique. La morphologie racinaire a prouvé sa capacité de contribuer de façon significative à l'attribution taxonomique de dents isolées provenant de collections de musée, de fouilles anciennes ou encore trouvées en contexte stratigraphique incertain. Nous insistons néanmoins sur le fait que la prudence doit rester de mise, et que la longueur racinaire ne doit pas être considérée comme suffisante pour une détermination taxonomique. La combinaison des caractères métriques et discrets renforce toujours une diagnose.

Les acquisitions micro-tomographiques de plus de spécimens représentatifs des débuts du genre *Homo* et d'hominidés plus anciens permettront de mieux comprendre la polarité des caractères des racines des dents antérieures, et peut-être aussi la signification fonctionnelle des traits morphologiques des racines. Les modélisations biomécaniques (par exemple, par la méthode des Eléments Finis) des différents régimes de charge que les Néanderthaliens pourraient avoir exercé sur leurs dents antérieures, permettraient de mieux cerner l'importance de l'adaptation fonctionnelle des morphologies racinaire et maxillo-faciale chez les Néanderthaliens.

APPENDIX

Max-Planck-Institut
für evolutionäre
Anthropologie
Max Planck Institute for Evolutionary Anthropology
Department of Human Evolution

MAX-PLANCK-GESELLSCHAFT

Adeline Le Cabec

Tel.: 00. 33. (0)4. 76. 88. 17. 50
Fax: 00. 33. (0)4. 76. 88. 22. 52
adeline.le-cabec@esrf.fr

Prof. Dr. Andrea Robitzki

Dean of the Faculty of Life Sciences, Pharmacy and Psychology

Brüderstraße 32

04103 Leipzig

Grenoble, November 22nd, 2012

Statement of Independent Work

Dear Prof. Dr. Andrea Robitzki,

I hereby declare that the present work has been produced independently, using only the aid mentioned. I certify that I have produced this work, expressed in my own words, involving the comments and advice of my co-authors and of the reviewers of the Journal of Human Evolution. All resources used are cited as full references. This work has not been submitted in any other instance for receiving any other academic degree.

Sincerely yours,

Adeline Le Cabec

Adeline Le Cabec

Anterior Dental Loading and Root Morphology in Neanderthals.

Statement of contribution of the co-authors

Title: Long Anterior Mandibular Tooth Roots in Neanderthals Are Not the Result of their Large Jaws

Authors: Adeline Le Cabec, Kornelius Kupczik, Philipp Gunz, José Braga, Jean-Jacques Hublin.

Journal: Journal of Human Evolution

DOI: 10.1016/j.jhevol.2012.07.003

Statement of contribution of Adeline Le Cabec

- contributed to research design.
- literature review.
- segmentation of all the specimens.
- linear, surface and volumetric measurements for all specimens.
- collection of landmarks datasets for centroid size estimation and mandibular shape analysis.
- performed some of the statistics in R.
- wrote the paper, interpret and discussed the results.

Statement of contribution of Kornelius Kupczik

- contributed to research design.
- commented on the manuscript.

Statement of contribution of Philipp Gunz

- performed the GPA and mandibular shape analysis.

- contributed to research design for the mandibular shape study and performed the associated statistical analysis.
- contributed to write the statistical part of the manuscript.
- commented on and improved the manuscript.

Statement of contribution of José Braga

- contributed to research design.

Statement of contribution of Jean-Jacques Hublin

- contributed to research design.
- provided facilities for scanning, image processing, and micro-CT data.
- discussed and contributed in interpreting the results.
- commented on the manuscript.

Adeline Le Cabec

Kornelius Kupczik

Philipp Gunz

José Braga

Jean-Jacques Hublin

Adeline Le Cabec

Anterior Dental Loading and Root Morphology in Neanderthals.

Statement of contribution of the co-authors

Title: Anterior Tooth Root Morphology and Size in Neanderthals: Taxonomic and Functional Implications.

Authors: Adeline Le Cabec, Philipp Gunz, Kornelius Kupczik, José Braga, Jean-Jacques Hublin.

Journal: Journal of Human Evolution

Statement of contribution of Adeline Le Cabec

- contributed to research design.
- literature review.
- data collection (micro-CT scanning, reconstruction, database) on the field during the two scanning trips, in France (2008) and in Israel (2011).
- pre-processing for some of the specimens: micro-CT scan, reconstruction of the scans.
- segmentation of all the specimens.
- linear, surface and volumetric measurements for all specimens.
- tested for methodological reliability (broken roots).
- contributed to design research for the root shape study.
- took landmarks and semi-landmark datasets for shape analysis.
- performed the statistics in R.
- wrote the paper, interpret and discussed the results.

Statement of contribution of Philipp Gunz

- facilitated access to fossils especially for the scanning trip to Israel.
- performed the PCA and CVA analyses.

- contributed to research design for the root shape study and performed the associated statistical analysis.
- commented on the manuscript.

Statement of contribution of Kornelius Kupczik

- contributed to research design.
- commented on the manuscript.

Statement of contribution of José Braga

- contributed to research design.
- provided micro-CT data.

Statement of contribution of Jean-Jacques Hublin

- contributed to research design.
- provided facilities for scanning acquisition and image processing, and micro-CT data.
- facilitated access to fossils especially for the two scanning trips.
- discussed and contributed in interpreting the results.
- commented on the manuscript.

Adeline Le Cabec

Philipp Gunz

Kornelius Kupczik

José Braga

Jean-Jacques Hublin

CURRICULUM VITAE – Adeline Le Cabec

adeline.le-cabec@esrf.fr

Date and Place of birth: 11th December 1984, Saint-Brieuc (Côtes-d'Armor, France)

Citizenship: French

Current personal address: 7, rue Pierre Sémard, 38000 Grenoble, France

Current work address: Beamline ID 19, European Synchrotron Radiation Facility, 6 rue Jules Horowitz, BP 220, 38043 Grenoble, France

Phone: 00 33 (0)4 76 88 17 50

Fax: 00 33 (0)4 76 88 22 52

Languages: French (mother tongue), English (read, spoken, written), German (basic conversation level).

EDUCATION

Febr. 2012-present — Junior scientist at the ID 19 Beamline, X-Ray Imaging Group, ESRF (Grenoble, France), supervised by Drs. Paul Tafforeau (ESRF) and Tanya Smith (Harvard University), and in collaboration with Dr. Anne Bonnin (ESRF, Grenoble, France).

2007-present — Ph.D. thesis at Max Planck Institute for Evolutionary Anthropology, Department of Human Evolution (Leipzig, Germany), Fakultät für Biowissenschaften, Pharmazie und Psychologie der Universität Leipzig (Germany), and UMR 5288 CNRS, Anthropobiologie et Imagerie Anatomique, Université Paul Sabatier (Toulouse, France). 'Anterior dental loading and root morphology in Neanderthals'. Ph.D. student at the IMPRS "The Leipzig School of Human Origins". Supervision: Prof. J.-J. Hublin (MPI-EVA) and Prof. J. Braga (UPS).

2006-2007 — Second year of M.Sc. 'Anthropology, genetic delimitation of human populations and health' (Mention Très Bien) University Paul Sabatier, Toulouse.

Dissertation supervised by Prof. J. Braga: 'Functional and evolutionary comparative study of the postcanine root complex

between the two species of chimpanzees (*Pan paniscus* and *Pan troglodytes schweinfurthi*)'.

2005-2006 First year of M.Sc. 'Biological Anthropology, Paleoanthropology and Prehistory' (Mention Bien) University of Bordeaux 1.

2004-2005 Third year of B.Sc. degree B.O.P. (Biology of Organisms and Populations) (Mention Bien) University of Rennes 1.

2002-2004 Classe Préparatoire aux Grandes Ecoles B.C.P.S.T. (for Biology, Chemistry, Physics, Earth Sciences, Mathematics), Lycée Chateaubriand, Rennes (France).

2002 Baccalauréat Scientifique (Mention Bien) at Notre-Dame de Campostal, Rostrenen (France).

TRAINING COURSES

February 2006 Internship in the Radiology Unit of the Teaching Hospital Pellegrin (Bordeaux, France). 'Initiation into radiological techniques allowing an estimate of the bone structure. Initiation into reading radiological simple views, TDM and RMI examinations, arthrography, ultrasonography, osteodensitometry. Approach of radiological anatomy: normal and variants, pathological.' Supervised by Prof. O. Hauger.

2004-2005 Voluntary internship in the Laboratory of Anthropology and Archeometry of University Rennes 1 (UMR 6566 – Civilisations Atlantiques & Archéosciences). 'Initiation into archeozoology and paleobotany.' From Nov. 2004 to June 2005. Supervised by Dr. J.-L. Monnier.

February 2000 Voluntary internship at the archeological center of Melrand, 'Le village de l'An Mil', Melrand, France. Supervised by Maud Le Clainche.

FIELD WORK

July - August 2011 Micro-CT scanning of the fossil collection at the Department of Anatomy and Anthropology, Sackler School of Medicine, Tel-Aviv University, Israel. Project leader: Dr. Philipp Gunz, MPI-EVA. Role: Organization of the work, scanning (on a SkyScan 1172), reconstruction of the scans, collection of data for the MPI-EVA database from museum records and literature.

Oct.-Nov. 2008	Micro-CT scanning of the fossil collection at the Musée National de la Préhistoire, Les-Eyzies-de-Tayac-Sireuil, France. Project leader: Prof. Jean-Jacques Hublin, MPI-EVA. Role: Organization of the work, collection of data for the MPI-EVA database from museum records and literature.
August 2006	Excavations at Les Pradelles (Marillac-Le-Franc, Charente, France), (Middle Palaeolithic), lead by Dr. B. Maureille.
August 2005	Excavations at Menez-Dregan (Plouhinec, Finistère, France), (Lower Palaeolithic habitat site), lead by Dr. J.-L. Monnier.

RESEARCH INTERESTS

- Virtual paleoanthropology
- Imaging techniques
- Image processing techniques
- Dental anthropology
- Tooth function
- Dental pathology and paleopathology

TECHNICAL SKILLS

- Scanning on a desktop micro-CT scanner - SkyScan 1172.
- Basic knowledge of scanning on a BIR ACTIS 225/300 industrial CT scanner.
- Reconstruction software: NRecon Reconstruction Software.
- 3D image analysis and visualization software: Avizo (Visualization Sciences Group), VGStudio MAX 2.1. (Volume Graphics).
- Microscribe digitizing.
- Statistical software: started using R statistical software.
- Participation in the MPI-EVA micro-CT database (structure, scanning trips, collecting information).

TEACHING/TRAINING EXPERIENCE

- 2008	Participation in the supervision of Gwendoline Chantreau, during the writing of her thesis for the first year of her Master's degree

in ‘Archeology and History’, entitled ‘Rapport de stage : Etude anthropologique des squelettes de la collection Simon, Genève.’ (Universities of Rennes 1, Rennes 2 and Nantes, France). Supervised by Dr. Jean-Laurent Monnier and Dr. Geneviève Perréard-Lopreno.

- 2007-2011 Training of several Ph.D. students, guest researchers, guest undergraduate students and student helpers to use Avizo and to follow the segmentation workflow in use for the Dental Tissue Group (MPI-EVA, Germany).

- 2006-2007 Advising other undergraduate students and guest researchers on using Amira (UPS, France).

PUBLICATIONS AND CONFERENCE PRESENTATIONS

PAPERS IN PEER-REVIEWED JOURNALS

Le Cabec, A., Gunz P., Kupczik, K., Braga, J. and Hublin, J.-J. (2013) – *Anterior Tooth Root Morphology and Size in Neanderthals: Taxonomic and Functional Implications.* Journal of Human Evolution, 64, 169-193. DOI: 10.1016/j.jhevol. 2012.08.011

Le Cabec, A., Kupczik, K., Gunz P., Braga, J. and Hublin, J.-J. (2012) – *Long Anterior Mandibular Tooth Roots in Neanderthals Are Not the Result of their Large Jaws.* Journal of Human Evolution, 63, 667-681. DOI: 10.1016/j.jhevol.2012.07.003

CONTRIBUTIONS TO EDITED BOOKS

Le Cabec A., Oueiss A., Egorova M., Gérault A., Baranov V., Rougé D., Braga J. (2007). – *Virtopsy de Kyys.* In: Crubézy E. & Alexeev A. (eds): Chamane, Kyys, jeune fille des glaces. Errance, Paris, pp. 28-29.

ORAL PRESENTATIONS

Le Cabec A., Tafforeau P., Smith T. M., Bonnin A., Spoor F., Alemseged Z. (2012). – *Insights into Early Hominids' Dentition using Synchrotron Tomography* – Science and Student Days, Val Cenis-Lanslevillard, France, 10th-12th October 2012.

Viola B., Markin S.V., Buzhilova A.P., Mednikova M.B., Dobrovolskaya M.V., Le Cabec A., Shunkov M.V., Derevianko A.P., Hublin J.-J. (2012). – *A Neanderthal mandible fragment from Chagyrskaya Cave (Altai Mountains, Russian Federation)* In: Abstracts of the 2nd Meeting for the European Society for the study of Human Evolution, Bordeaux, France, September 22nd 2012, p. 189.

Le Cabec A., Gunz P., Kupczik K., Braga J., Hublin J.-J. (2012*). – Anterior Tooth Root Morphology in Neanderthals and Anatomically Modern Humans: Quantification and Functional Implications.* 81st AAPA meeting, Portland, Oregon, USA. Published abstract in *AJPA* 147, S54: 189-190.

Le Cabec A., Kupczik K., Gunz P., Braga J., Hublin J.-J., (2011). – *Does anterior tooth root size correlate with symphyseal size in Neanderthals and modern humans?* In: Abstracts of the Inaugural Meeting for the European Society for the Study of Human Evolution, Leipzig, Germany, September 2011, p. 18.

Viola B., Le Cabec A., Markin S.V., Zenin A., Shunkov M.V., Derevianko A.P. (2011). – *Late Pleistocene dental remains from the Altai Mountains, Russian Federation*. – Characteristic features of the Middle to Upper Paleolithic transition in Eurasia: development of culture and evolution of *Homo* species. International Symposium at Denisova Cave, Russian Federation, July 3rd-11th 2011.

Le Cabec A., Verna C., Kupczik K., Toussaint M., Braga J., Bonjean D. and Hublin J.-J. (2011). – *Analyse microtomographique des racines des dents permanentes du néanderthalien de Scladina (Belgique).* – 1836e journées de la Société d'Anthropologie de Paris, Paris, France, January 26th-28th 2011.

Kupczik K., Le Cabec A., Hublin J.-J. (2010). – *Comparative morphology of incisor and molar roots in Neanderthals, Middle Pleistocene Homo and Homo sapiens*. 79th AAPA meeting, Albuquerque, New Mexico, USA. Published abstract in AJPA 141, S50: 148.

Le Cabec A., Crubézy E., Braga J., Dabernat H., Telmon N., Dedouit F. and Treil J. (2007). – *" Virtopsy " d'une momie naturelle : étude anthropologique classique (âge au decès, sexe, paléopathologie) au moyen de la tomodensitométrie et de la reconstruction tridimensionnelle.* – Congrès national des sociétés historiques et scientifiques – 132e congrès, Images et imagerie, Arles, France, April 16th-21st 2007.

POSTER PRESENTATIONS

Viola B., Markin S.V., Le Cabec A., Shunkov M.V., Derevianko A.P. (2011). – *Middle Palaeolithic associated hominin remains from Chagyrskaya Cave, Altai Mountains, Russian Federation*. – European Society for the study of Human Evolution - Inaugural Meeting, Leipzig, Germany, September 23th 2011.

Le Cabec A., Kupczik K., Toussaint M., Braga J., Hublin J.-J. (2010). – *Incisor and Molar Root Morphology of the Juvenile Neanderthal from Scladina Cave (Belgium).* 79th *AAPA meeting, Albuquerque, New Mexico, USA.* Published abstract in AJPA 141, S50: 148.

Le Cabec A., Kupczik K., Braga J., Hublin J.-J. (2009). – *Incisor Root Morphology in Neanderthals and Homo sapiens.* 78th *AAPA meeting, Chicago, Illinois, USA.* Published abstract in *AJPA 138*, S48: 263.

MEDIA COVERAGE

- ‘Будущее прошлого’ (‘The Future of the Past’), as part of the serial documentary ‘Вопрос времени’ (‘A Matter of Time’) broadcast on the channel ‘Россия 2’ (‘Russia 2’) on August 13, 2012, and on the channel ‘Наука 2.0’ (‘Science 2.0’). Main reporter: Andrey Shilov.

Russia 2 Online:
http://russia2.tv/video/show/brand_id/9818/video_id/143188/viewtype/picture (Russian)

- *Paläoanthropologie: Rivalen um die Weltherrschaft* – Der Spiegel, 5th September 2011, pp. 118-120. Main reporter: Johann Grolle.

Spiegel Online:
http://www.spiegel.de/spiegel/0,1518,784530-2,00.html (German)
http://www.spiegel.de/international/spiegel/0,1518,784921,00.html (English)

- ‘*Abenteuer Wissen - Der erste Amerikaner’*, Spiegel TV, 16th December 2009 (10.15 pm on ZDF). Main reporter: Amai Haukamp.

Spiegel Online:
http://www.spiegel.de/spiegel/print/d-68167796.html